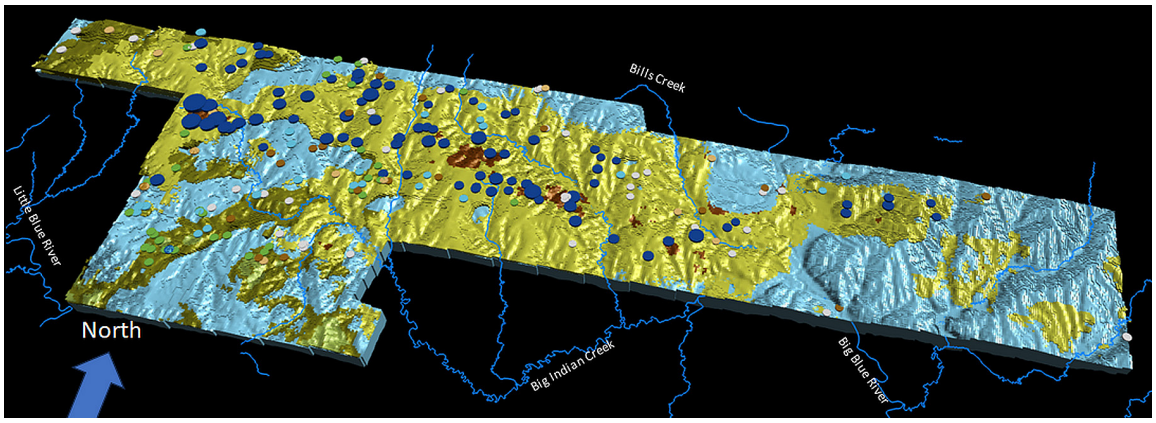
Airborne Electromagnetic Mapping and Hydrogeologic Framework of a Selected Area within the Lower Big Blue Natural Resources District



January 22, 2024

Prepared for the:
Lower Big Blue Natural Resources District
805 Dorsey Street, PO Box 826
Beatrice, NE 68310

Submitted by:
Aqua Geo Frameworks, LLC
10848 Ridge Road
Fort Laramie, WY 82212

Jared D. Abraham, P.G. #422
jabraham@aquageoframeworks.com

Theodore H. Asch, P.G. #430
tasch@aquageoframeworks.com

Tammi L. Renninger, ElephantFish, LLC
tammi@elephantfishco.com



Disclaimer: AGF conducted this project using the current standards of the geophysical industry and used in-house quality control standards to produce this geophysical survey and products. The geophysical methods and procedures described in this report are applicable to the particular project objectives, and these methods have been successfully applied by AGF to investigations and projects of similar size and nature. However, field or subsurface conditions may differ from those anticipated, and the resultant data may not achieve the project objectives. AGF's services were performed consistent with the professional skill and care ordinarily provided by professional geophysicists under the same or similar circumstances. No other warranty or representation, either expressed or implied, is made by AGF in connection with its services unless in writing and signed by an authorized representative of AGF.

Executive Summary

Aqua Geo Frameworks, LLC. (AGF) is pleased to submit this report titled "Airborne Electromagnetic Mapping and Hydrogeologic Framework of a Selected Area within the Lower Big Blue Natural Resources District". An understanding of the hydrogeological framework in the survey area is desired to assist in resource management. AGF entered into an agreement with the Lower Big Blue Natural Resources District (LBBNRD) to collect, process, and interpret airborne electromagnetic (AEM) data, and to use it in conjunction with other available background information to develop a 3D hydrogeologic framework.

The scope of work for this project was as follows:

1. SCOPE OF WORK

1.1 An AEM survey utilizing the SkyTEM304M system was flown over a portion of the southern part of LBBNRD. The area was from the border of the Little Blue Natural Resources District east of Fairbury, Nebraska encompassing the towns of Jansen, Harbine, Diller, Blue Springs, and Wymore. These flights have been provided as preliminary AEM inversions and the final AEM data and inversions are included as products attached to this data report.

1.2 AGF began project planning upon signing of the contract between AGF and the LBBNRD. This work included flight plans, database development, and review of hydrogeologic and geologic work for the area. The LBBNRD assisted in providing information such as water table measurements and water quality. The LBBNRD also assisted in obtaining powerline maps used in the flight planning process.

Upon conclusion of the design process, the LBBNRD flight lines had a maximum length of approximately 35 miles (57 km) in the east-west direction and about 10 miles (16 km) at their longest in the north-south direction. The flight lines were separated by approximately 0.93 mile (1.5 km) in both east-west and north-south directions.

1.4 AGF acquired AEM data over the LBBNRD, commencing 21 June 2023 and finishing on 22 June 2023, to support development of the hydrogeological framework. During this time frame, data collected over approximately 429 line-miles (691 line-kilometers) were acquired over the LBBNRD AEM survey area. Status reports of the flying were provided to the Contract Representative of LBBNRD daily, including the areas flown, production rates, and flight plan for the following day.

1.5 AGF processed and conducted quality assurance and quality control (QA/QC) procedures on all data collected from the acquisition system. AGF delivered preliminary data and inversions on June 23, 2023.

1.6 AGF inverted the AEM data. After final processing, approximately 347-line-miles (559-line kilometers) were retained for inversion amounting to a retention rate of 81.0%. This high rate is the result of careful flight line planning and design given the infrastructure that was encountered during the acquisition. These final inverted georeferenced data are delivered to the LBBNRD with this report. AGF-derived 2D sections, 3D electrical models, and interpreted geologic and hydrogeologic surfaces of the surveyed area are also delivered with this report.

1.7 AGF is providing a hydrogeologic framework report that includes maps of aquifer materials and their relationships to current test holes and production groundwater wells, estimated transmissivity

maps, areas of potential water quality concerns, and maps of estimated potential recharge areas under the AEM flight lines. This report, as mentioned above, also includes all data (acquired, processed, and developed) files. The report is delivered in PDF digital format and the data in native formats, ASCII, and ESRI map products.

2. KEY FINDINGS

2.1 Boreholes - Information from boreholes was used to analyze the AEM inversion results. These included CSD information on 27 test holes containing lithology and stratigraphic information, and four (4) test holes containing geophysical information. NE-DNR wells totaled 715 registered well records containing usable lithology information. These boreholes were essential in the interpretation of the AEM.

2.2 Digitizing Interpreted Geological Contacts - Characterization and interpretation of the subsurface was performed in cross-section and in derived surface grid formats. Contacts between the geologic units were digitized in 2D including: Quaternary (***Q***), Cretaceous Dakota Group (***Kd***), and the undifferentiated Permian (***P***) composed of the Permian Chase (***Pc***) and Council Grove Groups (***Pcg***). The interpretive process benefited from the use of CSD and NE-DNR borehole logs. Geological outcrop maps previously published were also used and critical in developing the geological contacts. Surface grids of the interpreted geologic formations were then produced. Each flight line profile with interpretation including the Quaternary/Cretaceous Dakota Group aquifer material mapping is included in the appendices as well as interpretative surface grids.

2.3 Resistivity/Lithology Relationship - Assessment of the sediment character in both the Quaternary (***Q***) and Cretaceous Dakota Group (***Kd***) aquifer system and the undifferentiated Permian bedrock was conducted to determine the overall composition of the major categories used to define the aquifer and aquitards in the survey area. A numerical assessment of the resistivity thresholds within the ***Q*** was used to characterize non-aquifer (<12 ohm-m), marginal (12-25 ohm-m), and aquifer (25-50 ohm-m), including coarse sand-rich intervals (>50 ohm-m), material.
The ***Kd*** within the LBBNRD AEM survey area was split into four parts based on empirical comparisons to lithology logs. The four parts were classified as follows: 1) 0-3 ohm-m as Shale/Clay Dominant materials; 2) 3-18 ohm-m as Siltstone/Silt Dominant materials; 3) 18-35 ohm-m as Sand/Silt Dominant; and 4) 35 ohm-m and greater as Sandstone/Sand Dominant materials. This is a modification of the splits that were used in the P-MRNRD reports from AGF (2021). Additional unpublished work in the Nebraska ***Kd*** using AEM data has led to a better understanding of the resistivity versus lithology within the ***Kd***. The undifferentiated Permian bedrock varied greatly but generally had moderate resistivities in the range of 15-30 ohm-m with the exception of the areas that contain saline waters; these areas had resistivities <7 ohm-m.

2.4 Hydrogeological Framework of the LBBNRD 2023 AEM Survey Area - The AEM reveals considerable variability in the Quaternary (***Q***) and Cretaceous Dakota Group (***Kd***) deposits across the AEM survey area. The groundwater within the LBBNRD 2023 AEM survey area is within the limited alluvial sediments of the present streams, glacial sediments, and the paleovalley sediments of the ***Q***. There is also groundwater in the fluvial and deltaic sediments of the ***Kd***. The actual groundwater availability is dependent upon the material type of both the ***Q*** and ***Kd***. In the western third of the survey area, the ***Q*** overlies the ***Kd*** and is in hydrogeological connection with the ***Kd***. In general, the ***Q*** groundwater is available within paleovalley sediments, and the ***Kd*** groundwater is available in the

sandstone and sand deposits of the fluvial deposits. Some NE-DNR wells are completed in both the ***Q*** and the ***Kd***.

An estimated Transmissivity (**T**) map was developed for the ***Q*** aquifers. This is related to the thickness of the saturated aquifer material and the estimated hydraulic conductivities. Most of the higher Specific Capacity (**SC**) values calculated from the NE-DNR well database are within the higher estimated **T** values of the paleovalley. A clear decrease in **T** is observed on the eastern side of the survey area where the paleovalley sediments thickness is reduced and the geology is dominated by thick glacial till deposits. Some isolated deposits of outwash gravel exist within the upper portions of the till and may be related to glacial-tectonic features associated with thrust sheets of outwash as was observed in areas of central Nebraska by Korus et al. (2021). Many of these sand and gravel deposits are unsaturated or partially saturated. Locally they can provide domestic water sources but are seldom large enough for sustainable large production wells.

The AEM successfully mapped the sand rich deposits of the ***Kd***. Many of the ***Kd*** completed wells are in this sand dominant region that has electrical resistivity > 25 ohm-m; these would be the sand dominant materials of the fluvial deposits of a paleochannel. The paleochannel deposits mapped by the AEM have many wells completed within it with SC on the order of 2 to 10 gallons per minute per foot (gpm/ft). While most of the ***Kd*** is saturated, the low yielding shales, siltstone, silts, and clays reduce the actual Specific Yield.

An estimated **T** map was developed for the ***Kd*** in the 2023 LBBNRD AEM survey area using the thickness of the sand dominant materials and hydraulic conductivities from published references (e.g., O'Connor (1987) and Gannon and Vogelgesang (2015)) in the area of eastern Nebraska and western Iowa. This map can be helpful, but needs to be used with caution due to the lack of local hydrogeological information on the ***Kd***.

2.5 Estimation of Aquifer Volume and Water in Storage in the LBBNRD AEM Survey Area - The values for the saturated Quaternary (***Q***) aquifer (based on the LBBNRD spring 2023 water table) and Cretaceous Dakota Group (***Kd***) aquifer volumes were calculated. Three-dimensional digital representation (3-D Voxel model) of the subsurface resulting from the AEM interpretation allowed the total saturated aquifer volume and the amount of extractable water to be estimated more accurately. An area of approximately 234 square miles (approximately 149,632 acres) of AEM data were collected in the LBBNRD 2023 AEM survey, and using estimates of porosity and specific yield from the published literature as well as the 3-D Voxel models, the total volume of groundwater in storage and the total volume of extractable groundwater within the saturated ***Q***, ***Kd***, and ***Q*** and ***Kd*** combined were calculated and are as follows:

- ***Q***
  - Total volume of saturated ***Q*** materials: **5,757,715** acre-ft (or approximately 33% of total ***Q*** material volume)
  - Estimated groundwater in storage: **1,559,226** acre-ft
  - Estimated extractable volume of groundwater: **826,072** acre-ft
- ***Kd***
  - Total volume of saturated ***Kd***: **6,010,404** acre-ft (or approximately 84% of total ***Kd*** volume)
  - Estimated groundwater in storage: **1,988,522** acre-ft
  - Estimated extractable volume of groundwater: **457,577** acre-ft
- ***Q*** and ***Kd*** combined
  - Total volume of saturated ***Q*** and ***Kd*** combined: **11,768,119** acre-ft (or approximately 48% of total ***Q*** and ***Kd*** combined volume)
  - Estimated groundwater in storage: **3,547,747** acre-ft
  - Estimated extractable volume of groundwater: **1,283,649** acre-ft

2.6 Groundwater Quality in the LBBNRD 2023 AEM Survey Area - The AEM provided information on the near-surface (unsaturated) materials in the 2023 LBBNRD AEM survey area. Near-surface occurrences of sandy soils and sand deposits (aquifer materials) may provide conduits for contaminants to migrate into the groundwater. Using the 3D interpretation of the AEM, a near-surface occurrence of the aquifer materials 2D grid was generated. A map depicting water quality (nitrate) data collected by the LBBNRD (*Personal Communication, Tyler Weishahn, January 2024*) overlying the near-surface occurrence of aquifer materials grid was made to visually determine if there is a correlation between the near-surface material type and water quality. While there is a very weak visual correlation of the nitrate concentrations within an area of near-surface sandy aquifer material along a portion of Sicily Creek, no other strong pattern exists. With the thick non- and marginal aquifer material in the survey area, it is unlikely that the nitrates are migrating through the clay-rich thicker till and loess deposits.
There is, however, a visual correlation of relatively high nitrate concentrations and the areas of the aquifer materials along the trend of the paleovalley aquifer (west-east).

2.7 Potential Recharge Zones within the LBBNRD 2023 AEM Survey Area - Using the AEM near-surface (unsaturated) 2D grid of the coarse and aquifer materials, a map was developed to assist in identifying and investigating areas where these materials could be used for recharge. Many of these areas are along the streams where the till and loess have been eroded away exposing the deeper coarse aquifer and aquifer material and may be considered windows into these deeper aquifer materials. On the eastern side of the survey area, many of the areas of coarse and aquifer materials that are depicted on the map are the isolated deposits of outwash in the upper portions of the till and may not have potential beneficial recharge impacts as they may not be connected to the deeper aquifer materials. The area along Sicily Creek is a good area to consider for recharge as it is underlain by the main paleovalley aquifer.
Utilizing the recharge target map to locate recharge areas can be done. However, it is imperative that accurate test holes, which may include sonic cores, are used to assess the geological materials. Any possible thin clay layers that were not detected with the AEM or may have been missed in the test hole drilling may be detected by calibrated borehole geophysical induction logs and natural gamma. Infiltration tests also need to be conducted to fully evaluate recharge rates. Additionally, determining the areas that are impacted by nitrates due to the configuration of the near-surface materials is critical because these same areas can also be targets for recharge due to the nature of the material type. The maps produced in this study can guide both management of nitrate control areas as well as allow implementation of recharge projects.

2.8 Using AEM Results to Implement Groundwater Management - All management plans can be improved as new information is gathered and considered for modifying the management practices. Much of this study was focused on the determination of the groundwater availability within the LBBNRD AEM survey area. Previous mapping was based on surficial exposures and limited test hole drilling coupled with monitoring well networks. While this provided some understanding of the hydrogeology, the AEM provides a much higher resolution of the aquifer configuration. The important findings that can have an impact on the management of the area are related to the estimated shape and configuration of the aquifers. Examples of these estimates are the transmissivity (**T**) maps that were made of both the ***Q*** and the ***Kd*** aquifers as part of this study. The hydraulic conductivity values used to estimate the ***Q*** transmissivity were based on the known material type (established with interpretation of the AEM) present within the survey area. The estimated transmissivity produced a **T** map that is in general agreement with the map produced by Summerside and Myers (2005). The AEM-produced **T** map provides a much higher resolution view of the area as compared with the previous mapping, but that is

expected and is the goal of this study. The hydraulic conductivity value used to estimate the transmissivity of the ***Kd*** aquifer was based on an average of two published values. The uncertainties in the hydrogeological parameters used in the ***Kd*** transmissivity estimates need to be acknowledged, but the map can serve as a starting point to the understanding of the area.

3. RECOMMENDATIONS

Recommendations provided to the LBBNRD in this section are based on the interpretation and understanding gained from the addition of the AEM data to existing information and from discussions with the LBBNRD about their management challenges.

3.1 Additional AEM Mapping - The aquifer maps provided in this report represent the detailed hydrogeologic framework developed for the LBBNRD 2023 AEM survey area. The AEM interpretations used to create the aquifer maps match well with the CSD and NE-DNR borehole lithologic, stratigraphic, and/or geophysical logs. It is recommended that additional areas be flown in the LBBNRD so that these aquifer maps may be broadened to cover a larger geographic extent. Additional survey flight lines can be of a reconnaissance nature to begin with but, later, closely spaced lines or "block flights" should be collected over project areas such as well fields, well head protection areas, and/or areas of detailed recharge projects to develop more detailed frameworks. The line spacing for the block flights should be on the order of 0.25 mile (1,320 ft). It is important to note that AEM data is not meant to replace existing data, such as borehole lithology or aquifer tests, but to provide a framework in which to place the existing hydrogeological data. Therefore, AEM mapping can assist with targeting areas where more expensive technologies including borehole drilling can be implemented, especially when a block flight is flown over an area.

Future AEM mapping projects could potentially be done in cooperation with the neighboring NRDs to get details on the continuous aquifer system that is shared in the area. The Little Blue NRD is a great example of an NRD the LBBNRD can partner with to share an AEM mapping project. A benefit for partnering with other NRDs is to have a combined comprehension of the estimates of groundwater storage capacity, which may be calculated by understanding the aquifer characteristics through AEM interpretation.

3.2 Siting new test holes and production wells - The AEM framework maps and profiles provided in this report give insight into the 3D relationship between current test holes and production groundwater wells and the material in which they are drilled into. At the time of this report, the current available lithology data for the LBBNRD area was used to help build the framework maps and profiles. It is recommended that the results from this report be used to site new test holes, monitoring wells, and/or water supply wells. Based on more data, the AEM framework maps and profiles provide detail in areas where the previously existing data may have been more regional in nature; this enables better decision-making when siting new wells.

The location of any future water supply wells can also use the results in this report to guide development of new water supply wells. Planners should locate wells in areas of greatest saturated thickness with the least potential for non-point source pollution.

3.3 Aquifer testing and borehole logging – Aquifer tests are recommended to improve estimates of aquifer characteristics. A robust aquifer characterization program is highly recommended at the state, regional (NRD's), and smaller municipal levels. Aquifer tests can be designed based on the results of AEM surveys and existing production wells.
Additional test holes with detailed, functional, and well calibrated geophysical logging for aquifer characteristics is highly recommended. The few test holes with calibrated geophysical logs in the LBBNRD survey area were inadequate. The borehole geophysical logs provided for this investigation demonstrate that additional calibrated and verified geophysical logs are required in the LBBNRD. Examples of additional logging would be borehole flow meter logs and geophysical logs including gamma, neutron, electrical, and induction logs. Detailed aquifer characteristics can be accomplished with nuclear magnetic resonance logging (NMR). This is a quick and effective way to characterize porosity and water content, estimates of permeability, mobile/bound water fraction, and pore-size distributions with depth. This is very cost effective when compared to traditional aquifer tests.

3.4 Groundwater Management: Control Areas, Recharge Areas - The hydrogeologic framework in this report provides the location and extent of high transmissive and saturated aquifers. Conversely, it also shows areas where high-capacity wells may be limited due to the aquifer characteristics. It is recommended that these areas be used to define the control areas based on empirical data of the AEM coupled with water quality and groundwater levels. The geospatial data products delivered with this report can be directly opened in ESRI's ArcGIS Pro and can be used to provide guidance in the establishment on control areas. These data can also be invaluable to the producers/developers within the area in replacing wells and drilling new wells. These data can be used by the LBBNRD in assessing the well permits of the area and assisting the interested parties to drill successful wells.
This study mapped areas that are windows to the deeper paleovalley aquifer. These areas may be considered for special recharge projects. These areas also may require additional protections to be added to avoid groundwater quality issues due to the direct conduit of the surface to the deeper aquifer systems. Any management decisions that would propose recharge would need to be weighed against current land use and recharge water availability.

4. DELIVERABLES

The following are included as deliverables:

- Raw Data Files - SkyTEM files *.gex, *skb, *.lin
- Raw EM Mag data as ASCII *.xyz
- SCI inversion as ASCII *.xyz in array column format
- Interpretations as ASCII *.xyz
- ESRI GIS files – raster grids (*.flt) and ESRI ArcGIS Pro map package (.mpkx).
- 2D profiles, Surfaces, and 3D fence diagrams of the AEM survey inversion results
- Files compatible with GeoScene3D and the Nebraska GeoCloud
- LBBNRD 2023 AEM 3D voxel files
- KMZs for LBBNRD AEM flight lines

Table of Contents

1 Introduction 1
1.1 Purpose of Current Project 1
2 Summary of the Geology and Hydrogeology of the Lower Big Blue Natural Resources District 5
2.1 Bedrock Geology 5
2.2 Hydrogeological Aspects Near the LBBNRD 7
3 Additional Background Information 19
3.1 Boreholes 19
4 Geophysical Methodology, Acquisition and Processing 21
4.1 Geophysical Methodology 21
4.2 Flight Planning/Utility Mapping 22
4.3 AEM Survey Instrumentation 23
4.4 Data Acquisition 25
4.4.1 Primary Field Compensation 31
4.4.2 Automatic Processing 31
4.4.3 Manual Processing and Laterally-Constrained Inversions 31
4.4.4 Power Line Noise Intensity (PLNI) 34
4.4.5 Magnetic Field Data 37
4.5 Spatially-Constrained Inversion 38
5 AEM Results and Interpretation 42
5.1 Interpretative Process 42
5.1.1 Merging AEM Flight Lines 42
5.1.2 Construction of the Project Digital Elevation Model 42
5.1.3 Borehole-Only Surface of the Bedrock 45
5.1.4 Interpretative 2D Profiles 46
5.1.5 Interpretative Surface Grids 54
5.1.6 Water Table 65
5.1.7 Transmissivity Maps 70
5.1.8 Specific Capacity Maps 73
5.1.9 Geologic Map Updates 73
5.1.10 3D Interpretative Voxel Grids 74
5.2 Comparison of AEM Inversion Resistivity to Borehole Geophysical Resistivity Logs 81

5.2.1 Resistivity Relationship in the Quaternary Aquifer System 84
5.2.2 Resistivity Relationship in the Cretaceous Dakota Group Aquifer System 85
5.3 Hydrogeological Framework of the LBBNRD 2023 AEM Survey Area 86
5.3.1 The Hydrogeology of the Quaternary 91
5.3.2 Hydrogeology of the Cretaceous Dakota Group 104
5.3.3 The Permian Bedrock Hydrology 115
5.3.4 Groundwater in LBBNRD 2023 AEM Survey Area 117
5.3.5 Estimation of Aquifer Volume/Water Storage for the 2023 LBBNRD AEM Survey Area 122
5.3.6 Groundwater Quality in the LBBNRD 2023 AEM Survey Area 127
5.3.7 Recharge in the LBBNRD 2023 AEM Survey Area 130
5.4 New Understanding of AEM Framework Applied to Water Management Efforts in in the LBBNRD 2023 AEM Survey Area 136
5.5 Key AEM Findings 137
5.5.1 Boreholes 137
5.5.2 Digitizing Interpreted Geological Contacts 137
5.5.3 Resistivity/Lithology Relationship 137
5.5.4 Hydrogeological Framework of the LBBNRD 2023 AEM Survey Area 138
5.5.5 Estimation of Aquifer Volume and Water in Storage in the LBBNRD AEM Survey Area 139
5.5.6 Groundwater Quality in the LBBNRD 2023 AEM Survey Area 139
5.5.7 Potential Recharge Zones within the LBBNRD 2023 AEM Survey Area 140
5.5.8 Using AEM Results to Implement Groundwater Management 140
5.6 Recommendations 141
5.6.1 Additional AEM Mapping 141
5.6.2 Siting new test holes and production wells 141
5.6.3 Aquifer testing and borehole logging 142
5.6.4 Groundwater Management: Control Areas, Recharge areas 142
6 Description of Data Delivered 143
6.1 Tables Describing Included Data Files 143
6.2 Description of Included Google Earth KMZ Data and Profiles 150
6.2.1 Included README for the LBBNRD 2023 Interpretation KMZ 150
7 References 155
Appendix 1. LBBNRD AEM Flight Line 2D Profiles and Surfaces A1-1

Appendix 2. LBBNRD 3D Images A2-1

Appendix 3. Data Deliverables

List of Figures

Figure 1-1. Natural resources district map showing the location of the Lower Big Blue Natural Resources District (LBBNRD) in southeastern Nebraska 3

Figure 1-2. Google Earth image of the LBBNRD 2023 AEM survey area including major roads 4

Figure 2-1. Nebraska bedrock geology map (Burchett and Pabian, 1992) 9

Figure 2-2. Upper-most bedrock geology units map of eastern Nebraska (from Divine and Sibray, 2017, originally Burchett, 1986) 10

Figure 2-3. Bedrock geology map of eastern Nebraska (from Burchett and Pabian, 1992) with 2023 AEM flight lines 11

Figure 2-4. Locations of wells in secondary aquifers relative to the High Plains aquifer 12

Figure 2-5. Areas of Nebraska underlain by paleovalley aquifers (modified from Korus et al. (2013)) 13

Figure 2-6. Areas of Nebraska underlain by glacial deposits (modified from Korus et al. (2013)) 14

Figure 2-7. Areas of Nebraska underlain by alluvial aquifers (modified from Korus et al. (2013)) 15

Figure 2-8. Average annual net recharge to groundwater based on data from 2000 to 2009 (modified from Szilagyi and Jozsa, 2012) 16

Figure 2-9. Elevation of the potentiometric surface in the paleovalley aquifers of eastern Nebraska (modified from Korus et al. (2013)) 17

Figure 2-10. Transmissivity of the primary aquifers of Nebraska, including the High Plains aquifer, alluvial aquifers, glacial aquifers, and paleovalley aquifers 18

Figure 3-1. NE-CSD and NE-DNR borehole logs used for quality control and interpretative purposes 20

Figure 4-1. Schematic of an airborne electromagnetic survey 21

Figure 4-2. A) Example of a dB/dt sounding curve. B) Corresponding inverted model values. C) Corresponding resistivity earth model. 22

Figure 4-3. SkyTEM304M frame, including instrumentation locations and X and Y axes. Distances are in meters. Instrumentation locations listed in Table 4-1. 24

Figure 4-4. Photo of the SkyTEM304M system in suspension beneath the helicopter 24

Figure 4-5. LBBNRD 2023 AEM flight lines grouped by acquisition date 26

Figure 4-6. LBBNRD 2023 AEM flight lines ground speed 27

Figure 4-7. LBBNRD 2023 AEM flight lines flight height above the ground surface 28

Figure 4-8. LBBNRD 2023 AEM flight lines pitch angle in the +/-X direction of travel 29

Figure 4-9. LBBNRD 2023 AEM flight lines Y roll angle perpendicular to the direction of travel 30

Figure 4-10. Example locations of electromagnetic coupling with pipelines or power lines. 32

Figure 4-11. A) Example of AEM data affected by electromagnetic coupling in the Aarhus Workbench editor. The top group of lines is the unedited data with the Low Moment on top and the High Moment on the bottom. The bottom group shows the same data after editing. 33

Figure 4-12. A) Example of Laterally-Constrained inversion results where AEM data affected by coupling with pipelines and power lines were not removed. B) Inversion results where AEM data affected by coupling were removed. 34

Figure 4-13. Power Line Noise Intensity (PLNI) map of the LBBNRD 2023 project area. 35

Figure 4-14. Locations of inverted data (blue lines) along the AEM flight lines (red lines) on the LBBNRD 2022 AEM survey area. 36

Figure 4-15. Residual magnetic Total Field intensity data for the LBBNRD 2023 AEM survey area corrected for diurnal drift, with the International Geomagnetic Reference Field (IGRF) removed 37

Figure 4-16. An example of an AEM profile illustrating increasing model layer thicknesses with depth. . 38

Figure 4-17. Data/model residual histogram for the LBBNRD 2023 SCI inversion results 40

Figure 4-18. Map of data inversion model residuals for the LBBNRD 2023 SCI inversion results 41

Figure 5-1. The flight lines and the connected merged lines for the 2023 LBBNRD AEM survey 43

Figure 5-2. Map of the Digital Elevation Model for the 2023 LBBNRD AEM Survey Area 44

Figure 5-3. Map of the project boundary showing the data points used to interpolate the bedrock surface elevation 49

Figure 5-4. 35-mile-long east-west line L500200 50

Figure 5-5. 29.5-mile-long east-west line L500500 51

Figure 5-6. 10-mile-long north south line L400801 52

Figure 5-7. 5-mile-long north south line L402801 53

Figure 5-8. Map of digitized bedrock outcrops overlaying map by Burchett et al. (1972) 56

Figure 5-9. Map displaying the elevation of the top of the Cretaceous Dakota (***Kd***) Group 57

Figure 5-10. Map displaying the elevation of the top of undifferentiated Permian units 58

Figure 5-11. Map displaying the elevation of the top of bedrock 59

Figure 5-12. Map displaying the depth to the top of Cretaceous Dakota (***Kd***) Group 60

Figure 5-13. Map displaying the depth to the top of undifferentiated Permian units 61

Figure 5-14. Map displaying the depth to the top of bedrock 62

Figure 5-15. Map of displaying the total thickness of the Quaternary (***Q***) material 63

Figure 5-16. Map displaying the total thickness of Cretaceous Dakota (***Kd***) Group..... 64

Figure 5-17. Map of water table elevation surface and the control points used to interpolate the surface 66

Figure 5-18. Map showing the elevation of the water table (ft bgs)..... 67

Figure 5-19. Map displaying the saturated thickness of Quaternary (***Q***) material..... 68

Figure 5-20. Map of displaying the saturated thickness of Cretaceous Dakota (***Kd***) Group 69

Figure 5-21. Map of the calculated transmissivities within the marginal, aquifer, and coarse aquifer materials of the ***Q*** deposits in the LBBNRD 2023 AEM survey area with an overlay of digitized contours from Summerside and Myers (2005)..... 71

Figure 5-22. Map of the calculated transmissivity within the marginal, aquifer, and coarse aquifer material of the **Q** deposits in the LBBNRD 2023 AEM survey area without the Summerside and Myers (2005) transmissivity contours 72

Figure 5-23. Map of the calculated transmissivities within the saturated ***Q*** deposits along with the specific capacity of the DNR wells designated as being completed within the ***Q*** deposits based on screen interval 75

Figure 5-24. Map of saturated ***Kd*** (over 18 ohm-m) along with the specific capacity of the DNR wells screened within the ***Kd*** 76

Figure 5-25. Map of saturated ***Kd*** (over 25 ohm) along with the specific capacity of the DNR wells screened within the ***Kd*** 77

Figure 5-26. Map of geologic units by Burchett (1986) with the refined extent of ***Kd*** shown in bright green 78

Figure 5-27. . Exploded 3D Voxel model of the stratigraphy of the LBBNRD 2023 AEM area showing unsaturated and saturated Quaternary (***Q***) and Cretaceous Dakota Group (***Kd***) material and undifferentiated Permian Chase and Council Grove Groups (***P***) 79

Figure 5-28. Interpreted depth to the top of the saline water interface 80

Figure 5-29. Graph of the four 16-inch normal resistivity log values and the inverted airborne electromagnetic average resistivity values within 2,800 feet 82

Figure 5-30. 10-mile-long north south line L400701 83

Figure 5-31. Plot displaying the resistivities by major Quaternary (***Q***) aquifer material color categories used in the LBBNRD 2023 AEM survey 84

Figure 5-32. Plot displaying the Cretaceous Dakota Group (***Kd***) resistivities by dominant material and the color categories used in the LBBNRD 2023 AEM survey..... 85

Figure 5-33. Bedrock map of the survey area modified from Burchett (1986) using the LBBNRD 2023 AEM survey results..... 87

Figure 5-34. 3D Fence diagram looking to the north of the interpreted distributions of aquifer material within the LBBNRD 2023 AEM survey area 88

Figure 5-35. 3D Fence Diagram looking to the northwest of the interpreted distributions of aquifer material within the LBBNRD 2023 AEM survey area 89

Figure 5-36. 3D exploded voxel model looking north of the LBBNRD 2023 AEM survey area showing ***Q*** (Quaternary) and ***Kd*** (Cretaceous Dakota Group) unsaturated and saturated, and the undifferentiated Permian Groups ***(P)*** 90

Figure 5-37. Map of the Quaternary (***Q***) total thickness within the LBBNRD 2023 AEM survey area 93

Figure 5-38. Map of the Quaternary (***Q***) total thickness of the coarse and aquifer materials within the LBBNRD 2023 AEM survey area 94

Figure 5-39. 3D Voxel diagram looking to the northwest of the interpreted distributions of total aquifer and coarse aquifer material of the Quaternary (***Q***) within the LBBNRD 2023 AEM survey area. 95

Figure 5-40. 3D Voxel diagram looking to the northwest of the interpreted distributions of the total non- and marginal-aquifer materials of the Quaternary (***Q***) within the LBBNRD 2023 AEM survey area 96

Figure 5-41. North-south AEM flight line L401701 97

Figure 5-42. East-west AEM flight line L500401 98

Figure 5-43. Map of the total saturated Quaternary (***Q***) thickness within the LBBNRD 2023 AEM survey area calculated using the Spring 2023 LBBNRD water levels 99

Figure 5-44. Map of the Quaternary (***Q***) aquifer and coarse aquifer material saturated thickness within the LBBNRD 2023 AEM survey area calculated using the Spring 2023 LBBNRD water levels 100

Figure 5-45. Map of the saturated Quaternary (***Q***) marginal aquifer materials, and saturated non-aquifer material thickness within the LBBNRD 2023 AEM survey area calculated using the Spring 2023 LBBNRD water levels 101

Figure 5-46. Map of the estimated transmissivity (gpf/feet) of the Quaternary (***Q***) marginal aquifer materials, aquifer materials, and coarse aquifer materials within the LBBNRD 2023 AEM survey area . 102

Figure 5-47. Map of the estimated transmissivity (gpf/feet) of the Quaternary (***Q***) marginal aquifer materials, aquifer materials, and coarse aquifer material transmissivity within the LBBNRD 2023 AEM survey area. Overlain with the transmissivity contours from Summerside and Myers (2005) 103

Figure 5-48. Map of the undifferentiated Permian (***P***) bedrock surface elevation 106

Figure 5-49. 3D Voxel diagram looking to the north of the interpreted Cretaceous Dakota Group (***Kd***) distributions of cemented sand and sand dominant as well as sand and silt dominant material > 18 ohm-m within the LBBNRD 2023 AEM survey area 107

Figure 5-50. 3D Voxel diagram looking to the north of the interpreted Cretaceous Dakota Group (***Kd***) distributions of cemented sand and sand dominant material > 25 ohm-m within the LBBNRD 2023 AEM survey area 108

Figure 5-51. North-south AEM flight line L400801 109

Figure 5-52. Map of the total Cretaceous Dakota Group (***Kd***) total thickness within the LBBNRD 2023 AEM survey area 110

Figure 5-53. Map of the Cretaceous Dakota Group (***Kd***) total saturated thickness within the LBBNRD 2023 AEM survey area 111

Figure 5-54. Map of the Cretaceous Dakota Group (***Kd***) total saturated thickness of the sandstone and sand-dominant materials within the LBBNRD 2023 AEM survey area with resistivities >25 ohm-m 112

Figure 5-55. Map of the estimated transmissivity (gpf/feet) of the Cretaceous Dakota Group (***Kd***) saturated thickness of the sandstone and sand dominant materials with resistivities > 25 ohm-m within the LBBNRD 2023 AEM survey area 113

Figure 5-56. Map of the estimated transmissivity (gpf/feet) of the Cretaceous Dakota Group (***Kd***) saturated thickness of the sandstone and sand dominant as well as the sand/silt dominant materials > 18 ohm-m within the LBBNRD 2023 AEM survey area 114

Figure 5-57. Map of the depth to the interpreted saline water surface within the undifferentiated Permian (***P***) units over the LBBNRD 2023 AEM survey area 116

Figure 5-58. Map of the estimated Transmissivity (**T**) (gpd/ft) of the Quaternary (***Q***) coarse, aquifer, and marginal aquifer materials with the Specific Capacity (SC) of the NE-DNR registered wells completed within the ***Q*** 118

Figure 5-59. Map of the estimated Transmissivity (**T**) (gpd/ft) of the Cretaceous Dakota Group (***Kd***) with resistivities > 18 ohm-m cemented sand and sand dominant as well as the sand/silt dominant aquifer materials with the Specific Capacity (SC) of the NE-DNR registered wells completed within the *Kd* 119

Figure 5-60. Map of the saturated Quaternary (***Q***) coarse, aquifer, and marginal aquifer materials plus the saturated Cretaceous Dakota Group (***Kd***) with resistivities >25 ohm-m cemented sand and sand dominant material with the Specific Capacity (SC) of the NE-DNR registered wells completed within the ***Q*** and ***Kd*** 120

Figure 5-61. 3D voxel model of the saturated Quaternary (***Q***) coarse and aquifer materials plus the saturated Cretaceous Dakota Group (***Kd***) with resistivities > 25 ohm-m cemented sand and sand dominant material with the Specific Capacity (SC) of the all NE-DNR registered wells completed within the area 121

Figure 5-62. Map of the Non- and Marginal Aquifer material within the unsaturated portion of the Quaternary (***Q***) potentially creating a confined aquifer beneath 126

Figure 5-63. Map of the thickness of the unsaturated coarse and aquifer material and the LBBNRD nitrates samples 128

Figure 5-64. Map of the thickness of the unsaturated non- and marginal aquifer material and the LBBNRD nitrates samples 129

Figure 5-65. Map of the thickness of the unsaturated coarse and aquifer material that is in the near surface that may provide recharge pathway to lower aquifers 131

Figure 5-66. East-west AEM flight line L500500 132

Figure 5-67. East-west AEM flight line L500401 133

Figure 5-68. North-south AEM flight line L401901 134

Figure 5-69. Map of the potential recharge locations based on the presence of coarse and aquifer materials in the near surface with connections to the deeper aquifers 135

Figure 6-1. Google Earth KMZ of the LBBNRD 2023 AEM survey area showing the AEM Interpretation locations. 152

Figure 6-2. Example of clicking on a location in the LBBNRD 2023 AEM survey area 153

Figure 6-3. Example of clicking on link to Profile image for line line L401401 in the LBBNRD 2023 Interpretation KMZ 154

List of Tables

Table 2-1. Percent coverage of the uppermost bedrock geological units in the Nebraska counties where the Lower Big Blue NRD is located 6

Table 2-2. Ranges of porosity and hydraulic conductivity for different materials (from Divine et al., 2009; adapted from Dominico and Schwartz, 1998) 8

Table 2-3. Ranges of intrinsic permeabilities and hydraulic conductivities for unconsolidated sediments (from Table 4-6, Fetter, 1988) 8

Table 4-1. Positions of instruments on the SkyTEM304M frame, using the center of the frame as the origin, in feet 25

Table 4-2. Positions of corners of the SkyTEM304M transmitter coil, using the center of the frame as the origin in feet 25

Table 4-3. Thickness and depth to bottom for each layer in the Spatially Constrained inversion (SCI) AEM earth models. The thickness of the model layers increase with depth as the resolution of the AEM technique decreases 39

Table 5-1. LBBNRD 2023 AEM lines merged 42

Table 5-2. Number of data points used to interpolate the elevation of the top of *Kd* and *Permian* surfaces 54

Table 5-3. Summary of the input into ESRI's raster calculator and the resultant output 55

Table 5-4. Summary of Hydraulic Conductivities, **K**, used to calculate transmissivities 70

Table 5-5. Volumes for Saturated Cretaceous Dakota Group (***Kd***) aquifer materials underlying the LBBNRD 2023 AEM survey area 125

Table 5-6. Volumes for Saturated Cretaceous Dakota Group (***Kd***) aquifer materials underlying the LBBNRD 2023 AEM survey area 125

Table 6-1. Raw SkyTEM data files.....144

Table 6-2. Channel name, description, and units for LBBNRD2023_EM_MAG_AUX.xyz with DEM, magnetic, DGPS, Inclinometer, altitude, and associated data.....144

Table 6-3. Channel name, description, and units for LBBNRD2023_AEM_SCI02_INV_v1.xyz with EM inversion results.....145

Table 6-4. Channel name description and units for the interpretation results file LBBNRD2023_InterpSurfaces.xyz 146

Table 6-5. Files containing LBBNRD 2023 raster datasets (.flt format)..... 147

Table 6-6. Relevant features and extents as LBBNRD 2023 ESRI Shapefiles 148

Table 6-7. Nebraska Geocloud-import file: LBBNRD2023_SCI02_InvResults_GeoCloud_v1.xyz 149

Table 6-8. Columns in LBBNRD 2023 AEM 3D Voxel files LBBNR23_Rho_Voxel_ALL, _Kd, _Q.....149

List of Abbreviations

2D	Two-dimensional
3D	Three-dimensional
A*m^2	Ampere meter squared
AEM	Airborne Electromagnetic
AGF	Aqua Geo Frameworks, LLC
AM	Aquifer Material
ASR	Aquifer Storage and Recovery
b	Saturated thickness
dB/dt	Change in amplitude of magnetic field with time
CA	Coarse Aquifer Material
CSD	Nebraska Conservation and Survey Division
DEM	Digital Elevation Model
DOI	Depth of Investigation
DGPS	Differential global positioning system
em, EM	Electromagnetic
FEM	Frequency-Domain Electromagnetic
FT	Fourier Transform
FT, ft	Feet
ft^3	cubic feet
Fm	Formation
GIS	Geographic Information System
gpm	Gallons per minute

Hr, hr	hours
Hz	Hertz (cycles per second)
IGRF	International Geomagnetic Reference Field
K	Hydraulic Conductivity
Kd	Cretaceous Dakota Group
Kgg	Cretaceous Greenhorn Limestone and Graneros Shale
Km, km	Kilometers
KMZ, kmz	Keyhole Markup language Zipped file
LCI	Laterally-constrained Inversions
LBBNRD	Lower Big Blue Natural Resources District
M, m	Meters
MAG	Magnetic (data); Magnetometer (instrument)
MCG	Minimum curvature gridding
mg/L	milligram per liter or parts per million (ppm)
mi^2	Miles squared
NAD83	North American Datum of 1983
MAR	Managed Aquifer Recharge
NAVD88	North American Vertical Datum of 1988
NE	Nebraska
NED	National Elevation Dataset
NE-DNR	Nebraska Department of Natural Resources
NMR	Nuclear Magnetic Resonance
NRD	Natural Resources Districts
OM	Geosoft Oasis montaj
Pc	Permian Chase Formation
Pcg	Permian Council Grove Formation
PFC	Primary Field Compensation
PLNI	Power Line Noise Intensity
Q	Quaternary
Rx	Receiver
recon	Reconnaissance
sec	second
SC	Specific Capacity
SCI	Spatially-Constrained Inversion
SPCS	State Plane Coordinate System
STD	Standard Deviation
T	Transmissivity
TEM	Transient, Time-Domain Electromagnetic
TDEM	Time-Domain Electromagnetic
Tx	Transmitter
UNL	University of Nebraska Lincoln
USGS	United States Geological Survey
UTM	Universal Transverse Mercator
VE	Vertical Exaggeration
V/m^2	Volts per meter squared
X, x	The x-direction in a cartesian coordinate system
Y, y	The y-direction in a cartesian coordinate system
Z, z	The z-direction (positive is up) in a cartesian coordinate system

1 Introduction

1.1 Purpose of Current Project

Sound management of groundwater and surface water in eastern Nebraska has become increasingly important in recent years. There are expanding pressures placed on the resources by the ever growing and dynamic demands of: agricultural production, population growth and urbanization, potential contamination from natural and anthropogenic sources, industrial and commercial needs; along with the persistent threat of drought. The discussion below is largely taken from the 2022 LBBNRD Water Sustainability Fund application that funded the 2023 AEM survey.

The Lower Big Blue NRD Airborne Electromagnetic Hydrogeologic Mapping (LBBNRD-AEM1) project is the District's latest and most comprehensive approach to understanding the character and vulnerability of its aquifer formations for use in establishing a hydrogeologic framework and assessing groundwater quantity and quality, particularly in areas of groundwater depletion and/or contamination, increased development and conflicts between groundwater users. More specifically, the aquifer formations of the LBBNRD are multiple and varied, including juxtaposition of Paleovalley and Maha (Dakota) aquifers in the east, northeast, south and southwest, as well as the High Plains aquifer in the west and northwest. This creates challenges in managing groundwater resources.

Historical groundwater quantity and quality monitoring in the District seem to bear out the relationships between subsurface composition, recharge and contamination (i.e., coarse sediments/thin unsaturated zones = higher recharge/more contamination vulnerability, fine-grained sediments/thick unsaturated zones = lower recharge/less contamination vulnerability) in single locations, but the extent of these potential impacts is not well understood. While the NRD's objective is to ultimately conduct AEM studies throughout the District, thereby providing a completely robust framework, funding and feasibility dictate a progressive and phased approach. This project aims to apply a more scientifically based approach to delineating those aquifer formations and the extent of any potential groundwater impacts in one of the District's most challenging areas. While limited, test holes have been the best available method for assessing aquifer characteristics until the recent improvement of AEM which essentially provides thousands of virtual test holes along the flight path, thereby collecting a nearly seamless cross-section of the aquifer materials. The AEM survey method can remotely cover large areas of the subsurface in a short amount of time and with detail. This type of seamless cross-section cannot be collected through any other known method in the same amount of time for AEM data acquisition.

Within the 235-square mile area proposed for this effort, the primary groundwater concerns revolve around quantity and recharge. The aquifer formations in the project area lend themselves more to quantity and recharge concerns than to contaminant concerns. The process of identifying and evaluating water availability using both traditional and state of the art techniques is critical to Nebraska's water planning activities and ensuring the sustainability and protection of Nebraska's water supply. AEM aids the NRD in more clearly assessing groundwater declines and their impacts, as well as delineating any potential Phase II Ground Water Quantity Management Areas (GWQMA). While LBBNRD rules dictate increased monitoring of established individually drilled boreholes to assess subsurface materials, the

remote sensing technique of AEM has the capability of collecting thousands of virtual boreholes at a fraction of the cost of traditional drilling and monitoring. AEM is quintessential to better understanding the aquifer connections and spatial extent, determining the extent of impacts, aiding in conflict resolution between groundwater users and ultimately managing groundwater resources. Combining AEM with existing studies and monitoring will result in a robust hydrogeologic framework from which to operate and will provide the best available information available to the LBBNRD.

Mapping results produced from the AEM data for this project have provided three-dimensional subsurface views of the aquifer materials and estimates of the extents and volumes of the ground water resources available (See Section 5 and *Appendix 2 – 3D Images*).

This project mapped a flight block across the Project Area in Jefferson and Gage counties, covering approximately 429 miles of AEM survey to develop a three-dimensional view of the subsurface. The project consisted of flight line planning within the block area, collection of AEM data along the flight lines, processing of the raw AEM data, interpretation of the processed data (tied to local geologic interpretations from traditional subsurface mapping), and reporting of the overall results. The AEM survey results have been incorporated into a Geographic Information System (GIS) (ESRI's ArcGIS Pro) for use by LBBNRD. The interpretations and GIS will be provided to Nebraska GeoCloud for public use, the CSD, and the NE-DNR at the time of this final report delivery.

District geologists will have the opportunity to evaluate the AEM survey results with cross-section and ancillary data to make interpretations of the regional geologic setting types encountered and evaluate how well the AEM results match up relative to the cross-sectional data. The resulting map publication and results will provide those interested in the hydrogeology of southeast Nebraska a comprehensive and improved understanding of the varying hydrogeological settings. That interpretation will likely follow the approach used for previous Eastern Nebraska Water Resources Assessment (ENWRA) areas. The LBBNRD will have groundwater aquifer delineations and associated maps to address groundwater quality problems occurring in this block and to help mitigate potential quantity concerns in the area.

A location map showing the LBBNRD is presented in Figure 1-1 and a flight line map is presented in Figure 1-2 and in *Appendix 3 – Deliverables\KMZ\FlightLines*.

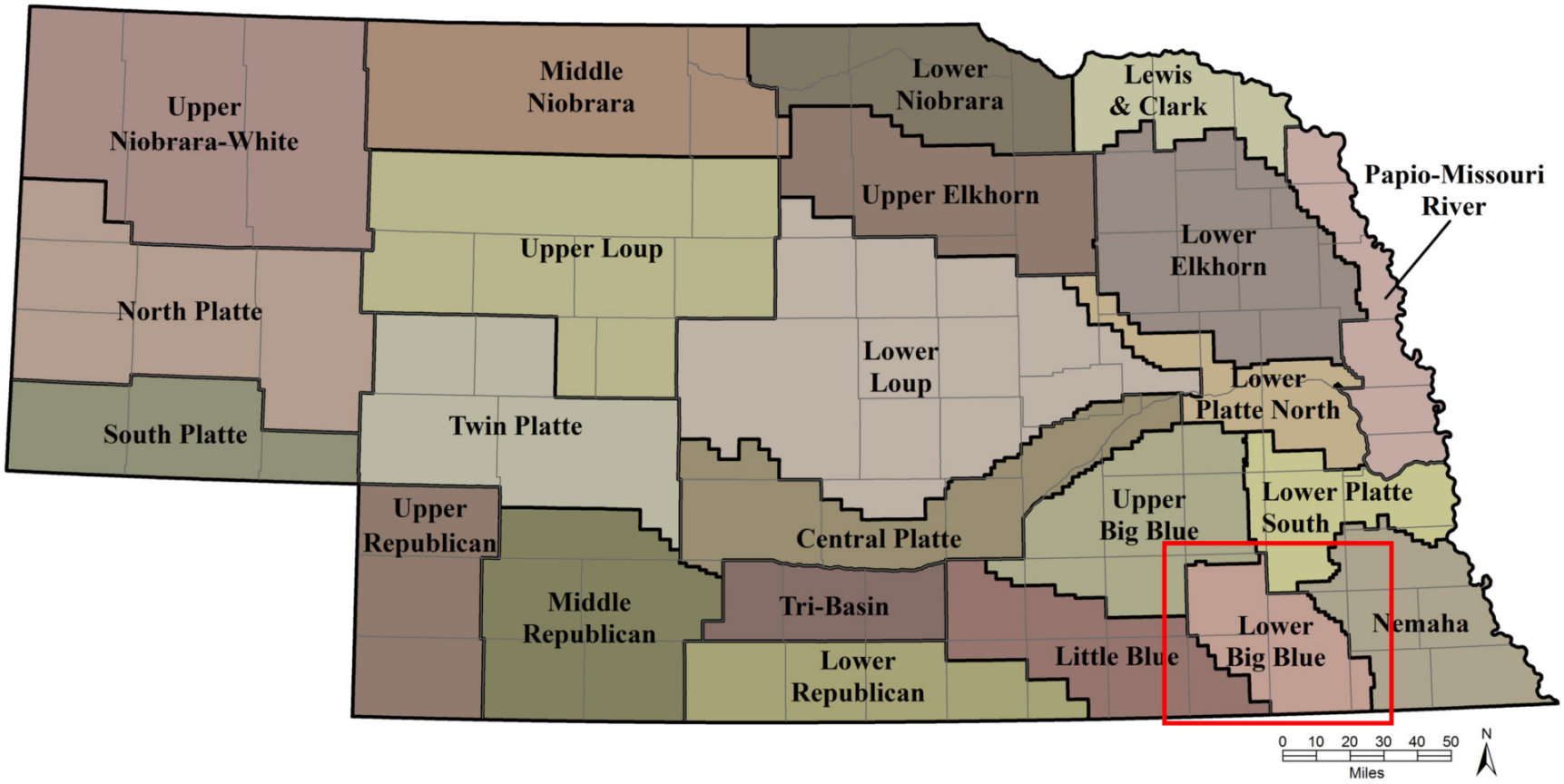


Figure 1-1. Natural resources district map showing the location of the Lower Big Blue Natural Resources District (LBBNRD) in southeastern Nebraska (https://www.lbbnrd.net/) in the red box.

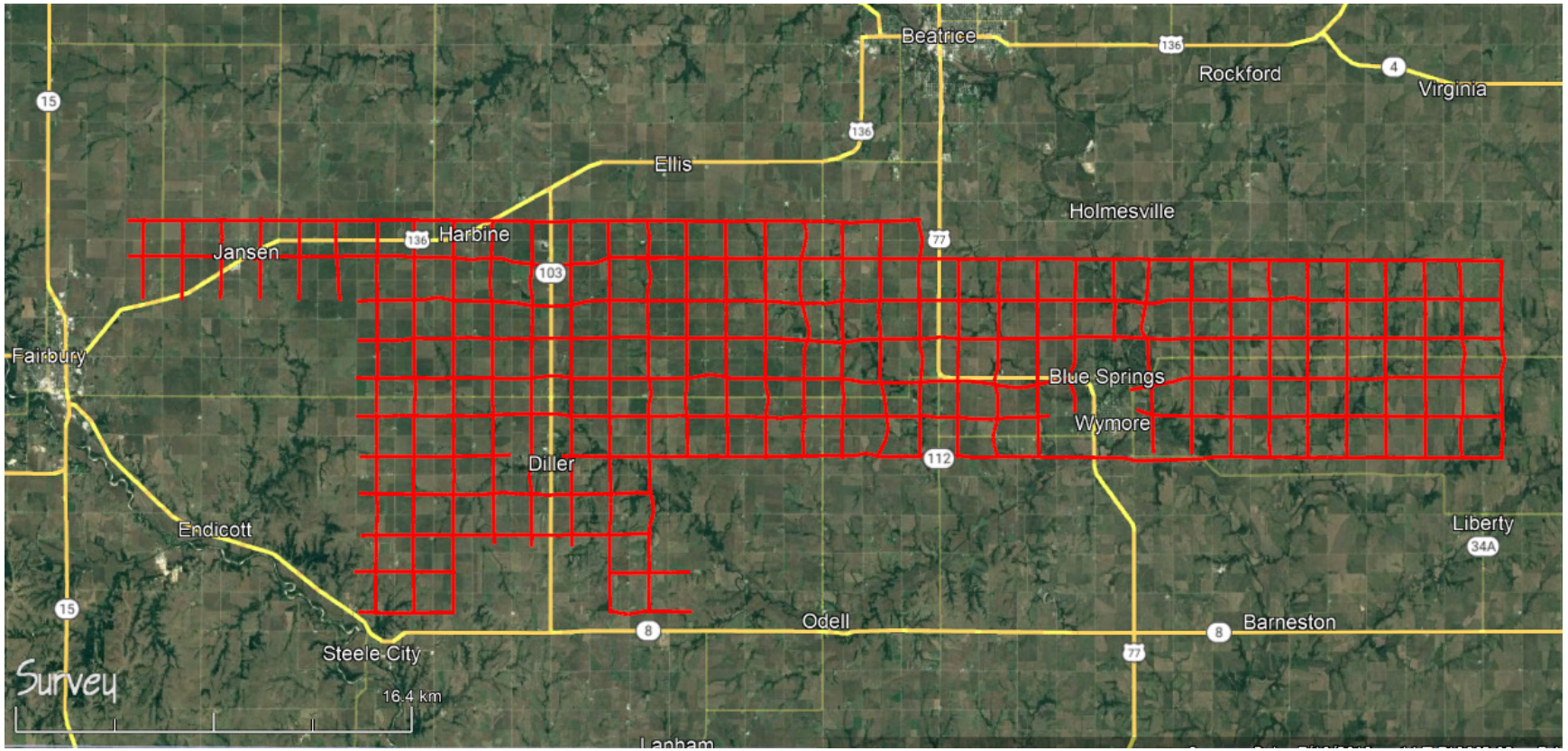


Figure 1-2. Google Earth image of the LBBNRD 2023 AEM survey area including major roads.

2 Summary of the Geology and Hydrogeology of the Lower Big Blue Natural Resources District

2.1 Bedrock Geology

The bedrock geology of southeastern Nebraska consists of several, well known, Late-Pennsylvanian to Late-Cretaceous units that have been discussed in many USGS, Nebraska Conservation and Survey Division, and Nebraska Department of Natural Resources reports including Reed (1959), Burchett and Reed (1967), Burchett (1986), Burchett and Pabian (1992), Stoeser et al. (2005), Divine et al. (2009), Korus et al. (2013), Divine and Sibray (2017), Joeckel et al. (2018), and Joeckel et al. (2019).

The geological formation descriptions below are from the USGS "MrData" website (USGS MrData, 2023). The bedrock geologic units in the counties in which the Lower Big Blue Natural Resources District is located, including Saline, Jefferson, Gage, and Pawnee counties, are:

Carlile Shale (Late Cretaceous) - Shale, limestone, and sandstone. At top, locally 5 feet of gray to pale-yellowish brown siltstone or very fine-grained sandstone. Upper 200 feet of shale is dark gray to medium gray; locally contains ironstone concretions, and interbedded with thin siltstone. Lower 80 feet of shale is medium gray, calcareous, and contains many very thin bedded, fossiliferous, shaly limestone and calcareous shale layers. Approximate maximum thickness of 300 ft.

Greenhorn Limestone and Graneros Shale (Late Cretaceous) - Greenhorn Limestone- medium- to light-gray limestone interbedded with argillaceous limestone, marl, and calcareous shale; contains Inoceramus fossils. Upper and lower contacts gradational. Approximate maximum thickness of 30 ft. Graneros Shale- medium- to dark-gray, partly calcareous shale. Interbeds of siltstone, sandstone, and carbonaceous shale, and thin bentonite layers in upper part. Approximate maximum thickness of 60 ft.

Dakota Group (Early Cretaceous) - Upper part is white, light-gray, brownish-gray, yellow, reddish-brown, and red sandstone and shale. Sandstone is very fine to coarse grained, friable, micaceous, cross-bedded, and lenticular; locally contains gravel near base. contains numerous zones of ironstone and siltstone concretions of variable thickness. Middle part is light-gray, yellow, red brown and dark-gray, sandy carbonaceous shale; commonly contains a zone of concretions near top. Lower part is sandstone similar to that in the upper part except there are zones of siderite concretions and, locally, a basal zone of chert pebbles. Approximate maximum thickness of 600 ft.

Chase Group (Permian) - Limestone and shale. Limestone is light gray to dark gray, yellowish gray to pale yellowish brown. Two limestones in the upper part are thin bedded to medium bedded, argillaceous, cherty and fossiliferous. Two limestones in the lower part of the Chase Group are medium to massive bedded, very cherty, and fossiliferous. Shale is gray, green, red, reddish brown, calcareous, arenaceous, fossiliferous, and, locally, fissile. Approximate maximum thickness of 300 ft.

Council Grove Group (Permian) - Shale and interbedded limestone. Shale is gray, green, red, reddish brown, or maroon, sandy, calcareous, fossiliferous, locally fissile; several fissile black shale beds are in the lower 75 feet. Interbedded dark- to light-gray, medium- to thick-bedded, argillaceous, cherty

limestone beds are very fossiliferous and locally contain shale partings. Approximate maximum thickness of 300 ft.

Admire Group (Permian) - Shale and interbedded limestone. Shale is dark gray to light gray, brown, red, or green, sandy, calcareous, and fossiliferous. The Admire Group is interbedded dark- to light-gray, very thin to medium bedded, argillaceous, very fossiliferous limestone beds. Near top of the Admire Group is a fine-grained, micaceous sandstone bed that underlies a stromatolite limestone bed which has distinctive lobate bedding. Approximate maximum thickness of 150 ft.

Wabaunsee Group (Late Pennsylvanian - Virgilian) - Shale, sandstone, and interbedded limestone. Shale is light gray to dark gray, greenish gray, red, or blacks that contains very thin layers of siltstone and is, locally, very fossiliferous and carbonaceous. The sandstone is brownish gray to yellowish gray, or gray, argillaceous, and micaceous. The limestone is dark gray to medium gray, yellowish gray, thin bedded to thick bedded; very fossiliferous. The Wabaunsee Group contains coal beds less than 1 ft. thick. The Wabaunsee Group has an approximate maximum thickness of 300 ft.

Shawnee Group (Late Pennsylvanian - Virgilian) - Limestone, shale, and siltstone. Limestone is dark gray to very light gray, yellowish gray, very thin bedded to massive bedded, and fossiliferous. Locally, thin beds are argillaceous and other beds are oolitic and a few contain chert. The shale is medium gray, greenish gray, pale red, dark reddish brown, black, sandy fossiliferous and calcareous. Black shale is, in part, fissile. Siltstone is light gray to greenish yellow, massive, calcareous, and, locally, sandy. The Shawnee Group has an approximate maximum thickness of 200 ft.

A bedrock geology map of all of Nebraska from Burchett and Pabian (1992) is presented in Figure 2-1. The bedrock geology of just eastern Nebraska is presented in Figure 2-2 and a zoom-in on the bedrock geology of the LBBNRD area along with the 2023 AEM flight lines is presented in Figure 2-3. Table 2-1 presents the percentage of surface area for the different geologic units in the counties in which the LBBNRD is located.

Table 2-1. Percent coverage of the uppermost bedrock geological units in the Nebraska counties where the Lower Big Blue NRD is located (modified from USGS MrData, 2023).

Unit name	Age	Saline (% at surface)	Jefferson (% at surface)	Gage (% at surface)	Pawnee (% at surface)
Carlile Shale	Late Cretaceous	7.6	0.5	-	-
Greenhorn Limestone and Graneros Shale	Late Cretaceous	28.5	10.6	-	-
Dakota Group	Early Cretaceous	63.8	88.2	21.0	-
Chase Group	Permian	-	0.3	48.7	10.0
Council Grove Group	Permian	< 0.1	0.6	26.6	36.4
Admire Group	Permian	-	-	3.7	10.7
Wabaunsee Group	Late Pennsylvanian - Virgilian	-	-	-	42.1
Shawnee Group	Late Pennsylvanian - Virgilian	-	-	-	0.8

2.2 Hydrogeological Aspects Near the LBBNRD

This section presents images of hydrogeological features in Nebraska that have relevance to the hydrogeological framework in the LBBNRD. Figure 2-4 presents the spatial distribution of the High Plains Aquifer and shows that the northwest half of the LBBNRD includes access to the High Plains Aquifer (modified from Divine and Sibray, 2017). Figure 2-5 presents areas of Nebraska, particularly in southeastern Nebraska, that are underlain by paleovalley aquifers and that the LBBNRD has several areas with paleovalley aquifers, including the area over which the 2023 AEM survey was conducted (Korus et al., 2013). Figure 2-6 shows areas of eastern Nebraska that are underlain by glacial deposits and Figure 2-7 shows areas of Nebraska that are underlain by alluvial aquifers including the LBBNRD (Korus et al., 2013).

A map of the average annual net recharge to groundwater in Nebraska (Korus et al., 2013), based on data from 2000 to 2009 (modified from Szilagyi and Jozsa, 2012), is presented in Figure 2-8. The map in Figure 2-8 shows that the LBBNRD has a positive net recharge from 2000 to 2009.

A map of the elevation of the potentiometric surface in the paleovalley aquifers of eastern Nebraska is presented in Figure 2-9 (Korus et al., 2013). In the LBBNRD, the potentiometric surface has an elevation of about 1300 ft to 1400 ft.

A map of the transmissivity of the primary aquifers of Nebraska including the High Plains aquifer, alluvial aquifers, glacial aquifers, and paleovalley aquifers is presented in Figure 2-10 (Korus et al., 2013). The map in Figure 2-10 shows that the paleovalley aquifers in the LBBNRD have moderate to good transmissivity.

Table 2-2 lists different materials and their measured porosity and hydraulic conductivity (**K**) per Dominico and Schwartz (1998). Note that Transmissivity (**T**) (L^2/T) = Hydraulic Conductivity (L/T) x Aquifer Thickness (L) (i.e., **T = K*b**).

Table 2-3 presents another set of permeabilities and hydraulic conductivities from Fetter (1988) that were utilized to developed the transmissivities used in the 2023 LBBNRD AEM interpretation.

Table 2-2. Ranges of porosity and hydraulic conductivity for different materials (from Divine et al., 2009; adapted from Dominico and Schwartz, 1998)

	Material porosity (%)	Hydraulic conductivity (ft/day)	Hydraulic conductivity (m/s)
Gravel	25 to 40	85 to 8,500	$3x10^{-4}$ to 0.03
Coarse sand	30 to 45	0.2 to 1,700	$9x10^{-7}$ to $6x10^{-3}$
Fine sand	25 to 50	0.06 to 60	$2x10^{-7}$ to $2x10^{-4}$
Sandstone	5 to 30	$9x10^{-5}$ to 1.7	$3x10^{-10}$ to $6x10^{-6}$
Silt, loess	35 to 60	$3x10^{-4}$ to 6	$1x10^{-9}$ to $2x10^{-5}$
Till	25 to 40	$3x10^{-7}$ to 0.6	$1x10^{-12}$ to $2x10^{-6}$
Clay	35 to 60	$3x10^{-6}$ to $1x10^{-3}$	$1x10^{-11}$ to $5x10^{-9}$
Shale	0 to 10	$3x10^{-8}$ to $6x10^{-4}$	$1x10^{-13}$ to $2x10^{-9}$

Table 2-3. Ranges of intrinsic permeabilities and hydraulic conductivities for unconsolidated sediments (from Table 4-6, Fetter, 1988).

Material	Intrinsic Permeability (darcys)	Hydraulic Conductivity (cm/s)
Clay	10^{-6} - 10^{-3}	10^{-9} - 10^{-6}
Silt,sandy silts, clayey sands, till	10^{-3} - 10^{-1}	10^{-6} - 10^{-4}
Silty sands, fine sands	10^{-3} - 1	10^{-5} - 10^{-3}
Well-sorted sands, glacial outwash	1 - 10^{2}	10^{-3} - 10^{-1}
Well-sorted gravel	10 - 10^{3}	10^{-3} - 10^{0}

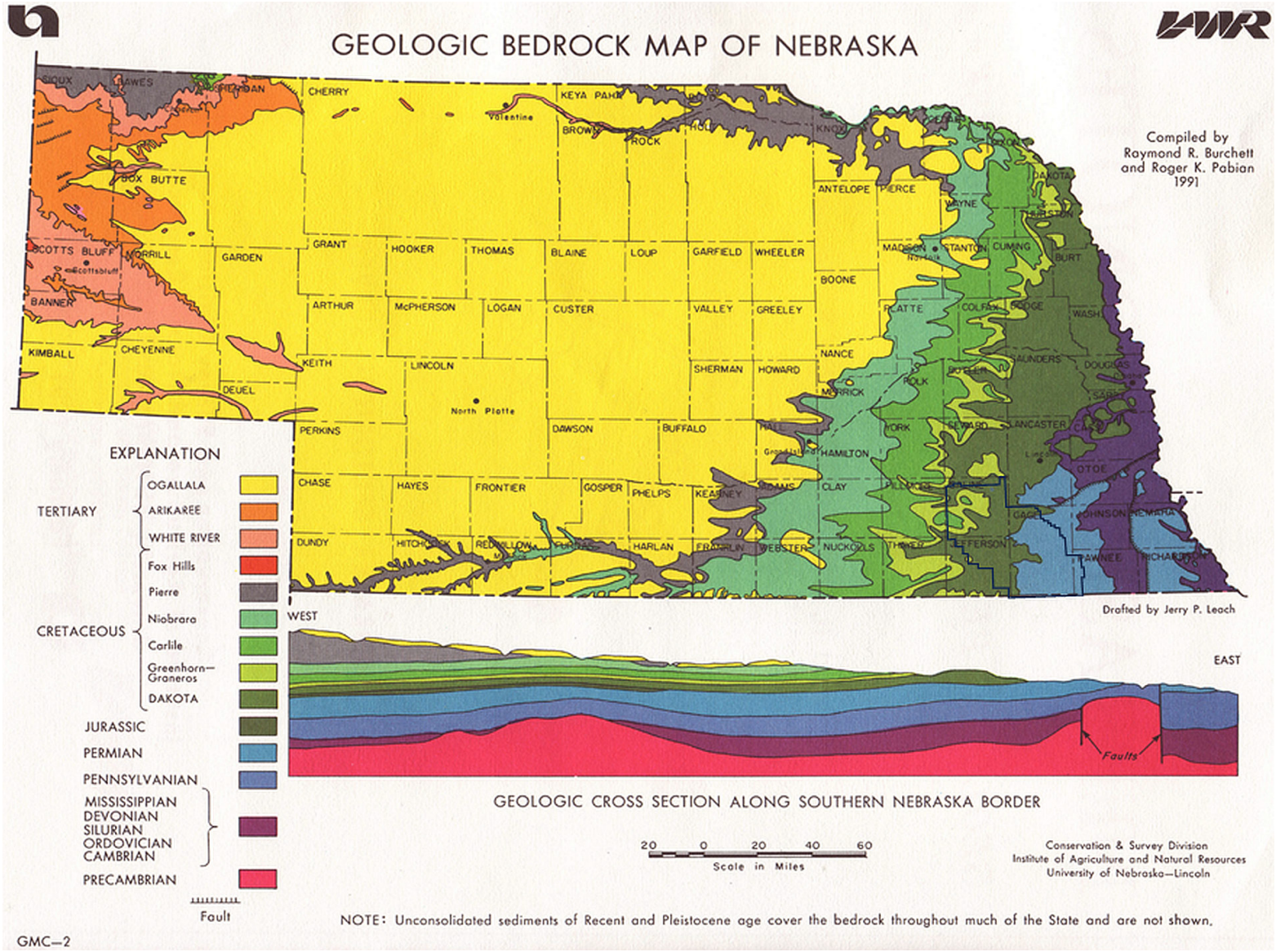


Figure 2-1. Nebraska bedrock geology map (Burchett and Pabian, 1992). Black polygon in southeast corner is the approximate location of the Lower Big Blue Natural Resources District.

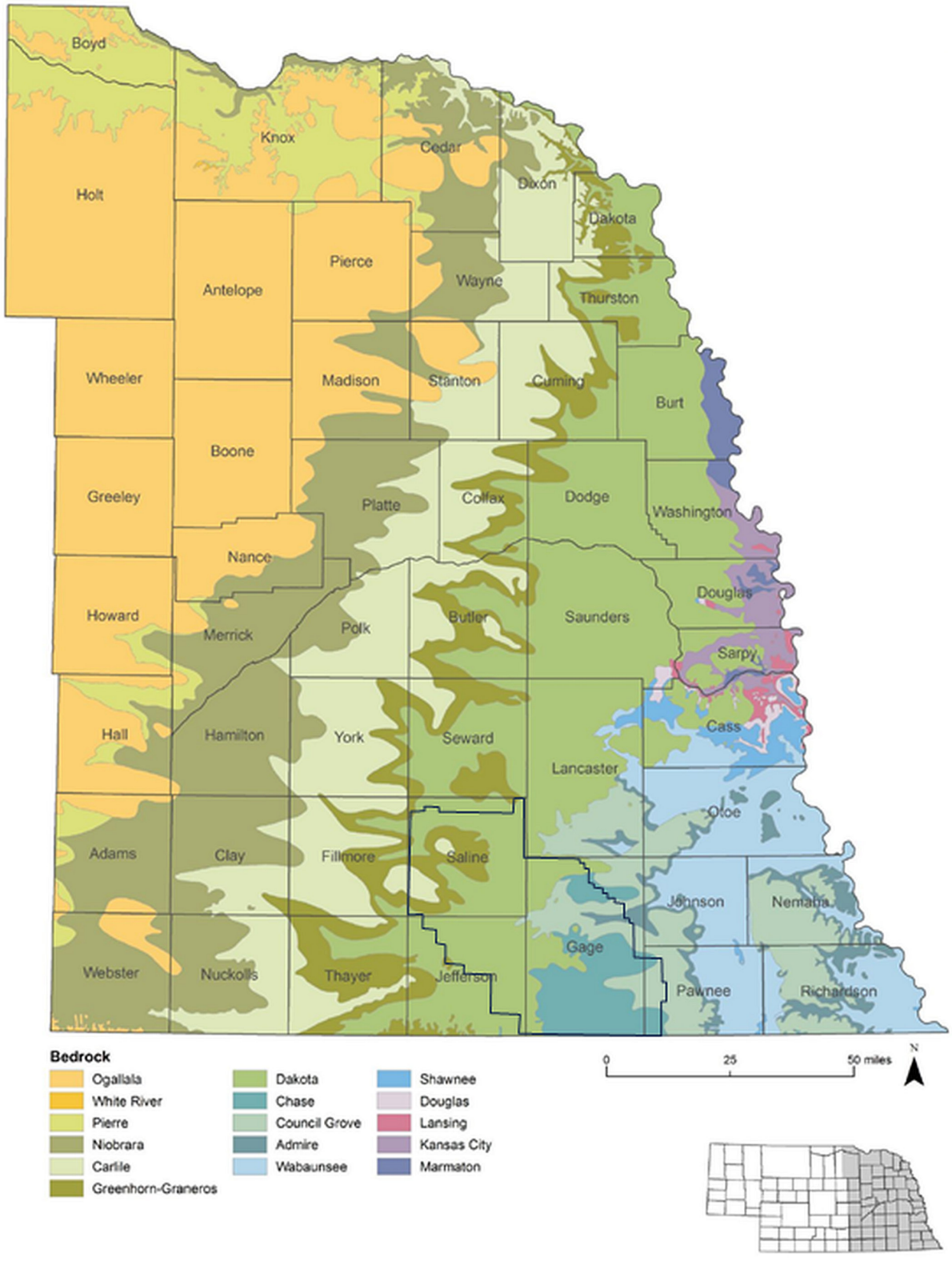


Figure 2-2. Upper-most bedrock geology units map of eastern Nebraska (from Divine and Sibray, 2017, originally Burchett, 1986). Black polygon in southeast corner is the approximate location of the Lower Big Blue Natural Resources District.

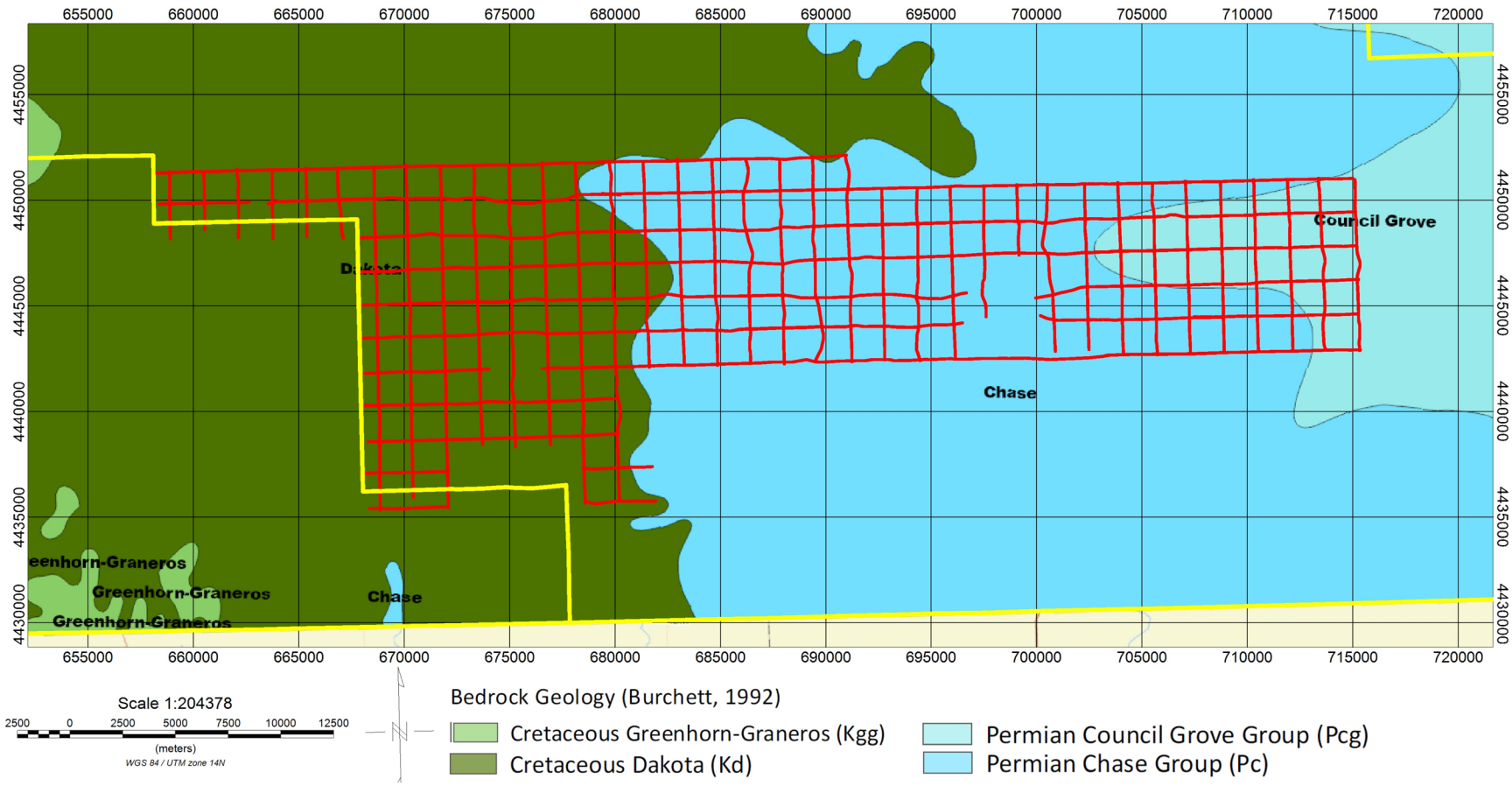


Figure 2-3. Bedrock geology map of eastern Nebraska (from Burchett and Pabian, 1992) with 2023 AEM flight lines (red lines). Map projection is WGS84, UTM14N, meters.

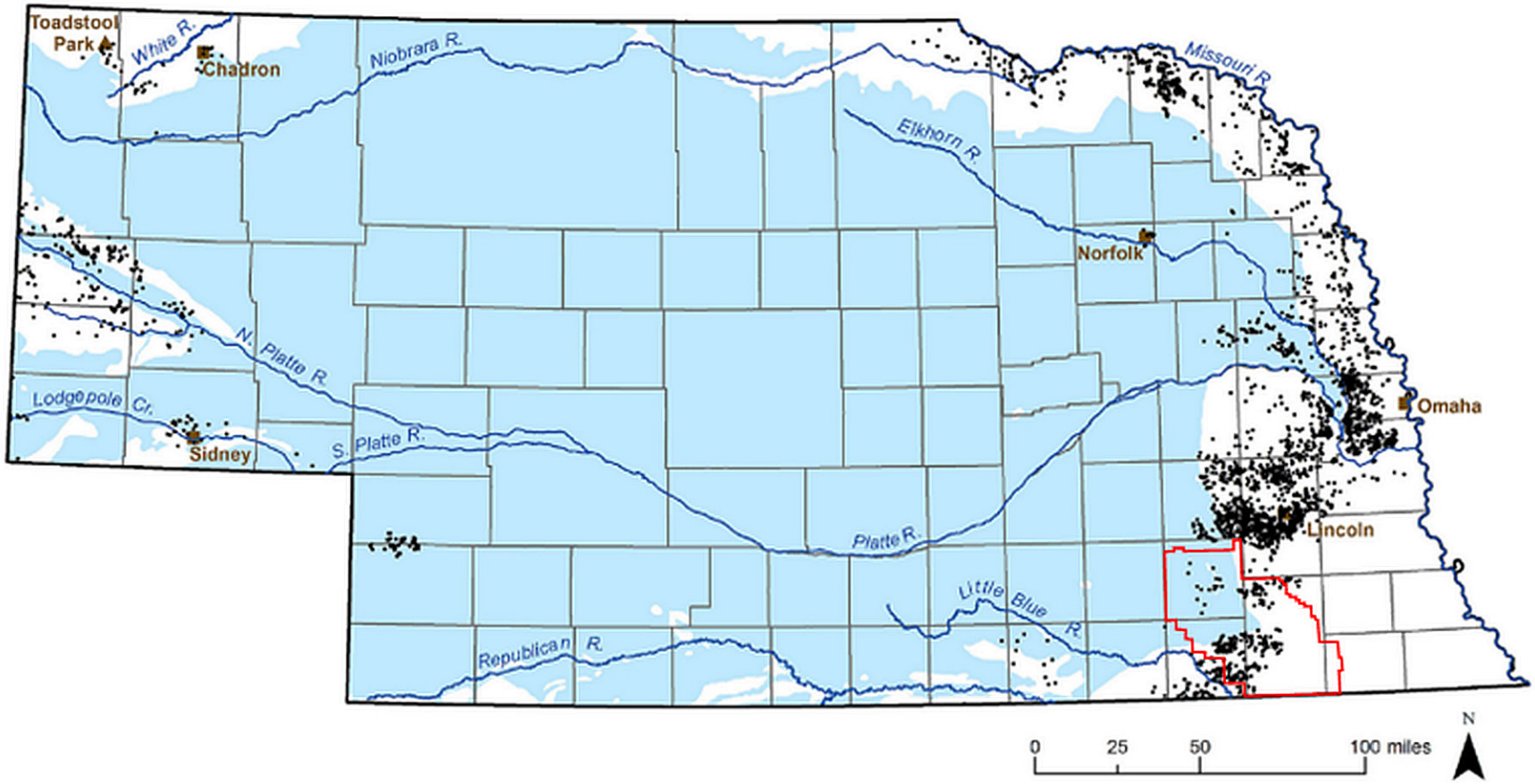


Figure 2-4. Locations of wells in secondary aquifers (black dots) relative to the High Plains aquifer (shown in blue). The approximate position of the Lower Big Blue Natural Resources District is indicated with the red polygon. Modified from Divine and Sibray (2017). The red polygon is the approximate location of the Lower Big Blue Natural Resources District.

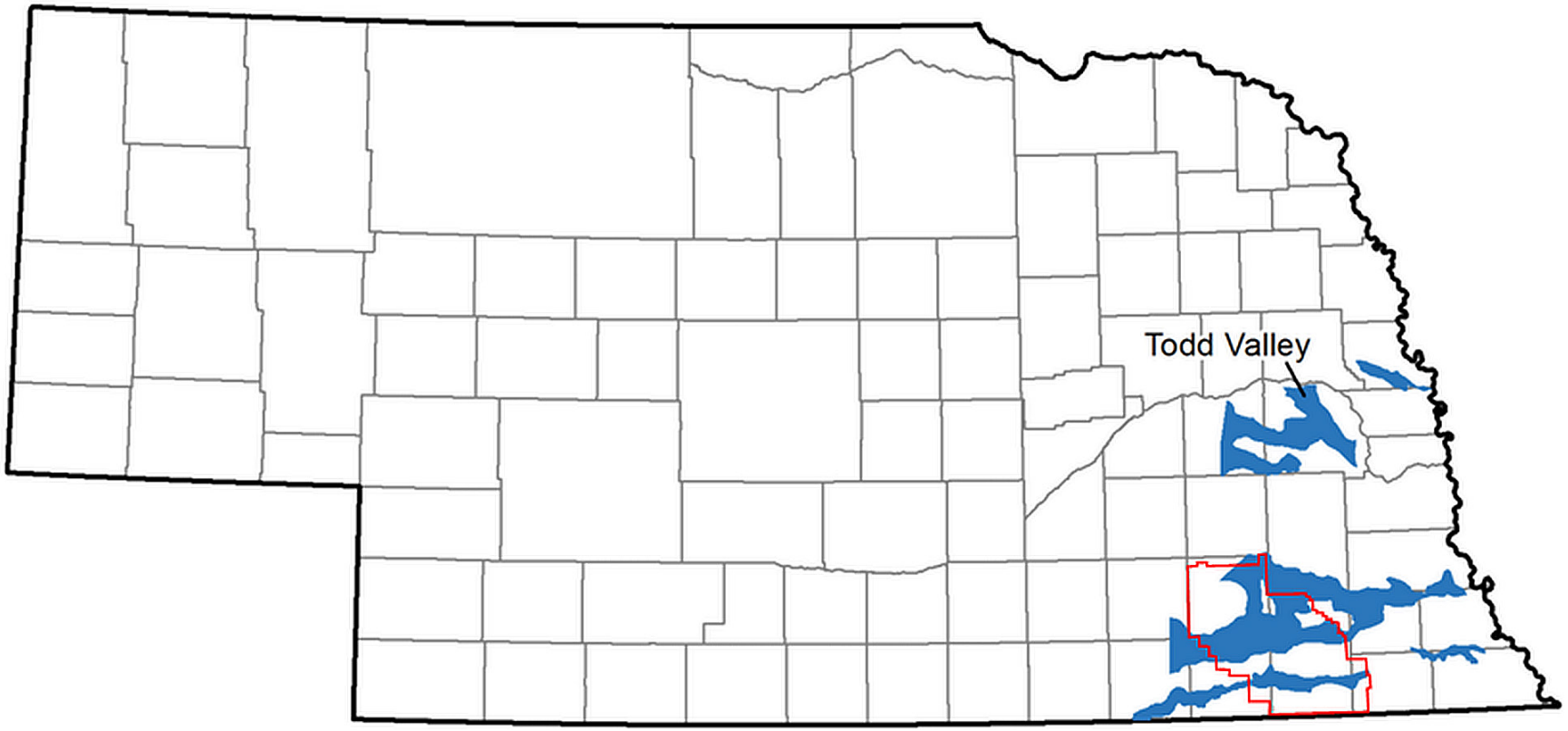


Figure 2-5. Areas of Nebraska underlain by paleovalley aquifers (modified from Korus et al. (2013)). The red polygon is the approximate location of the Lower Big Blue Natural Resources District.

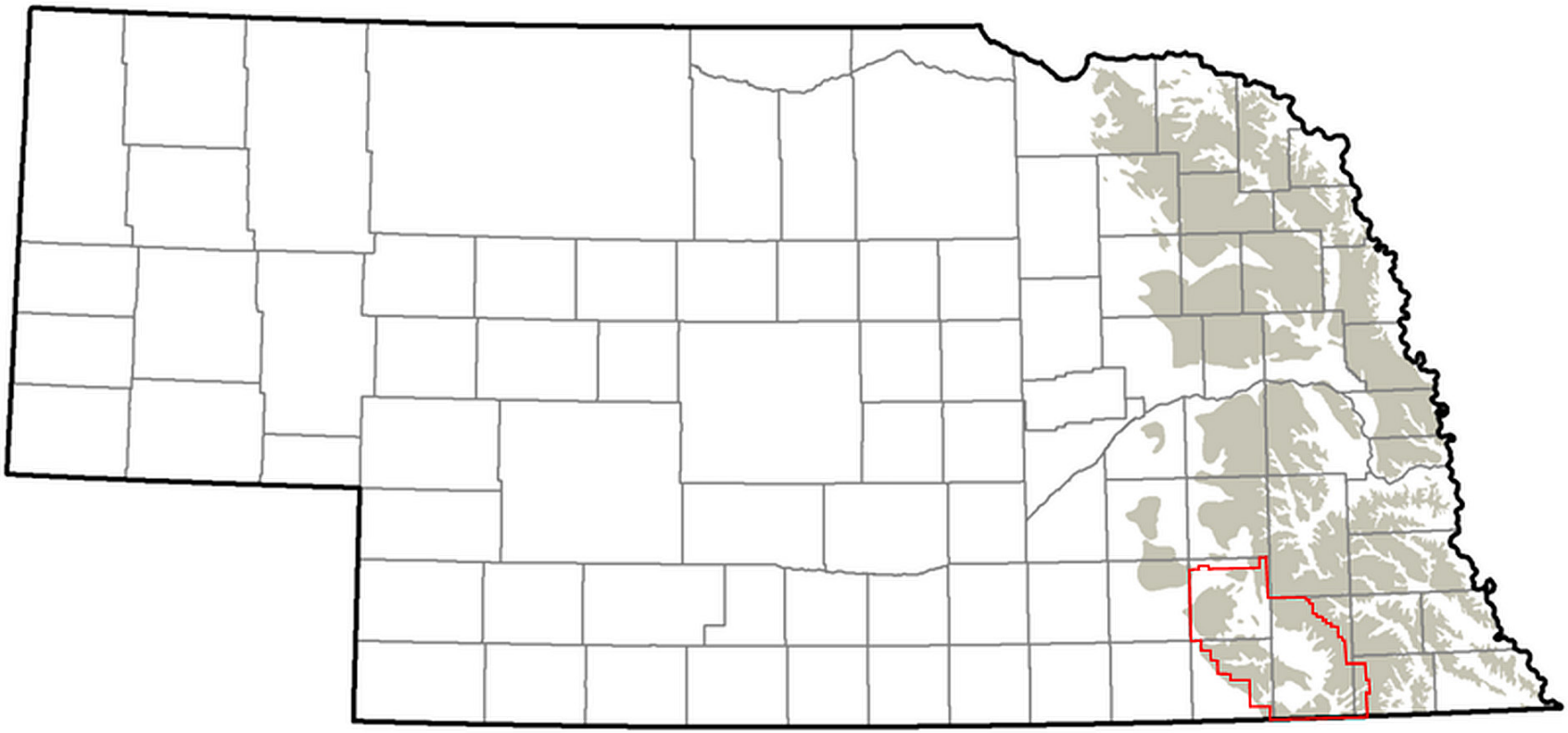


Figure 2-6. Areas of Nebraska underlain by glacial deposits (modified from Korus et al. (2013)). The red polygon is the approximate location of the Lower Big Blue Natural Resources District. Localized aquifers are contained within these deposits.

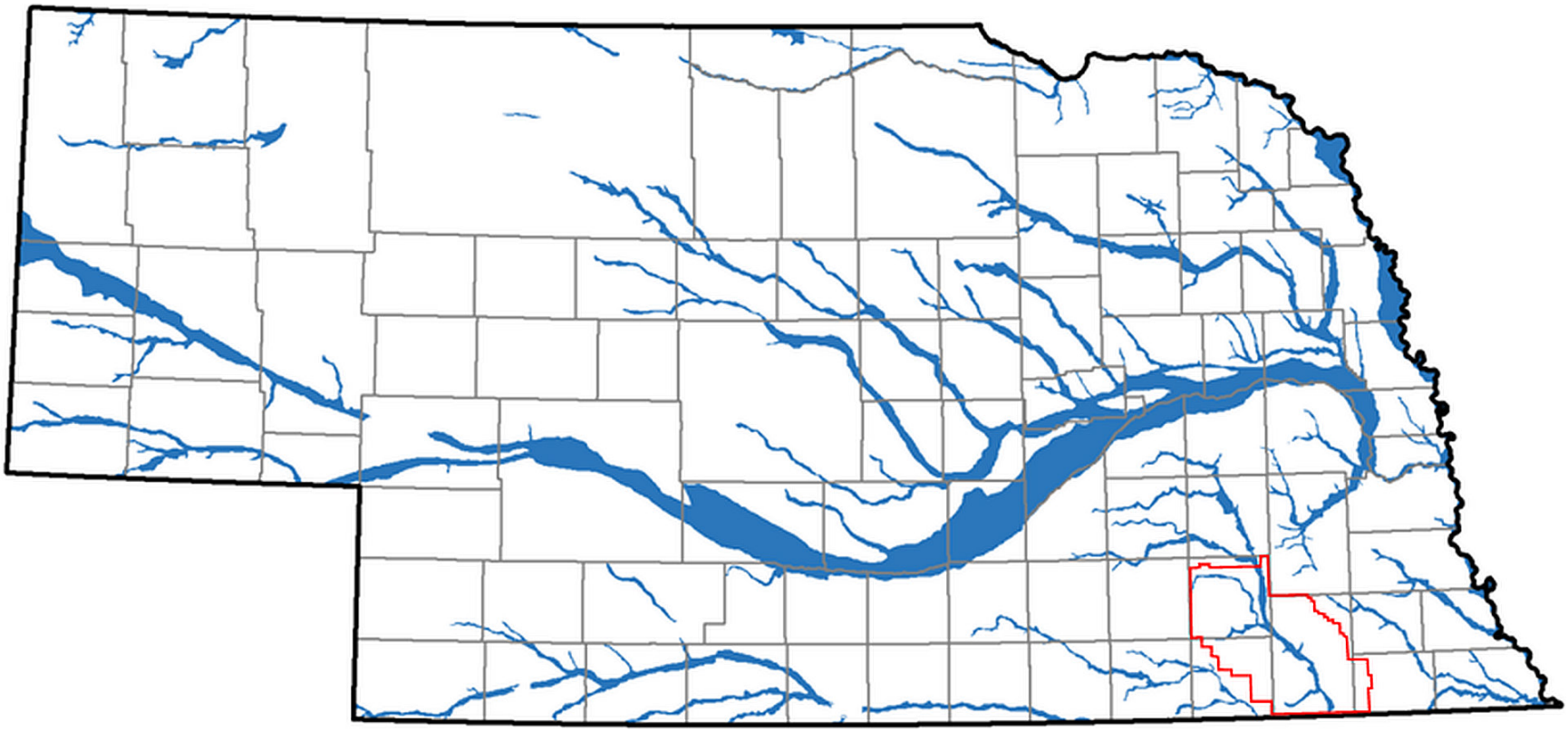


Figure 2-7. Areas of Nebraska underlain by alluvial aquifers (modified from Korus et al. (2013)). The red polygon is the approximate location of the Lower Big Blue Natural Resources District.

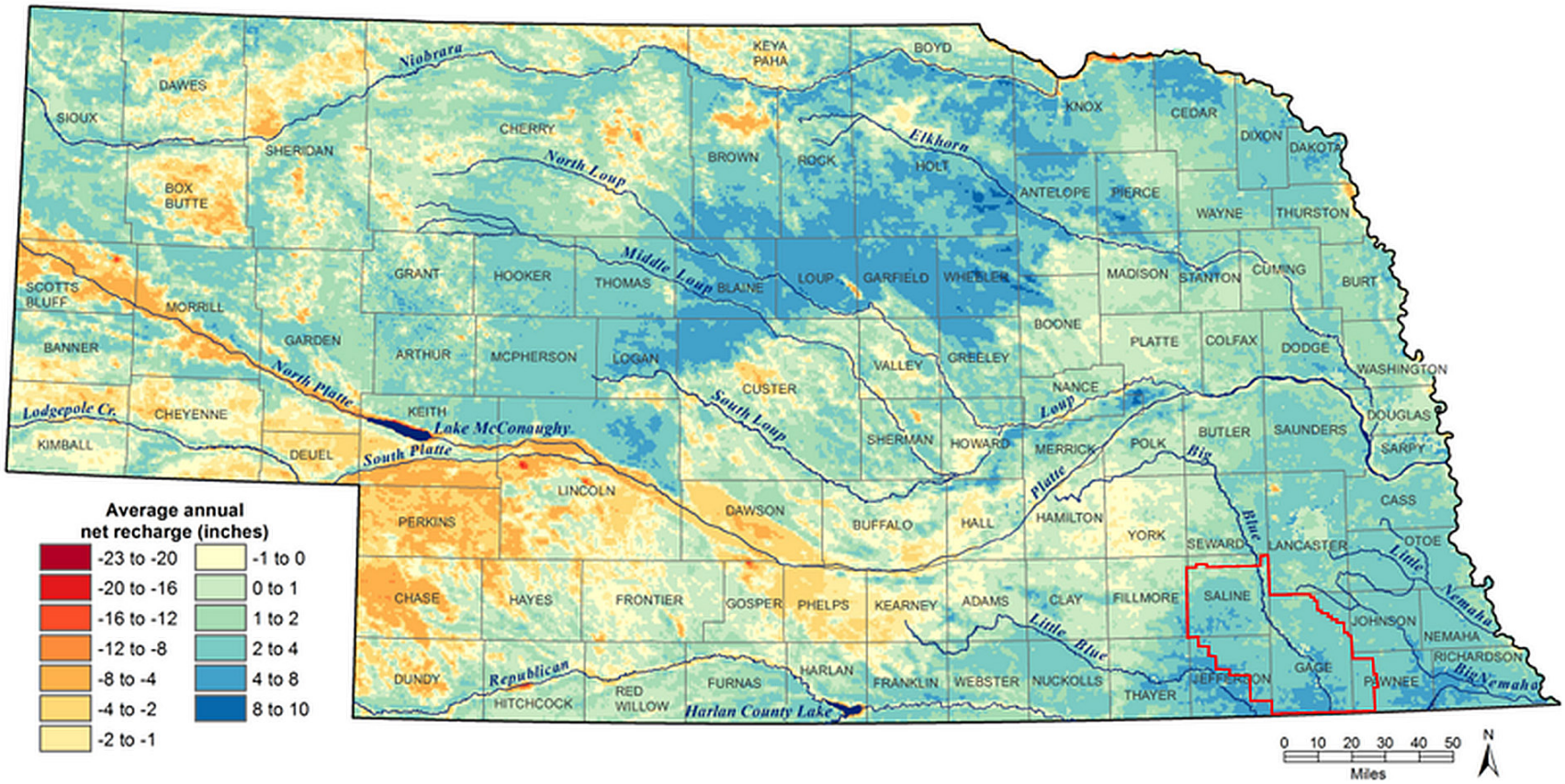


Figure 2-8. Average annual net recharge to groundwater based on data from 2000 to 2009 (modified from Szilagyi and Jozsa, 2012). Negative values indicate that evapotranspiration is greater than precipitation (modified from Korus et al. (2013)). The red polygon is the approximate location of the Lower Big Blue Natural Resources District.

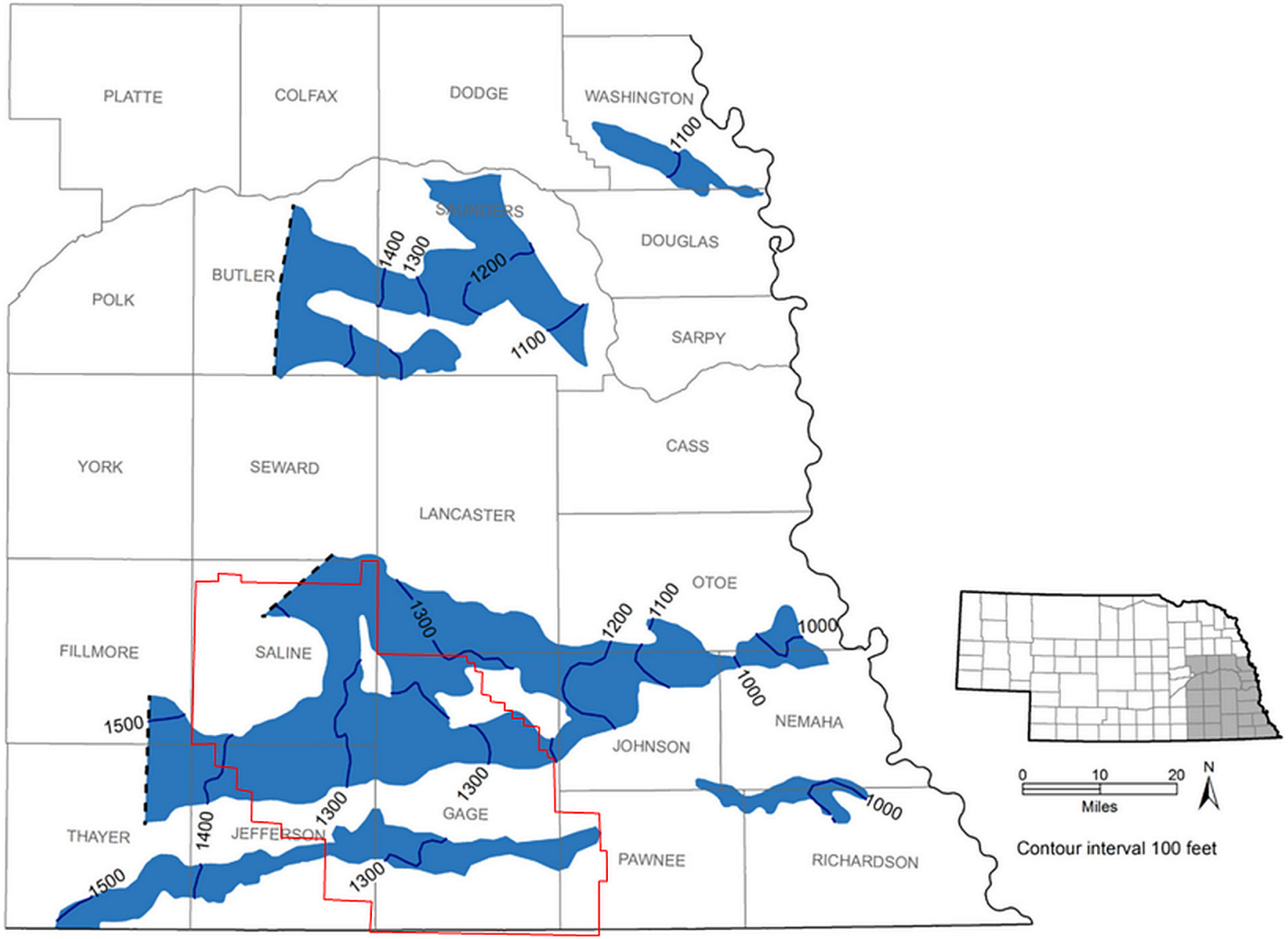


Figure 2-9. Elevation of the potentiometric surface in the paleovalley aquifers of eastern Nebraska (modified from Korus et al. (2013)). The red polygon is the approximate location of the Lower Big Blue Natural Resources District.

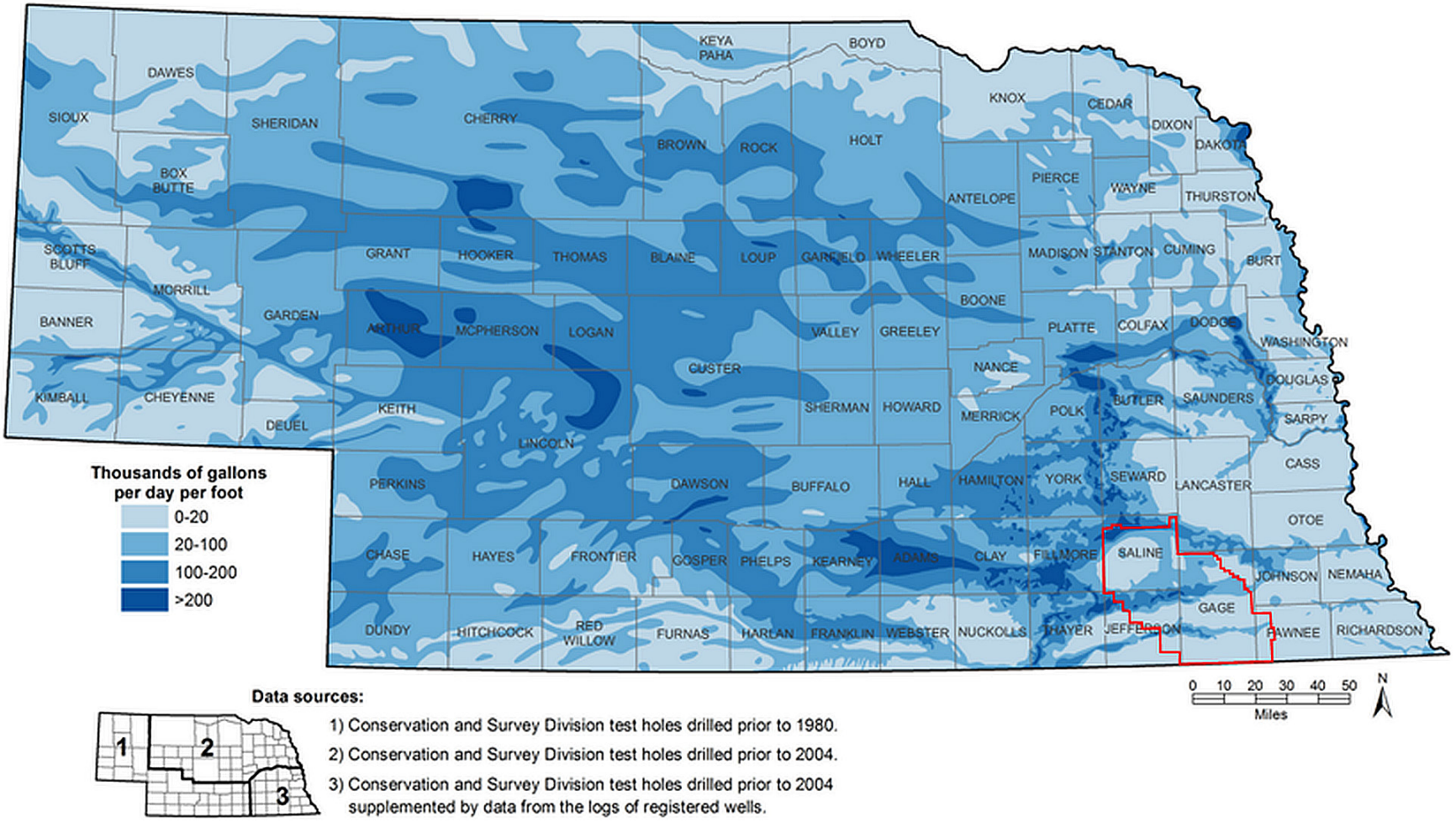


Figure 2-10. Transmissivity of the primary aquifers of Nebraska, including the High Plains aquifer, alluvial aquifers, glacial aquifers, and paleovalley aquifers. Sources of data vary by area, shown in inset map: 1) modified from an unpublished CSD map, 2) modified from Summerside et al. (2005), and 3) modified from Summerside et al. (2005), in which test hole data were supplemented by data from the logs of registered wells (modified from Korus et al. (2013)). The red polygon is the approximate location of the Lower Big Blue Natural Resources District.

3 Additional Background Information

3.1 Boreholes

Borehole data for this project consisted of a combination of lithologic, stratigraphic, and downhole geophysical logs (Figure 3-1). The borehole information was gathered from two sources: 1) CSD Nebraska Statewide Test Hole Database (UNL, 2023), including 29 wells within and adjacent to the project boundary with information from boreholes (lithology and stratigraphy) drilled between 1930 and 2022 by the CSD and other cooperating agencies; and 2) NE-DNR registered wells database, including 715 wells within and adjacent to the project boundary (Nebraska Department of Natural Resources, 2023). Four (4) of the CSD wells in the LBBNRD 2023 AEM survey area had geophysical logs.

The boreholes used in this study can be found as ESRI shapefiles in the *Appendix 3 – Deliverables\ESRI Products*.

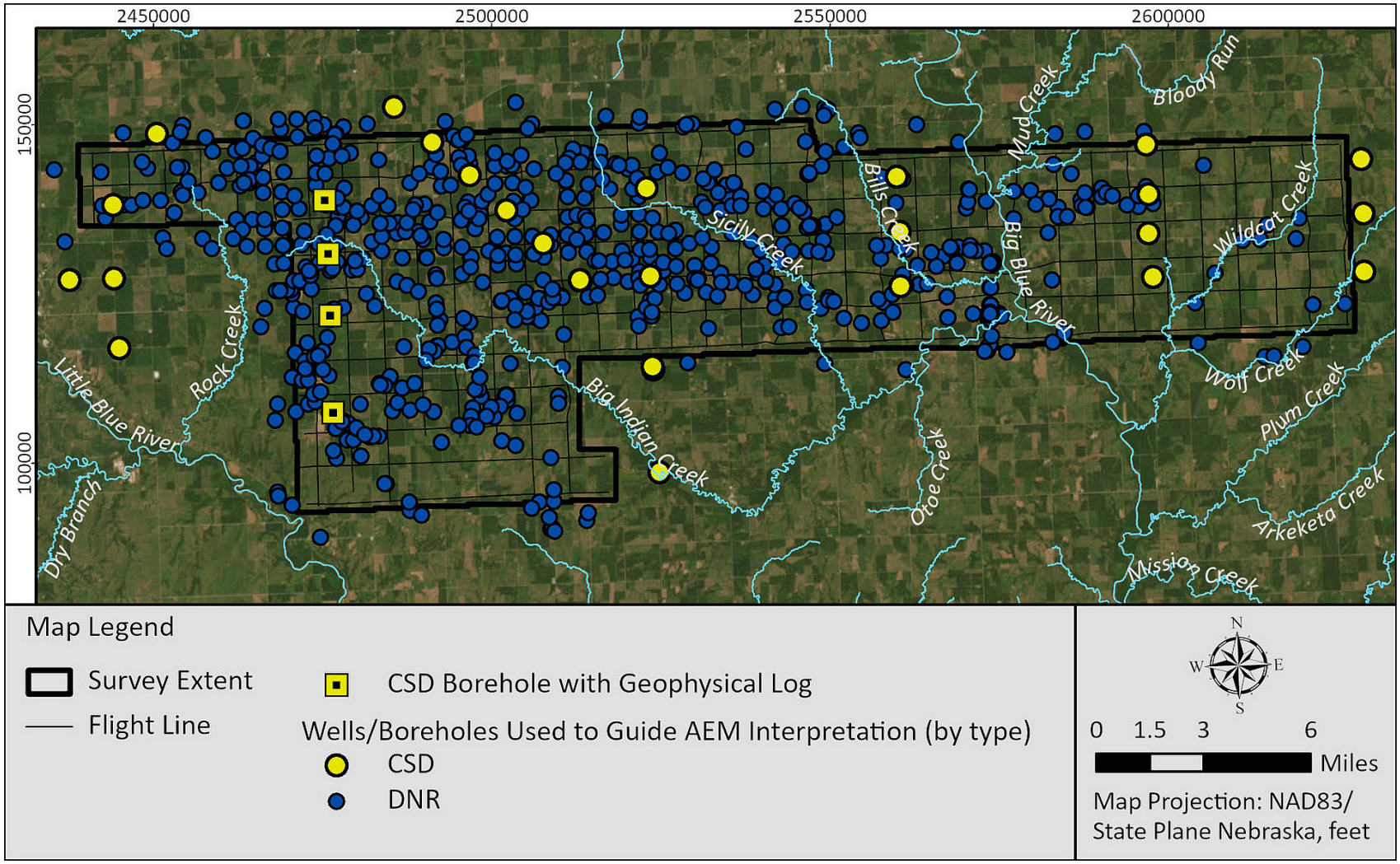


Figure 3-1. Map of the Nebraska CSD and DNR boreholes used to guide the LBBNRD 2023 AEM interpretation.

4 Geophysical Methodology, Acquisition and Processing

4.1 Geophysical Methodology

Airborne Transient Electromagnetic (TEM) or airborne Time-Domain Electromagnetic (TDEM), or generally AEM, investigations provide characterization of electrical properties of earth materials from the land surface downward using electromagnetic induction. Figure 4-1 gives a conceptual illustration of the airborne TEM method.

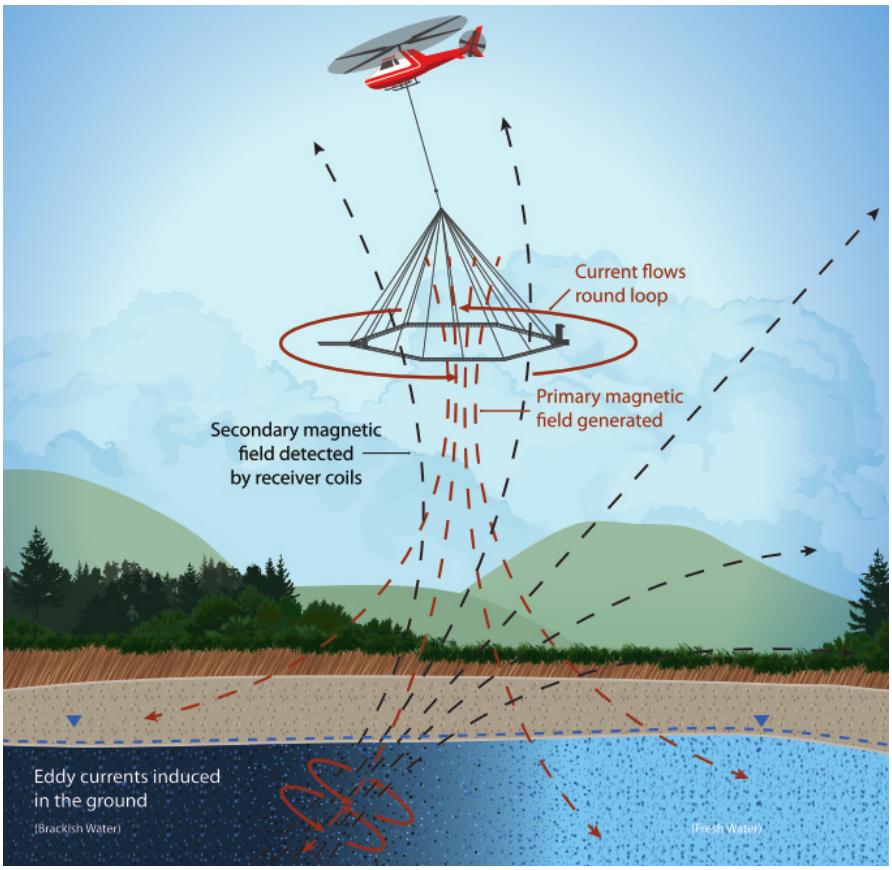


Figure 4-1: Schematic of an airborne electromagnetic survey, modified from Carney et al. (2015).

To collect TEM data, an electrical current is sent through a large loop of wire consisting of multiple turns which generates an electromagnetic (EM) field. This is called the transmitter (Tx) coil. After the EM field produced by the Tx coil is stable, it is switched off as abruptly as possible. The EM field dissipates and decays with time, traveling deeper and spreading wider into the subsurface. The rate of dissipation is dependent on the electrical properties of the subsurface (controlled by the material composition of the geology including the amount of mineralogical clay, the water content, the presence of dissolved solids, the metallic mineralization, and the percentage of void space). At the moment of turnoff, a secondary EM field, which also begins to decay, is generated within the subsurface. The decaying secondary EM field generates a current in a receiver (Rx) coil, per Ampere's Law. This current in the Rx coil is measured at several different moments in time (each moment being within a time band called a "gate"). From the

induced current, the time rate of decay of the magnetic field, B, is determined (dB/dt). When compiled in time, these measurements constitute a “sounding” at that location. Each TEM measurement produces an EM sounding at one point on the surface.

The sounding curves are numerically inverted to produce a model of subsurface resistivity as a function of depth. Inversion relates the measured geophysical data to probable physical earth properties. Figure 4-2 shows an example of a dual-moment TEM dB/dt sounding curve and the result of the inversion, the corresponding electrical resistivity model.

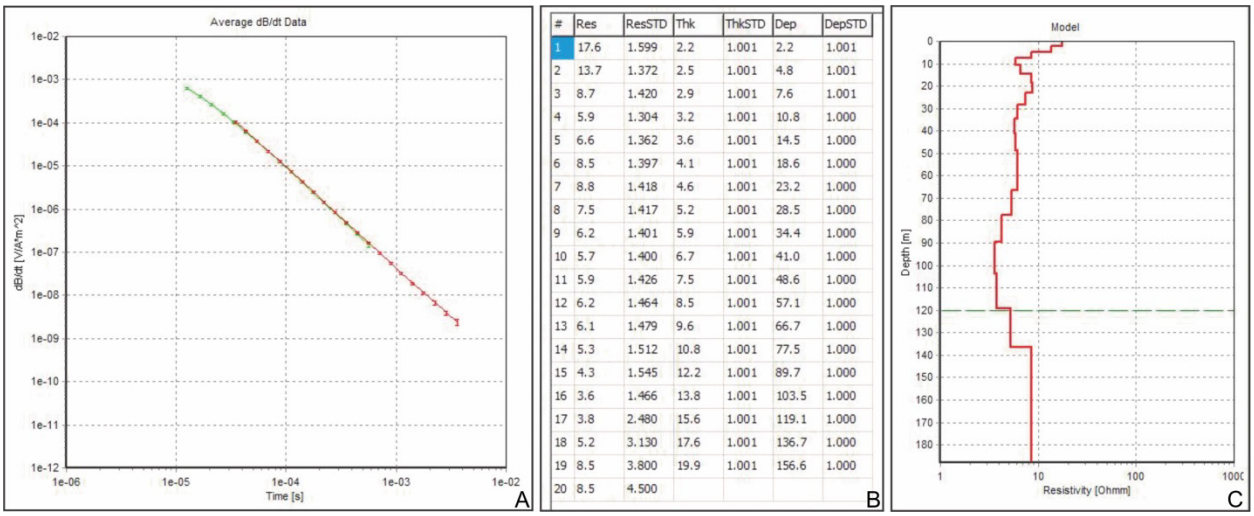


Figure 4-2: A) Example of a dB/dt sounding curve. B) Corresponding inverted model values. C) Corresponding resistivity earth model.

4.2 Flight Planning/Utility Mapping

The primary source of noise in geophysical electromagnetic surveys are other electromagnetic devices that are part of typical municipal utility infrastructure. These include, but are not limited to, power lines, railroads, pipelines, and water pumps. Prior to AEM data acquisition in the LBBNRD, three types of utilities (pipelines, railroads, and power lines) were located by inspection from Google Earth imagery.

The locations of the flight lines were modified from a regularly spaced grid to one with flight lines optimized to avoid electromagnetic coupling with identified utilities. This was done by moving along each flight line in ESRI ArcGIS Pro to inspect the path for visible power lines, radio towers, railroads, highways and roads, confined feeding operations and buildings, and any other obstructions that needed to be avoided during flight.

Upon conclusion of the design process, the LBBNRD flight lines had a maximum length of approximately 35 miles (57 km) in the east-west direction and about 10 miles (16 km) at their longest in the north-south direction. The flight lines were separated by approximately 0.93 mile (1.5 km) in both east-west and north-south directions.

4.3 AEM Survey Instrumentation

AEM data were acquired using the SkyTEM304M (304) airborne electromagnetic system (SkyTem Airborne Surveys Worldwide, 2023). The 304 is a rigid frame, dual-magnetic moment (Low and High) TEM system. The area of the 304 Tx coil is 342 m^2 and the coil contains four (4) turns of wire. A peak current of nine (9) amps is passed through one turn of wire in the Tx for Low Moment measurements and a peak current of about 110 amps is passed through the four turns of wire for High Moment measurements. This results in peak Tx Low and High magnetic moments of ~3,000 Ampere-meter-squared ($A*m^2$) and ~150,000 $A*m^2$, respectively.

The SkyTEM304M system utilizes an offset Rx positioned slightly behind the Tx resulting in a 'null' position which is a location where the intensity of the primary field from the system transmitter is minimized. This is desirable as to minimize the amplitude of the primary field at the Rx to maximize the sensitivity of the Rx to the secondary fields. The SkyTEM304M multi-turn Rx coil has an effective area of 105 m^2. In addition to the Tx and Rx that constitute the TEM instrument, the SkyTEM304M is also equipped with a Total Field magnetometer (MAG) and data acquisition systems for both instruments. The SkyTEM304M also includes two each of laser altimeters, inclinometers/tilt meters, and differential global positioning system (DGPS) receivers. Positional data from the frame mounted DGPS receivers are recorded by the AEM data acquisition system. The magnetometer includes a third DGPS receiver whose positional data is recorded by the magnetometer data acquisition system. Figure 4-3 gives a simple illustration of the SkyTEM304M frame and instrument locations. The image is viewed along the +z axis looking at the horizontal x-y plane. The axes for the image are labeled with distance in meters. The magnetometer is located on a boom off the front of the frame (right side of image). The Tx coil is located around the octagonal frame and the Rx Coil is located at the back of the frame (left side of image).

The coordinate system used by the 304 defines the +x direction as the direction of flight, the +y direction is defined 90 degrees to the right, and the +z direction is downward. The center of the transmitter loop, mounted to the octagonal SkyTEM frame is used as the origin in reference to instrumentation positions. Table 4-1 lists the positions of the instruments (in feet) and Table 4-2 lists the corners of the transmitter loop in feet (whereas units of meters are presented in Figure 4-3). Figure 4-4 displays a couple of images of the 304 in operation.

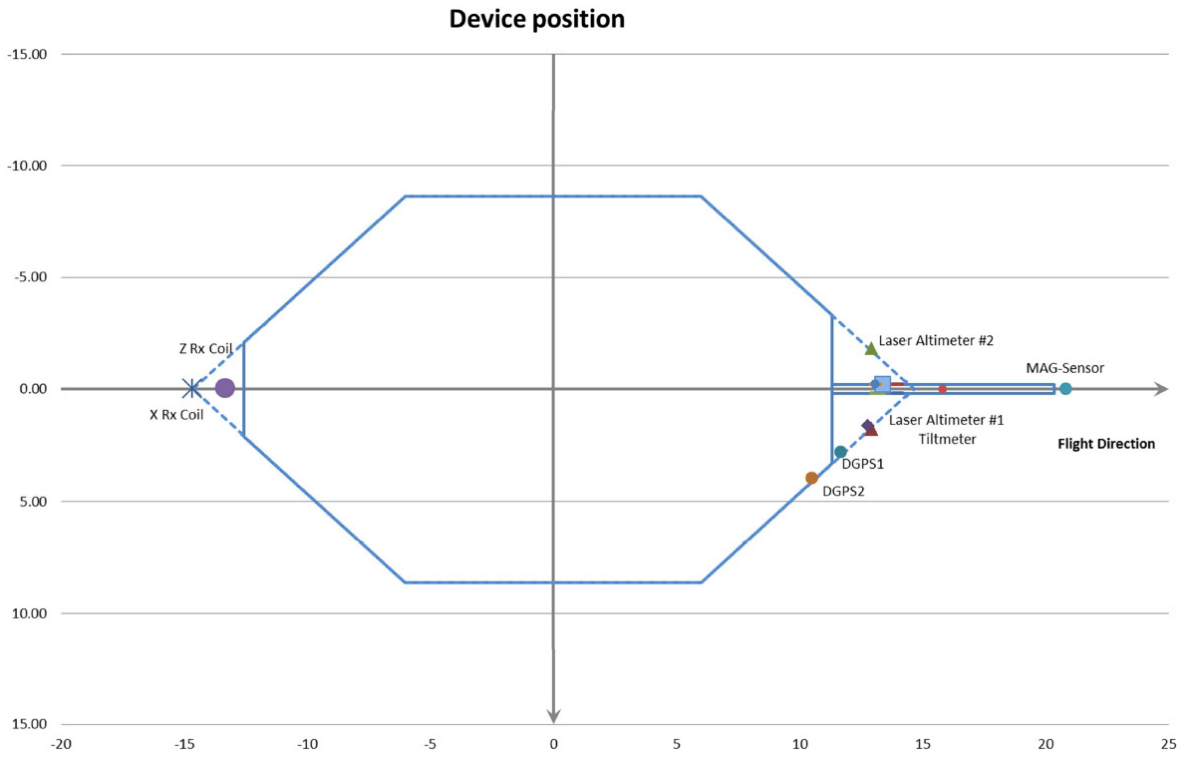


Figure 4-3: SkyTEM 304M frame, including instrumentation locations and X and Y axes. Distances are in meters. Instrumentation locations listed in Table 4-1.



Figure 4-4: Photos of the SkyTEM 304M system in suspension beneath the helicopter.

Table 4-1: Positions of instruments on the SkyTEM 304M frame, using the center of the frame as the origin, in feet.

	DGPS 1	DGPS 2	Inclinometer 1	Inclinometer 2	Altimeter 1	Altimeter 2	Magnetic Sensor	Rx Coil
X	39.08	34.15	42.36	41.95	42.44	42.44	67.24	-43.46
Y	9.15	12.96	5.38	-5.38	5.87	-5.87	0	0
Z	-0.52	-0.52	-0.39	-0.39	-0.39	-0.39	-1.71	-6.56

Table 4-2: Positions of corners of the SkyTEM 304M transmitter coil, using the center of the frame as the origin in feet.

Tx Corners	1	2	3	4	5	6	7	8
X	-41.16	-19.78	18.83	37.19	39.19	18.83	-19.78	-41.16
Y	-6.89	-27.98	-28.18	-10.85	10.85	28.18	27.98	6.89

4.4 Data Acquisition

All SkyTEM systems are calibrated to a ground test site in Lyngby, Denmark prior to being used for production work (HydroGeophysics Group Aarhus University, 2010; HydroGeophysics Group Aarhus University, 2011; Foged et al., 2013). The calibration process involves acquiring data with the system hovering at different altitudes, from 16 ft to 164 ft, over the Lyngby site. Acquired data are processed and a scale factor (time and amplitude) is applied so that the inversion process produces the model that approximates the known geology at Lyngby.

Installation of the navigational instruments in the helicopter and assembly of the SkyTEM304 system commenced at the beginning of the 2023 AGF AEM project campaign and the system was ferried to the Beatrice Municipal Airport on June 20, 2023. Calibration test flights were flown to ensure that the equipment was operating within technical specifications. Survey set-up procedures included measurement of the transmitter waveforms, verification that the receiver was properly located in a null position, and verification that all positioning instruments were functioning properly. A high-altitude test, used to verify system performance, was flown prior to the beginning of the survey's production flights. In the field, quality control of the operational parameters for the EM and magnetic field sensors including current levels, positioning sensor dropouts, acquisition speed, and system orientation were conducted with proprietary SkyTEM software following each flight.

Approximately 429.2 line-miles (690.5 line-kilometers) were acquired over the LBBNRD AEM survey area between 21 June 2023 and finishing on 22 June 2023. A data acquisition map for the flight lines is presented in Figure 4-5, grouped by acquisition date. For this LBBNRD project, the 304 was flown at an average speed of 66.0 mi/hr (106.2 kilometers/hr) and at an average flight height of 111.9 ft (34.1 m) above land surface, using the sling-load cargo system of a Eurocopter AS350 B2 helicopter. The average pitch (tilt angle in the +/- X direction of travel) was -1.81 degrees and the average roll (tilt angle perpendicular to the direction of travel) was -0.48 degrees. Images of the LBBNRD AEM survey ground speeds are presented in Figure 4-6. Flight heights are presented in Figure 4-7. Images of the pitch (X) angle and yaw (Y) angle are presented in Figure 4-8 and Figure 4-9, respectively.

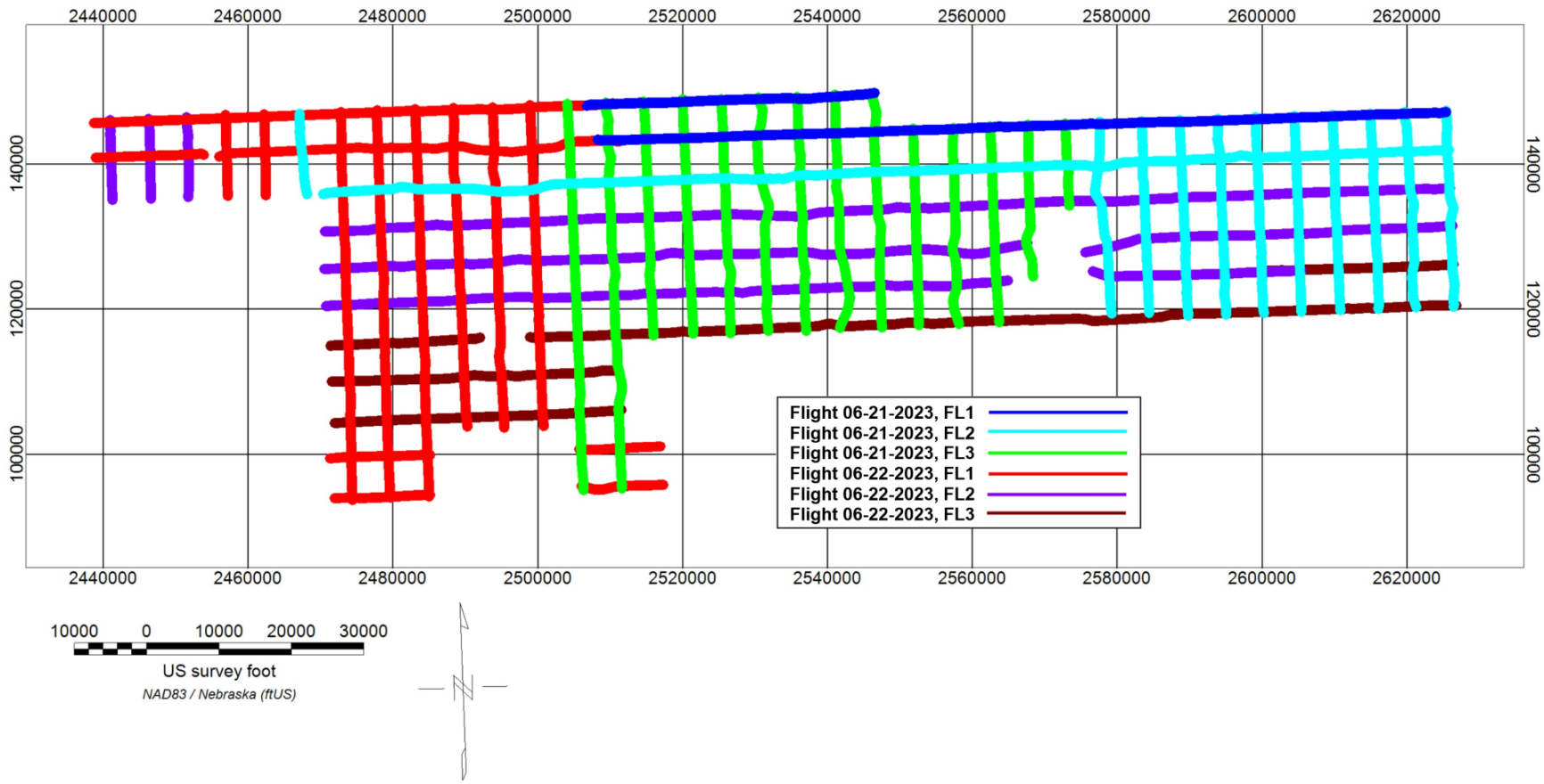


Figure 4-5. LBBNRD 2023 AEM flight lines grouped by acquisition date. Projection is Nebraska State Plane NAD83, feet.

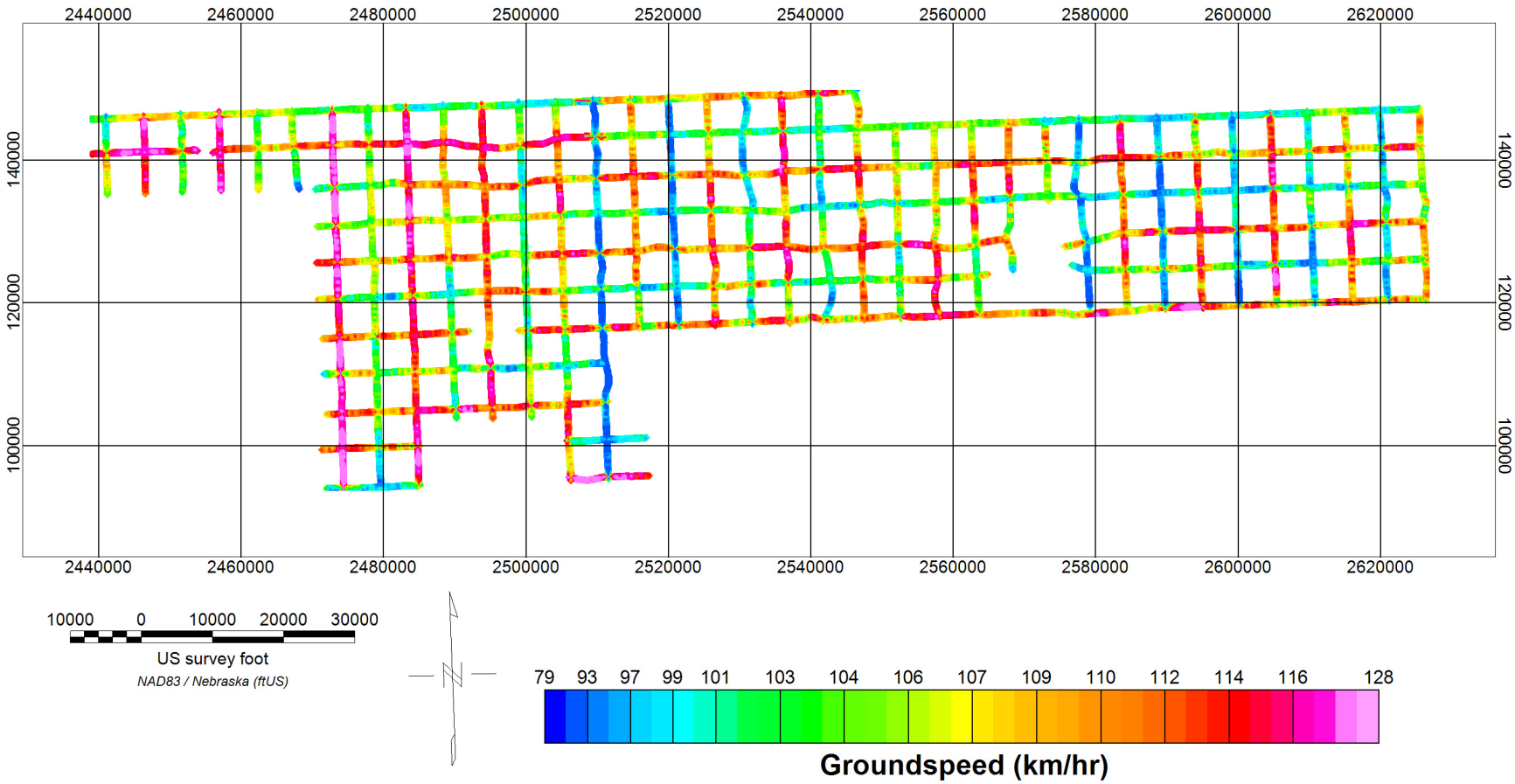


Figure 4-6. LBBNRD 2023 AEM survey ground speed. Projection is Nebraska State Plane NAD83, feet.

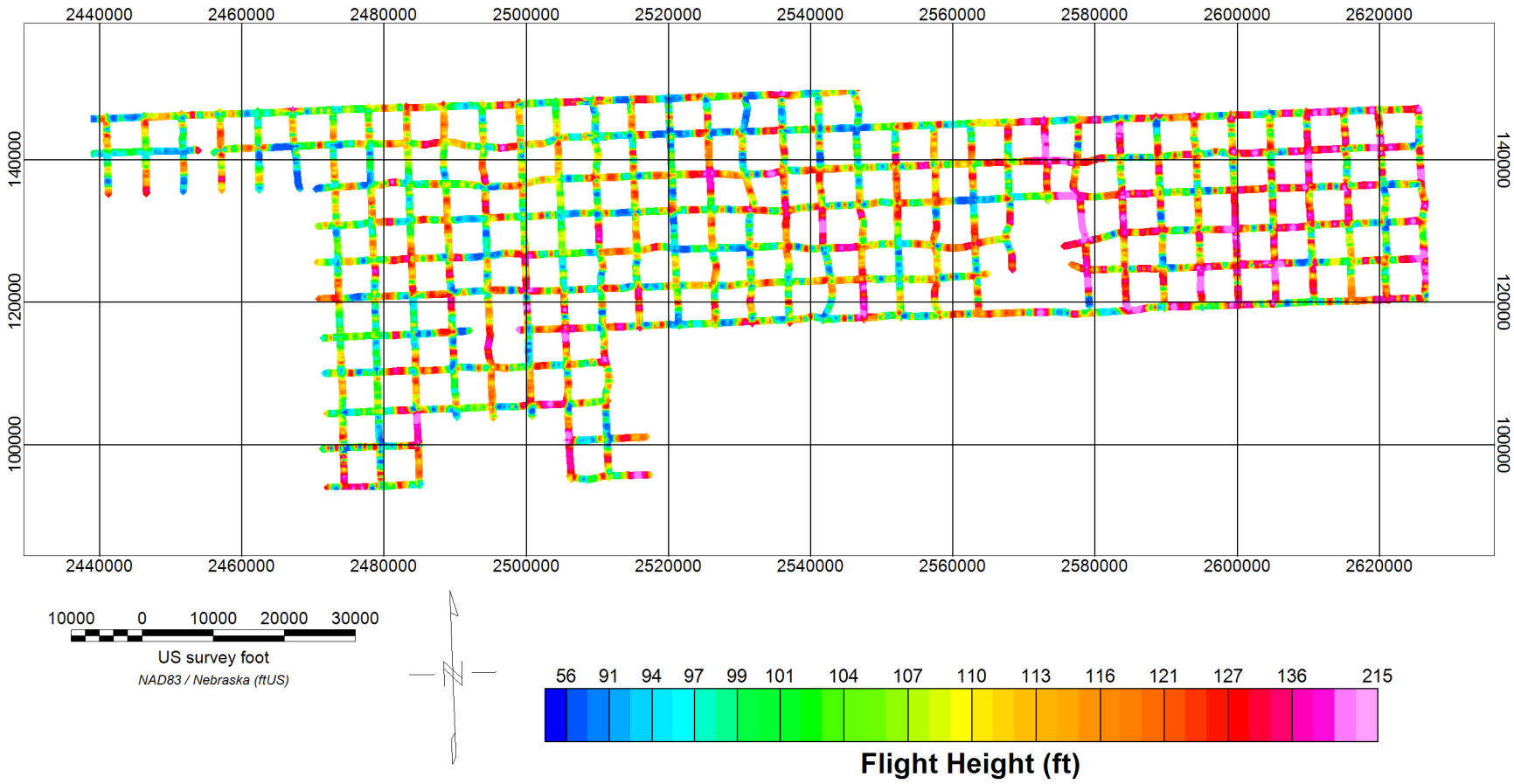


Figure 4-7. LBBNRD 2023 AEM flight lines flight height above the ground surface. Projection is Nebraska State Plane NAD83, feet.

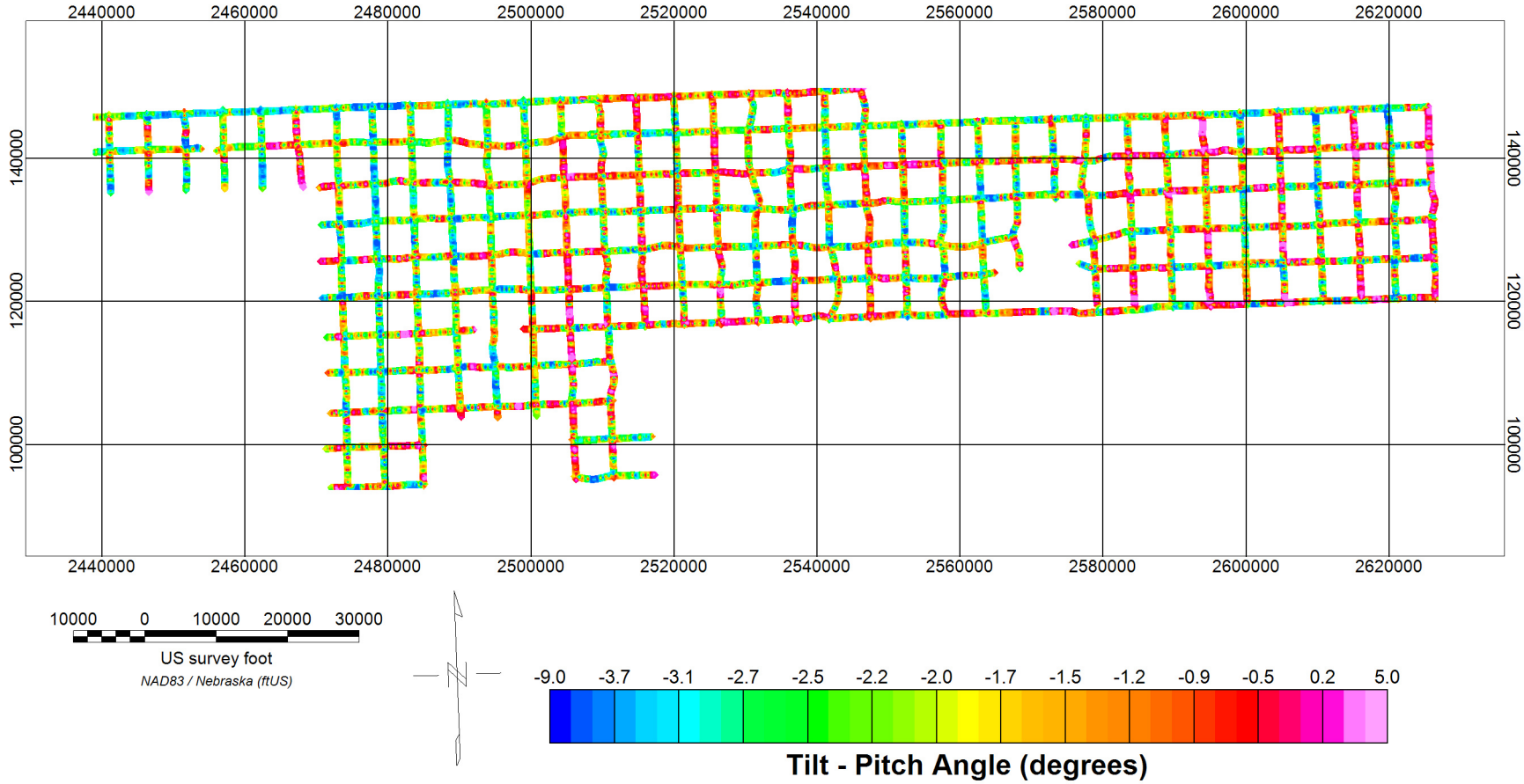


Figure 4-8. LBBNRD 2023 AEM flight lines pitch angle in the +/-X direction of travel. Projection is Nebraska State Plane NAD83, feet.

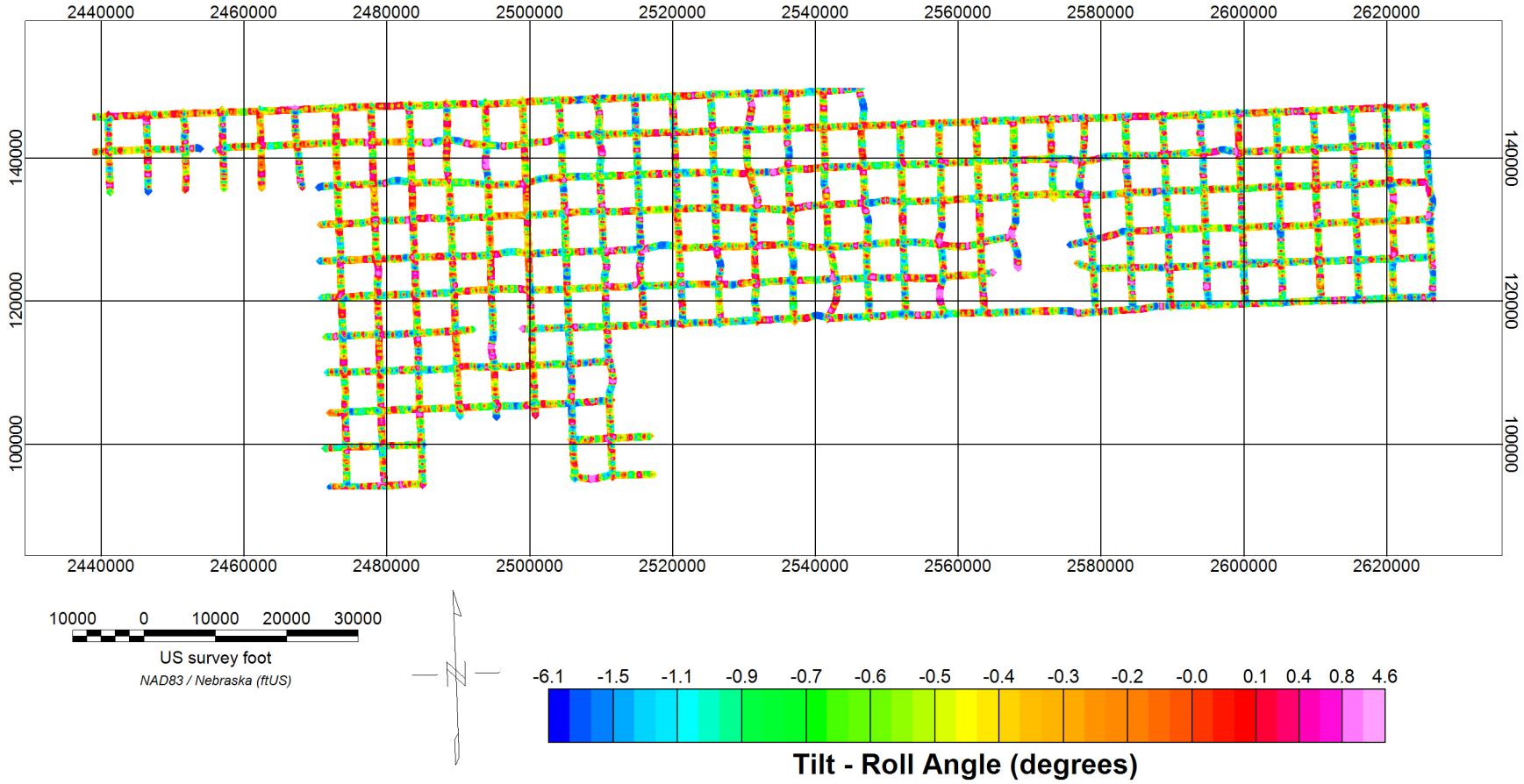


Figure 4-9. LBBNRD 2023 AEM flight lines Y roll angle perpendicular to the direction of travel. Projection is Nebraska State Plane NAD83, feet.

4.4.1 Primary Field Compensation

A standard SkyTEM data acquisition procedure involves review of acquired raw data by SkyTEM in Denmark for Primary Field Compensation (PFC) prior to continued data processing by AGF (Schamper et al., 2014). The primary field of the transmitter affects the recorded early time gates, which in the case of the Low Moment, are helpful in resolving the near surface resistivity structure of the ground. The Low Moment uses a saw tooth waveform which is calculated and then used in the PFC correction to correct the early time gates.

4.4.2 Automatic Processing

The AEM data collected by the 304 were processed using Aarhus Workbench version 6.8.0.0 (Aarhus Geosoftware (https://www.aarhusgeosoftware.dk/aarhus-workbench) described in HydroGeophysics Group, Aarhus University (2011).

Automatic processing algorithms provided within the Workbench program are initially applied to the AEM data. DGPS locations were filtered using a stepwise, second-order polynomial filter of ten seconds with a beat time of 0.5 seconds, based on flight acquisition parameters. The AEM data are corrected for tilt deviations from level and so filters were also applied to both tilt meter readings with a median filter of three seconds and an average filter of two seconds. The altitude data were corrected using a series of two polynomial filters. The lengths of both eighth-order polynomial filters were set to 15 seconds with shift lengths of twelve (12) seconds. The lower and upper thresholds were 1 and 100 meters, respectively.

Trapezoidal spatial averaging filters were next applied to the AEM data. The times used to define the trapezoidal filters for the Low Moment were $1.0x10^{-5}$ sec, $1.0x10^{-4}$ sec, and $1.0x10^{-3}$ sec with widths of 3, 6, and 18 seconds. The times used to define the trapezoid for the High Moment were $1.0x10^{-4}$ sec, $1.0x10^{-3}$ sec, and $1.0x10^{-2}$ sec with widths of 6, 12, and 36 seconds. The trapezoid sounding distance was set to 1.0 seconds and the left/right setting, which requires the trapezoid to be complete on both sides, was turned on. The spike factor and minimum number of gates were both set to 25 percent for both moments. Lastly, the locations of the averaged soundings were synchronized between the two moments.

4.4.3 Manual Processing and Laterally-Constrained Inversions

After the implementation of the automatic filtering, the AEM data were manually examined using a sliding two-minute time window. The data were examined for possible electromagnetic coupling with surface and buried utilities and metal, as well as for late time-gate noise. Data affected by these were removed. An example of flight light passing over possible sources of EM coupling is shown in Figure 4-10 Figure 4-11 displays what an EM coupling looks like in Aarhus Workbench both before and after removal. Example inversion results with coupling and that coupling removed are shown in Figure 4-12. Data were also removed where the system height was greater than 230 feet (70 m) which causes a decrease in the signal level. This occurred at several locations due to object avoidance.

The AEM data were then inverted using a Laterally-Constrained Inversion (LCI) algorithm (HydroGeophysics Group Aarhus University, 2011). The profile and depth slices were examined, and any remaining electromagnetic couplings were masked out of the data set. Once acceptable LCI results were obtained, the data were then inverted using the Spatially Constrained Inversion (SCI) discussed below.

After final processing, 347.5 line-miles (559.2 line-kilometers) were retained for inversion amounting to a retention rate of 81.0%. This high rate is the result of careful flight line planning and design to avoid the infrastructure present in the survey area.

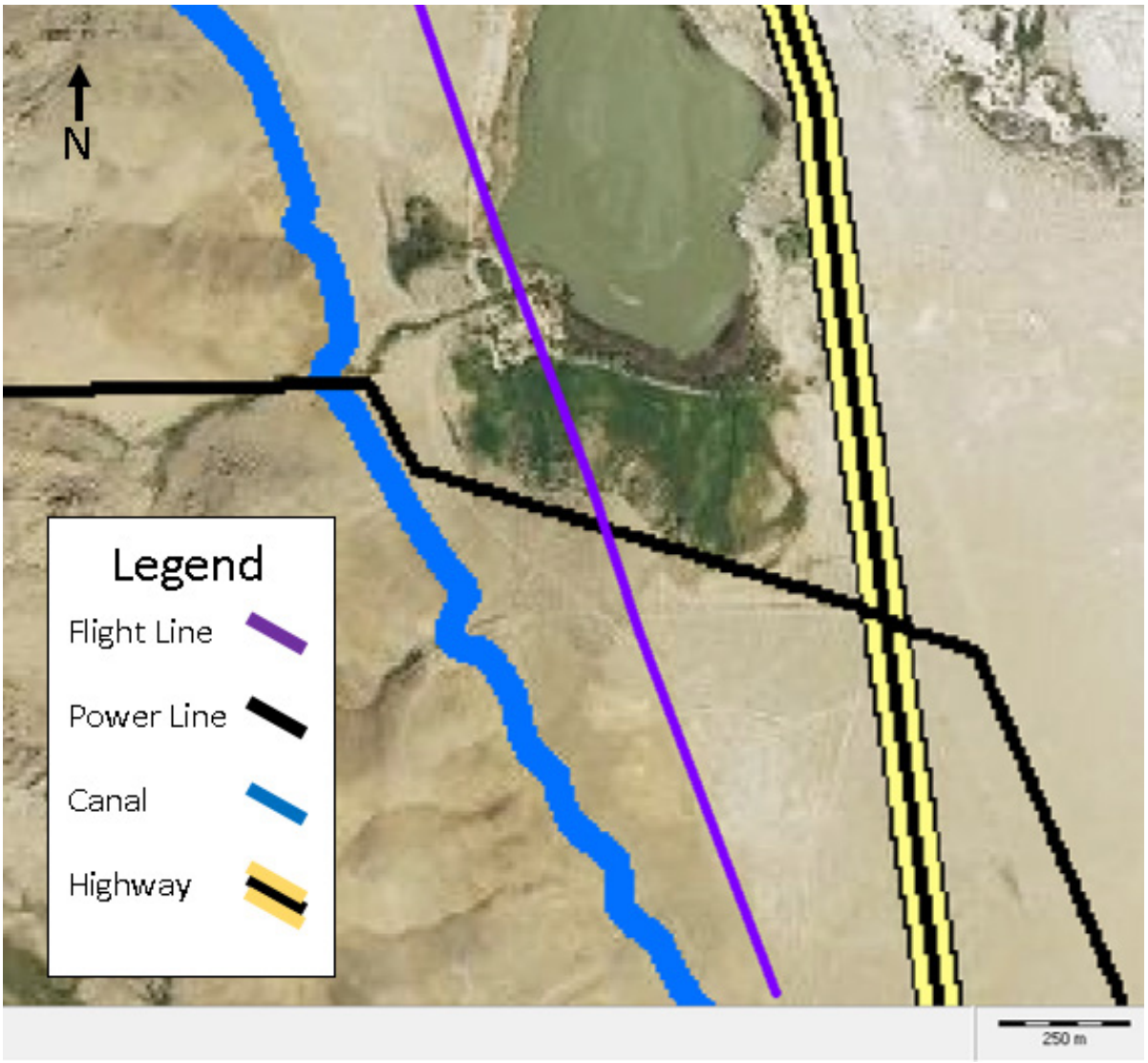


Figure 4-10: Example locations of electromagnetic coupling with pipelines or power lines.

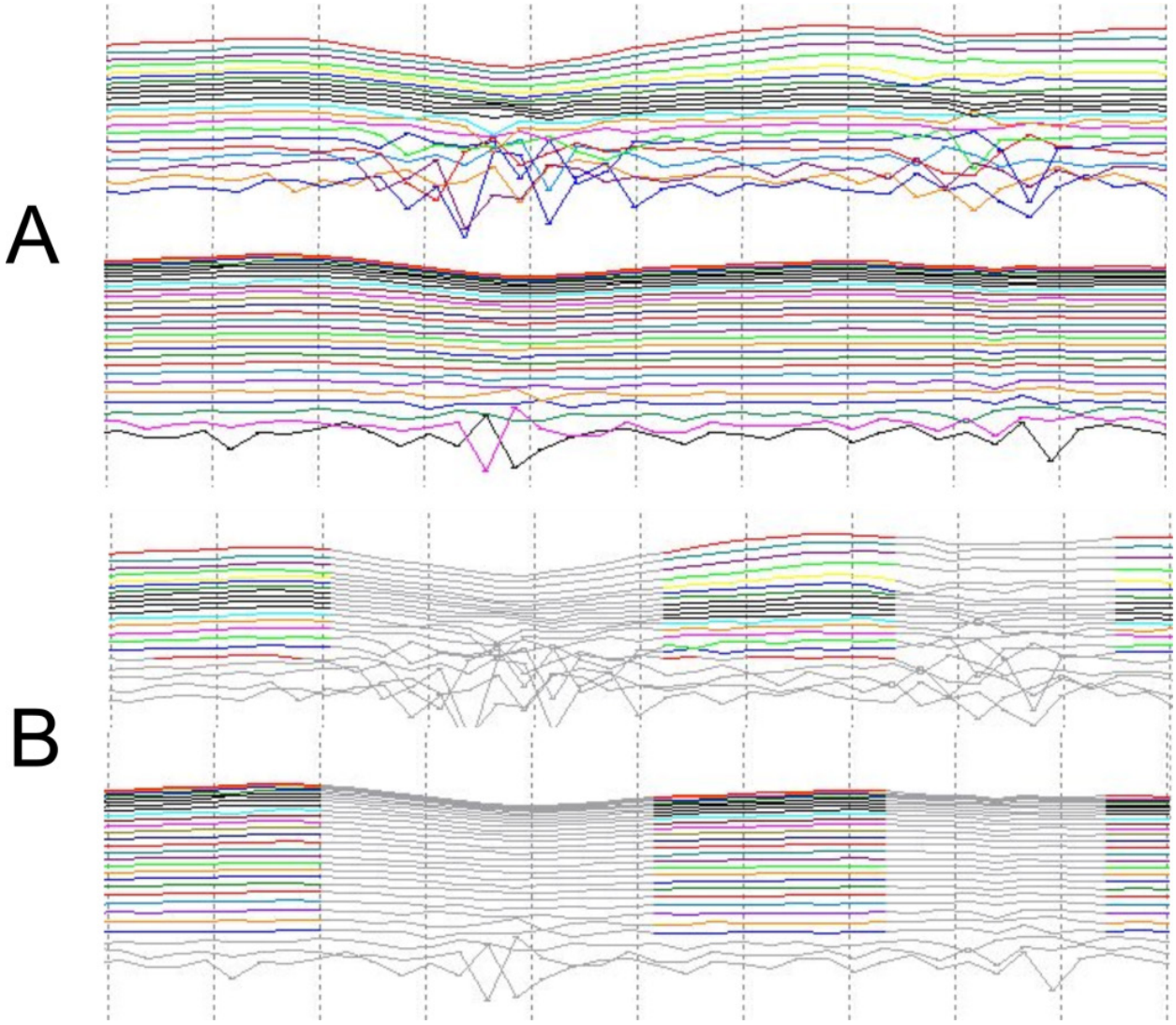


Figure 4-11: A) Example of AEM data affected by electromagnetic coupling as presented in the Aarhus Workbench editor. The top group of lines is the unedited data with the Low Moment on top and the High Moment on the bottom. The bottom group shows the same data after editing.

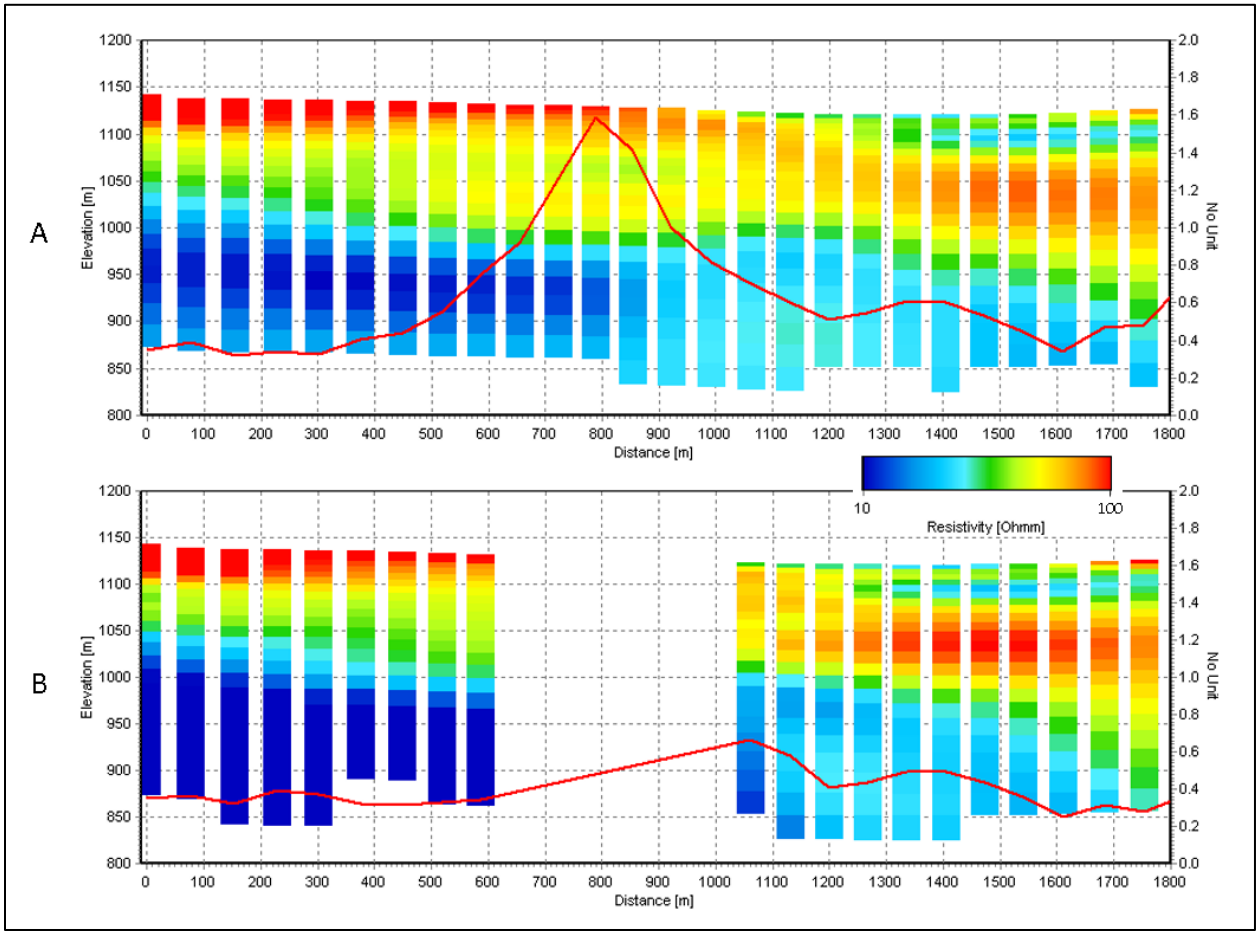


Figure 4-12: A) Example of Laterally-Constrained inversion results where AEM data affected by coupling with pipelines and power lines were not removed. B) Inversion results where AEM data affected by coupling were removed.

4.4.4 Power Line Noise Intensity (PLNI)

The Power Line Noise Intensity (PLNI) channel assists in identifying possible sources of noise from power lines. Pipelines, unless they are cathodically-protected, are not mapped by the PLNI. The PLNI is produced by performing a spectral frequency content analysis on the raw received Z-component SkyTEM data. For every Low Moment data block, a Fourier Transform (FT) is performed on the latest usable time gate data. The FT is evaluated at the local power line transmission frequency (60 Hz) yielding the amplitude spectral density of the local power line noise. The PLNI data for the LBBNRD 2023 AEM survey are presented as a grid in Figure 4-13. The LBBNRD 2023 survey As-Flown data and the data retained for inversion are presented in Figure 4-14. The blue lines represent the 81.0% of data retained for inversion and red lines representing data removed due to infrastructure and noise.

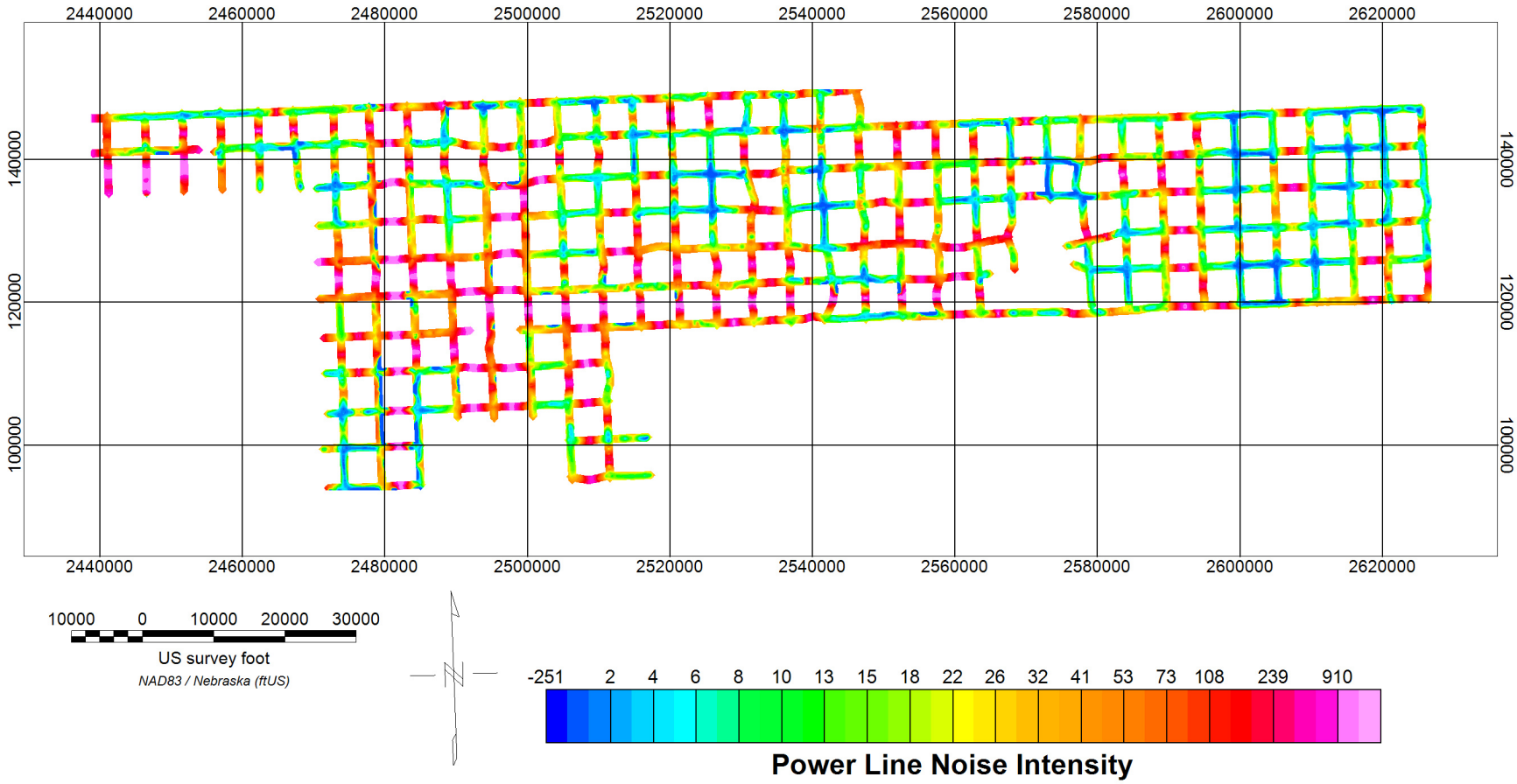


Figure 4-13: Power Line Noise Intensity (PLNI) map of the LBBNRD 2023 project area. Projection is Nebraska State Plane NAD83, feet.

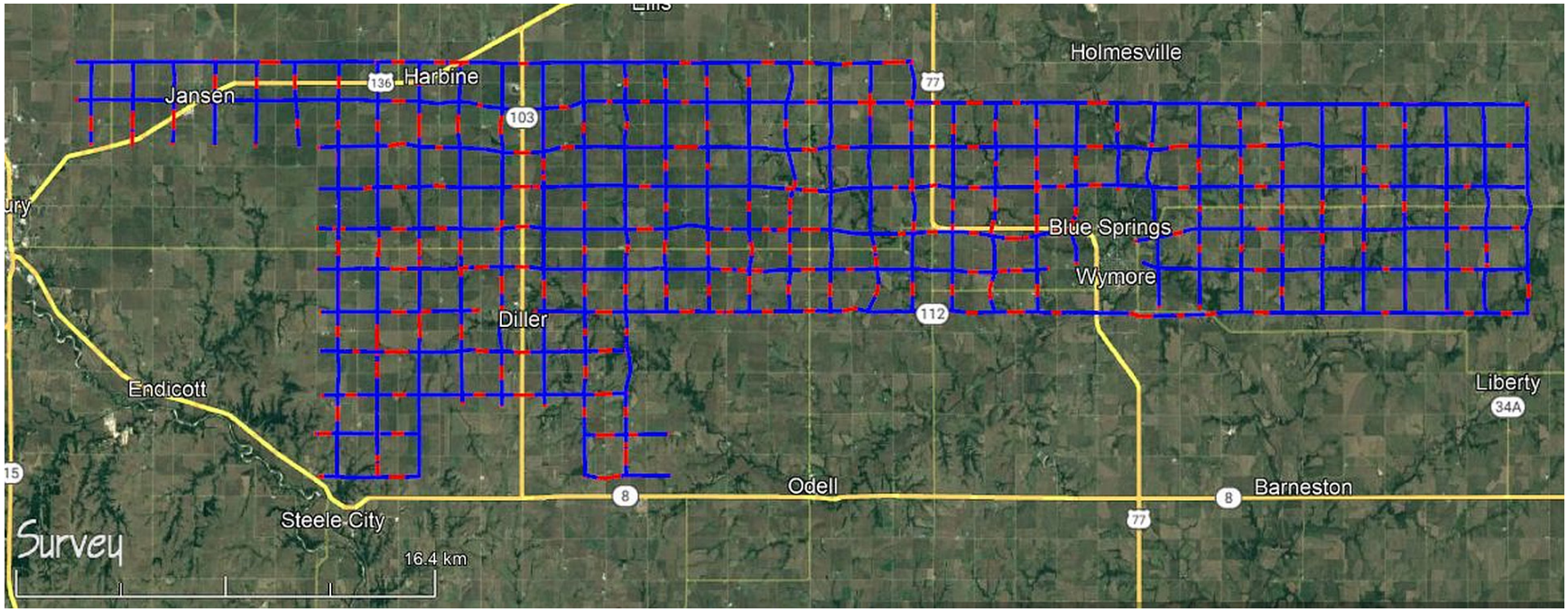


Figure 4-14. Locations of inverted data (blue lines) along the AEM flight lines (red lines) on the LBBNRD 2023 AEM survey area in Google Earth. Where blue lines are not present indicates decoupled (removed) data. Google Earth kmz's of the inverted data locations as well as the "as-flown" flight lines are included in Appendix 3\KMZ.

4.4.5 Magnetic Field Data

As discussed above, the SkyTEM 304 includes a Total Field magnetometer. The magnetic Total Field data can yield information about infrastructure as well as geology. Figure 4-15 shows the residual magnetic Total Field (RMF) intensity data for the LBBNRD AEM survey area after correcting for diurnal drift and removing the International Geomagnetic Reference Field (IGRF). This data is used in decoupling efforts.

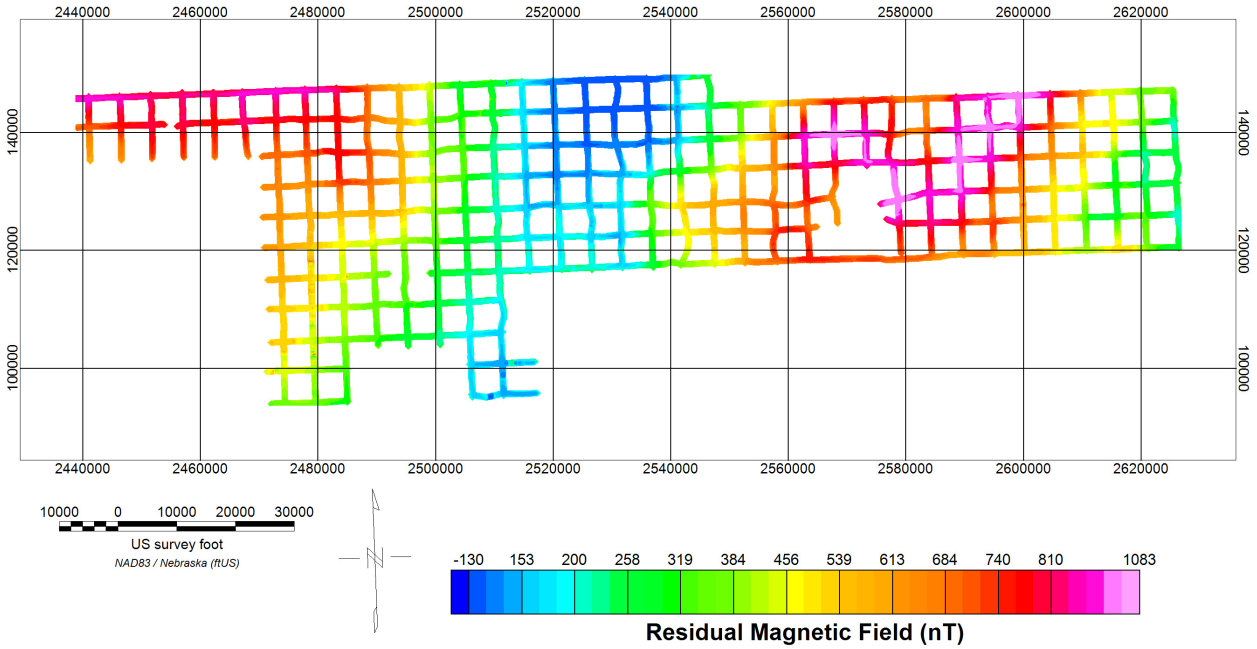


Figure 4-15. Residual magnetic Total Field intensity data for the LBBNRD 2023 AEM survey area corrected for diurnal drift, with the International Geomagnetic Reference Field (IGRF) removed. Projection is Nebraska State Plane NAD83, feet.

4.5 Spatially-Constrained Inversion

Following the initial decoupling and LCI analysis, Spatially-Constrained Inversions (SCI) were performed. SCIs use EM data along, and across, flight lines within user-specified distance criteria (Viezzoli et al., 2008).

The LBBNRD 2023 AEM data were inverted using a 40-layer model structure. The SCI inversions used smooth models, each with a starting resistivity of 10 Ohm-m (equivalent to a 10 ohm-m halfspace). The thicknesses of the first layers of the models were about 6.6 ft (2 m) with the thicknesses of the consecutive layers increasing approximately by a factor of 1.01. The depths to the bottoms of the 39th layers were set to 325.0 ft, with thicknesses up to about 21.6 ft. The thicknesses of the layers increase with depth (Table 4-3 and Figure 4-16) as the resolution of the EM technique decreases. The spatial reference distance, ***s***, for the inversion constraints was set to 328 ft (100 m) with a power law falloff of 0.75. The vertical and lateral constraints, ***ResVerSTD*** and ***ResLatStD***, were set to 2.4 and 1.4, respectively, for all layers.

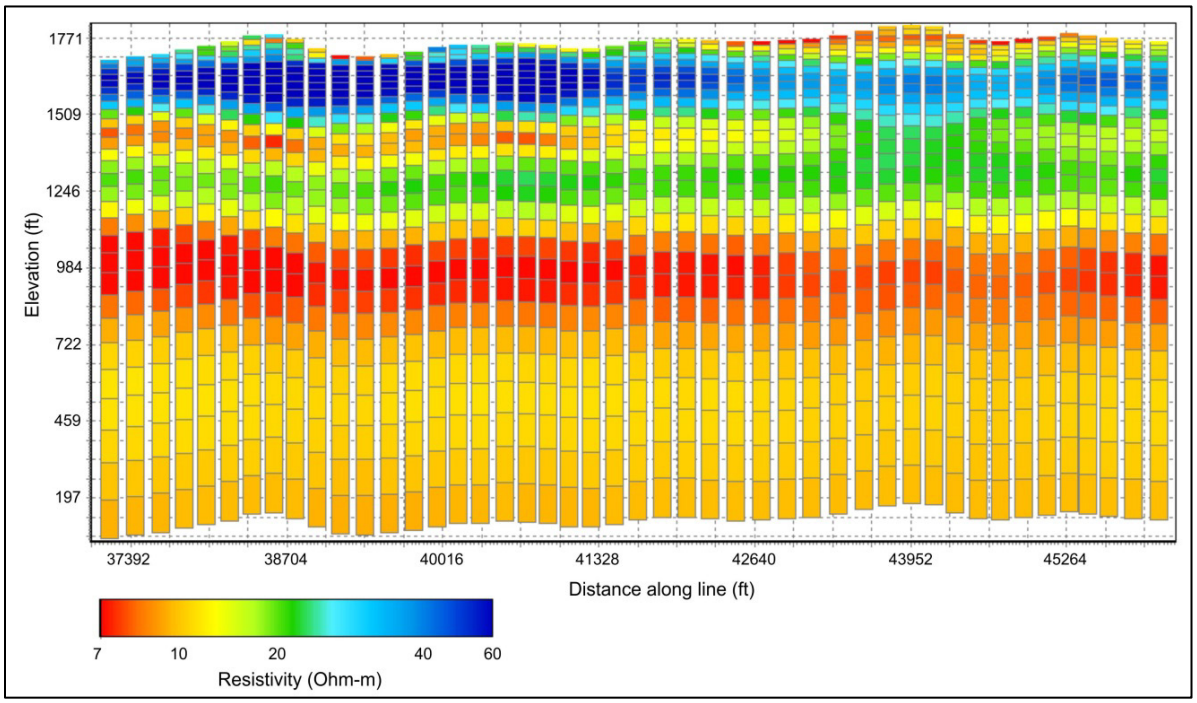


Figure 4-16. An example of an AEM profile illustrating increasing model layer thicknesses with depth.

In addition to the recovered resistivity models, the SCIs also produce data residual error values (single sounding error residuals) and Depth of Investigation (DOI) estimates. The data residuals compare the measured data with the forward modeled response of the individual inverted models (Christensen et al., 2009). The DOI provides a general estimate of the depth to which the AEM data are sensitive to changes in the resistivity distribution at depth (Christiansen and Auken, 2012). Two DOI's are calculated: an "Upper" DOI at a cumulative sensitivity of 1.2 and a "Lower" DOI set at a cumulative sensitivity of 0.6. A more detailed discussion on the DOI can be found in Asch et al. (2015).

Table 4-3: Thickness and depth to bottom for each layer in the Spatially Constrained Inversion (SCI) AEM earth models. The thickness of the model layers increase with depth as the resolution of the AEM technique decreases.

Layer	Depth to Bottom (ft)	Thickness (ft)	Depth to Bottom (m)	Thickness (m)	Layer	Depth to Bottom (ft)	Thickness (ft)	Depth to Bottom (m)	Thickness (m)
1	6.6	6.6	2.0	2.0	21	276.6	23.0	84.3	7.0
2	13.5	6.9	4.1	2.1	22	301.2	24.6	91.8	7.5
3	21.0	7.5	6.4	2.3	23	327.1	25.9	99.7	7.9
4	28.9	7.9	8.8	2.4	24	355.0	27.9	108.2	8.5
5	37.4	8.5	11.4	2.6	25	384.5	29.5	117.2	9.0
6	46.3	8.9	14.1	2.7	26	415.7	31.2	126.7	9.5
7	55.8	9.5	17.0	2.9	27	449.2	33.5	136.9	10.2
8	65.9	10.2	20.1	3.1	28	484.9	35.8	147.8	10.9
9	76.8	10.8	23.4	3.3	29	522.7	37.7	159.3	11.5
10	88.3	11.5	26.9	3.5	30	563.0	40.4	171.6	12.3
11	100.7	12.5	30.7	3.8	31	606.0	43.0	184.7	13.1
12	113.9	13.1	34.7	4.0	32	651.9	45.9	198.7	14.0
13	127.6	13.8	38.9	4.2	33	700.5	48.6	213.5	14.8
14	142.4	14.8	43.4	4.5	34	752.3	51.8	229.3	15.8
15	158.1	15.7	48.2	4.8	35	807.5	55.1	246.1	16.8
16	174.9	16.7	53.3	5.1	36	866.2	58.7	264.0	17.9
17	192.9	18.0	58.8	5.5	37	928.9	62.7	283.1	19.1
18	212.0	19.0	64.6	5.8	38	995.5	66.6	303.4	20.3
19	232.3	20.3	70.8	6.2	39	1066.3	70.9	325.0	21.6
20	253.6	21.3	77.3	6.5					

Figure 4-17 presents a histogram of the LBBNRD 2023 SCI inversion data/model residuals and a map of data to model error residuals comparison is presented in Figure 4-18.

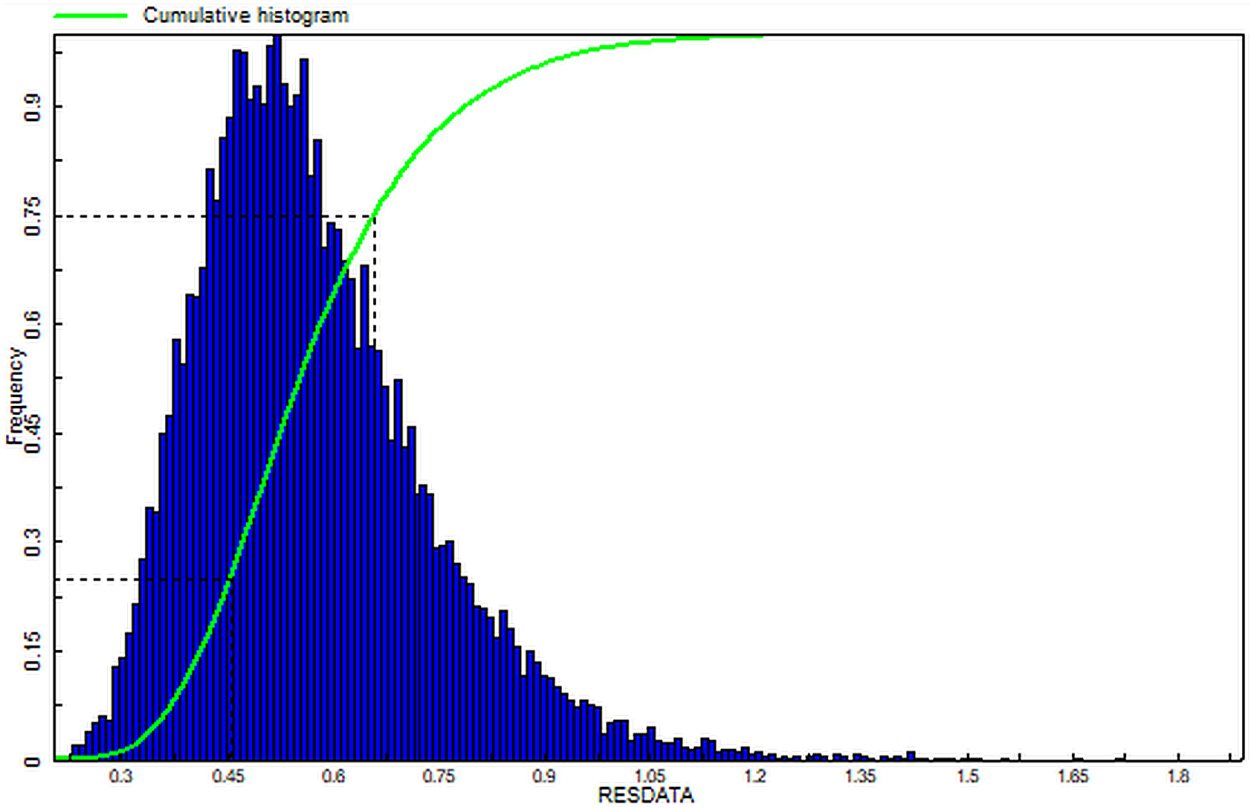


Figure 4-17. Data/model residual histogram for the LBBNRD 2023 SCI inversion results.

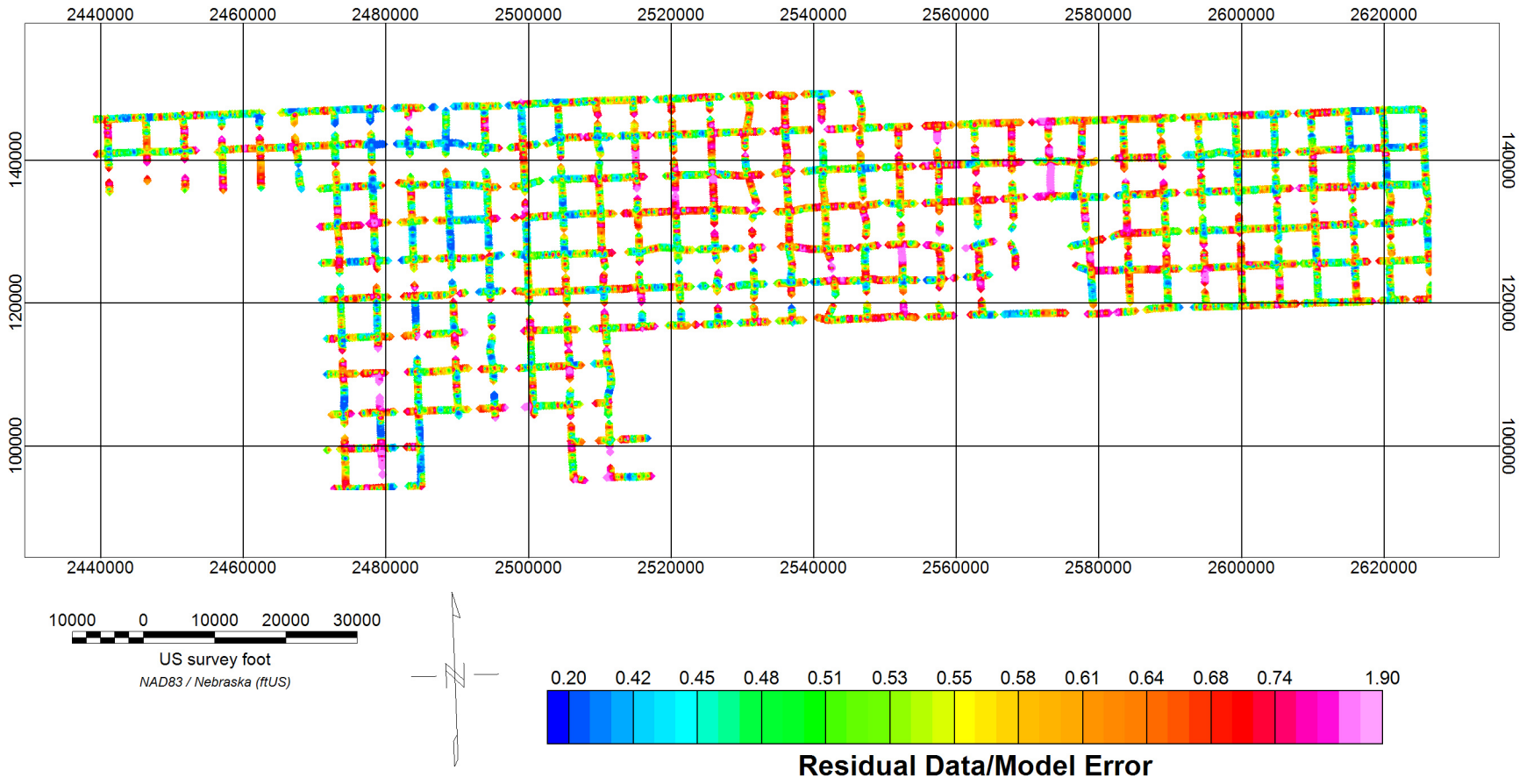


Figure 4-18. Map of data-inversion model residuals for the LBBNRD 2023 SCI inversion results. Projection is Nebraska State Plane NAD83, feet.

5 AEM Results and Interpretation

This section provides the details involved in the interpretation of the LBBNRD 2023 AEM data and inversion results.

5.1 Interpretative Process

5.1.1 Merging AEM Flight Lines

After the inversion process, flight lines from the 2023 LBBNRD data set were combined to create continuous lines in areas where an east-west line was flown in two parts due to infrastructure and or flight planning. These continuous lines allow for improved viewing and interpretation of the AEM inversions results across the LBBNRD area. A compiled table listing the originally flown lines from the AEM inversions and the newly combined lines are shown in Table 5-1. This would be used if referring to the original as-flown lines within the raw acquired data and the inverted data sets. Figure 5-1 presents a map showing the merged segments where the lines were connected.

Table 5-1. LBBNRD 2023 AEM lines merged.

Direction	Original Line 1	Original Line 2	Original Line 3	New Line
East-West	500101	500102		500100
East-West	500201	500202	500203	500200
East-West	500501	500502		500500
East-West	500601	500602	500603	500600
East-West	500701	500702		500700
East-West	501001	501002		501000
East-West	501101	501102		501100

5.1.2 Construction of the Project Digital Elevation Model

To ensure that the elevation used in the project is constant for all the data sources (i.e., boreholes and AEM) a ground surface Digital Elevation Model (DEM) was downloaded and processed for the 2023 LBBNRD survey (Figure 5-2). The raster dataset was downloaded from the National Map Data Download Application (U.S. Geological Survey, 2023) at a resolution of 1/3 arc-second or approximately 30 ft. The native geographic coordinates are North American Datum of 1983 (NAD 83) and the elevation values are referenced to the North American Vertical Datum of 1988 (NAVD 88). The original 30 ft resolution was resampled to 300 ft and project products such as 2D grids and 3D voxel products were snapped to this 300 ft resolution. The map in Figure 5-2 of the ground surface DEM shows a vertical relief of 335 ft with a minimum elevation of 1,164 ft and a maximum elevation of 1,499 ft and an average elevation of 1,360 ft. This DEM was used to reference all elevations within the AEM and borehole datasets.

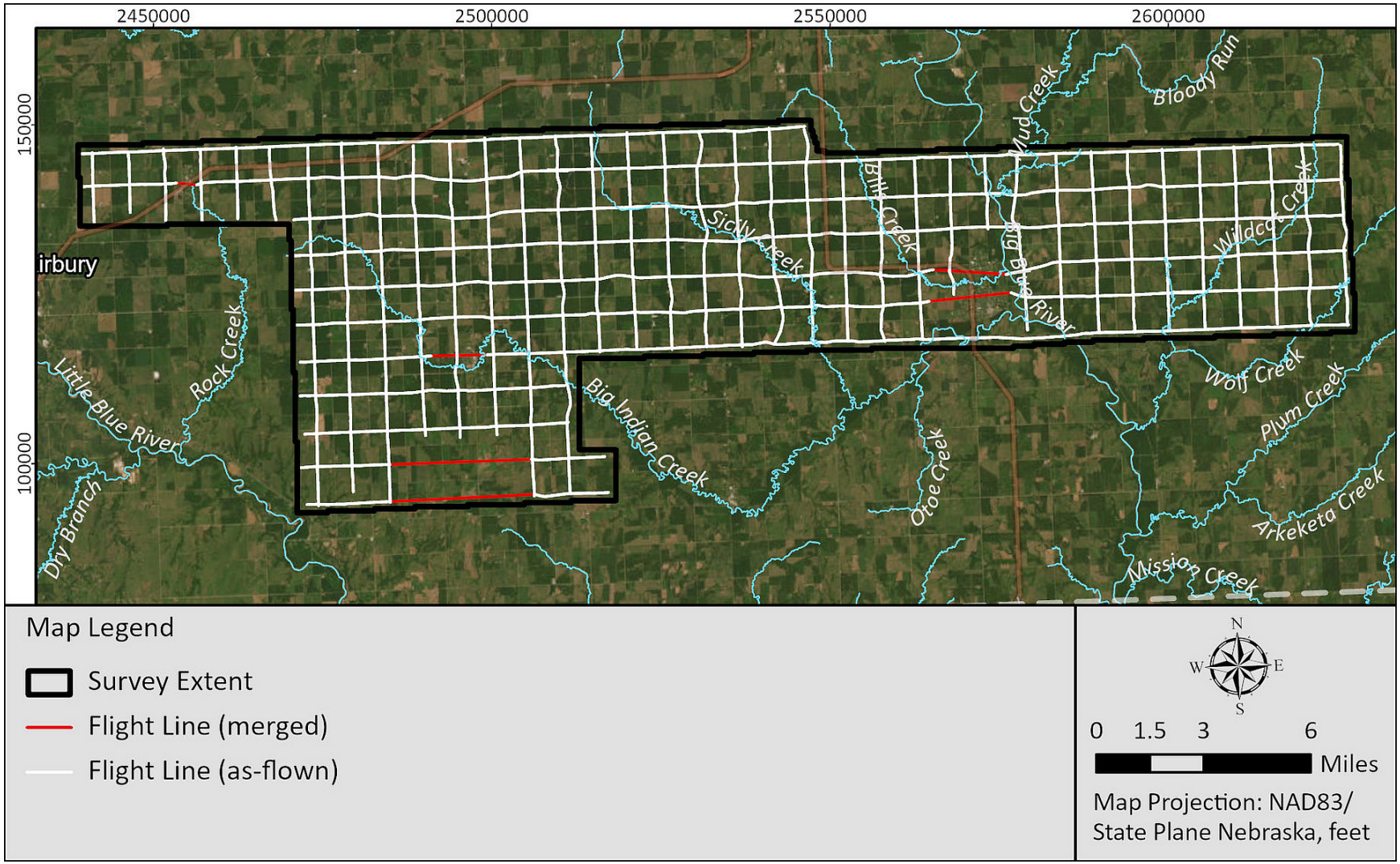


Figure 5-1. The flight lines and the connected merged lines for the 2023 LBBNRD AEM survey.

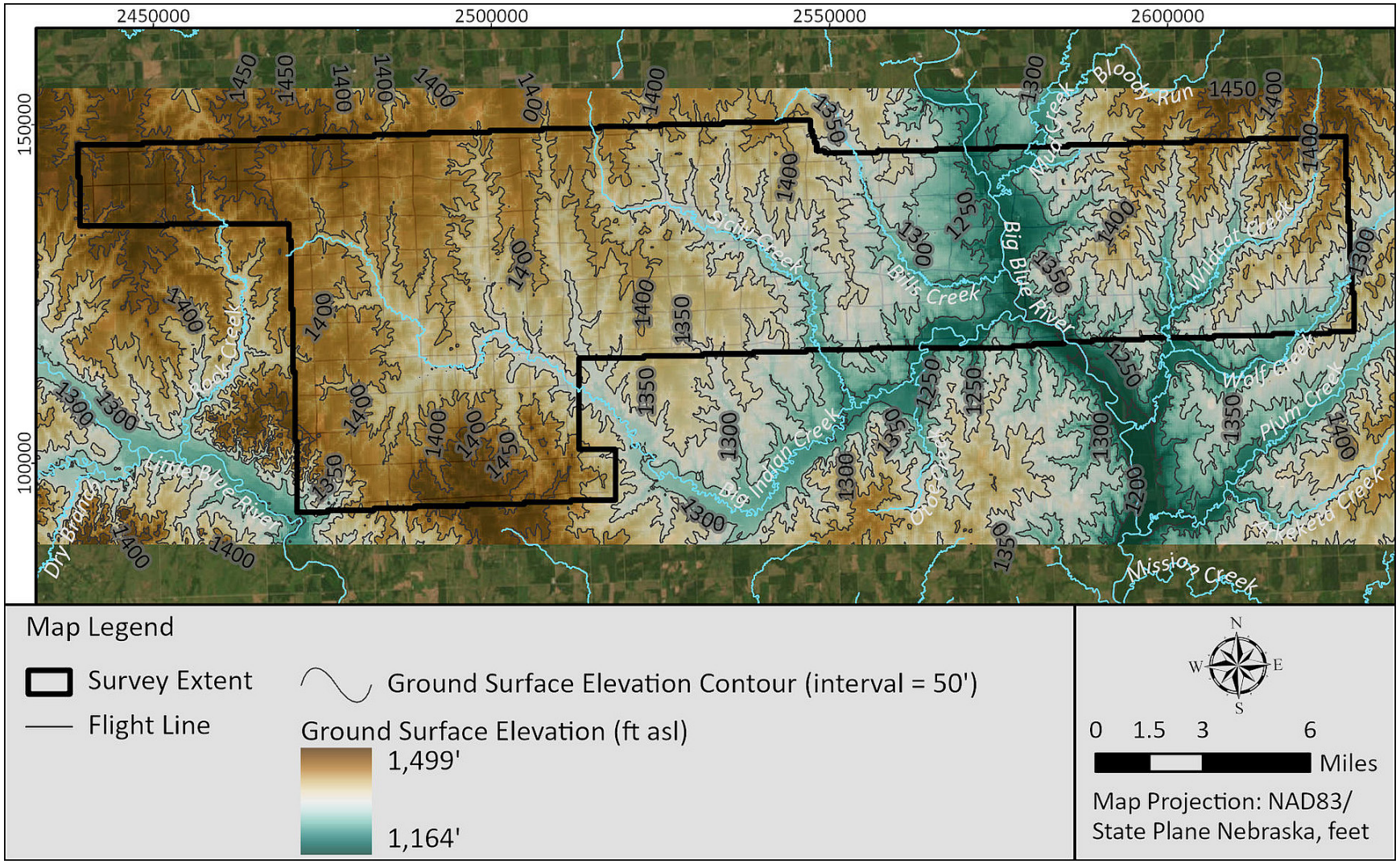


Figure 5-2. Map of the ground surface DEM for the 2023 LBBNRD AEM survey.

5.1.3 Borehole-Only Surface of the Bedrock

As a guide in the interpretation of the AEM, a bedrock surface was prepared using CSD and NE-DNR borehole logs in combination with published geologic maps. For conciseness, the bedrock surface interpolation process is described in the following list:

Data used:

- Most up to date NE-DNR and CSD borehole data downloaded from the Nebraska GeoCloud (2023)
- NE-DNR borehole processing
    - Extracted NE-DNR boreholes within 1 mile of the planned flight lines.
    - Extracted project ground surface elevation to the NE-DNR boreholes.
    - In a spreadsheet, categorized each borehole's lithology description as either 'Bedrock' or 'Unconsolidated' based on the description type.
        - For example:
            - Sandstone, Shale, Siltstone, Limestone, Chalk = 'Bedrock'
            - Clay, silt, gravel/boulders, etc. = 'Unconsolidated'
    - Extracted the depth/elevation of the first 'Bedrock' encountered for each borehole.
    - Saved the extracted data as a new working table.
- CSD borehole processing
    - Extracted CSD boreholes within 1 mile of planned flight lines.
    - Extracted project ground surface elevation to the CSD boreholes.
    - Used the stratigraphy table associated with the CSD borehole database to determine the depth/elevation of the first encountered 'Bedrock'.
    - Added the CSD borehole bedrock depths to the working table.

Borehole bedrock elevation interpolation:

- Converted the working table of NE-DNR and CSD bedrock boreholes into a point shapefile.
- Interpolated the borehole point shapefile into a continuous raster dataset using the kriging geostatistical model and exported to a 300 ft cell size grid, snapped to the project ground surface DEM.
- Calculated the residuals of the actual measured top of bedrock elevation to the interpolated top of bedrock elevation.
- Reviewed any borehole where the residual was > 30 ft or < -30 ft. The value of 30 was used because it is a general representation of the degree of error while logging a borehole with mud rotary drilling techniques as it is approximately one drill stem length. Flagged and reviewed those boreholes that appeared to be anomalous.
    - Most, if not all, of the reviewed wells contained lithology that was a mix of bedrock and unconsolidated material making it unclear about where the top of bedrock actually was in the log. In these cases, the borehole was removed from the point shapefile used for interpolation.
- Re-interpolated the point shapefile following the same kriging geostatistical model and snapped to the 300 ft project ground surface DEM.

- The final borehole shapefile used for interpolation of the borehole-only bedrock surface contained 429 data points and is depicted in Figure 5-3 below.

The bedrock surface was used as a guide in the interpretation of the bedrock within the AEM data profiles described next.

5.1.4 Interpretative 2D Profiles

After final combination of the AEM data, characterization of the subsurface was performed in cross-section format using Datamine Discover Profile Analyst (Datamine, 2024). During interpretation, the horizontal and vertical scale of the profiles were adjusted to facilitate viewing. The color scale of the resistivity data was also adjusted to illuminate subtle differences in the resistivity structure within the inverted AEM resistivity data related to the area being interpreted.

The first step in the interpretation is digitizing the contacts between the geologic units including: Quaternary (***Q***), Cretaceous Dakota Group (***Kd***), and the undifferentiated Permian Chase Group and the Permian Council Grove Group (***P***). The interpretive process benefited from the use of CSD and NE-DNR borehole logs which provided lithologic, stratigraphic, and geophysical information. The interpretations were simultaneously checked against the CSD's Nebraska bedrock geology map (Burchett, 1986) and the geological outcrop map (Burchett et al., 1972). However, horizontal extents of geologic units may differ from Burchett (1986) due to the final interpretation of the AEM.

The interpretation began with picking the ***P/Kd*** and ***P/Q*** contact. The borehole-only surface was mapped on the profiles and was used as a guide for the interpretation. The interpretation of the ***P*** included examining the AEM profile section for a high electrical resistivity layer that was also indicated in the borehole logs as the base of aquifer. Many of the CSD as well as the NE-DNR borehole logs stop at the ***P*** due to that stratigraphic unit not being considered an aquifer since it is composed predominantly of limestone and shale. Many of the CSD boreholes have stratigraphic calls that assist in the location of the ***P***. For the profiles, the clipping distance from the flight line, or maximum distance from the flight line at which a borehole is displayed on the profile, was set independently for the CSD boreholes and the NE-DNR boreholes. Typically, the CSD clipping distance was set to 1,320 ft and the NE-DNR boreholes was set to 1,000 ft. The inversion DOI was also inspected during interpretation of the profiles. The ***P*** can be challenging to interpret due to the variable nature of the limestone and shale and the often lack of electrical contrast with the variable electrical resistivity of the ***Kd***. This is the reason the borehole-only surface was used as a reference in the interpretation of the ***P/Kd*** and ***P/Q*** contact.

The interpretation of the ***Kd/Q*** contact included examination of the CSD and NE-DNR boreholes and comparison with the AEM resistivities. The borehole information is critical in the determination of an estimated top of the ***Kd***. The following borehole log characteristics were used to locate the top of the ***Kd***: 1) ***Kd*** is indicated on the CSD borehole stratigraphic logs; 2) There is an indication of sandstone, siltstone, or shale in the CSD borehole lithology logs; 3) There is an indication of sandstone, siltstone, shale in the NE-DNR lithology logs; and 4) There is a resistivity change or layer indicating ***Q*** loess or till deposits.

Patterns in the resistivity were also used to match the difference in the ***Q*** and the ***Kd***. In the areas of coarse ***Kd*** deposits and Quaternary ***Q*** deposits, the interpretation is more challenging due to a lack of resistivity contrast. Resistivity zone patterns were used to match these areas and continuations of the ***Kd*** from under the low resistivity loess/till deposits were used to estimate the contact.

It should be noted that the top of the ***Kd*** as interpreted is an estimate. This is due to the challenge of both the lithology interpretation of drill cuttings of the ***Kd*** and the low electrical resistivity contrast. Throughout this report the ***Kd*** will be shown as a dashed line and care needs to be exercised in the use of the interpreted top of ***Kd*** surfaces. The white areas within the profiles are zones that were cut from the AEM data due to EM-coupling.

East-west flight line L500200, presented in Figure 5-4, is approximately 35-mile-long and crosses Hwy 136, Elm Creek, Hwy 77, the Big Blue River, and 162nd Rd on the northern edge of the survey area. There are two CSD test holes along the line within 1,320 feet (1/4 mile), *63-B-44 and 70-B-49*. Both the AEM and CSD test hole *63-B-44* indicates the ***Kd*** at depth and test hole *70-B-49* indicates the Permian Chase Group (***P***) at depth. The eastern portion of the flight line is dominated by low electrical resistivity materials within the Quaternary (***Q***) section indicating clay rich tills. *70-B-49* also indicates till and clays in the ***Q*** section.

An area of high electrical resistivity material is noted in the central portion of the flight line and is in the area that indicates sands. Several NE-DNR registered wells are in the area and indicate sands. On the western end of the flight line, several NE-DNR registered wells indicate sandstone of the ***Kd***. The high resistivity zone where the flight line crosses the Big Blue River indicates the high bedrock of the Permian Chase Group.

At the bottom of the profile a low resistivity area is encountered throughout the LBBNRD AEM survey area where the resistivities are all < 7 ohm-m. These areas are interpreted as saline water. Note that the AEM section extends below the depth of the profile (~ 450 feet) as indicated in Table 4.3 (over 1000 ft).

East-west flight line L500500, presented in Figure 5-5, is approximately 29.5-mile-long and crosses Hwy 103, Elm Creek, Hwy 77, the Big Blue River, and 162nd Rd in the center of the survey area. There are two CSD test holes along the line within 1,320 feet (1/4 mile), *66-B-44 and 77-B-44*. The AEM and both the CSD test holes indicate the ***Kd*** at depth. CSD test hole *77-B-44* indicates the ***P*** at depth. The eastern portion of the flight line is again dominated by low electrical resistivity materials within the ***Q*** section indicating clay rich tills.

There is a small deposit of high resistivity materials above the water table that may be a good sand and gravel deposit. An area of high electrical resistivity material is noted in the central portion of the flight line and is in the area that indicates sands as was observed along line L500200 in Figure 5-4. Several NE-DNR registered wells are in the area and indicate sands and some gravel. On the western end of the flight line several NE-DNR registered wells indicate sandstone of the ***Kd***.

As before, the white areas within the profiles are zones that were cut from the AEM data due to EM-coupling from powerlines or other infrastructure. The low resistivity zone is also observed at the base of the profiles indicating saline water.

North-south line L400801, presented in Figure 5-6, is approximately 10-mile-long and crosses PWF Road, Indian Creek, and Hwy 136 on the western end of the survey area. There are no CSD test holes within 1,320 feet of the flight line. The AEM and the NE-DNR registered wells both indicate that the ***Kd*** and ***P*** are present. Several of the NE-DNR registered wells indicate the top of the ***P*** due to their depth extent and the ***P*** not being an aquifer and several NE-DNR registered wells indicate sandstone.

The areas of the ***Q*** are dominated by clay and silt. At approximately northing 130000 there is the presence of a high resistivity zone in the ***Q*** materials directly above the ***Kd***. On the southern end of the line there are several registered wells within the ***Kd*** that are also high in electrical resistivity indicating sand and sandstone. A low resistivity zone is observed at the base of the profile within 250 feet of the surface in the southern portions of the profile which likely indicate saline water.

North-south line L402801, presented in Figure 5-7, is approximately 5-mile-long and is east of the Big Blue River within the eastern third of the survey area. There are no CSD test holes within 1,320 feet of the flight line. The AEM and the NE-DNR registered wells both indicate ***P*** bedrock. Two NE-DNR registered wells also indicate the top of the ***P*** due to their depth extent and the ***P*** not being an aquifer. The two NE-DNR registered wells indicate sand and gravel at their bases with a thick sequence of overlying clay in the ***Q***.

A shallow well on the northern side of the flight line indicates clay overlying a thin sand zone. Low electrical resistivity materials are composed of clay rich tills overlying sand and gravels that are deposited on the ***P***. The ***P*** bedrock is high on the southern end of the flight line and has a thin layer of low electrical resistivity ***Q*** material overlying. A low resistivity zone is observed at the base of the profile within 200 feet of the surface throughout most of the profile indicating saline water.

The above examples illustrate the interpretive process that was used on the profiles provided within this report. All the flight lines are presented in *Appendix 1 – 2D Profiles* with the resulting hydrogeological interpretations. Details for each flight line is presented as well as the corresponding CSD and NE-DNR registered wells within the specified distances.

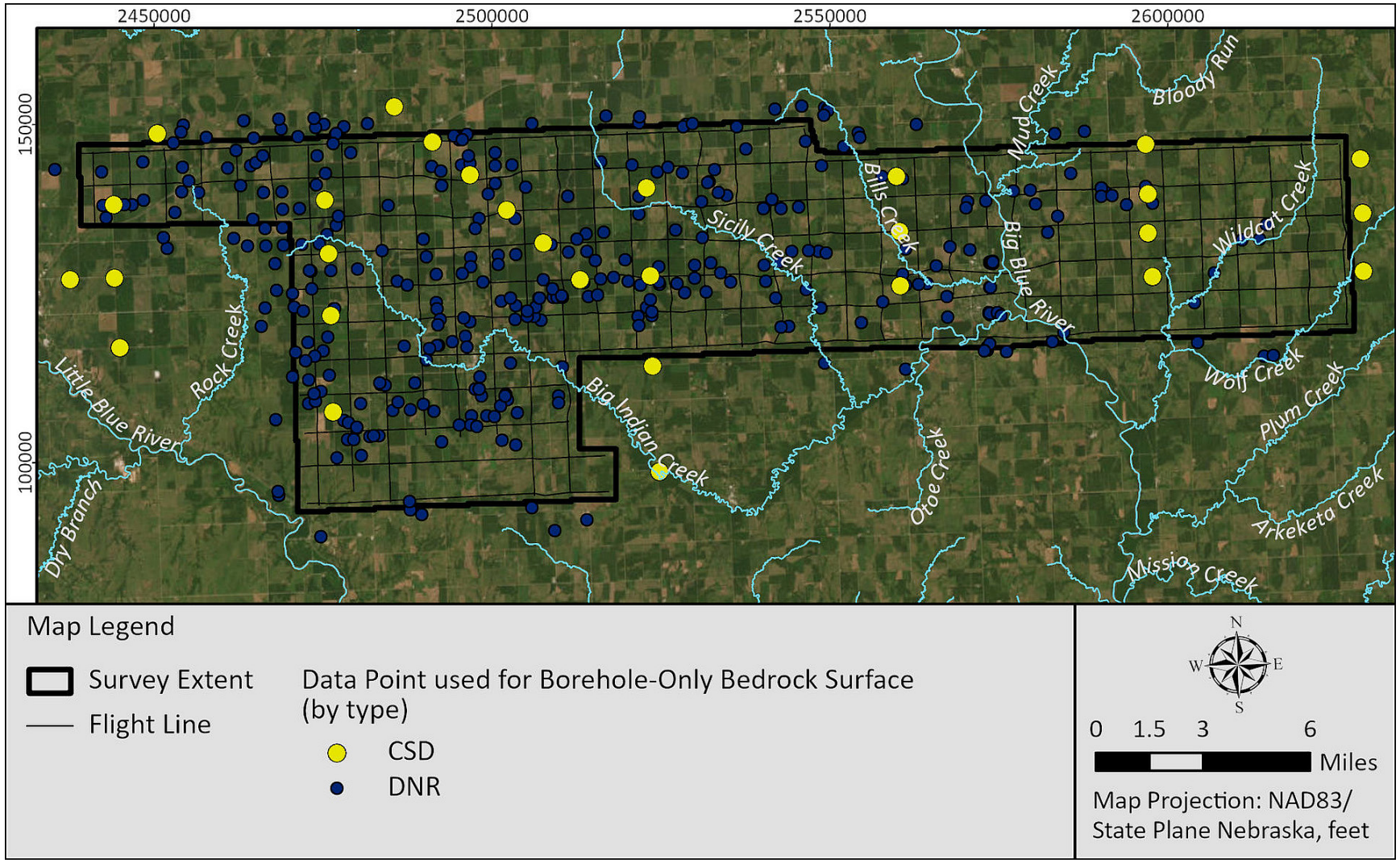


Figure 5-3. Map of the project boundary showing the data points used to interpolate the bedrock surface elevation. This "borehole only" interpolated bedrock surface was used as a guide in the interpretation of the AEM data. The projection is NAD83 State Plane Nebraska (feet).

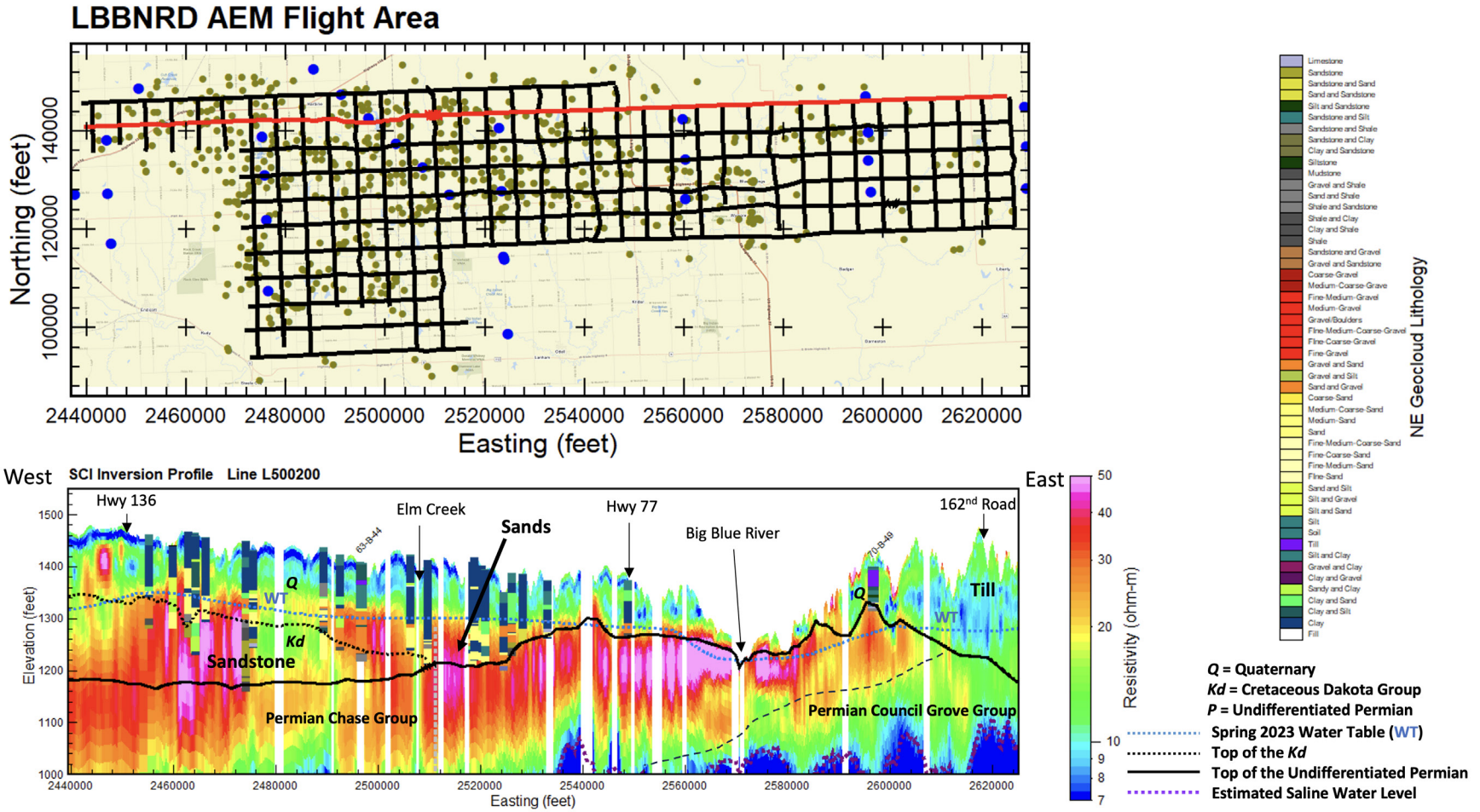


Figure 5-4. 35-mile-long east-west line L500200. The top map displays the flight lines as black lines and the flight line shown in the profile as a red line on a general map of the area. Blue dots indicate CSD test holes and olive dots are the NE-DNR registered wells. Lithology from CSD test holes within 1,320 feet and NE-DNR registered wells within 1,000 feet are projected on the flight line. Gaps in the profile are due to EM decoupling from infrastructure or areas that were not flown due to FFA regulations. Projection is NAD83 State Plane Nebraska (feet), the vertical datum is NAVD88 (feet).

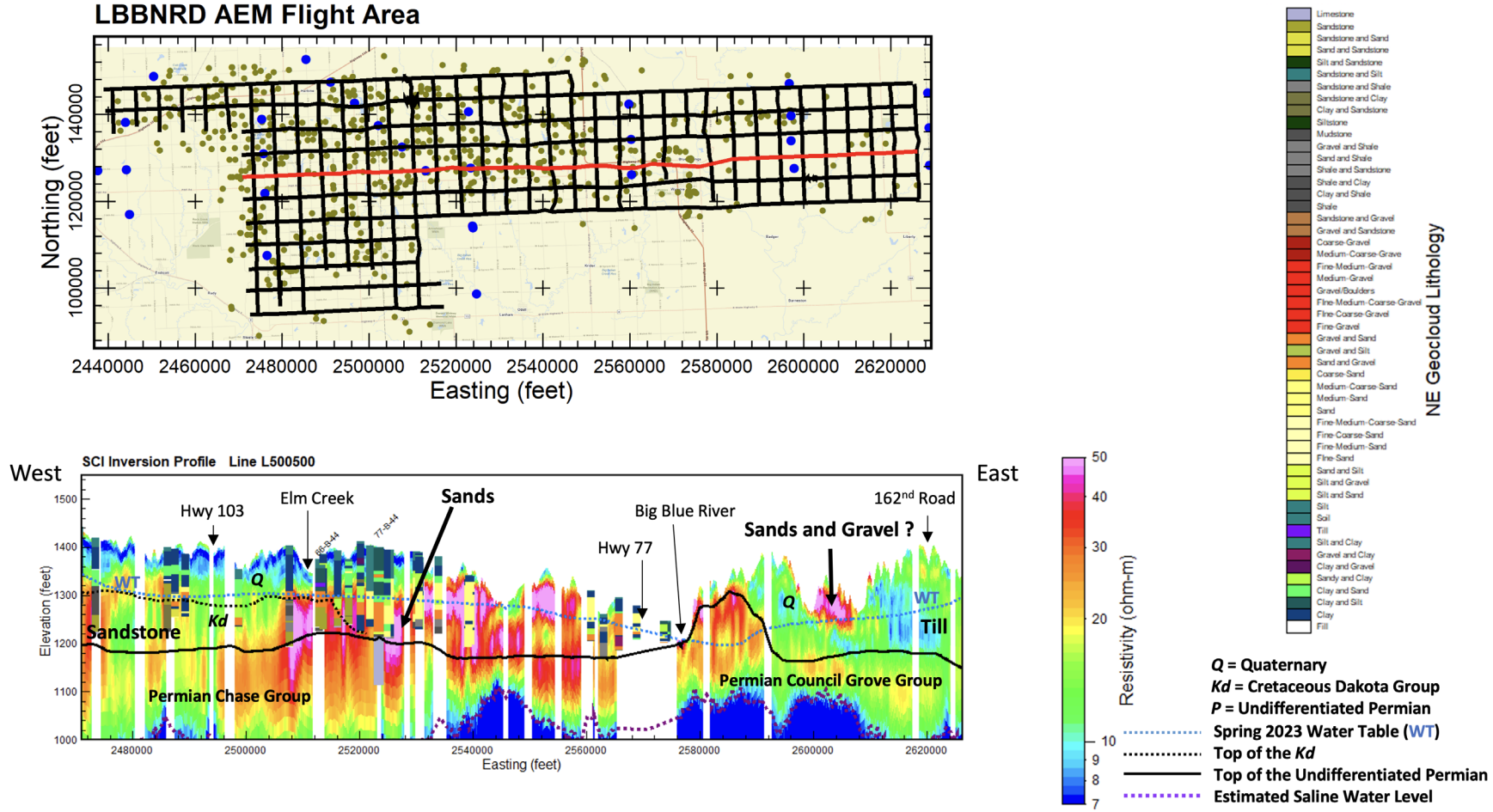


Figure 5-5. 29.5-mile-long east-west line L500500. The top map displays the flight lines as black lines and the flight line shown in the profile as a red line on a general map of the area. Blue dots indicate CSD test holes and olive dots are the NE-DNR registered wells. Lithology from CSD test holes within 1,320 feet and NE-DNR registered wells within 1,000 feet are projected on the flight line. Gaps in the profile are due to EM decoupling from infrastructure or areas that were not flown due to FFA regulations. Projection is NAD83 State Plane Nebraska (feet), the vertical datum is NAVD88 (feet).

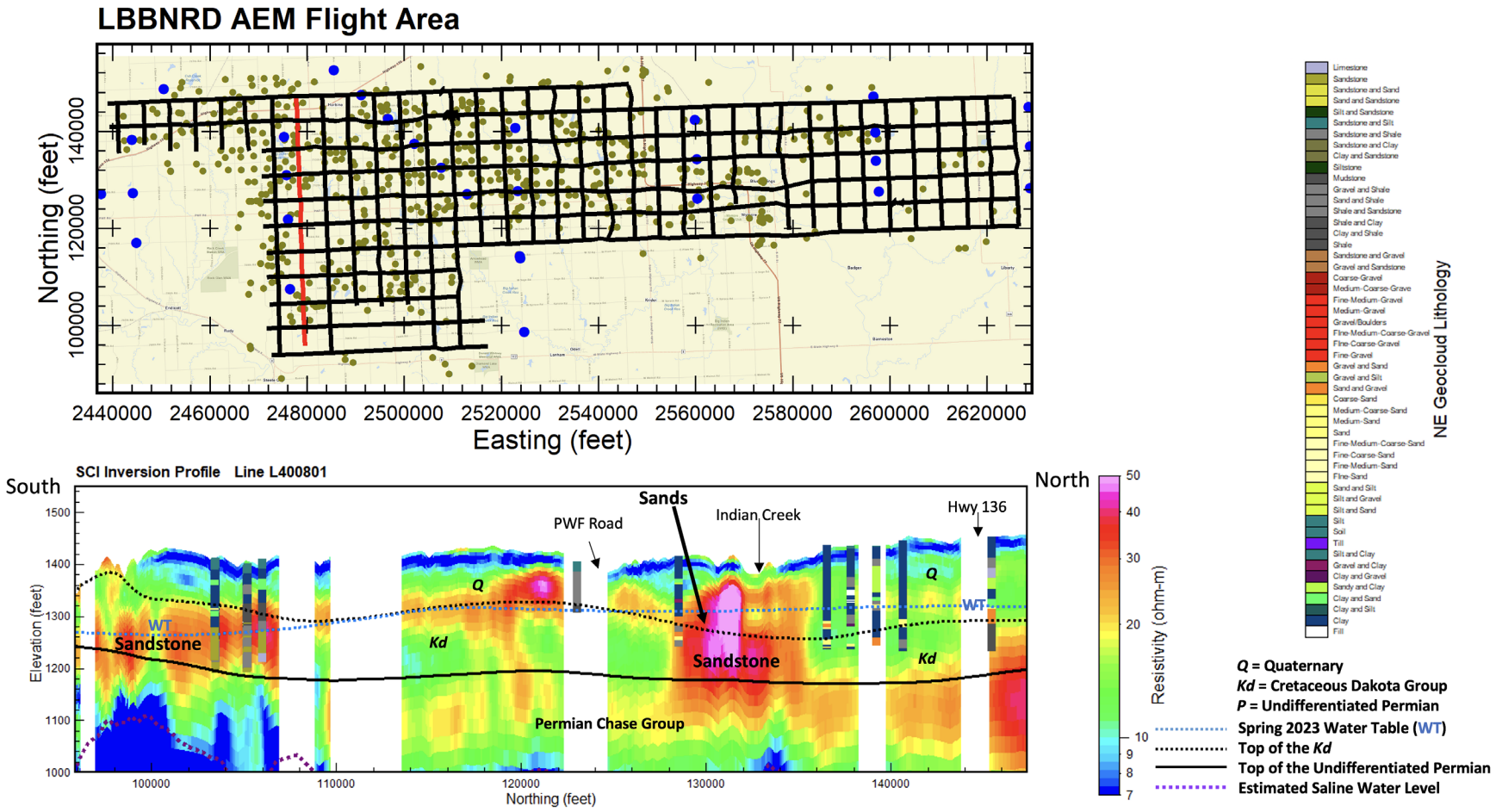


Figure 5-6. 10-mile-long north south line L400801. The top map displays the flight lines as black lines and the flight line shown in the profile as a red line on a general map of the area. Blue dots indicate CSD test holes and olive dots are the NE-DNR registered wells. Lithology from CSD test holes within 1,320 feet and NE-DNR registered wells within 1,000 feet are projected on the flight line. Gaps in the profile are due to EM decoupling from infrastructure or areas that were not flown due to FFA regulations. Projection is NAD83 State Plane Nebraska (feet), the vertical datum is NAVD88 (feet).

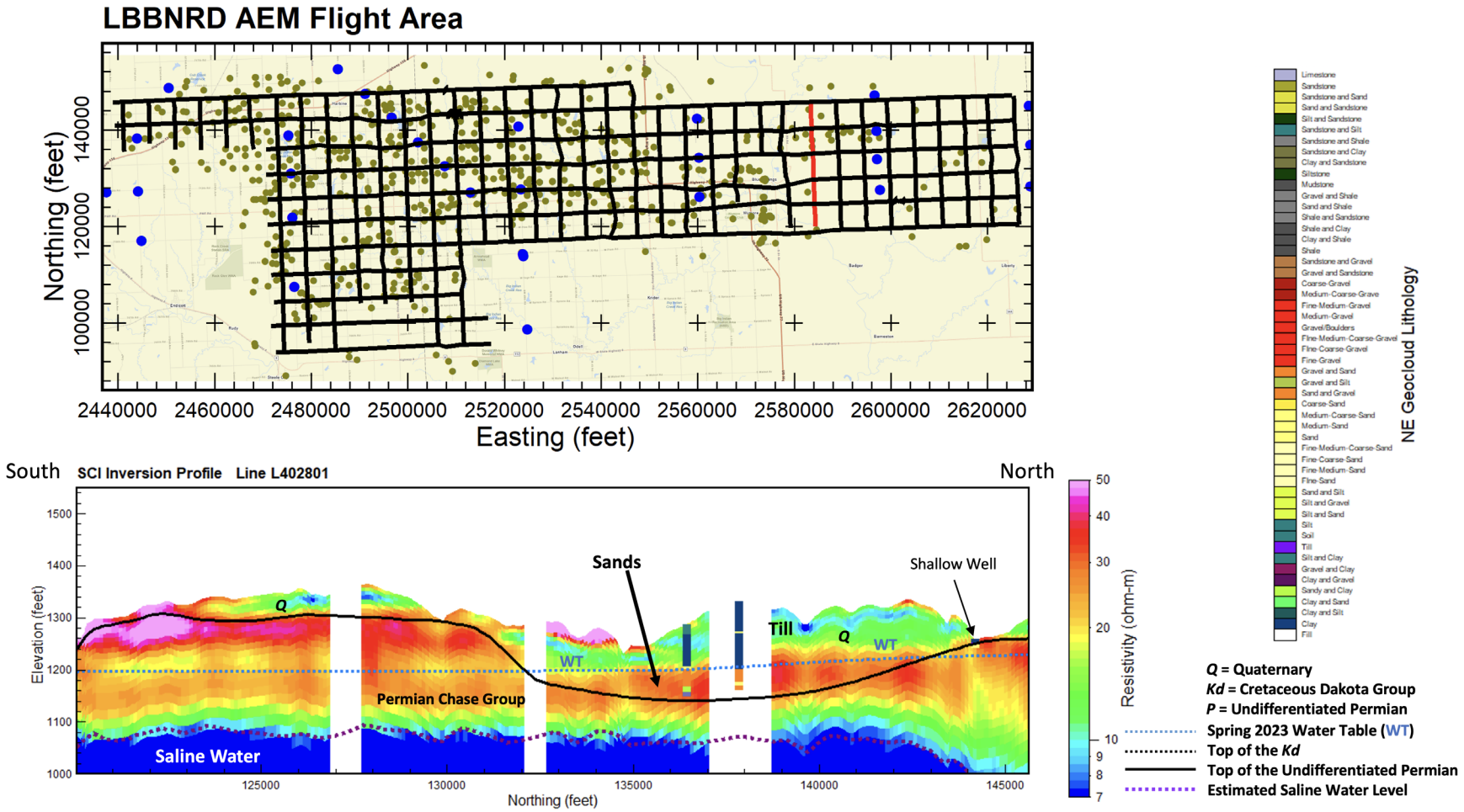


Figure 5-7. 5-mile-long north south line L402801. The top map displays the flight lines as black lines and the flight line shown in the profile as a red line on a general map of the area. Blue dots indicate CSD test holes and olive dots are the NE-DNR registered wells. Lithology from CSD test holes within 1,320 feet and NE-DNR registered wells within 1,000 feet are projected on the flight line. Gaps in the profile are due to EM decoupling from infrastructure or areas that were not flown due to FFA regulations. Projection is NAD83 State Plane Nebraska (feet), the vertical datum is NAVD88 (feet).

5.1.5 Interpretative Surface Grids

After the AEM data were interpreted, the interpretations (i.e., points with elevations that represent the top of specific geologic units) were extracted into a GIS shapefile so that continuous raster surfaces could be developed. Please note that the terms grid, surface, and raster are used interchangeably, and all refer to a continuous dataset made up of cells, with each cell being a 300 ft by 300 ft area, where each cell contains elevation data representative at that cell location.

In addition to the AEM data interpretation points, CSD boreholes and outcrop points with elevation data were added to the AEM interpretation point shapefile. Outcrop points represent those approximate locations where a bedrock outcrop (either ***Kd*** and/or ***P***) was noted on the map by Burchett et al. (1972). On the map (Burchett et al., 1972) the outcrops are approximate and are denoted by black markings. A GIS polygon shapefile was digitized from those black markings and points were made within those outcrop polygons to act as "dummy" points for the interpolation process.

Figure 5-8 displays digitized outcrop polygons overlaying the Burchett et al. (1972) map. Table 5-2 displays the number of data points used to interpolate each surface.

Table 5-2. Number of data points used to interpolate the elevation of the top of *Kd* and *Permian* surfaces.

Geologic Unit	# of AEM Data Points	# of CSD Boreholes	# of Outcrop Points
Cretaceous Dakota Group (*Kd*)	**408**	**15**	**43**
Undifferentiated Permian (*P*)	**657**	**14**	**45**

The elevation point data were interpolated for each geologic unit into a continuous surface using the kriging geostatistical model and exported to 300 ft cell size resolution raster datasets. The surfaces were corrected with the 300 ft resolution ground surface DEM so that each surface was restrained to less than or equal to the DEM minus 3' elevation.

Figure 5-9 and Figure 5-10 are maps displaying the top elevation surfaces of the ***Kd*** and Permian ***P*** within the 2023 LBBNRD AEM survey area, respectively. Using the top elevation grids for the ***Kd*** and ***Permian*** units, a top of bedrock elevation surface was produced by mosaicking, or stitching, the two grids together. Figure 5-11 is a map of the elevation of the top of bedrock surface within the 2023 LBBNRD AEM survey area.

Each top elevation surface was subtracted from the DEM to calculate the depth (in feet) to the top of each surface. Figure 5-12, Figure 5-13, and Figure 5-14 are maps displaying the depth to the tops of the ***Kd,*** Permian ***P,*** and bedrock, respectively.

Total thickness for the ***Q*** and ***Kd*** were calculated using the top of elevation surfaces and DEM in ESRI's raster calculator. Table 5-3 summarizes the raster calculator input and output for each thickness calculation. The output was set to 'snap' to the 300 ft DEM and then was clipped to each geologic unit extent.

Table 5-3. Summary of the input into ESRI's raster calculator and the resultant output.

Raster Calculator Input	Output Result
DEM – Bedrock	**Q Thickness**
Top of *Kd* - Top of *P*	***Kd* Thickness**

Figure 5-15 and Figure 5-16 are maps displaying the total thickness of ***Q*** and ***Kd***, respectively.

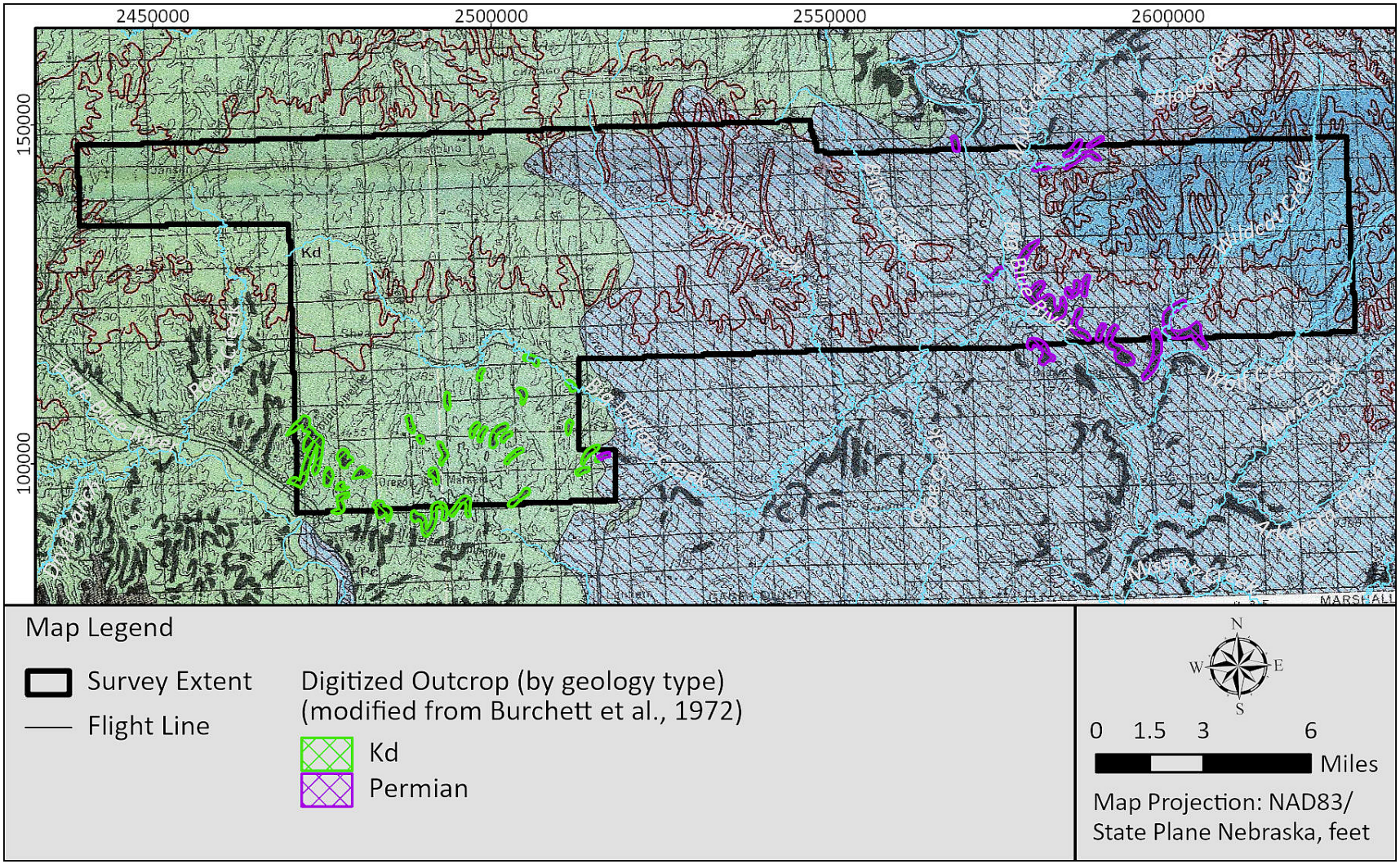


Figure 5-8. Map of digitized bedrock outcrops overlaying map by Burchett et al. (1972). The projection is NAD83 State Plane Nebraska (feet).

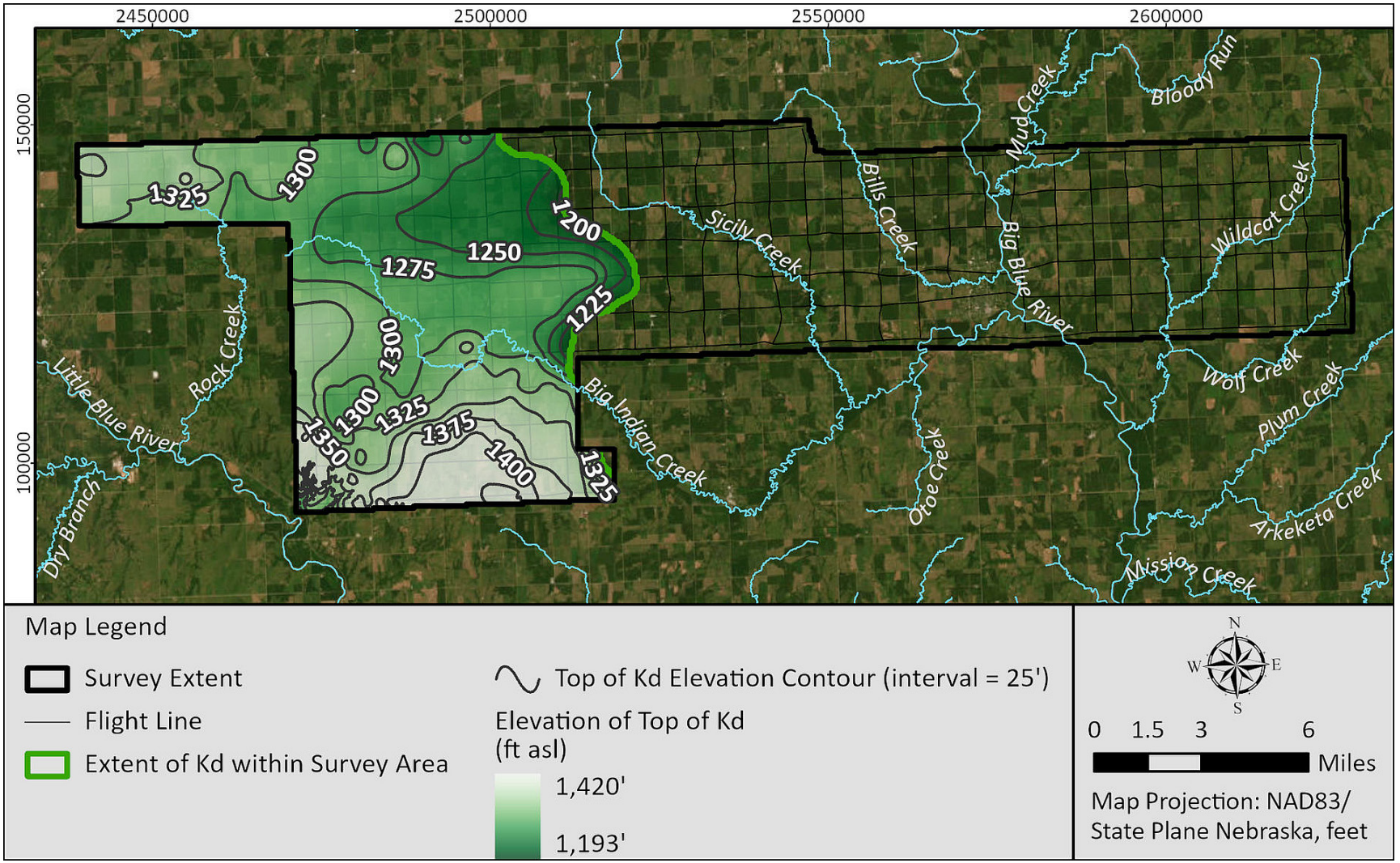


Figure 5-9. Map displaying the elevation of the top of the Cretaceous Dakota (*Kd*) Group. The extent of the *Kd* within the survey area is shown in bright green. Map projection is NAD83 State Plane Nebraska (feet).

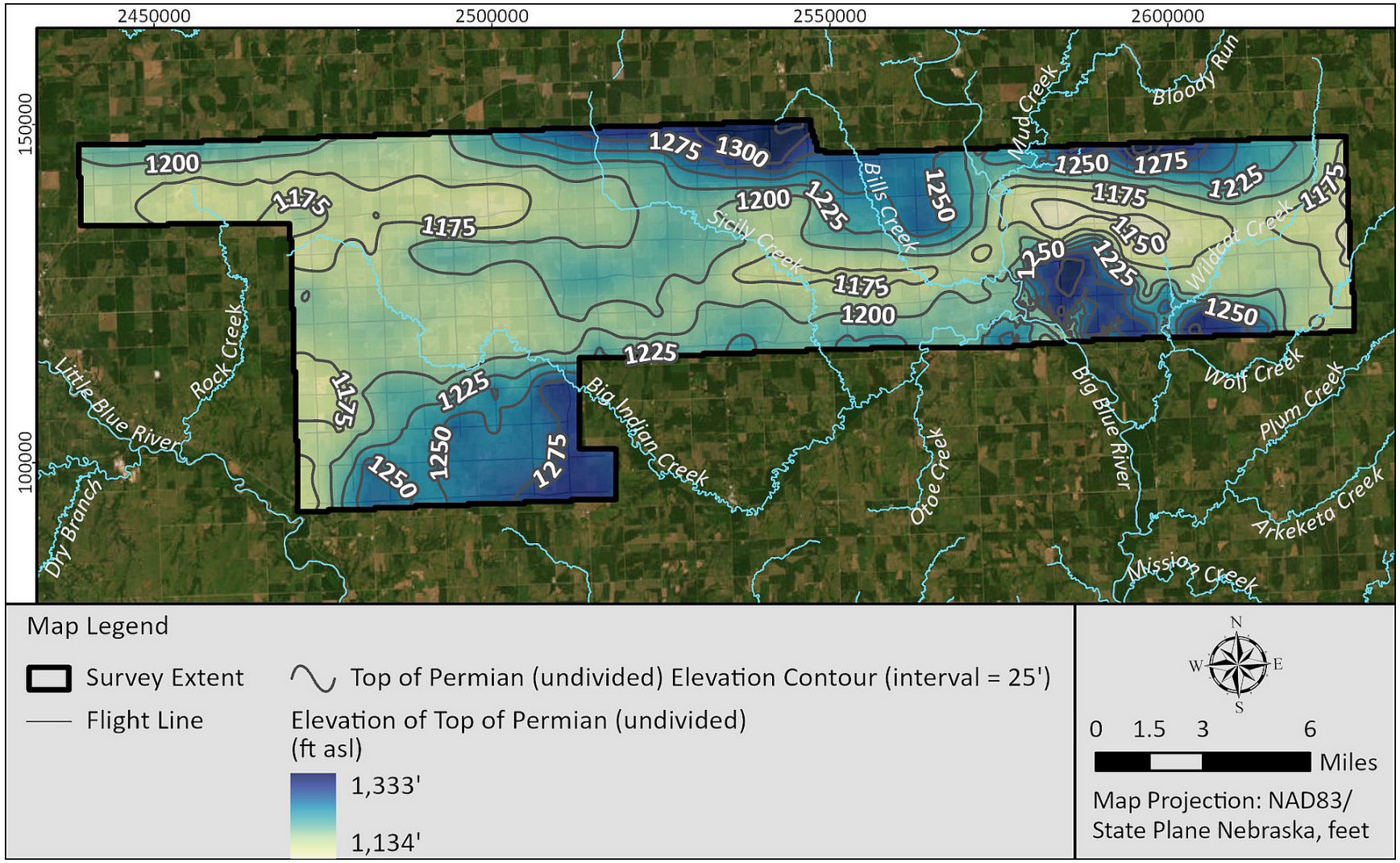


Figure 5-10. Map displaying the elevation of the top of undifferentiated Permian units. Map projection is NAD83 State Plane Nebraska (feet).

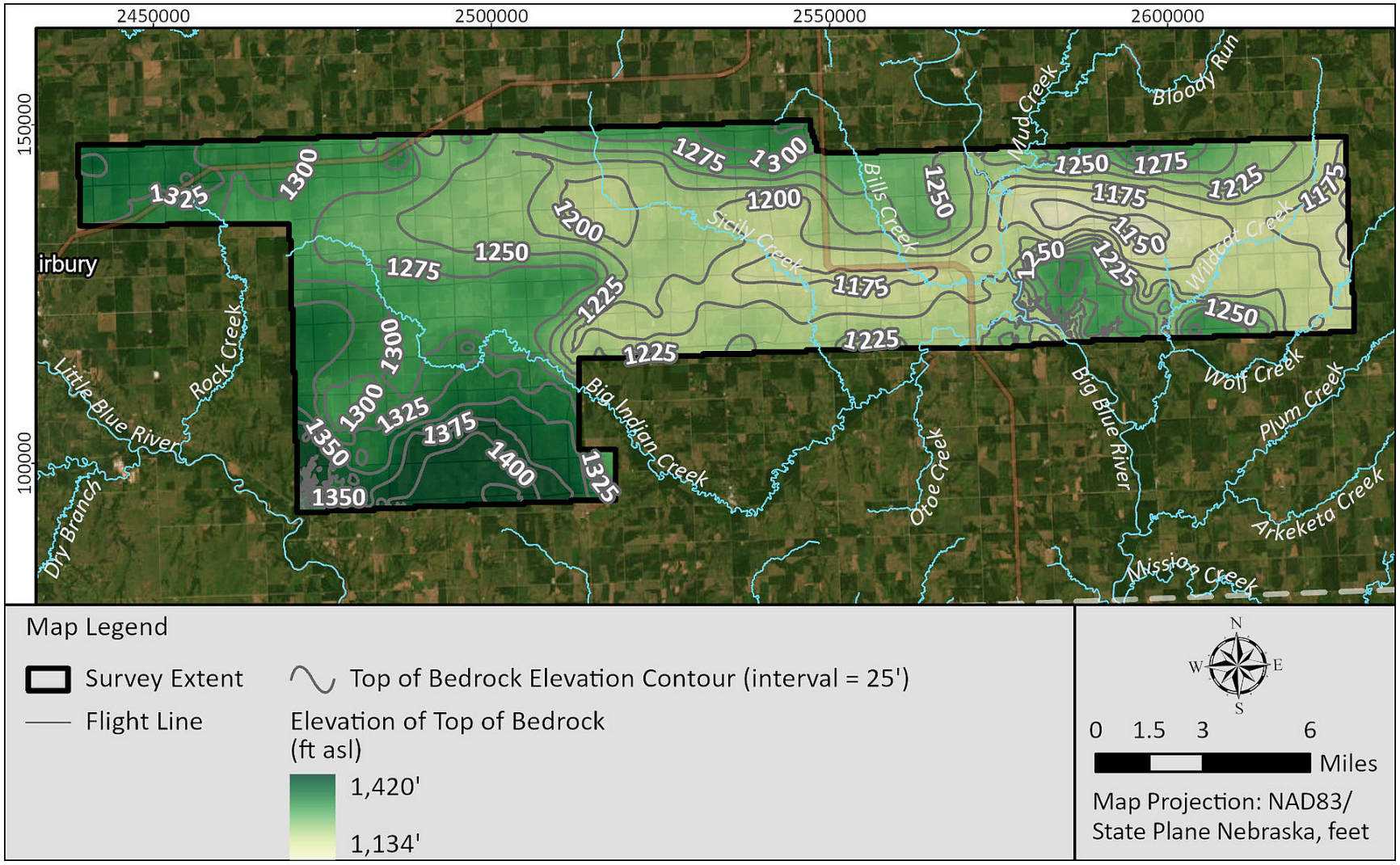


Figure 5-11. Map displaying the elevation of the top of bedrock. Map projection is NAD83 State Plane Nebraska (feet).

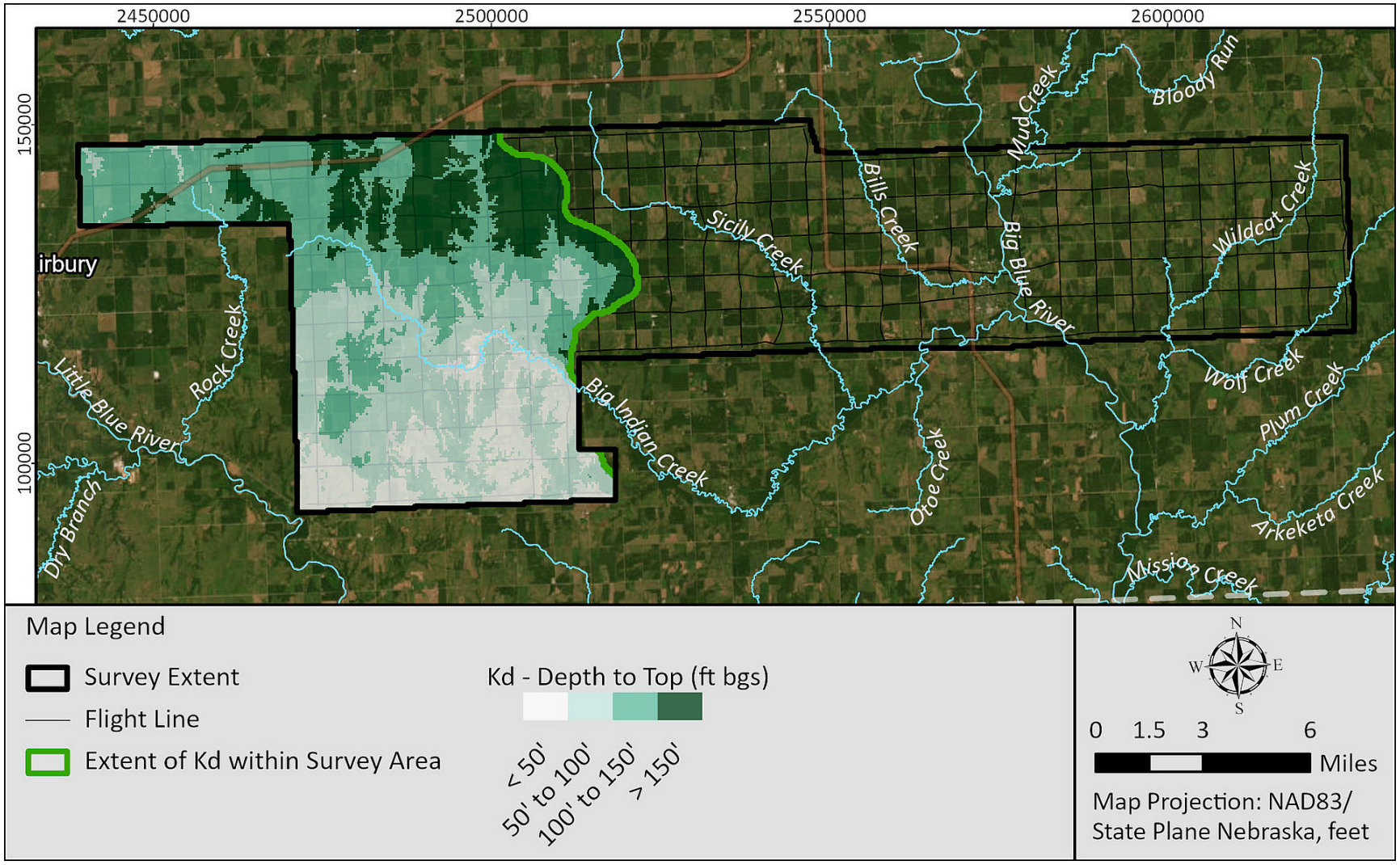


Figure 5-12. Map displaying the depth to the top of Cretaceous Dakota (*Kd*) Group. The extent of the *Kd* within the survey area is shown in bright green. Map projection is NAD83 State Plane Nebraska (feet).

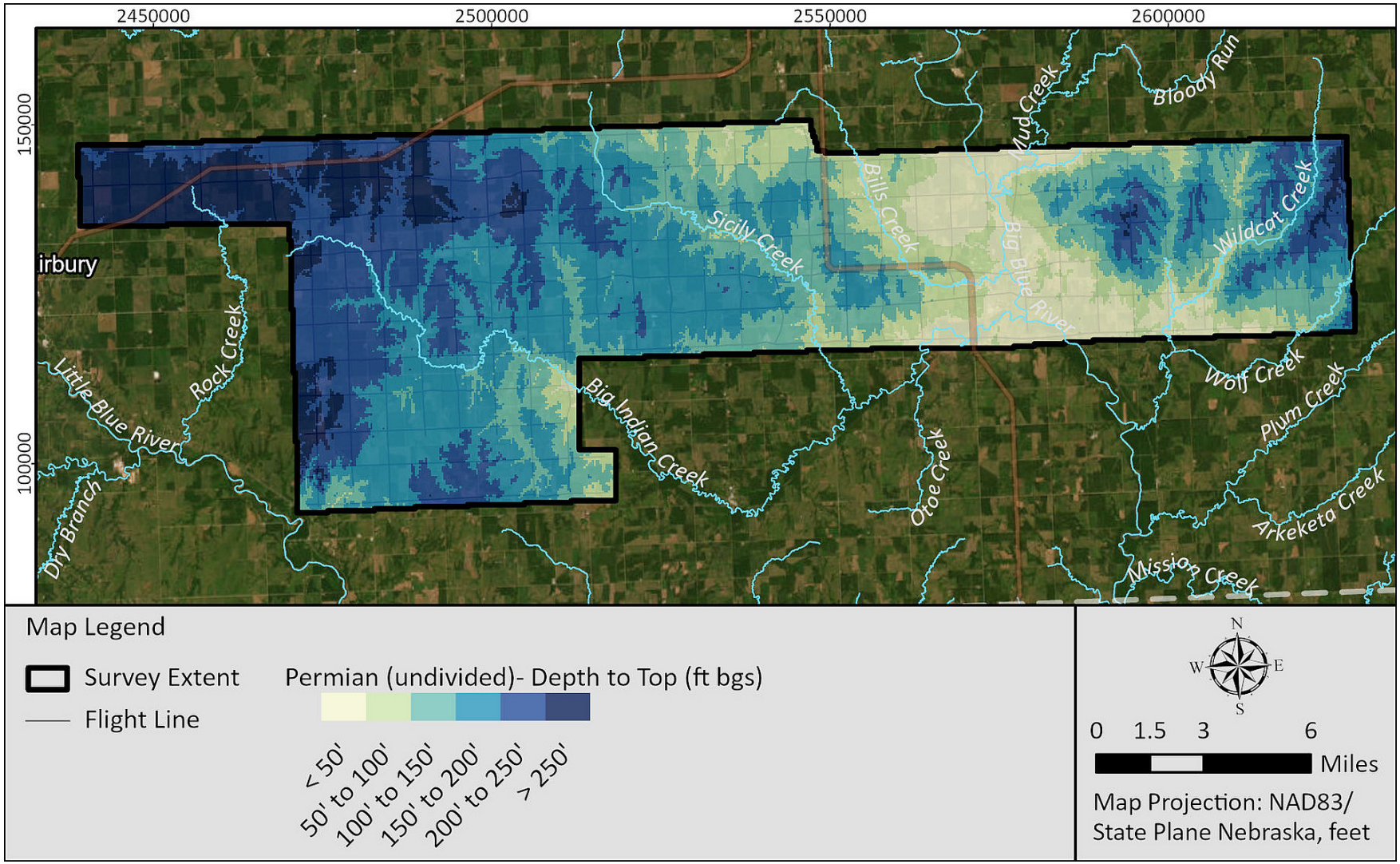


Figure 5-13. Map displaying the depth to the top of undifferentiated Permian units. Map projection is NAD83 State Plane Nebraska (feet).

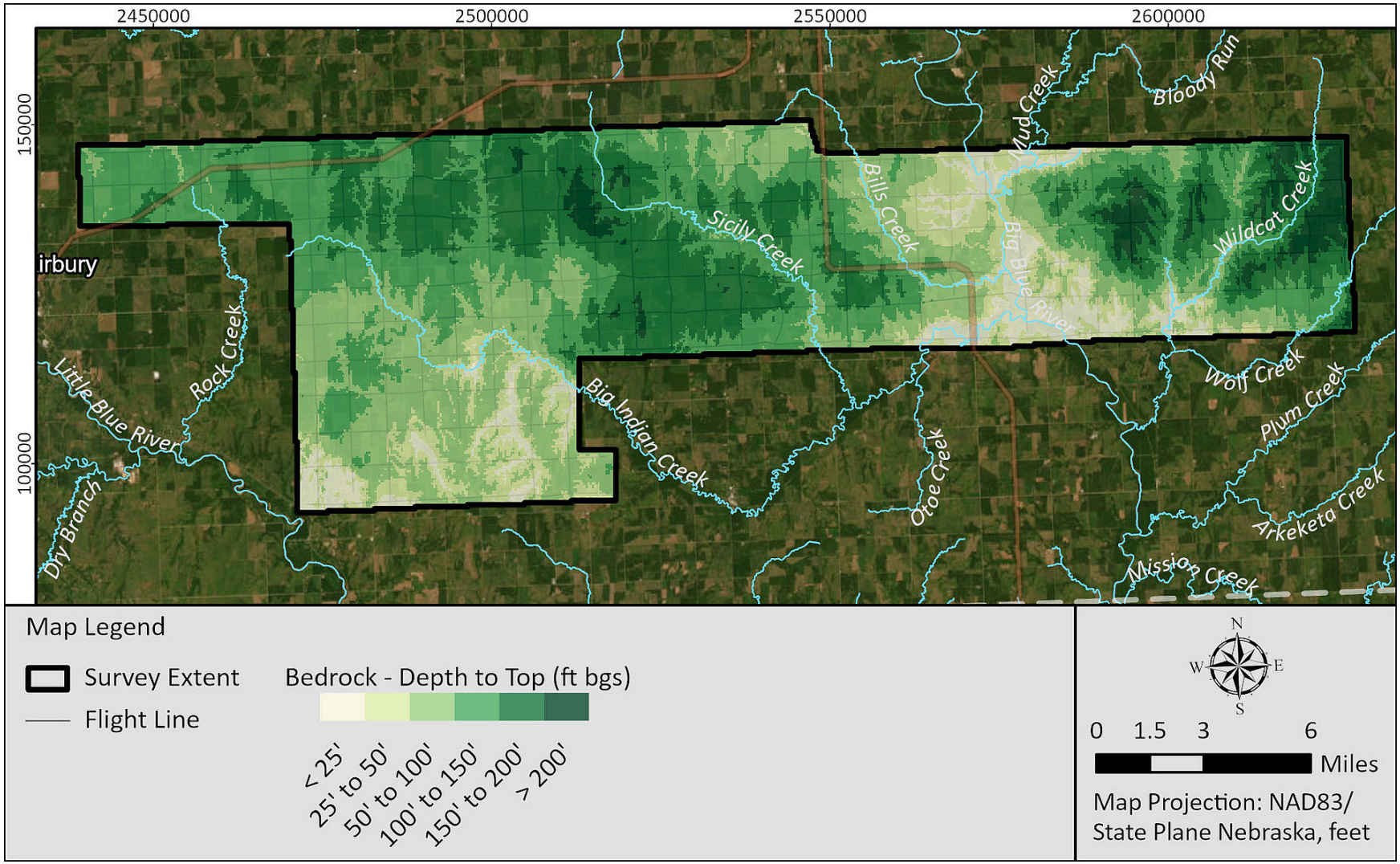


Figure 5-14. Map displaying the depth to the top of bedrock. Map projection is NAD83 State Plane Nebraska (feet).

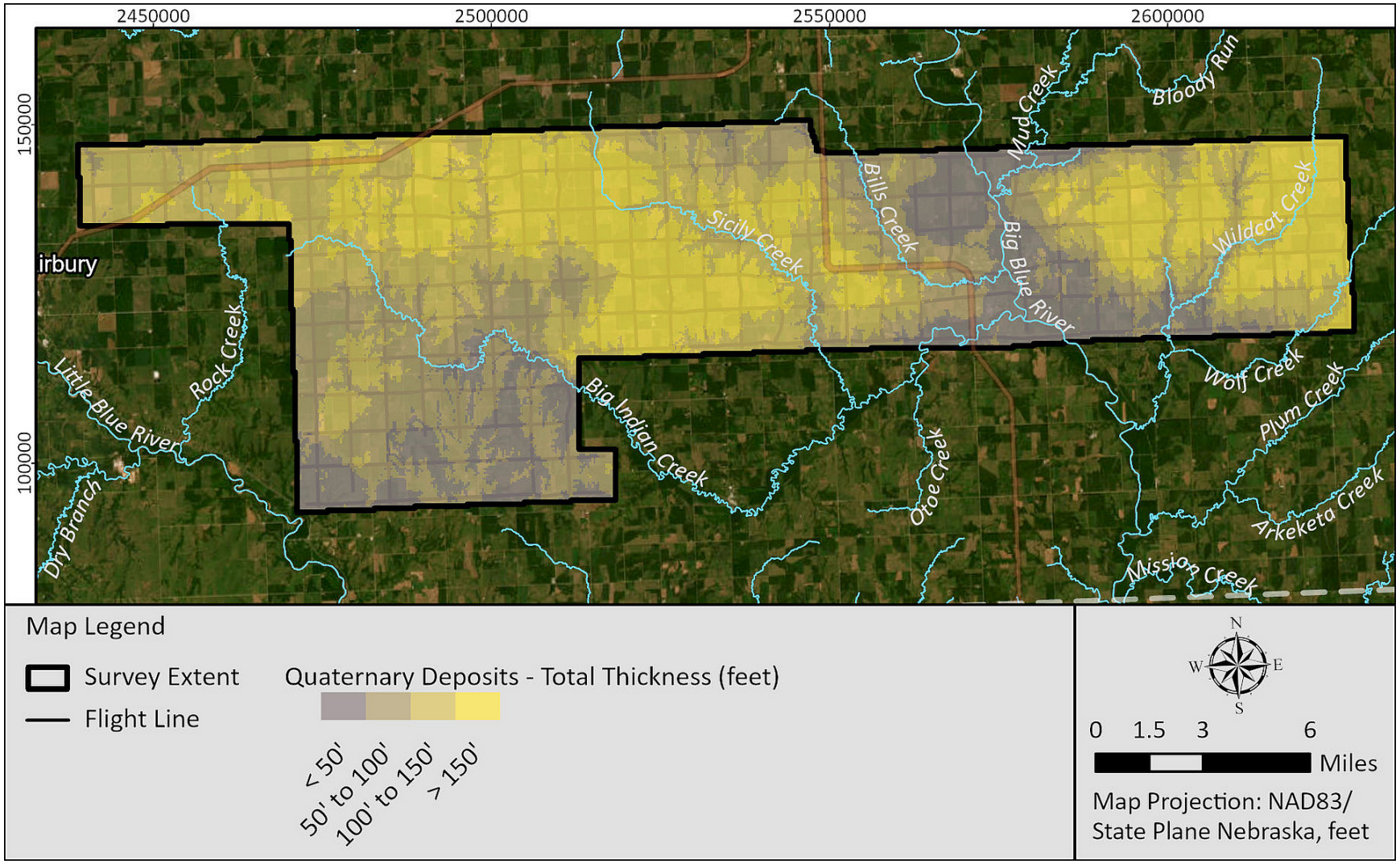


Figure 5-15. Map of displaying the total thickness of the Quaternary (*Q*) material. Map projection is NAD83 State Plane Nebraska (feet).

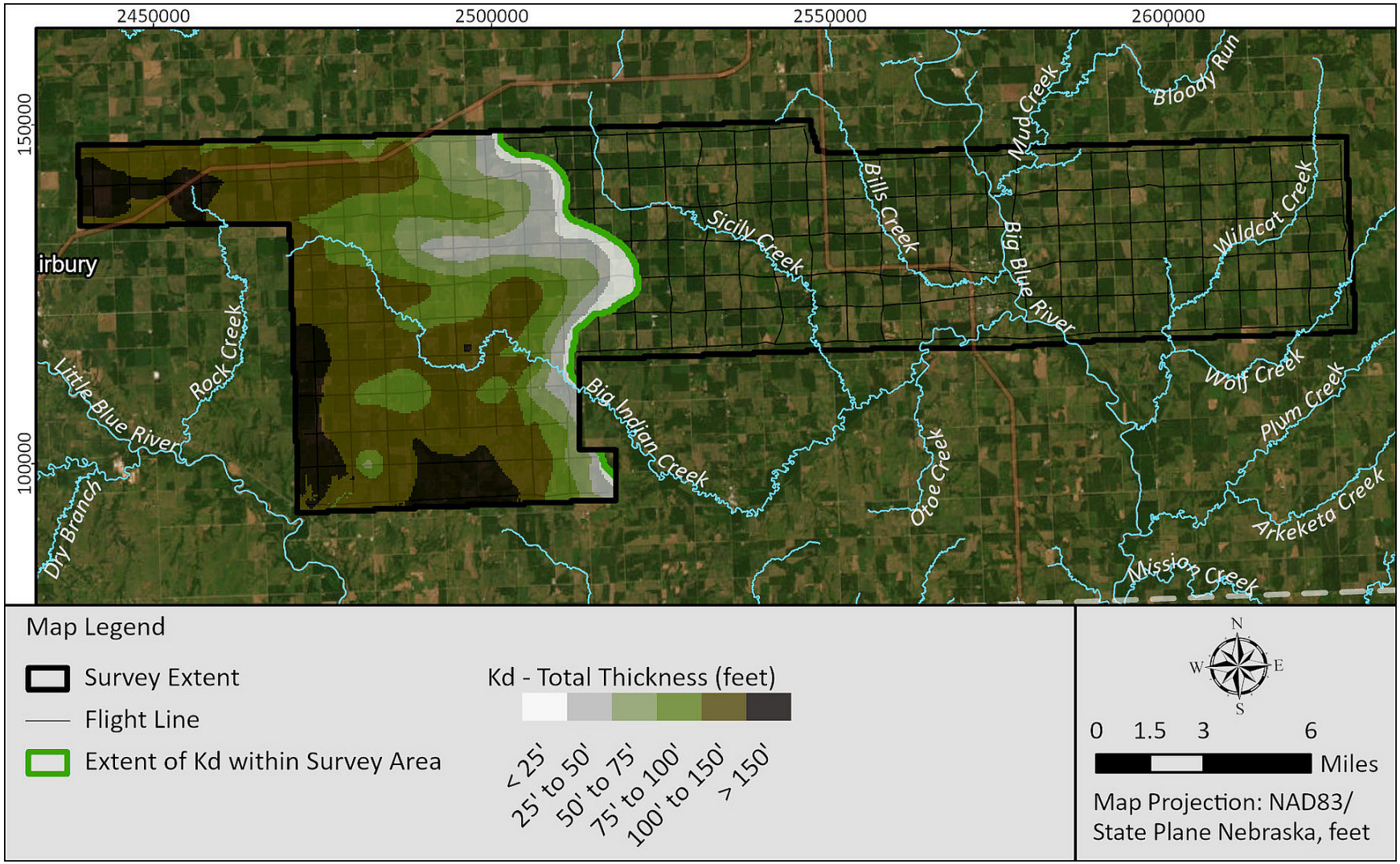


Figure 5-16. Map displaying the total thickness of Cretaceous Dakota (*Kd*) Group. The extent of the *Kd* within the survey area is shown in bright green. Map projection is NAD83 State Plane Nebraska (feet).

5.1.6 Water Table

To assist in the approximation of the saturated materials along the surveyed AEM flight lines, a water table was created. Water level data were provided by LBBNRD as shapefiles, including *County_Measuring_Wells.shp* and *Monitoring_Wells.shp* (Personal communication Tyler Weishahn Assistant Manager LBBNRD December 19, 2023). Both shapefiles provided a robust, consistent dataset of historic water levels and most useful to this project were the water level readings from Spring 2023. Wells from the shapefiles within and adjacent to the survey area were extracted into a single dataset for interpolation into a continuous raster dataset.

However, before interpolating a water table surface, some geographic data gaps, specifically on the east and southwest areas of the survey extent, needed to be filled in as best as possible (if possible at all). To try to fill in some of the data gaps Nebraska Department of Natural Resources (NE-DNR) wells were reviewed to assess the usefulness of the water level data provided in the database. The most useful water levels are the most recent, so wells that were constructed no more than 10 years ago were extracted from the NE-DNR database. Then, wells that fell within the geographic data gaps were selected. The selected data points included eight wells constructed (and water level measured) between 2014 and 2018. These water levels were added to the LBBNRD Spring 2023 water level point dataset. Streams/rivers that flow within the survey area were taken into consideration by adding "stream points" to the water level point dataset. These stream points were added along perennial streams and the ground surface elevation was extracted to each point to represent the water level at that location.

After these four datasets were compiled (two datasets from LBBNRD, NE-DNR wells, and stream points), a surface was interpolated using the inverse distance weighted method in ArcGIS Pro. The interpolated surface was contoured and contours were hand-edited, as needed, to better represent the data, especially the water levels provided by LBBNRD. The contours were converted to a raster surface and a comparison between the actual and interpolated water table elevation (the residuals) was reviewed. Contours were re-edited based on the residuals, if needed, and another raster surface was made from those contours. The final surface was corrected with the project ground surface DEM so that no part of the water table surface was higher in elevation than the ground surface. Figure 5-17 below displays the water table elevation surface along with the control points used to interpolate the surface. The water table elevation was subtracted from the project ground surface DEM to determine the depth to the top of the water table. Figure 5-18 displays the depth to water table in feet.

The saturated thickness of both ***Q*** and ***Kd*** were calculated using both the mosaic tool and raster calculator with the water table, top of bedrock, and top of ***Kd*** surfaces. Figure 5-19 and Figure 5-20 are maps displaying the total saturated thickness of ***Q*** and ***Kd***, respectively.

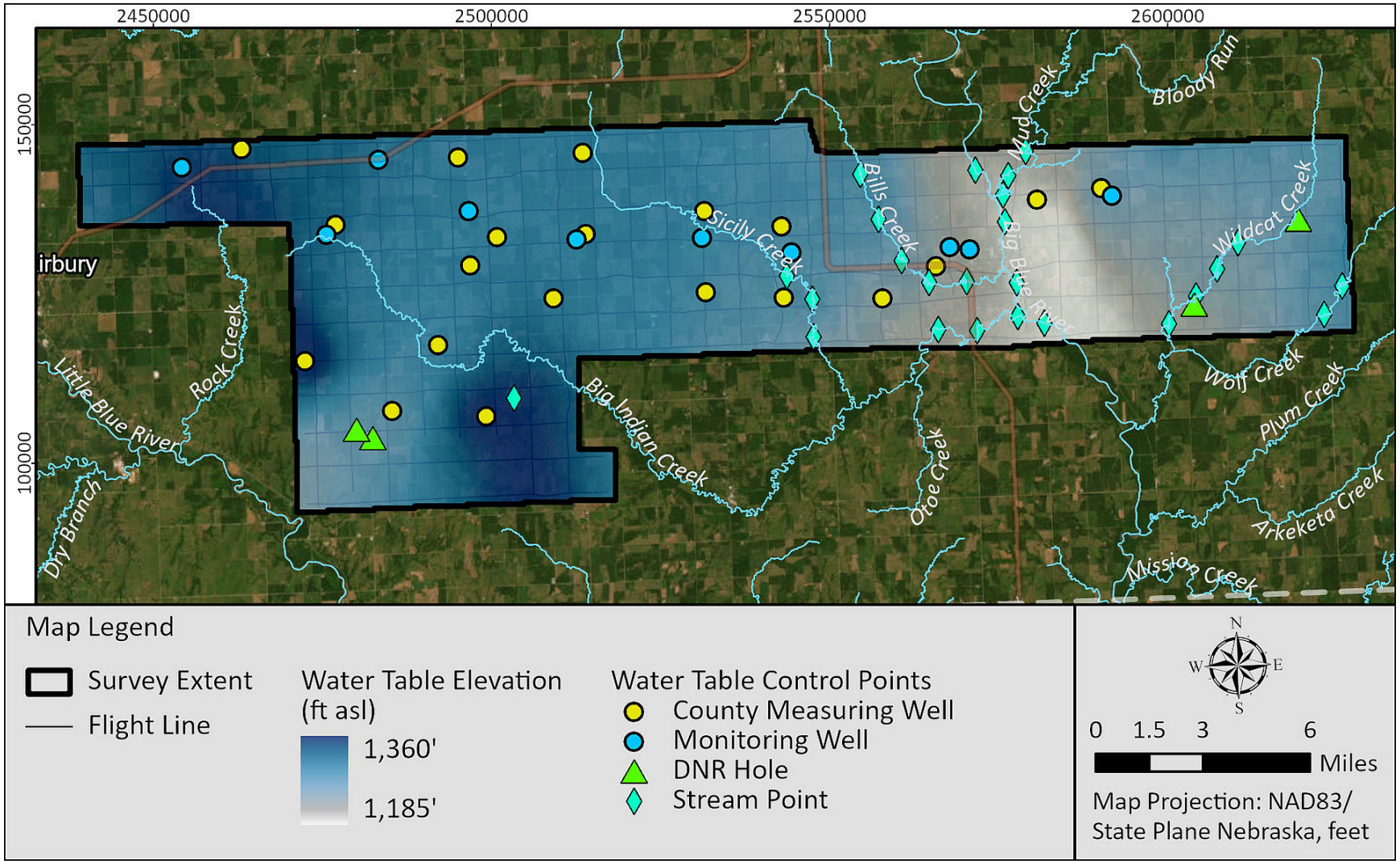


Figure 5-17. Map of water table elevation surface and the control points used to interpolate the surface. The projection is NAD83 State Plane Nebraska (feet).

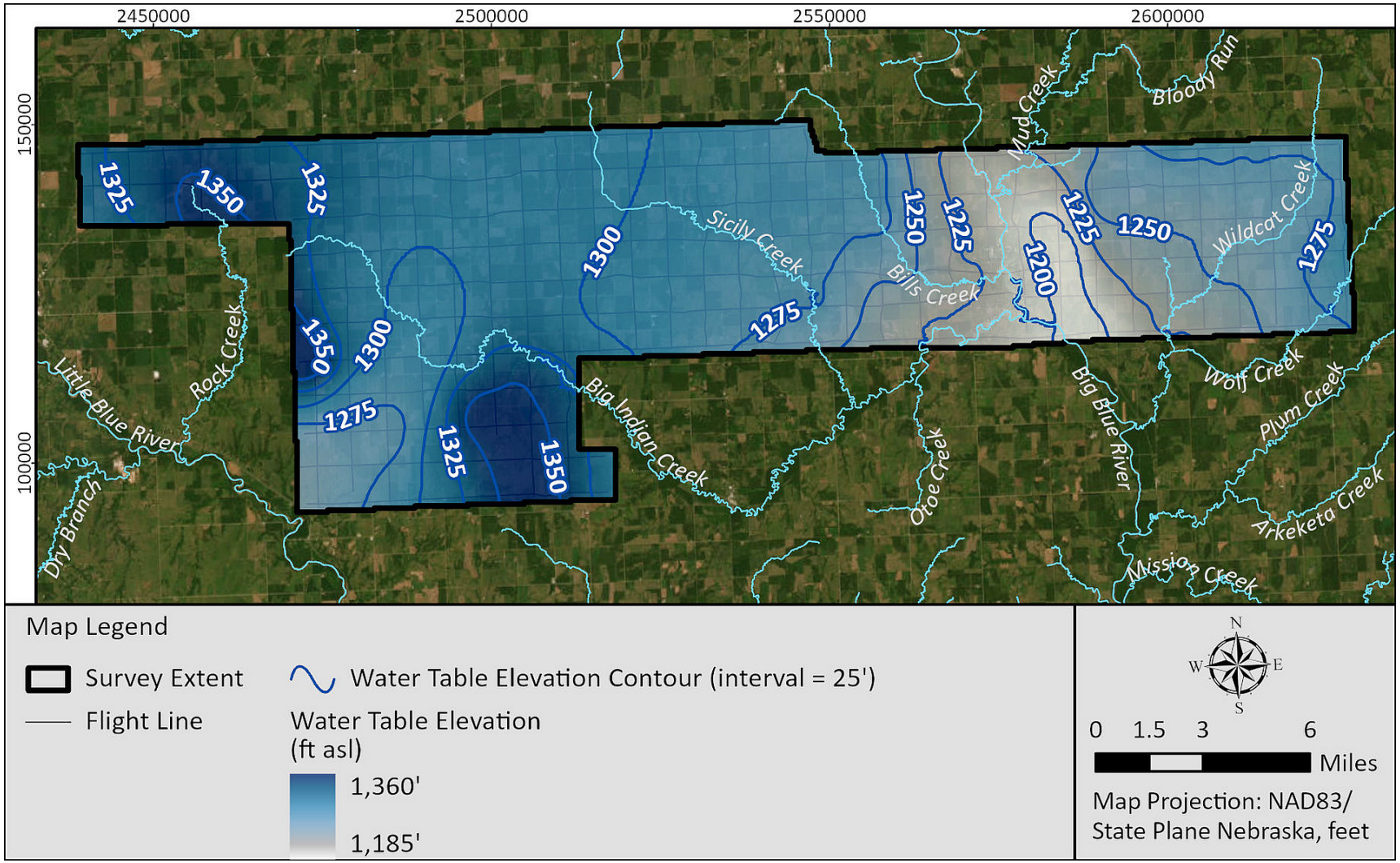


Figure 5-18. Map showing the elevation of the water table (ft bgs). The projection is NAD83 State Plane Nebraska (feet).

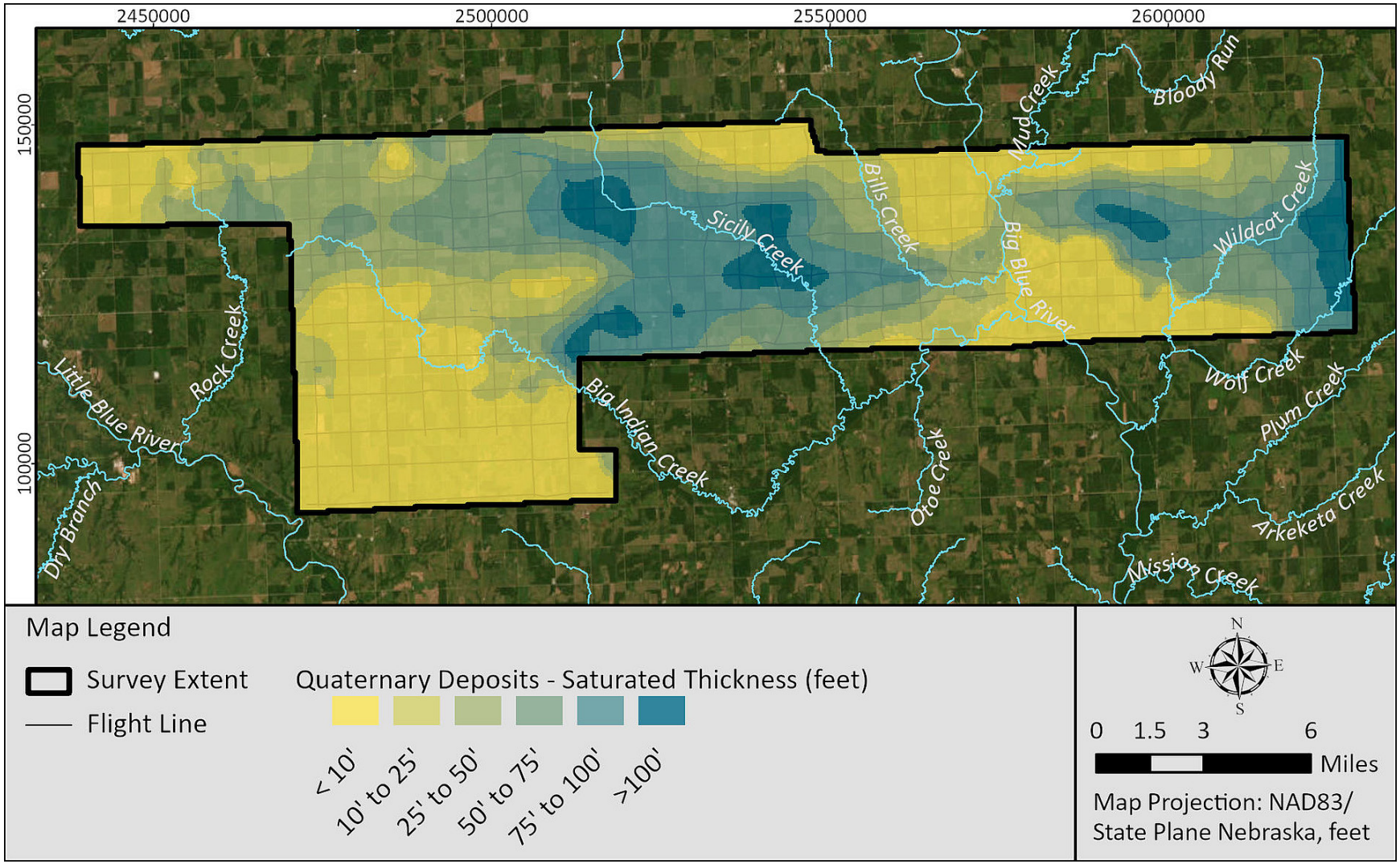


Figure 5-19. Map displaying the saturated thickness of Quaternary (*Q*) material. The projection is NAD83 State Plane Nebraska (feet).

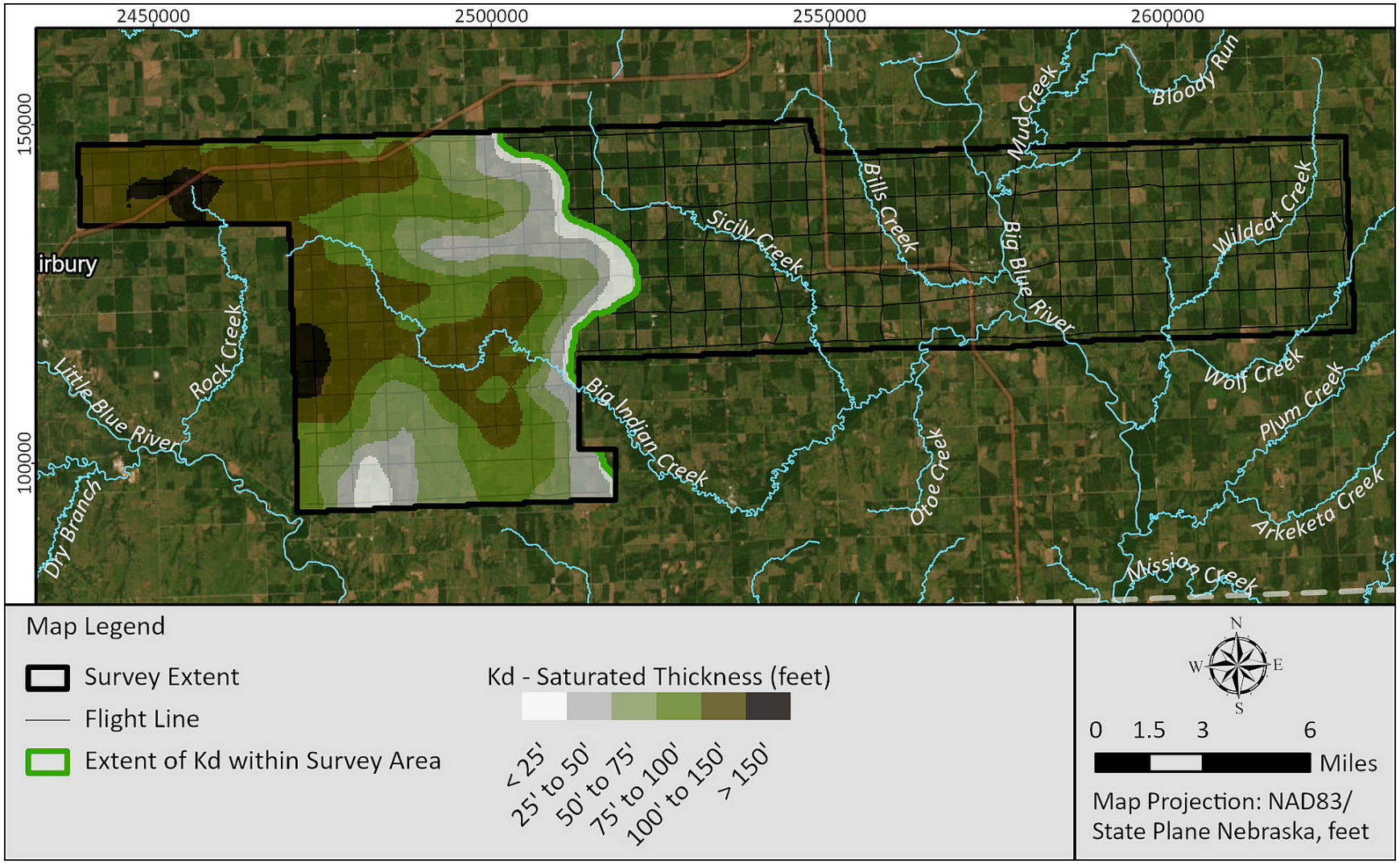


Figure 5-20. Map of displaying the saturated thickness of Cretaceous Dakota (*Kd*) Group. The extent of the *Kd* within the survey area is shown in bright green. Map projection is NAD83 State Plane Nebraska (feet).

5.1.7 Transmissivity Maps

The transmissivity (**T**), or the ability of an aquifer to transmit water, of the unconsolidated saturated material was calculated. The transmissivity, as discussed above in Section 2.2, was calculated using the equation:

$$\mathbf{T = K * b}$$

where **K** is the hydraulic conductivity (ft/sec) and **b** is the saturated aquifer thickness (ft).

The **K** values used to calculate transmissivity within the 2023 LBBNRD survey area were determined based on Fetter (1988, Table 4.6). The Fetter (1988) table lists ranges of **K** values based on material type. LBBNRD project **K** values were selected from the table based on known material type determined through AEM interpretation. Table 5-4 lists the **K** values that were used to calculate transmissivity for the LBBNRD survey area and represent the middle of the range given in the Fetter (1988) table for each material type:

Table 5-4. Summary of Hydraulic Conductivities, K, used to calculate transmissivities.

Q Deposits Material Type	K used for Transmissivity calculation (ft/sec)
Marginal	**1.7×10^{-5} (Silty sands, fine sands)**
Aquifer and Coarse	**1.7×10^{-3} (Well-sorted sands glacial outwash)**

The transmissivity of each saturated material type (marginal; and aquifer and coarse aquifer) for ***Q*** were calculated separately and then added together to determine the overall transmissivity of saturated materials for marginal, aquifer, and coarse aquifer materials.

The resultant raster datasets were compared to the values displayed in "Transmissivity of Principal Aquifer Lincoln and Nebraska City Quadrangles, Nebraska" (Summerside and Myers, 2005). The comparison showed that the AEM-derived values were relatively similar to the values in the published map in Summerside and Myers (2005), but showed more detail and variation. This is to be expected because the AEM data provided a more expansive data coverage to calculate the transmissivity.

Figure 5-21 displays the range of transmissivities for the ***Q*** marginal, aquifer, and coarse aquifer saturated materials in the 2023 LBBNRD AEM survey as compared to the digitized contours from Summerside and Myers (2005). Figure 5-22 presents the same data but without the Summerside and Myers (2005) contours.

It is apparent that the transmissivity results indicate a likely paleochannel feature in the subsurface of the 2023 LBBNRD AEM survey area.

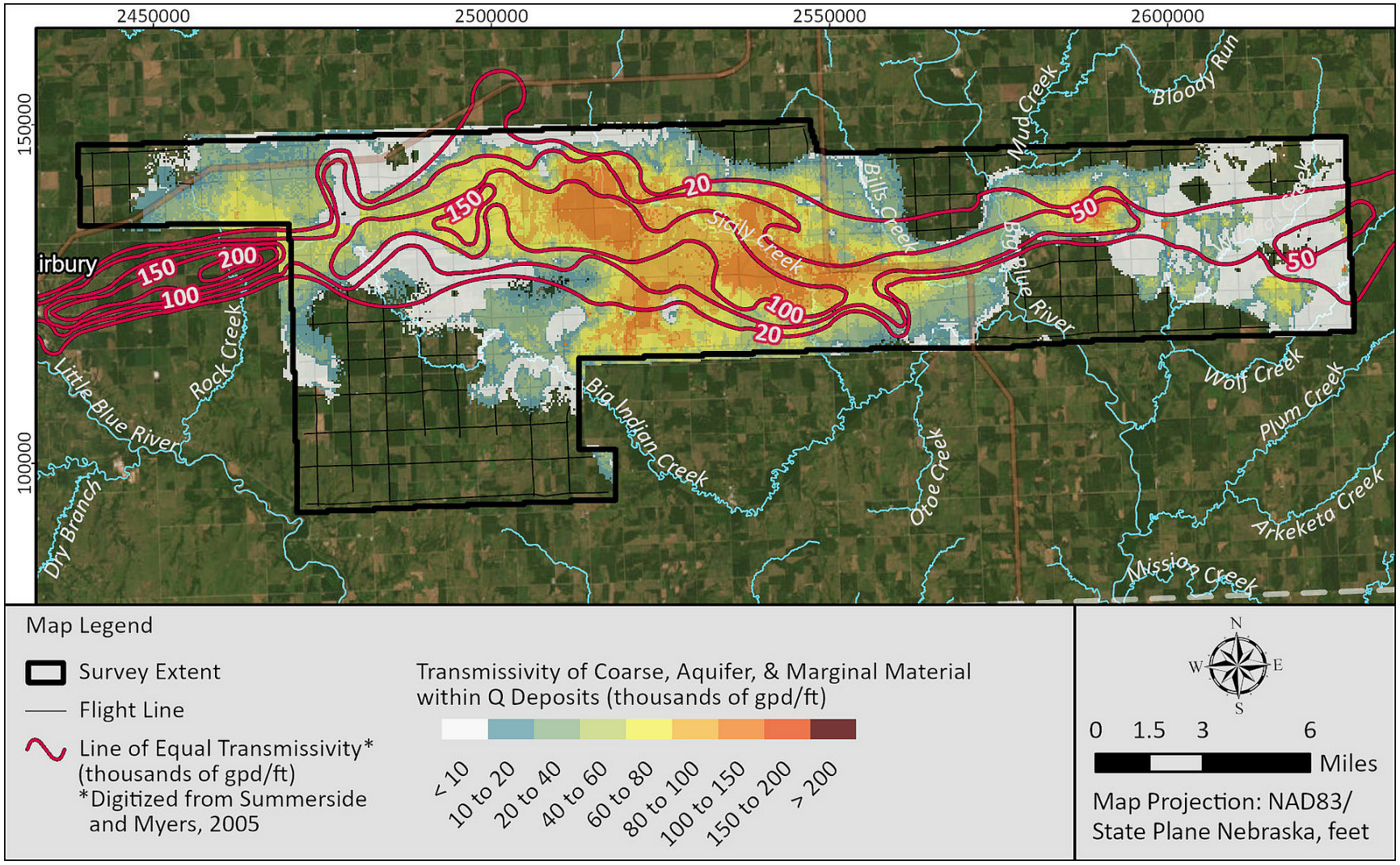


Figure 5-21. Map of the calculated transmissivities within the marginal, aquifer, and coarse aquifer materials of the *Q* deposits in the LBBNRD 2023 AEM survey area with an overlay of digitized contours from Summerside and Myers (2005). Flight lines are depicted as black lines and published transmissivity contours were digitized and added to the map for a visual comparison. The map projection is NAD83 State Plane Nebraska (feet).

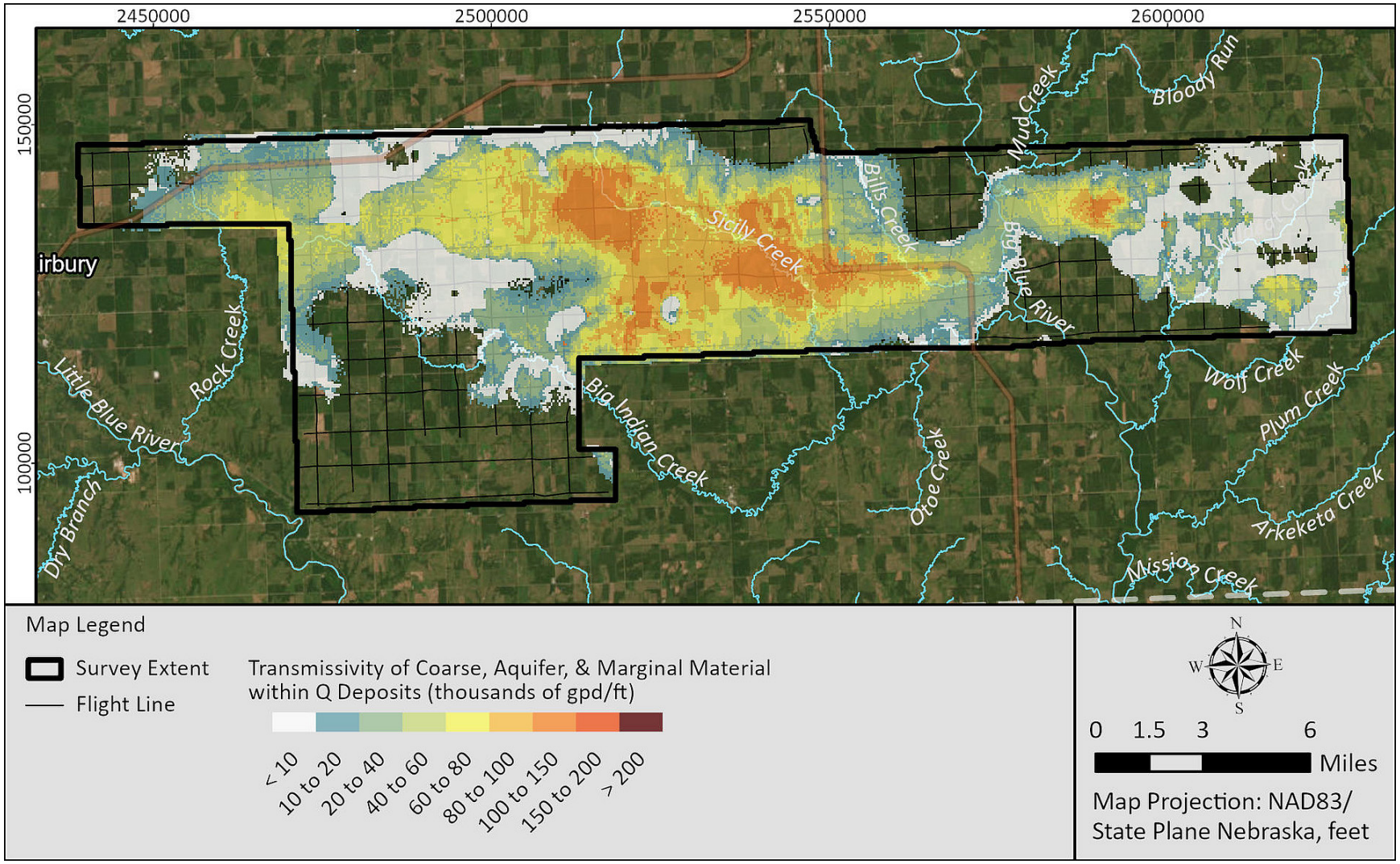


Figure 5-22. Map of the calculated transmissivity within the marginal, aquifer, and coarse aquifer material of the Q deposits in the LBBNRD 2023 AEM survey area without the Summerside and Myers (2005) transmissivity contours. Flight lines are depicted as black lines. The map projection is NAD83 State Plane Nebraska (feet).

5.1.8 Specific Capacity Maps

An estimate of specific capacity was made for the Nebraska Department of Natural Resources (NE-DNR) wells based on the following:

- Screen data (i.e. depth of top and bottom of the screen interval) were extracted from the Nebraska GeoCloud (2023) and data such as static water level, pumping water level, and well yield were extracted from the NE-DNR well shapefile for DNR wells located within the survey area.
- Screen top and bottom depths/elevations were compared to the depth/top elevation of bedrock extracted from the surfaces constructed from the AEM data for each well.
- Based on the comparison, each well was designated with a "completion aquifer" (either ***Q***, Bedrock, or completed in both). For example, if the top of a well screen was below the bottom of ***Q*** deposits, then the well was designated as "Bedrock".
- After the well was designated with a completion aquifer, the Specific Capacity was calculated for each well based on the equation:
    - SC = pumping rate / drawdown (pumping water level minus static water level)
- The calculated Specific Capacity values are only as accurate as the pumping data provided in the NE-DNR dataset (i.e., the well logs). The Specific Capacity values should be considered as approximate, but they do give a helpful, general overview of well production rates.
    - There were 235 wells with the data required to calculate Specific Capacity and assign the well to a completion aquifer. More than half were designated as completed within the ***Q*** deposits.

Figure 5-23 displays the transmissivity of saturated marginal, aquifer, and coarse aquifer material of ***Q*** along with the Specific Capacity of wells screened within the ***Q*** deposits. Figure 5-24 presents saturated thickness of ***Kd*** over 18 ohm-m with the Specific Capacity of wells screened within the ***Kd***. Figure 5-25 presents saturated thickness of ***Kd*** over 25 ohm-m with the Specific Capacity of wells screened in the ***Kd***, respectively.

5.1.9 Geologic Map Updates

Based on the addition of AEM data within the 2023 LBBNRD survey area, minor refinements were made to the published geologic map (Burchett, 1986), specifically to the extent of the ***Kd***. The refinement made to the ***Kd*** extent is based on the resistivity of the material and "picks" made during the interpretation portion of the project. Figure 5-26 is a map displaying the published geologic map (Burchett, 1986) and the refined extent.

5.1.10 3D Interpretative Voxel Grids

A voxel grid was completed for the LBBNRD 2023 AEM survey area. The voxel grids were made using a 300 feet grid cell size and the model layer thickness (from Table 4-3). A minimum curvature method was used within Datamine Discover PA (Datamine Discover, 2024). All layers were referenced to their depth from the surface and then projected on the area DEM.

After the grid was calculated, the grid was split at the interpreted top of the Cretaceous Dakota Group (***Kd***) and the top of the undifferentiated Permian (***P***) using the surface elevation grids discussed above in Section 5.1.5. The resulting voxel grids can be used to explore the distribution of the aquifer materials within the area in 3D. Specifically, these grids can allow for visual inspection of the volume of materials above the bedrock as well as surface materials.

The Quaternary (***Q***) and ***Kd*** materials can also be separated by thresholds developed for four lithology classes (see Section 5.2.1 and Section 5.2.2 below). Utilizing the voxel grids of the ***Q*** and ***Kd***, analysis can be made of the thickness of the different materials within the section. Additionally, the ***Q*** and ***Kd*** voxel can be split into unsaturated and saturated portions utilizing the LBBNRD Spring 2023 water table (Section 5.1.6).

Figure 5-27 is an exploded diagram of the plot of the stratigraphy of the area, including the ***Q, Kd,*** and ***P***, looking to the north. The voxel grids can be found in *Appendix 3-Deliverables\Voxel*.

The voxel model was also used to develop the depth to the saline water is at in the area by using a threshold on the resistivity of 7 ohm-m. Figure 5-28 is a depth to the top of the interpreted saline water.

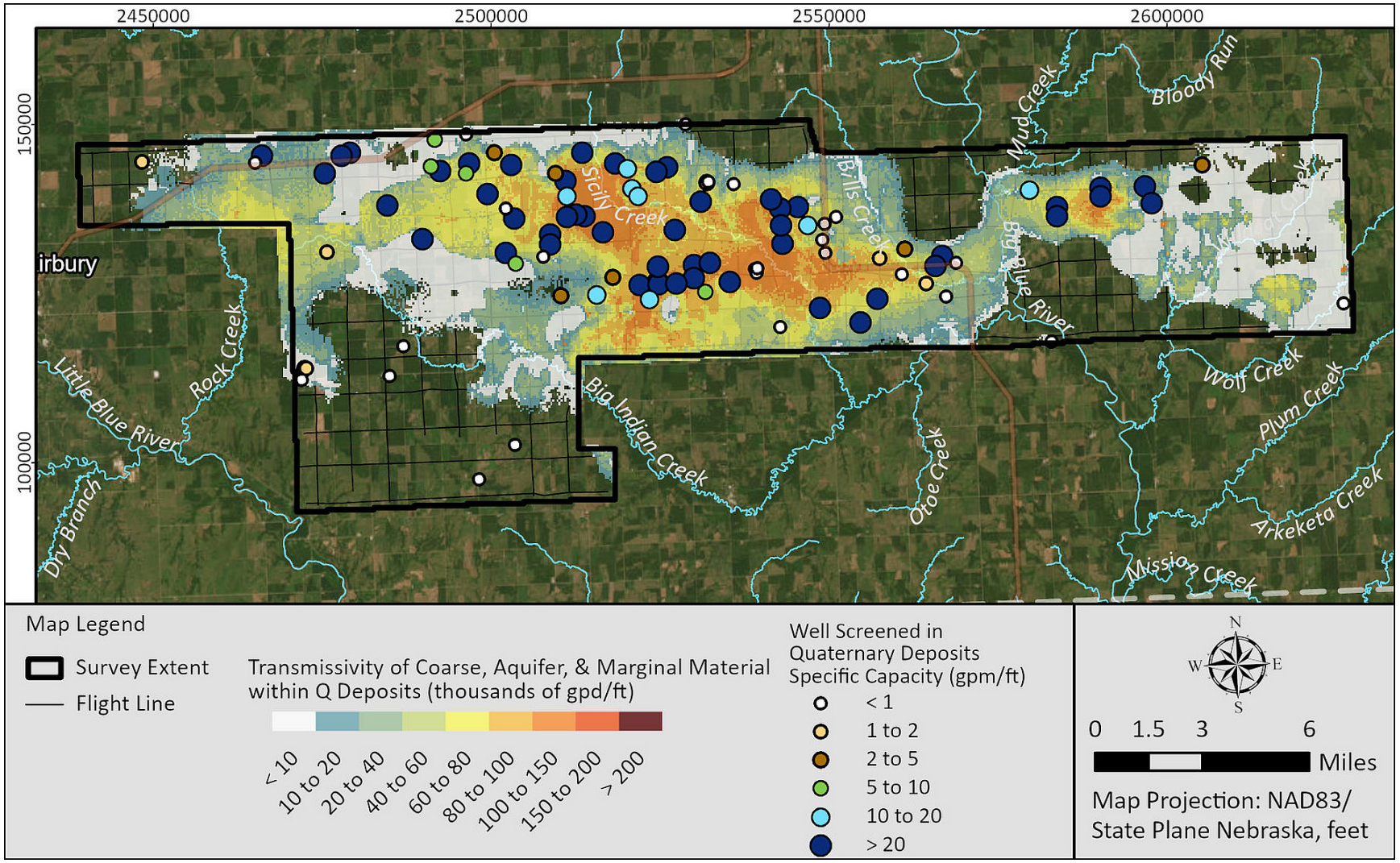


Figure 5-23. Map of the calculated transmissivities within the saturated coarse, aquifer, and marginal materials within the *Q* deposits along with the specific capacity of the DNR wells designated as being completed within the *Q* deposits based on screen interval. Flight lines are depicted as black lines. The map projection is NAD83 State Plane Nebraska (feet).

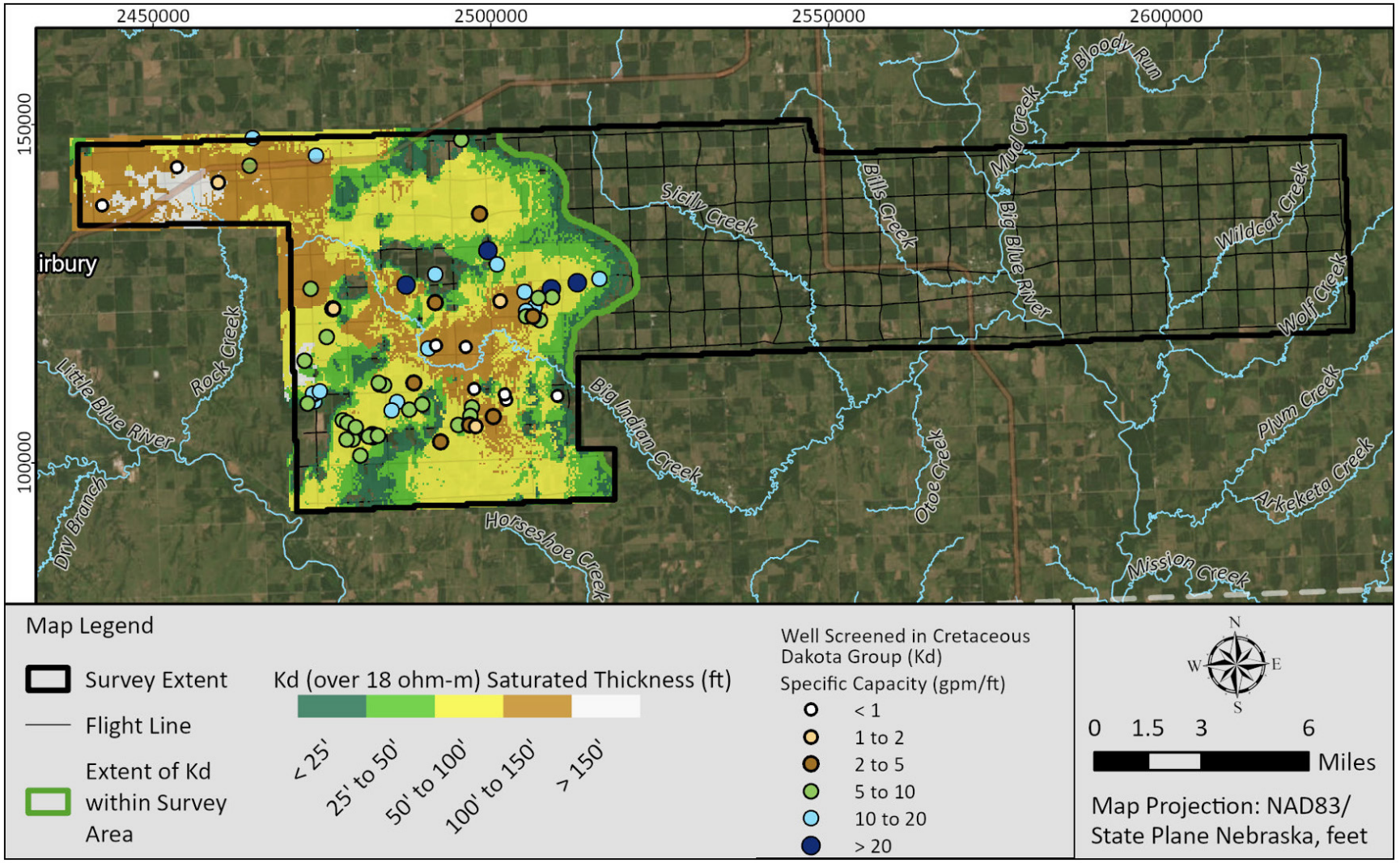


Figure 5-24. Map of saturated *Kd* (over 18 ohm-m) along with the specific capacity of the DNR wells screened within the *Kd*. Flight lines are depicted as black lines. The map projection is NAD83 State Plane Nebraska (feet).

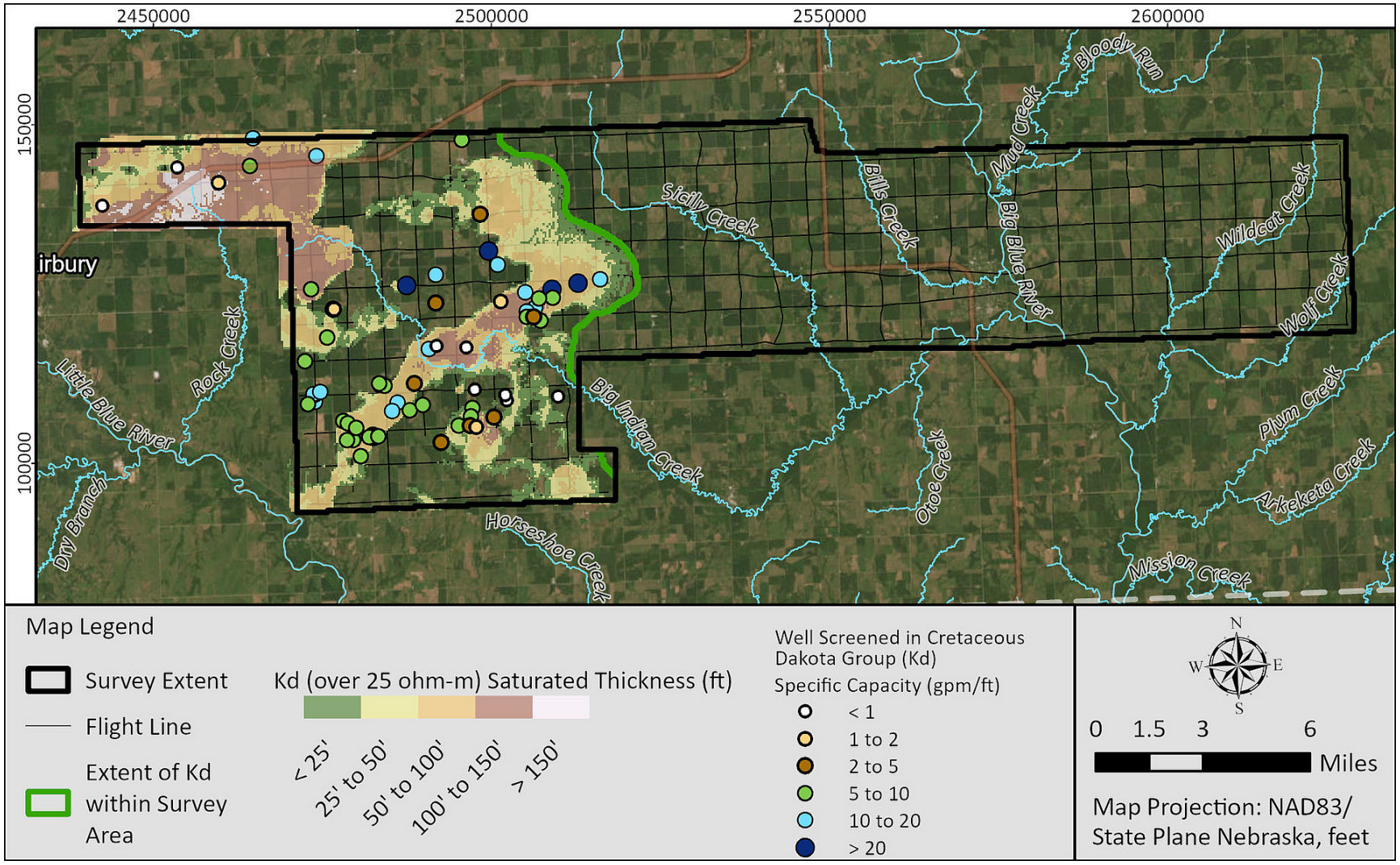


Figure 5-25. Map of saturated *Kd* (over 25 ohm-m) along with the specific capacity of the DNR wells screened within the *Kd*. Flight lines are depicted as black lines. The map projection is NAD83 State Plane Nebraska (feet).

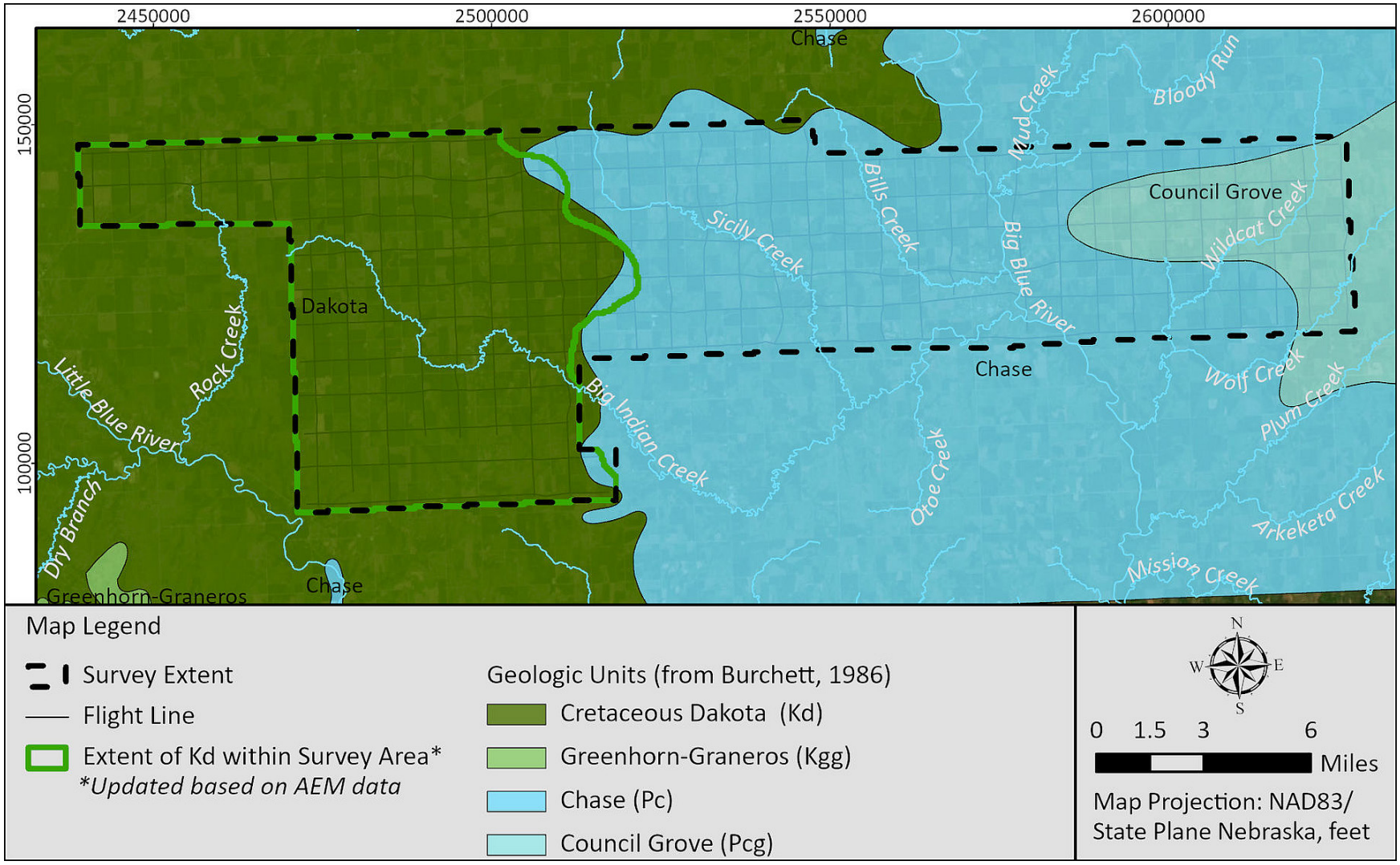


Figure 5-26. Map of geologic units by Burchett (1986) with the refined extent of Kd shown in bright green. Flight lines are depicted as black lines. The map projection is NAD83 State Plane Nebraska (feet).

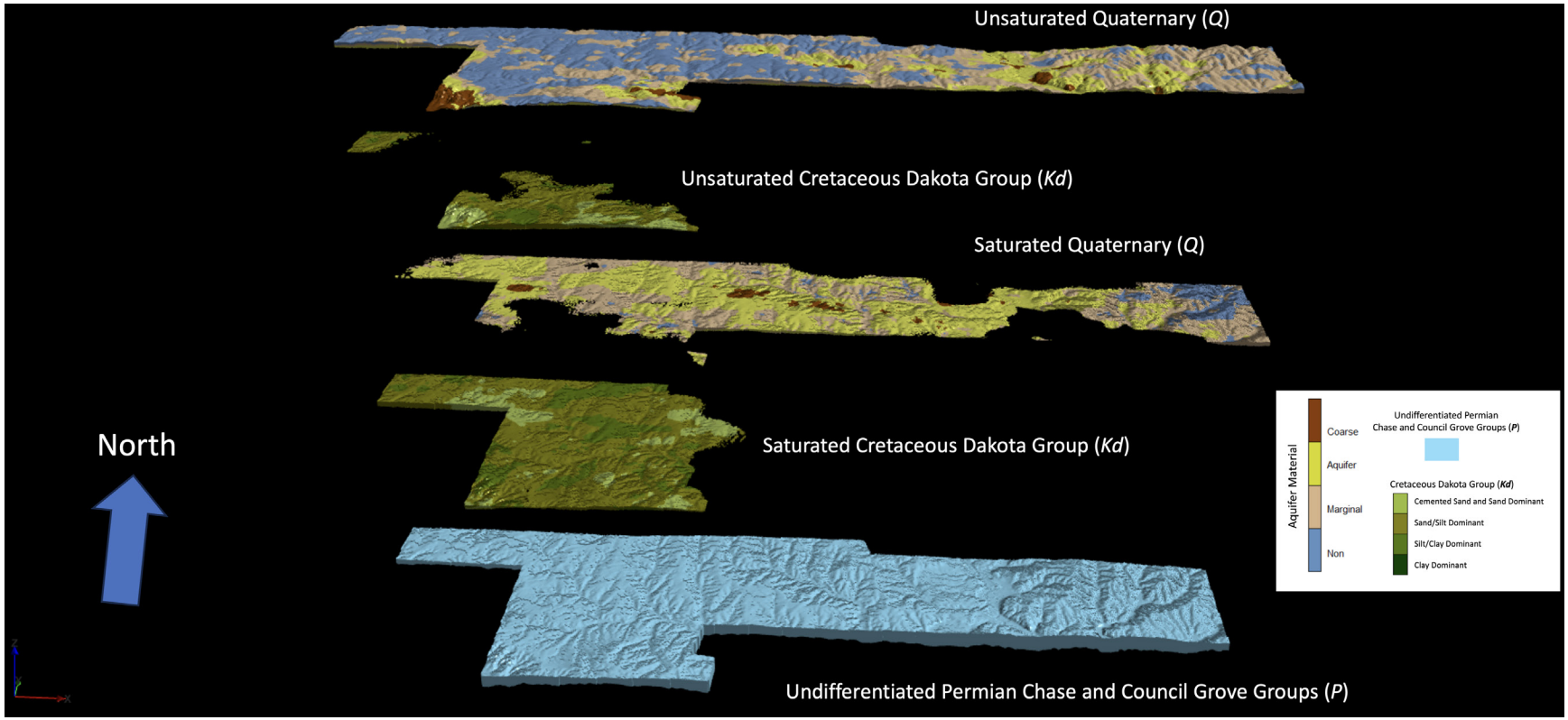


Figure 5-27. Exploded 3D Voxel model of the stratigraphy of the LBBNRD 2023 AEM area showing unsaturated and saturated Quaternary (*Q*) and Cretaceous Dakota Group (*Kd*) material and undifferentiated Permian Chase and Council Grove Groups (*P*). Not to scale.

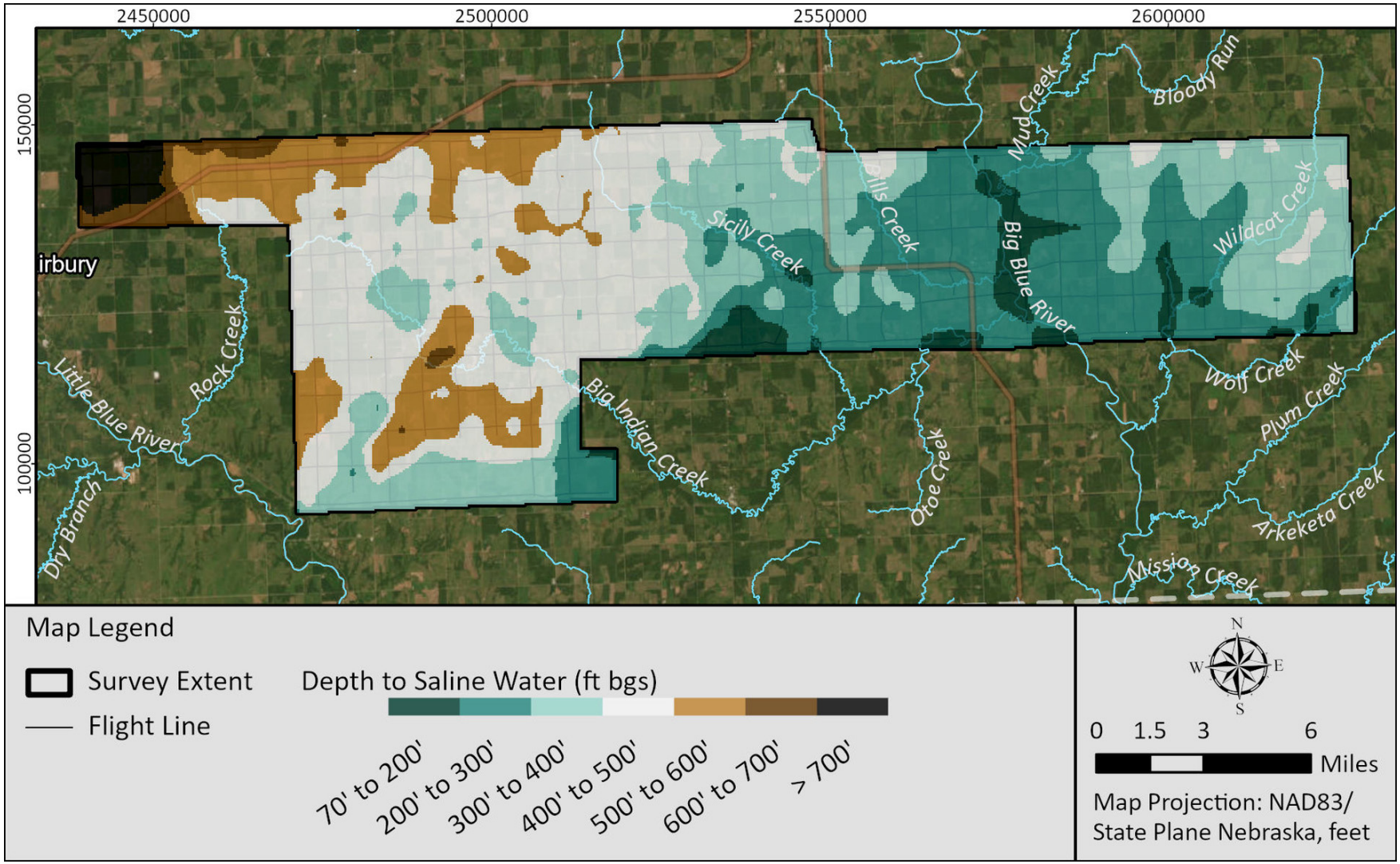


Figure 5-28. Interpreted depth to the top of the saline water interface. The map projection is NAD83 State Plane Nebraska (feet).

5.2 Comparison of AEM Inversion Resistivity to Borehole Geophysical Resistivity Logs

Four geophysical logs existed in the CSD database within the 2023 LBBNRD AEM survey area. These included *3-B-65*, *4-B-65*, *5-B-65*, and *6-B-65*. These logs included a 16-inch Short Normal geophysical resistivity log or electric log (E-log) digitized from paper logs. The resistivity logs within the CSD database are of various vintages and conducted by various staff with differing equipment. However, logs located within the survey area would seem to have been collected in a single year of drilling in 1965.

A critical examination of the absolute values of the resistivity needs to include an awareness of errors in calibration and in the proper operation of the equipment. Many of the early 1940-1980's electric logs were paper logs that were scanned and digitized and then included in the database. There is a long-standing issue with using geophysical logs as ground truth when comparing to AEM acquisition systems and inversions that are well calibrated using modern techniques. Throughout much of the geophysical logging at the time it was acquired, the relative deflections of the resistivity measurements were all that was required or expected from a geophysical log. Operators were seldom trained in the proper operation of a calibrated sonde or in the ability to recognize high contact resistance of a cable head. This has led to many geophysical logs that are uncalibrated within the CSD database. Note that these logs still have scientific merit in their ability to relatively indicate an increase or a decrease in the formation resistivity.

The logs used herein are for qualitative comparison to the AEM because detailed calibration and corrections would need to be carried out for the resistivity values in the logs to be directly used as numerical constraints in the inversion of the AEM data (Ley-Cooper and Davis, 2010). In order to compare the E-logs to the AEM data, a 2,800 feet search radius was used around each of the boreholes and any AEM soundings within that distance were averaged and a mean and standard deviation was calculated.

Figure 5-29 is a graph of the four wells' 16-inch Short Normal resistivity logs plotted with the inverted AEM average resistivity and standard deviation within 2,800 feet. There is general agreement to the shape of the resistivity curves with some being more calibrated than others. The one discrepancy is in *5-B-65* where the AEM show a low resistivity zone and the E-log shows a high resistivity zone at the bottom of the log. This may be related to local variations over the 2,800 feet interval.

Figure 5-30 is the north south survey line L400701. The E-logs are plotted on the same color scale as the AEM and are within 2,800 feet of the flight line.

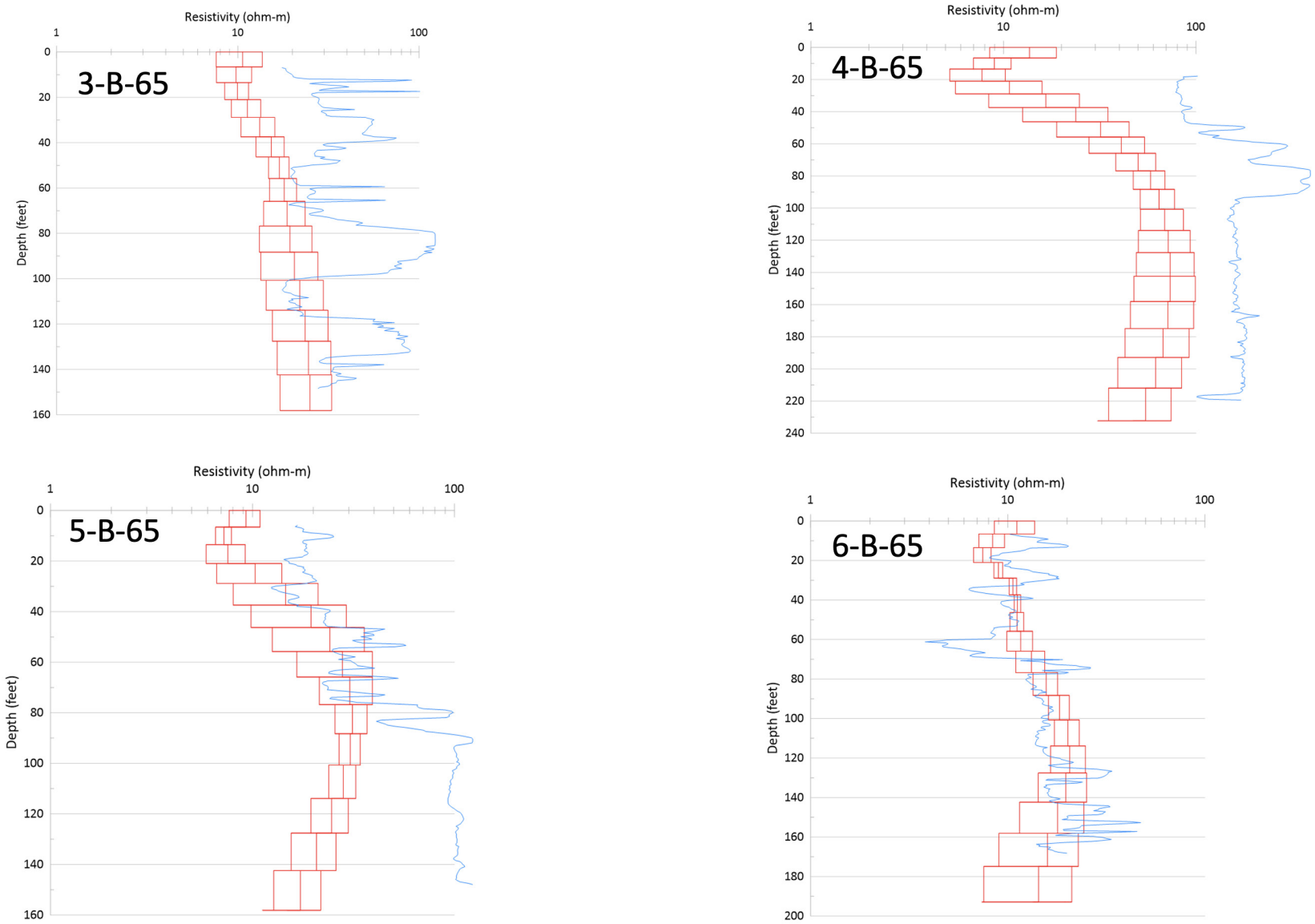


Figure 5-29. Graph of the four 16-inch normal resistivity log values (blue line) and the inverted airborne electromagnetic average resistivity values (red line) within 2,800 feet. Error bars indicated one standard deviation.

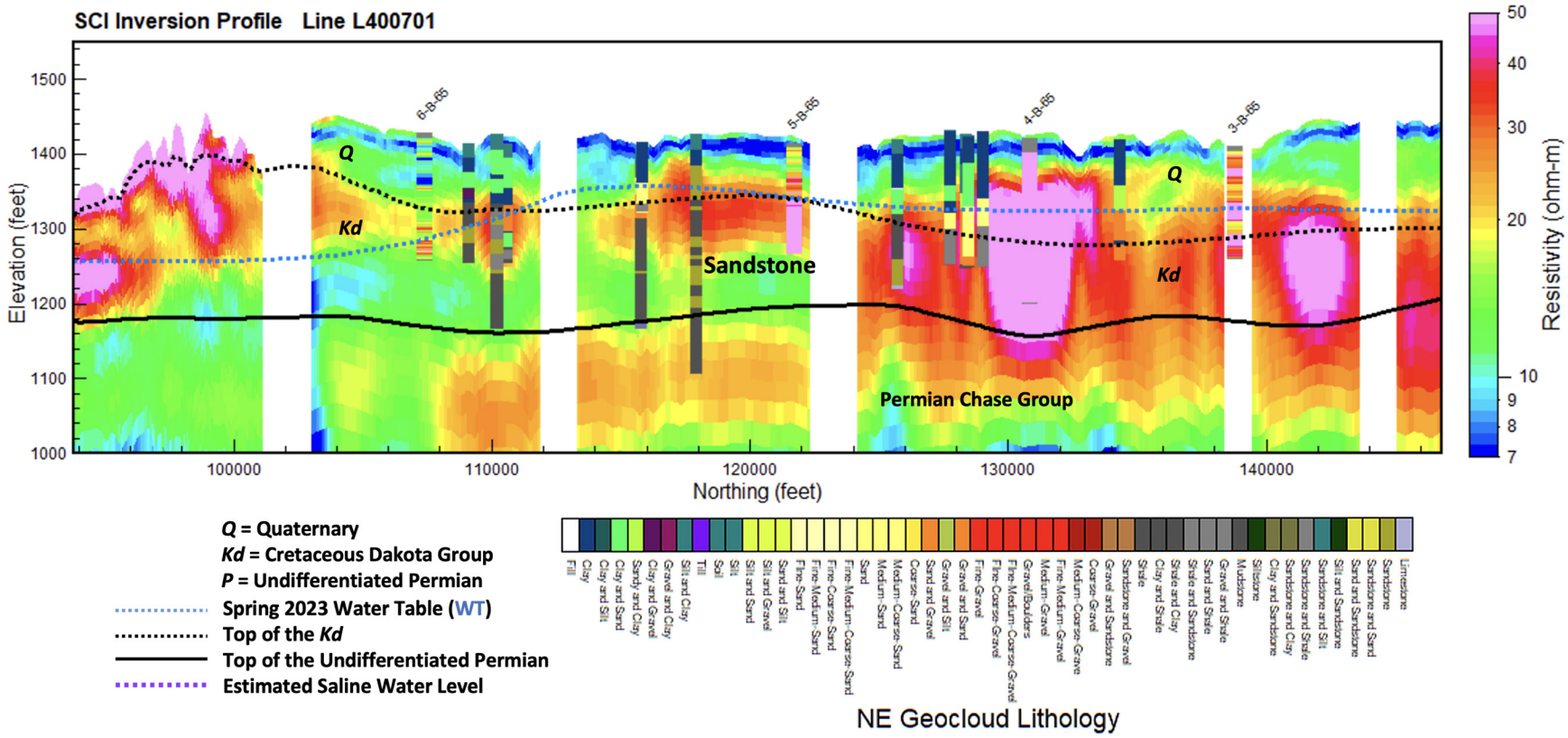


Figure 5-30. 10-mile-long north south line L400701. Resistivity from CSD test holes within 2,800 feet and NE-DNR registered wells lithology within 1,000 feet are projected on the flight line. Gaps in the profile are due to EM decoupling from infrastructure or areas that were not flown due to FFA regulations. Projection is NAD83 State Plane Nebraska (feet), the vertical datum is NAVD88 (feet).

5.2.1 Resistivity Relationship in the Quaternary Aquifer System

A critical aspect of a geophysical survey is assessing the nature of the material detected by the geophysical method applied in the investigation. Regarding the 2023 LBBNRD AEM survey area, assessment of the sediment character in the Quaternary (***Q***) aquifer system is required to determine the overall composition of the major categories used to define the aquifer and aquitards. This is typically done by utilizing the borehole geophysical logs associated with lithology.

In the LBBNRD 2023 AEM survey area there are four geophysical logs to complete this analysis, but they are of the older type that were digitized from paper logs and are not calibrated. Unlike the work that was presented in Carney et al. (2015), uncalibrated logs are inadequate within the LBBNRD 2023 AEM survey area. An assessment of the resistivity thresholds used to characterize non-aquifer, marginal, aquifer, and coarse aquifer materials was conducted using a comparison to the lithologies in the well logs and the AEM resistivity. This allowed for the characterization of the ranges of resistivities present in the ***Q*** units described in this report. It was determined that the Carney et al. (2015) report adequately mapped the aquifer materials that were interpreted for this project; therefore, the analysis presented in Carney et al. (2015) was used for the categorization of the Quaternary aquifer system within the LBBNRD survey area. The ***Q*** aquifers were broken down by resistivity for aquifer materials (less than 12 ohm-m for non-aquifer material, 12-20 ohm-m for marginal aquifer material, 20-50 ohm-m for aquifer material, and greater than 50 ohm-m for coarse aquifer material). Figure 5-31 is a plot of the color bar used and the resistivity ranges for the four aquifer material types.

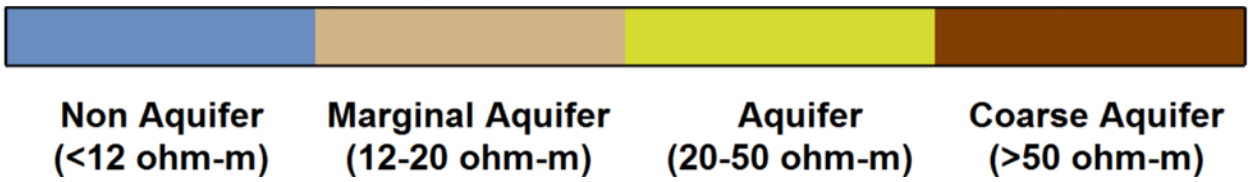


Figure 5-31. Plot displaying the resistivities by major Quaternary (*Q*) aquifer material color categories used in the LBBNRD 2023 AEM survey: blue- non-aquifer materials, tan- marginal aquifer materials, yellow- aquifer materials, brown- coarse aquifer materials (Carney et al., 2015).

5.2.2 Resistivity Relationship in the Cretaceous Dakota Group Aquifer System

As discussed above a critical aspect of a geophysical survey is assessing the nature of the material detected by the geophysical method applied in the investigation. Regarding the 2023 LBBNRD AEM survey area, assessment of the sediment character in the Cretaceous Dakota Group (***Kd***) aquifer system, or as sometimes referred to as the Maha Aquifer (Divine and Sibray, 2017), is required to determine the overall composition of the major categories used to define the aquifer and aquitards.

The ***Kd*** within the LBBNRD was split into four parts based on empirical comparisons to lithology logs. 0-3 ohm-m was classified as Shale/Clay Dominant materials, 3-18 ohm-m as Siltstone/Silt Dominant materials, 18-35 ohm-m Sand/Silt Dominant, and 35 ohm-m and greater as Sandstone/Sand Dominant materials. This is a modification of the splits that were used in the P-MRNRD reports from AGF (2021). Additional unpublished work in the Nebraska ***Kd*** using AEM data has led to a better understanding of the resistivity versus lithology with the ***Kd***.

Lacking the quality geophysical well logs in the ***Kd*** that exist in the ***Q***, it is difficult to produce a more robust statistical distribution of the resistivity versus lithology as was done for the ***Q*** materials (Carney et al., 2015). Figure 5-32 is an image of the color scale that was used in the interpretation of the ***Kd***.

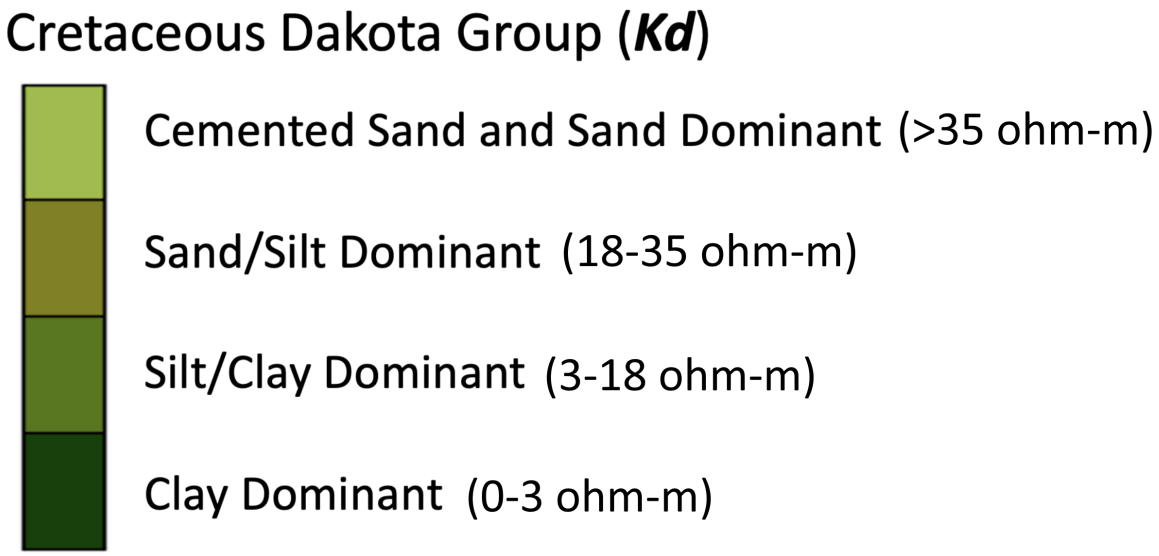


Figure 5-32. Plot displaying the Cretaceous Dakota Group (*Kd*) resistivities by dominant material and the color categories used in the LBBNRD 2023 AEM survey.

5.3 Hydrogeological Framework of the LBBNRD 2023 AEM Survey Area

The priority for this survey was to build a detailed hydrogeologic framework to better understand the aquifers within the areas of southern Gage and eastern Jefferson Counties in the southern portion of the LBBNRD. The end goal is to establish a scientific-based approach to defining new management boundaries.

The AEM reveals variability of the aquifer materials within the Quaternary (***Q***) and Cretaceous Dakota Group (***Kd***) deposits, which provide the groundwater supply, and their spatial relationship to each other and the surface water. These spatial relationships can provide insight into groundwater supply in the AEM survey area. The Permian Chase Group (***Pc***) and Permian Council Grove Group (***Pcg***) is under much of the survey area and beneath the ***Q*** and ***Kd***. The ***Pcg*** underlies the ***Q*** in the eastern side of the survey area. The ***Pcg*** also underlies the ***Pc***. The term bedrock in this report represents the Cretaceous bedrock units of the ***Kd*** and the undifferentiated Permian (***P***) units. The ***Kd*** is only on the western third of the survey area. Figure 5-33 is the revised geology map of the area based on the interpretation of the AEM. This figure is based on Burchett (1986) with modifications due to the higher resolution AEM data.

The ***Q*** is expressed in the resistivity color scale as shown in Section 5.2.1 to present locations of aquifer materials composed of non-aquifer (blue color in figures), marginal aquifer (tan color in figures), aquifer (yellow color in figures), and coarse aquifer materials (brown color in figures). The ***Q*** materials are composed predominantly of preglacial alluvial deposits and glacial outwash and till with a loess cover in some areas. The ***Kd*** is expressed in the resistivity color scale as shown in Section 5.2.2 representing cemented sand and sand dominant, sand/silt dominant, slit clay dominant, and clay dominant. The ***Kd*** is consolidated, semi-consolidated, and non-consolidated fluvial and deltaic sediments.

Figure 5-34 and Figure 5-35, displayed as 3D fence diagrams, present the overall distribution of ***Q***, ***Kd***, and ***P*** (as described in Section 2) across the LBBNRD 2023 AEM survey area. The ***Q*** aquifer materials can generally be characterized by alluvial/outwash materials in a paleochannel through the center of the survey area. The ***Kd*** in the western part of the survey area is directly deposited on the ***P*** units. The ***Kd*** is composed of consolidated and semi consolidated clay, silt, sand, sandstone, siltstone, and shale. The deposits are in fluvial deposits associated with the delta front that existed east of the survey area and underwent multiple regression and transgressive sequences in the Cretaceous (Witzke et al., 1983).

The undifferentiated Permian groups (***P***) are impermeable shale and limestone, and they are considered aquicludes or boundaries to groundwater flow that is present throughout the survey area. The combined ***P*** surface can be considered the bottom of the aquifer. Within the ***P*** units saline water exists at depth and is widespread in the LBBNRD area of Nebraska (Korus et al., 2013).

Figure 5-36 presents an exploded 3D voxel model of the unsaturated ***Q***, unsaturated ***Kd***, saturated ***Q,*** saturated ***Kd***, and ***P*** units. Note that the saturated ***Q*** follows a paleochannel path and there are gaps where the ***Kd*** and the ***P*** units are higher than the water table. Much of the ***Kd*** in the west is saturated with the southern-most part unsaturated.

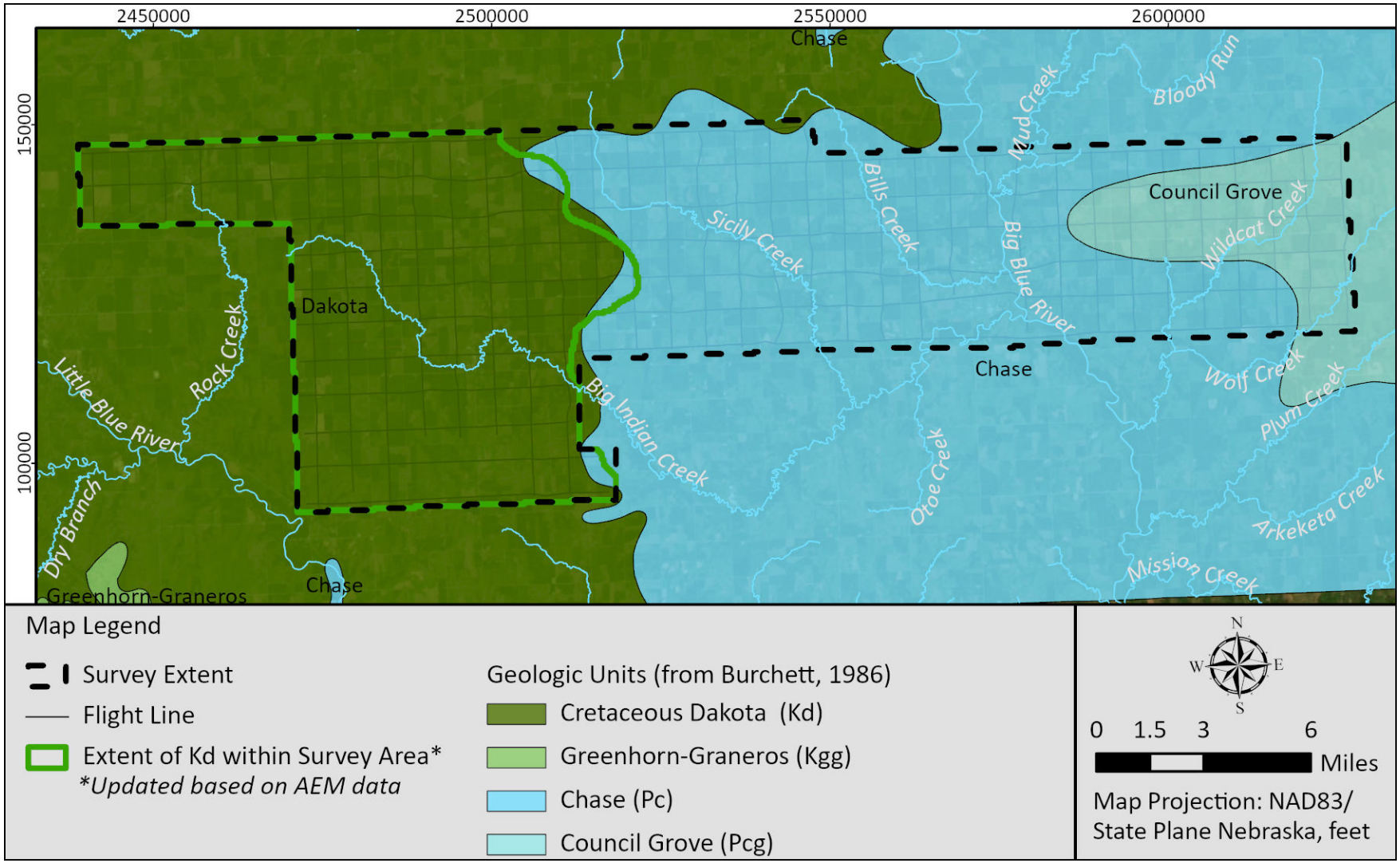


Figure 5-33. Bedrock map of the survey area modified from Burchett (1986) using the LBBNRD 2023 AEM survey results.

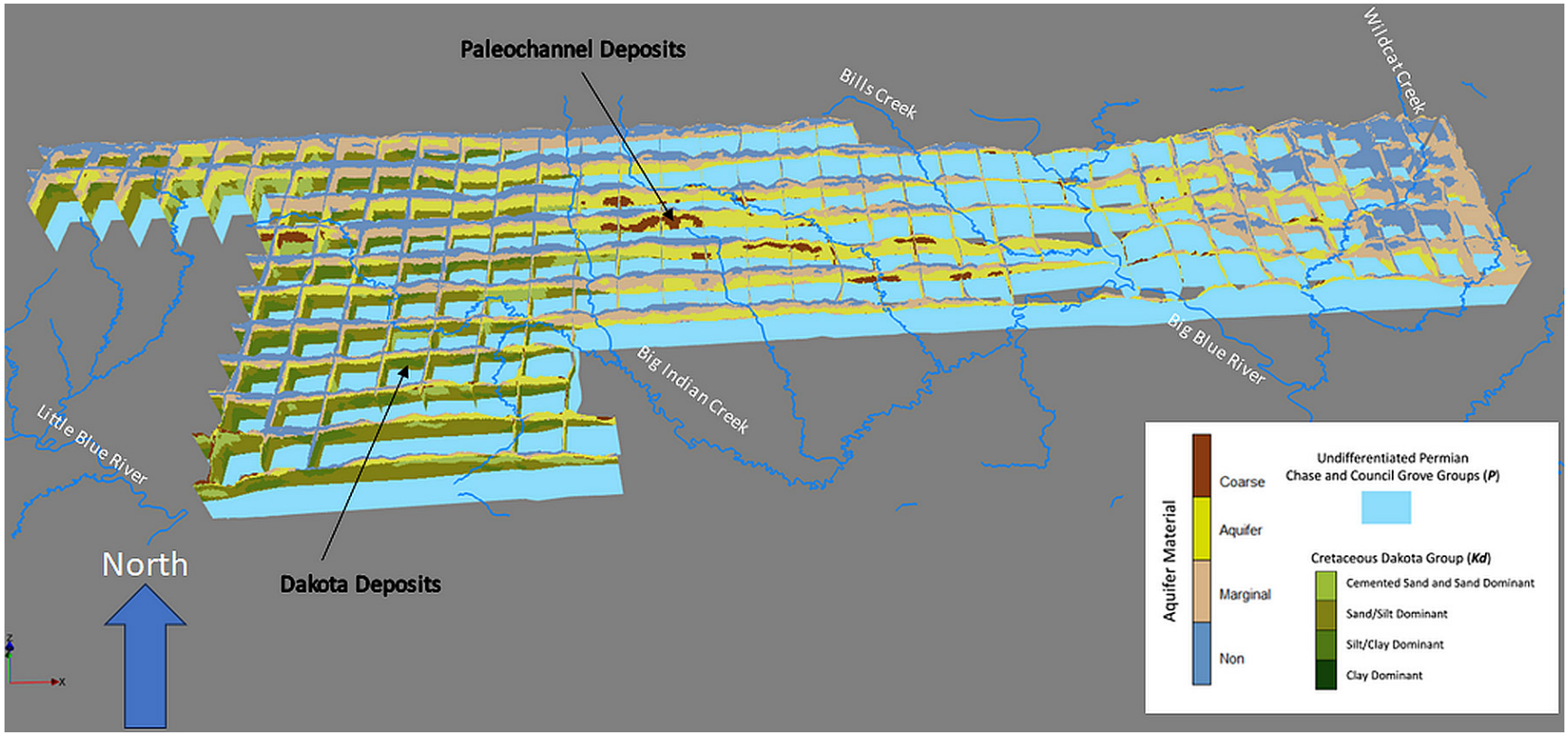


Figure 5-34. 3D Fence diagram looking to the north of the interpreted distributions of aquifer material within the LBBNRD 2023 AEM survey area. Flight lines are indicated by black lines. V.E.=20x.

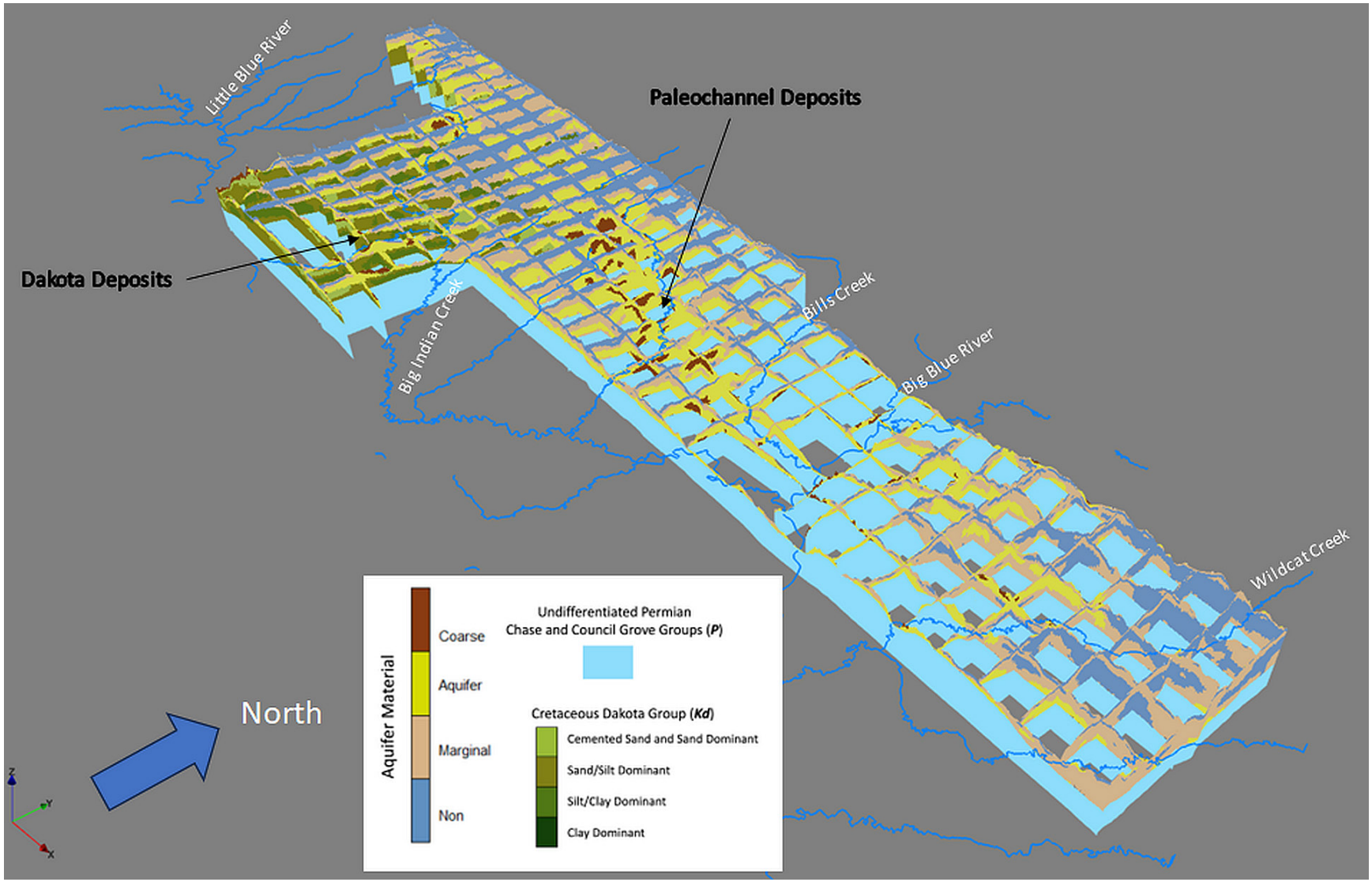


Figure 5-35. 3D Fence Diagram looking to the northwest of the interpreted distributions of aquifer material within the LBBNRD 2023 AEM survey area. Flight lines are indicated by black lines. V.E.=20x.

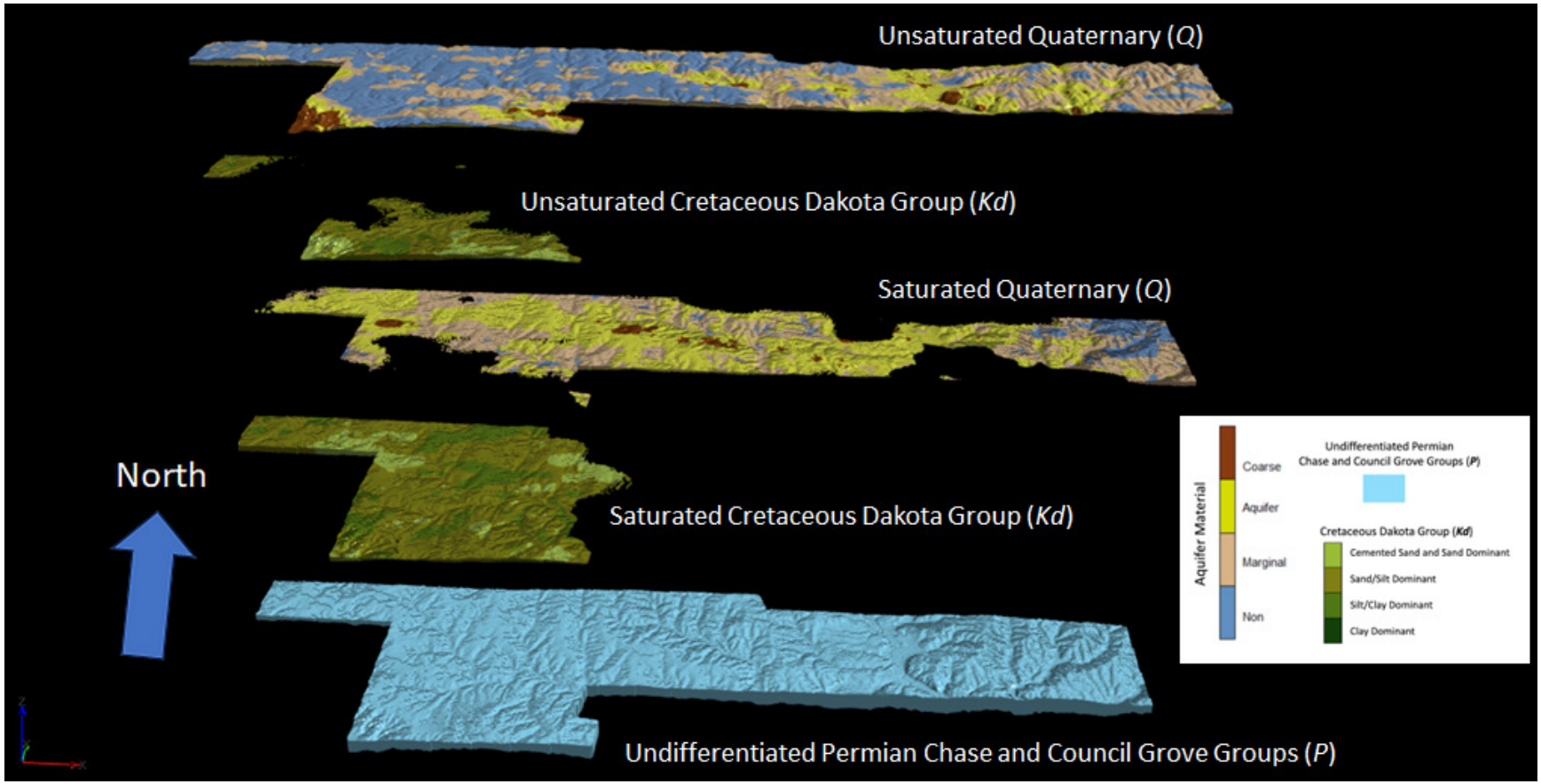


Figure 5-36. 3D exploded voxel model looking north of the LBBNRD 2023 AEM survey area showing *Q* (Quaternary) and *Kd* (Cretaceous Dakota Group) unsaturated and saturated, and the undifferentiated Permian Groups *(P*).

5.3.1 The Hydrogeology of the Quaternary

The Quaternary (***Q***) materials of the LBBNRD 2023 AEM survey area are predominantly composed of two zones: 1) the alluvial sediments dominated by sands and gravels of the paleovalleys, and 2) the glacial deposits of till, outwash and loess deposits. The total thickness of the ***Q*** (including both zones of ***Q***) is shown in Figure 5-37. The paleochannel is not easily discernable in the ***Q*** total thickness map. The thickness of the ***Q*** is controlled by the topography of the area, but the thicker section of > 150 feet extends in a general east-west trend, disrupted by a relatively thin ***Q*** area running north-south at the Big Blue River.

The first zone, mentioned above, is aquifer material in the ***Q*** fluvial paleochannel sediments (yellow color in figures) and coarse aquifer materials (brown color in figures) that indicate sands and gravels of the paleovalley aquifers. Small deposits of outwash above the paleovalley can also add to the total thickness of the aquifer materials (Figure 5-38); there are some aquifer materials on the southern end of the survey area that are from the weathered ***Kd*** that is near the surface. A 3D view of the voxel model of the total ***Q*** aquifer and coarse aquifer materials (Figure 5-39) shows the distribution of those materials with the undifferentiated Permian (***P***) surface in the background.

As noted above, the second ***Q*** zone is the loess and glacial tills containing silts and clays which make up the marginal aquifer and non-aquifer material and are poor aquifers. Figure 5-40 illustrates the 3D distribution of the marginal (tan color in figures) and non-aquifer (blue color in figures) materials. There are some windows in the till and loess deposits that can be seen in the areas of the Big Blue River and other drainages.

An enhanced understanding of the distribution of ***Q*** aquifer materials can be gained by an examination of the flight line profiles. North-south profile Line L401701 (Figure 5-41) is a good example of the ***Q*** section crossing the paleovalley aquifer. On Figure 5-41 the LBBNRD AEM flight area map inset on the upper right indicates all the flight lines as black lines. The line displayed in the profiles is indicated in red and boreholes are indicated as blue dots from the CSD database and small olive dots from NE-DNR database. The flight line location map on the upper left indicates the flight line location on an air photo. The middle profile is the SCI inversion result which shows the results of the inversion as electrical resistivity. Gaps in the resistivity profile are a result of editing areas of EM-coupling out of the data or of areas that were not over flown due to infrastructure. Located on the profile are lithology indicated on the Nebraska GeoCloud lithology legend from the CSD and NE-DNR databases that are within 1,320 and 1,000 feet respectively of the flight line. When present on the profile (due to displayed elevation range), the Depth of Investigation (DOI) is indicated by dashed gray lines. The Cretaceous Dakota Group (***Kd***) is indicated by a dashed black line and the top of the undifferentiated Permian (***P***) is by a solid black line. The Spring 2023 LBBNRD water table is indicated by the dashed blue line.

The interpretation profile on the bottom of Figure 5-41 shows the results of the hydrogeological framework interpretation. Located on the profile are NE-DNR database boreholes (gray) within 1,000 feet of the flight line with the screen intervals colored (indicated in the legend) with the specific capacity in gpm/ft. The Cretaceous Dakota Group (***Kd***) and undifferentiated Permian (***P***) are indicated by the

colors in the legend. The Spring 2023 LBBNRD water table is indicated by the dashed blue line. Estimated aquifer materials are represented by the colors in the legend.

The presence of the high electrical resistivity paleochannel deposits are observed in the 'SCI Inversion Profile'. Confirmation is seen in the three NE-DNR wells within 1,000 feet of the flight line. The low electrical resistivity of the tills and the loess that is overlying the paleochannel can also be observed. Below this resistivity area is interpreted as aquifer materials in the 'Interpretation Profile'. One NE-DNR well (*183739*) had the information to calculate a specific capacity and indicated a higher SC value in the paleochannel deposits.

Examining Figure 5-42 of east-west line L500401 several features can be seen in the ***Q*** aquifer system. The paleochannel is seen in the center of the profile just to the west of the Permian bedrock high and the aquifer and coarse aquifer materials are overlain by tills and loess deposits. On the east end of the profile the aquifer materials are less and are likely outwash deposits as seen higher in the section. The western end of the profile also shows the relationship of the ***Q*** to the ***Kd***. Several NE-DNR registered wells have information that allowed for the calculation of Specific Capacity (SC).

Using the LBBNRD Spring 2023 water table estimates, saturated thickness can be derived from the data. Figure 5-43 is the total saturated thickness of the ***Q*** and Figure 5-44 is the saturated thickness of the aquifer and coarse aquifer material. These figures illustrate the paleochannel deposits and the paleovalley aquifer in the ***Q*** sediments. As indicated above, the marginal aquifer material class can provide some water but at a much lower rate due to the interlayering of clays and silts.

As a comparison, the ***Q*** marginal and non-aquifer material saturated thickness is indicated in Figure 5-45. These deposits are thickest in the east and are on the margins of the main paleochannel.

Using the calculated transmissivity maps (Section 5.1.7) and plotting the registered wells with specific capacity data for completions within the ***Q***, an image of the ***Q*** aquifer can be better illuminated (Figure 5-46**)**. Most completions within the ***Q*** are within the paleovalley aquifer in the higher transmissive materials. The correlation is excellent with the Specific Capacity values and the position of the AEM estimated transmissivity. This can be compared with what has been previously published about the paleovalley aquifer by overlying transmissivity contours from Summerside and Myers (2005) on the AEM estimated transmissivity map (Figure 5-47). A good general agreement is observed, and more details revealed, by the AEM due to the high density of observations.

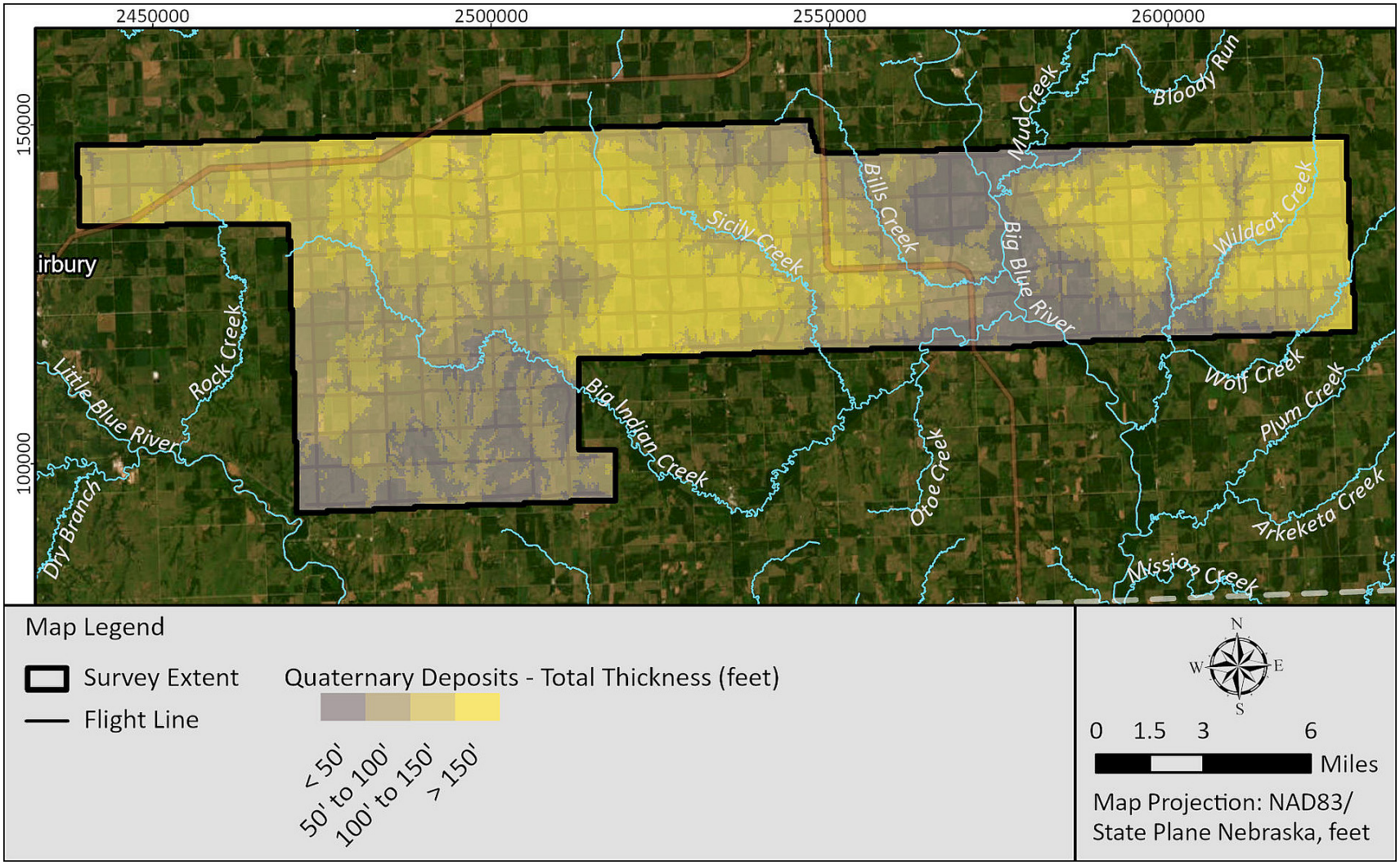


Figure 5-37. Map of the Quaternary (*Q*) total thickness within the LBBNRD 2023 AEM survey area.

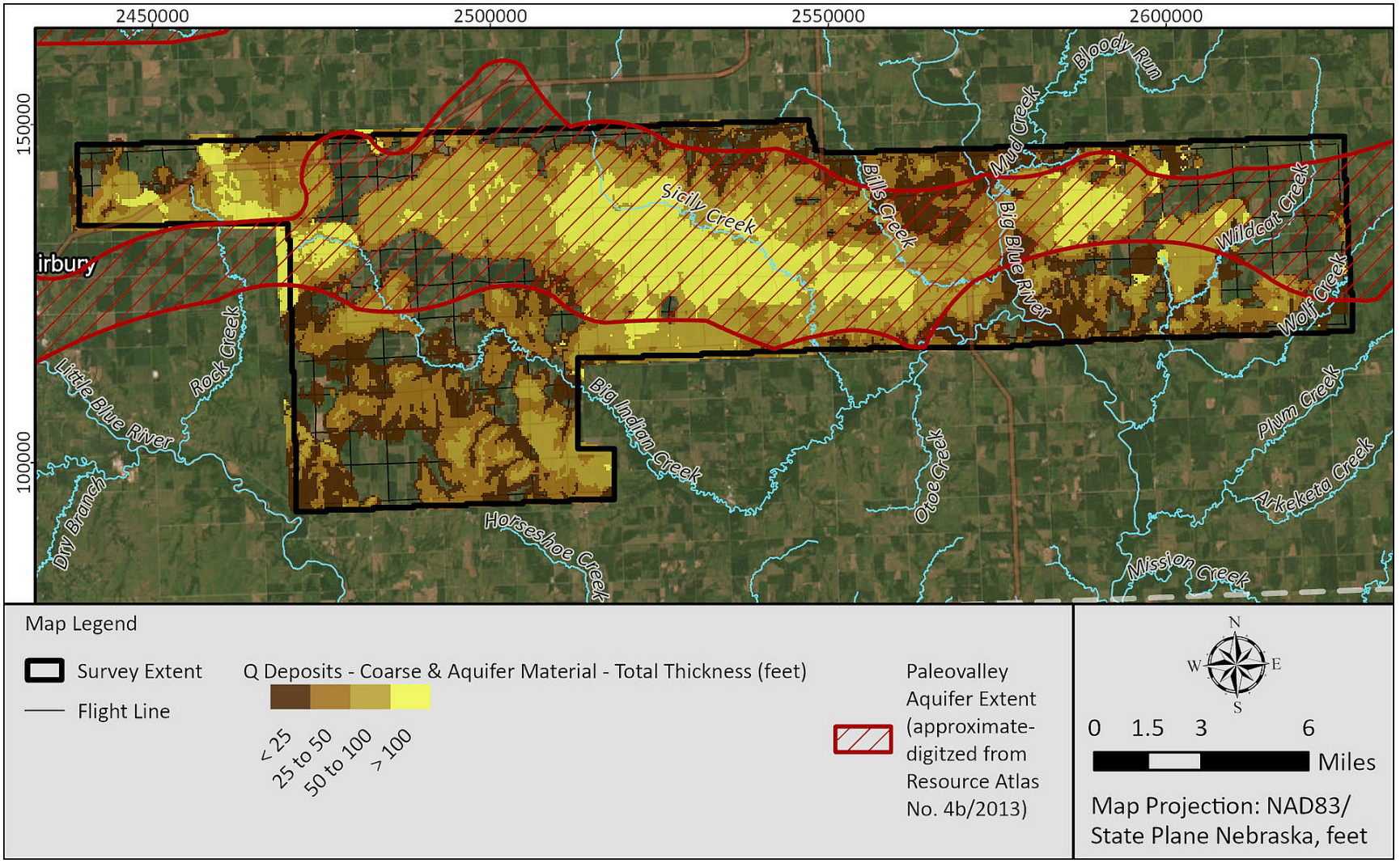


Figure 5-38. Map of the Quaternary (*Q*) total thickness of the coarse and aquifer materials within the LBBNRD 2023 AEM survey area. The shaded/hatched area is from Korus (2013).

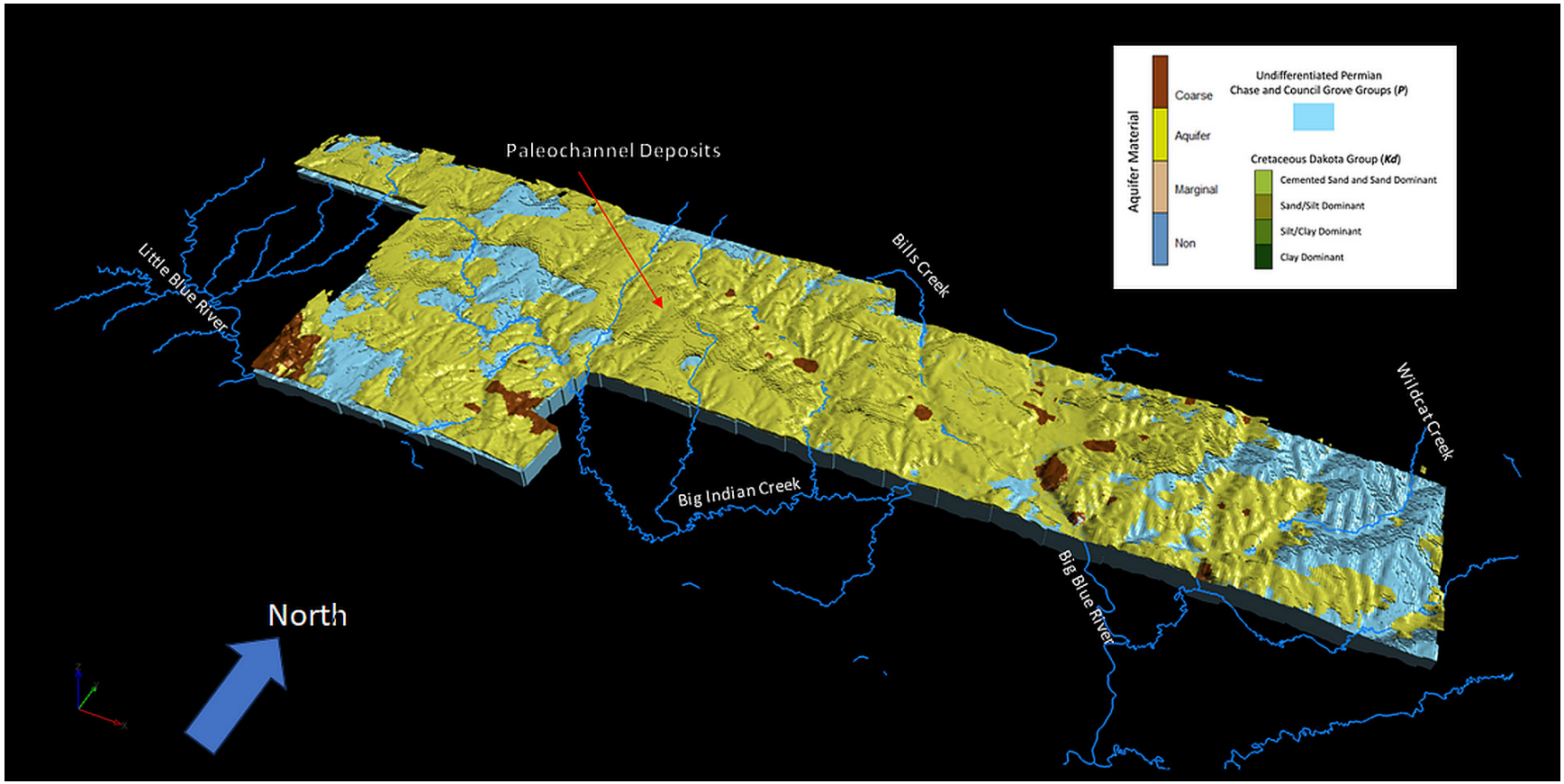


Figure 5-39. 3D Voxel diagram looking to the northwest of the interpreted distributions of total aquifer and coarse aquifer material of the Quaternary (*Q*) within the LBBNRD 2023 AEM survey area. V.E.=20x.

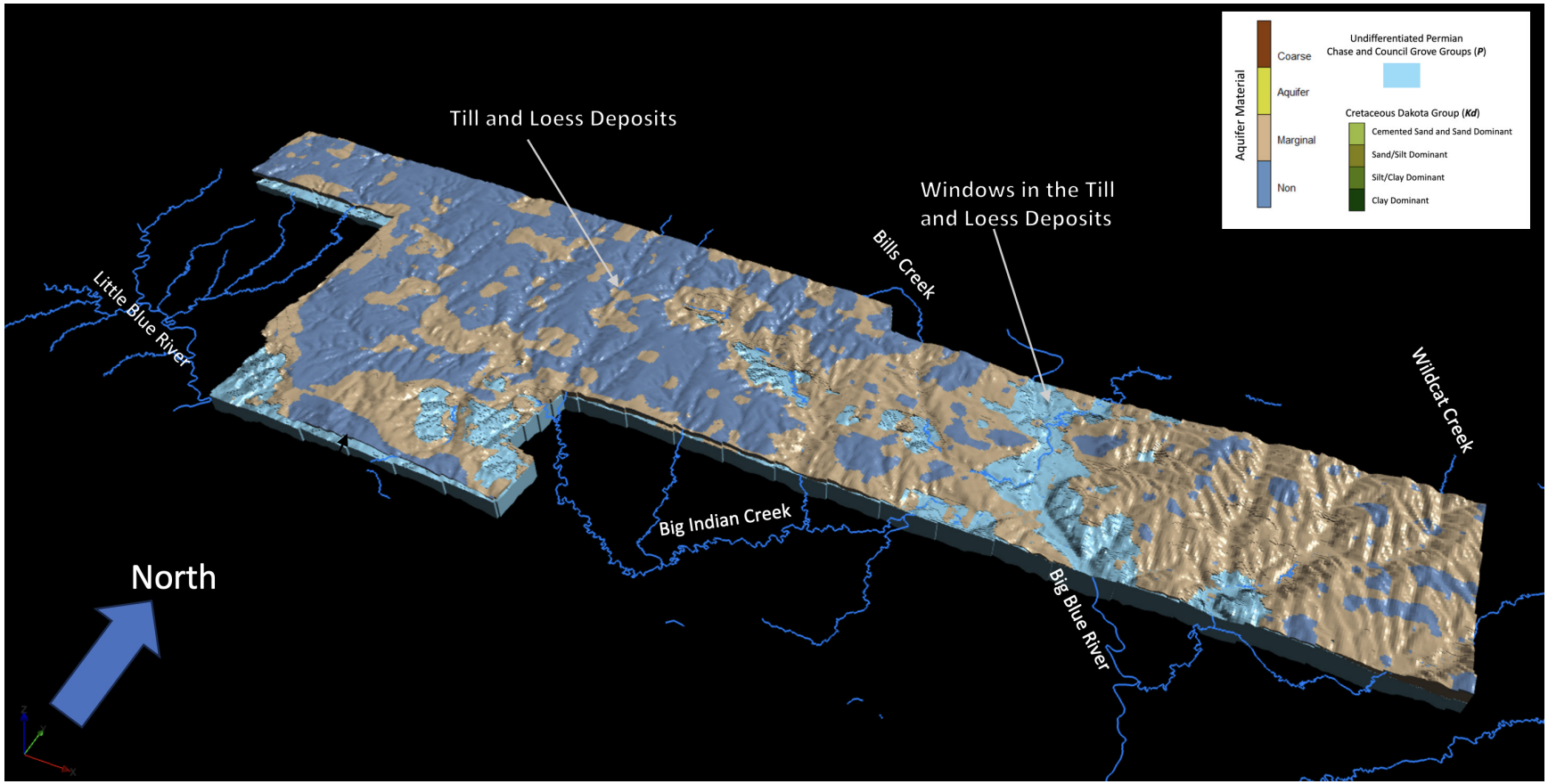


Figure 5-40. 3D Voxel diagram looking to the northwest of the interpreted distributions of the total non- and marginal-aquifer materials of the Quaternary (*Q*) within the LBBNRD 2023 AEM survey area. V.E.=20x.

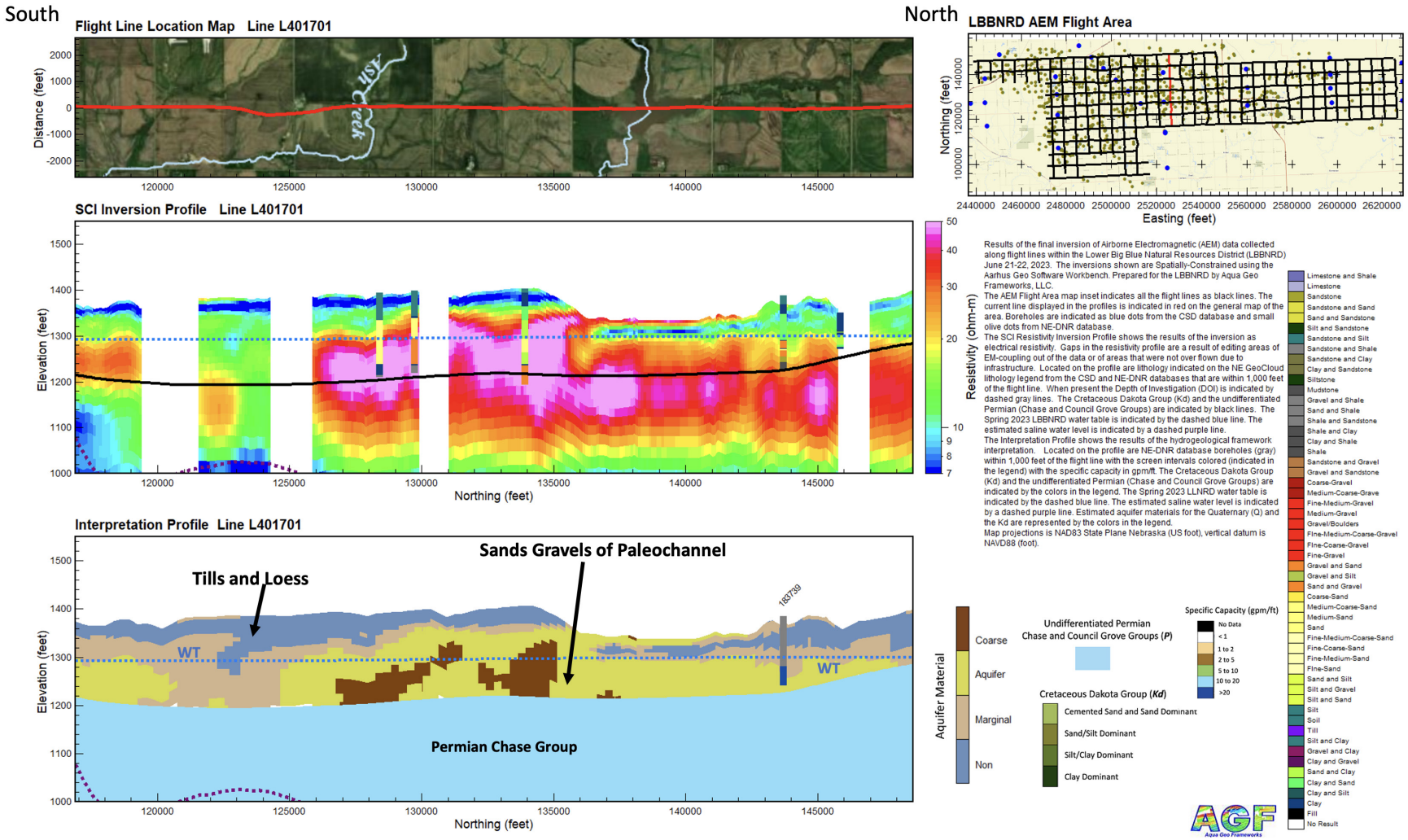


Figure 5-41. North-south AEM flight line L401701. A location map is on the upper right. On the left the top profile shows the air photo along the flight line. The middle profile is the SCI resistivity inversion result showing borehole lithologies and the bottom profile is an interpretative section showing the undifferentiated Permian (*P*) underlying Quaternary (Q) subdivided into interpreted aquifer materials. Boreholes in the bottom section indicate measured Specific Capacity.

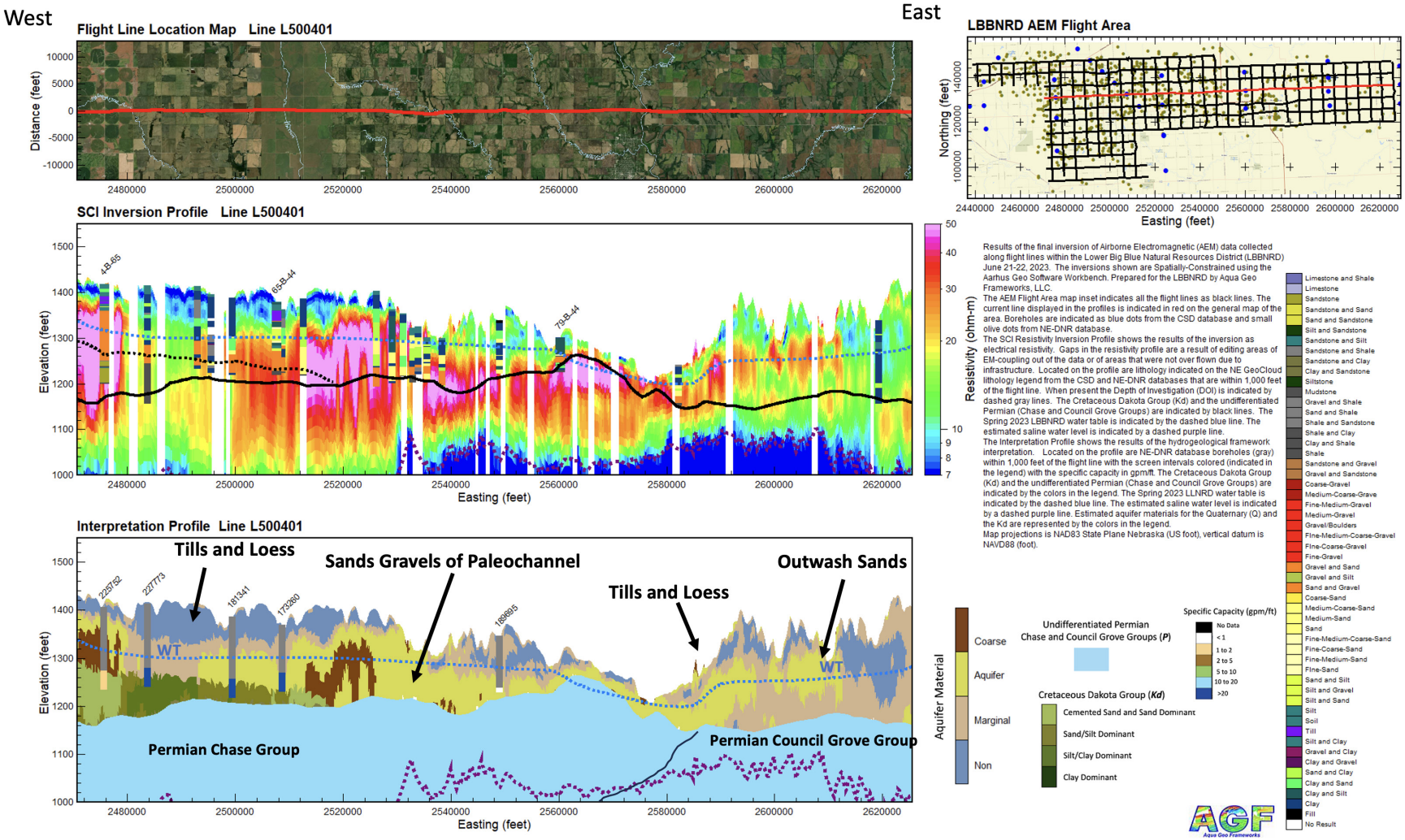


Figure 5-42. East-west AEM flight line L500401. A location map is on the upper right. On the left the top profile shows the air photo along the flight line. The middle profile is the SCI resistivity inversion result showing borehole lithologies and the bottom profile is an interpretative section showing the undifferentiated Permian (*P*) underlying the Cretaceous Dakota Group (*Kd*) on the west and the Quaternary (*Q*) subdivided into interpreted aquifer materials. Boreholes in the bottom section indicate measured Specific Capacity.

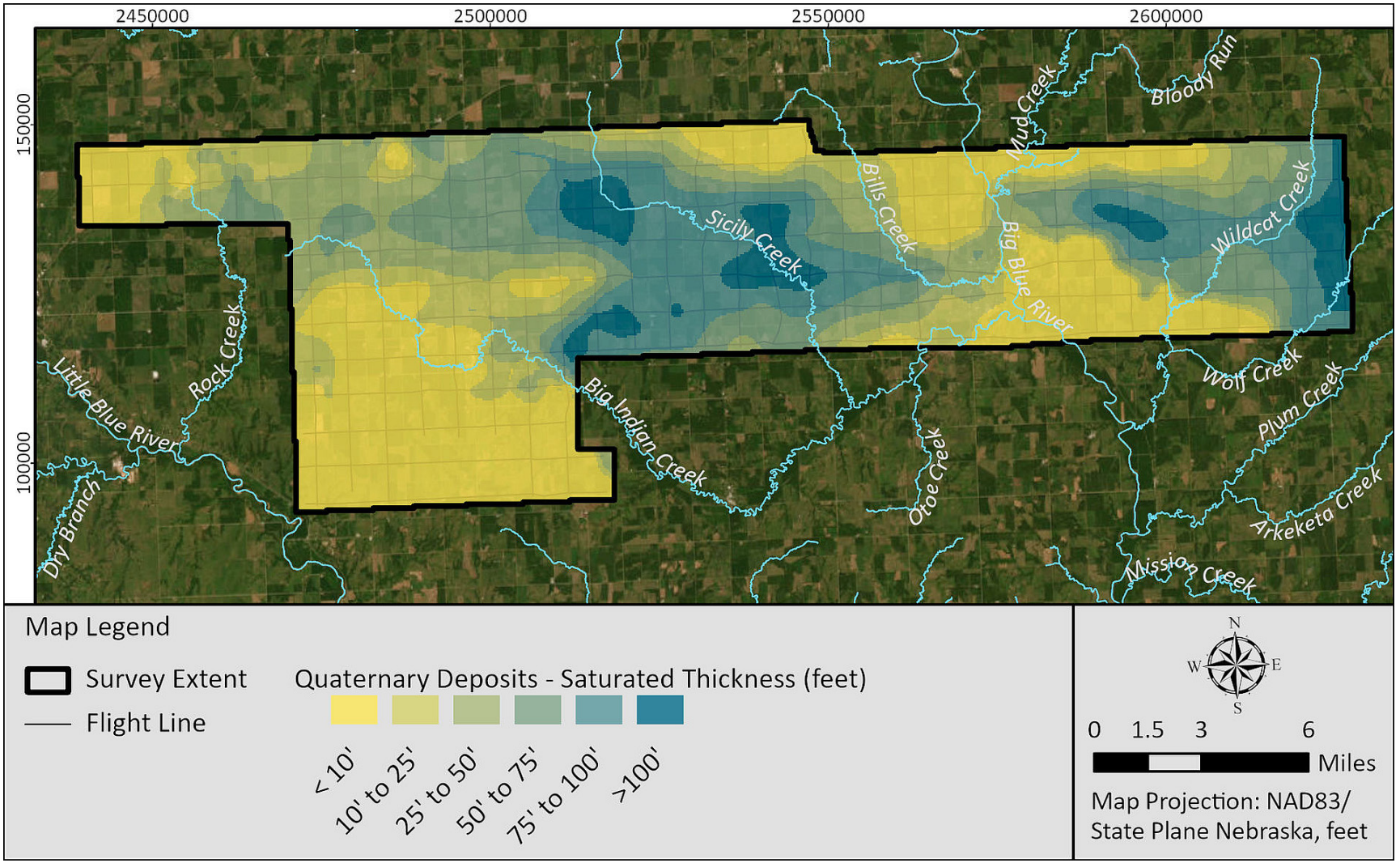


Figure 5-43. Map of the total saturated Quaternary (*Q*) thickness within the LBBNRD 2023 AEM survey area calculated using the Spring 2023 LBBNRD water levels.

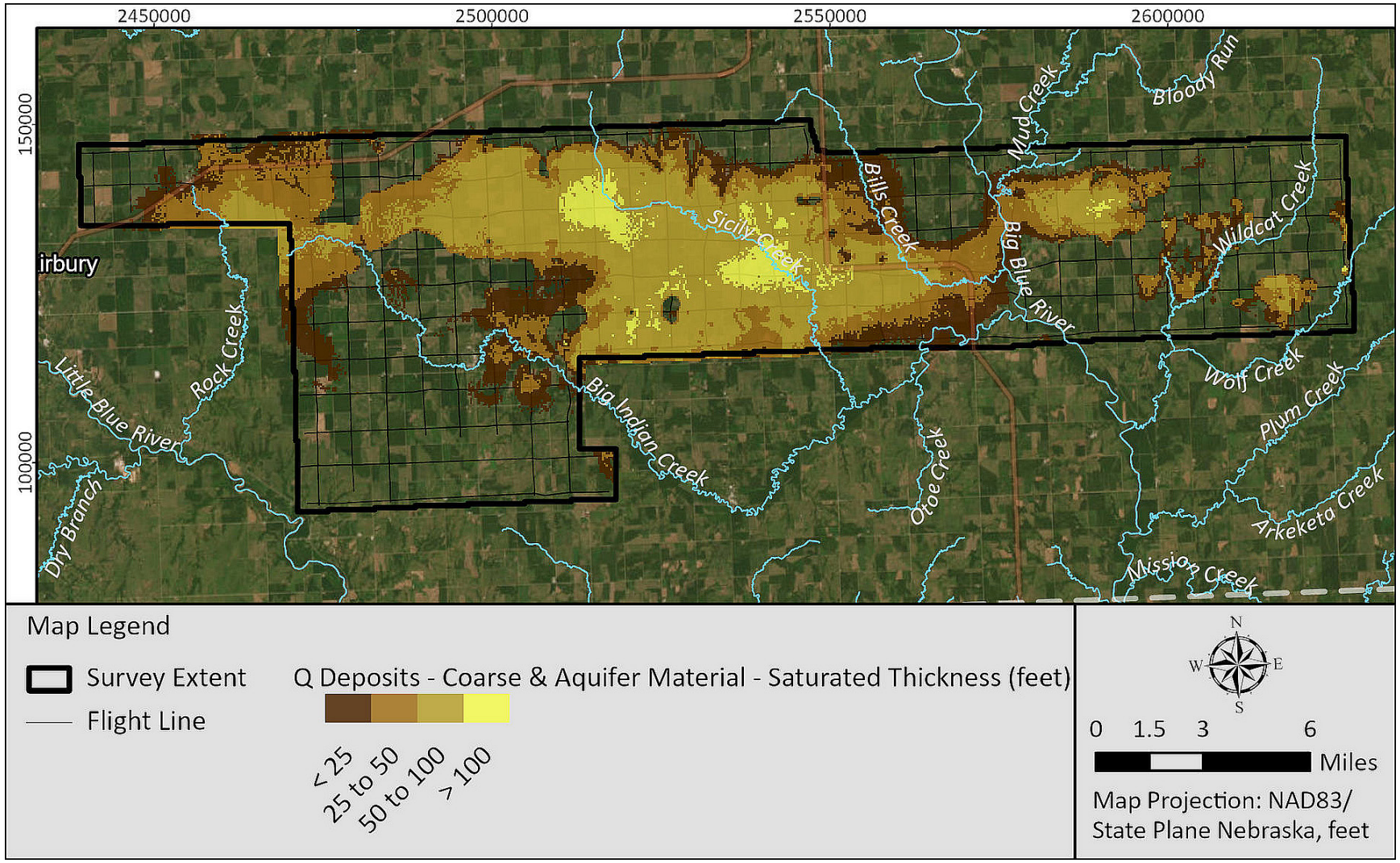


Figure 5-44. Map of the Quaternary (*Q*) aquifer and coarse aquifer material saturated thickness within the LBBNRD 2023 AEM survey area calculated using the Spring 2023 LBBNRD water levels.

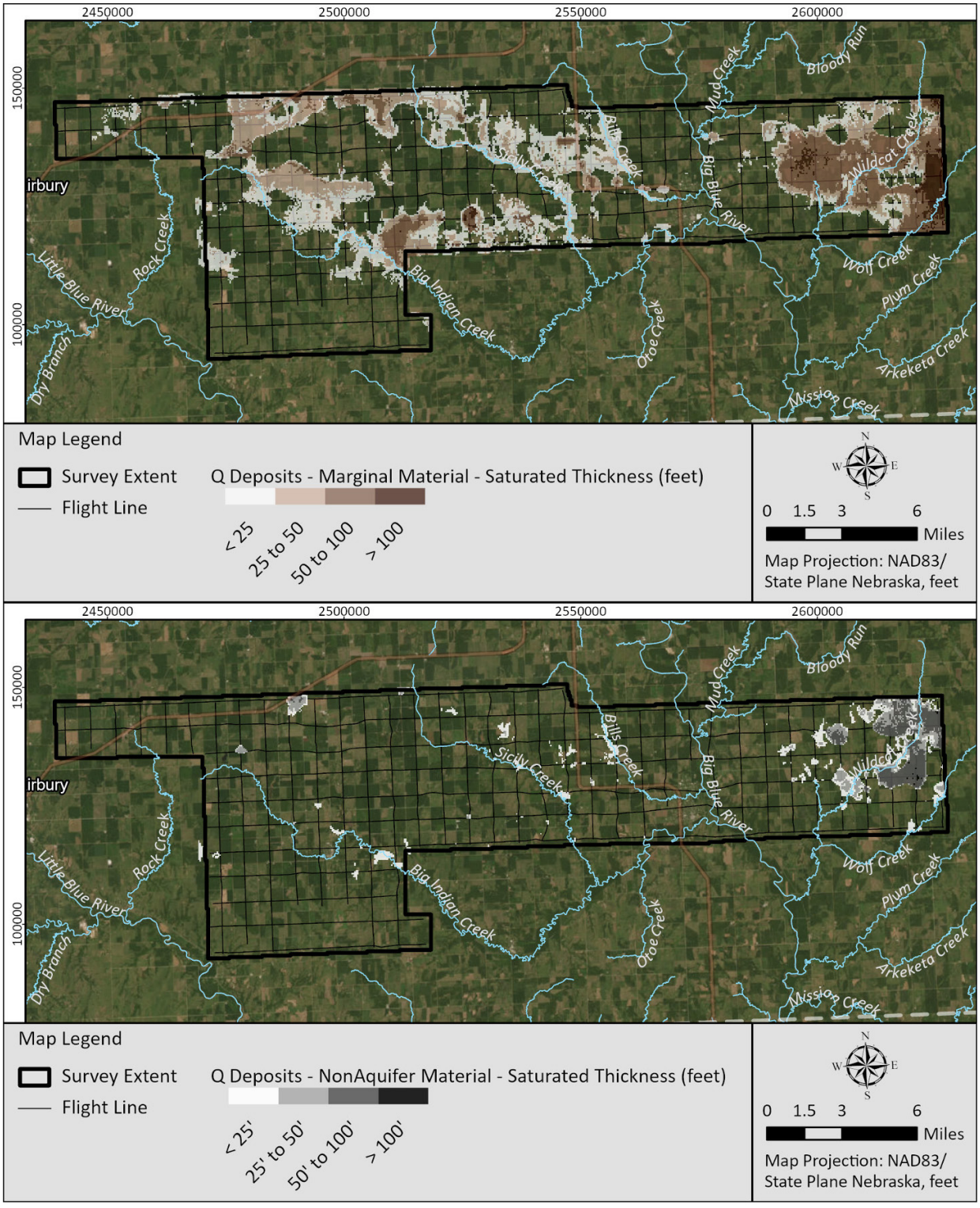


Figure 5-45. Map of the saturated Quaternary (*Q*) marginal aquifer materials (top), and saturated non-aquifer material thickness (bottom) within the LBBNRD 2023 AEM survey area calculated using the Spring 2023 LBBNRD water levels.

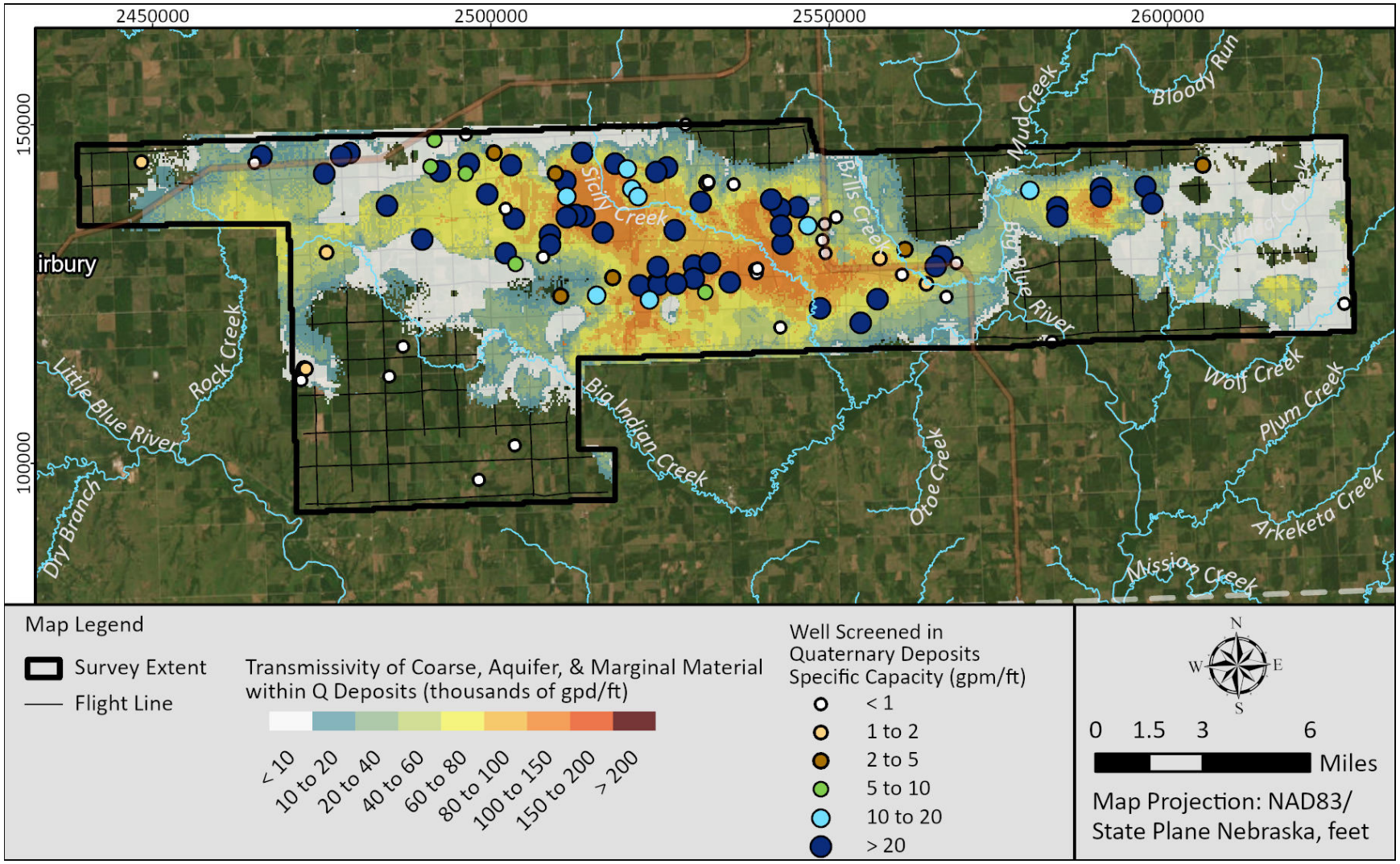


Figure 5-46. Map of the estimated transmissivity (gpf/feet) of the Quaternary (Q) marginal aquifer materials, aquifer materials, and coarse aquifer materials within the LBBNRD 2023 AEM survey area. Specific Capacity values from the NE-DNR registered well database for wells screen in the Q are shown as indicated by the legend.

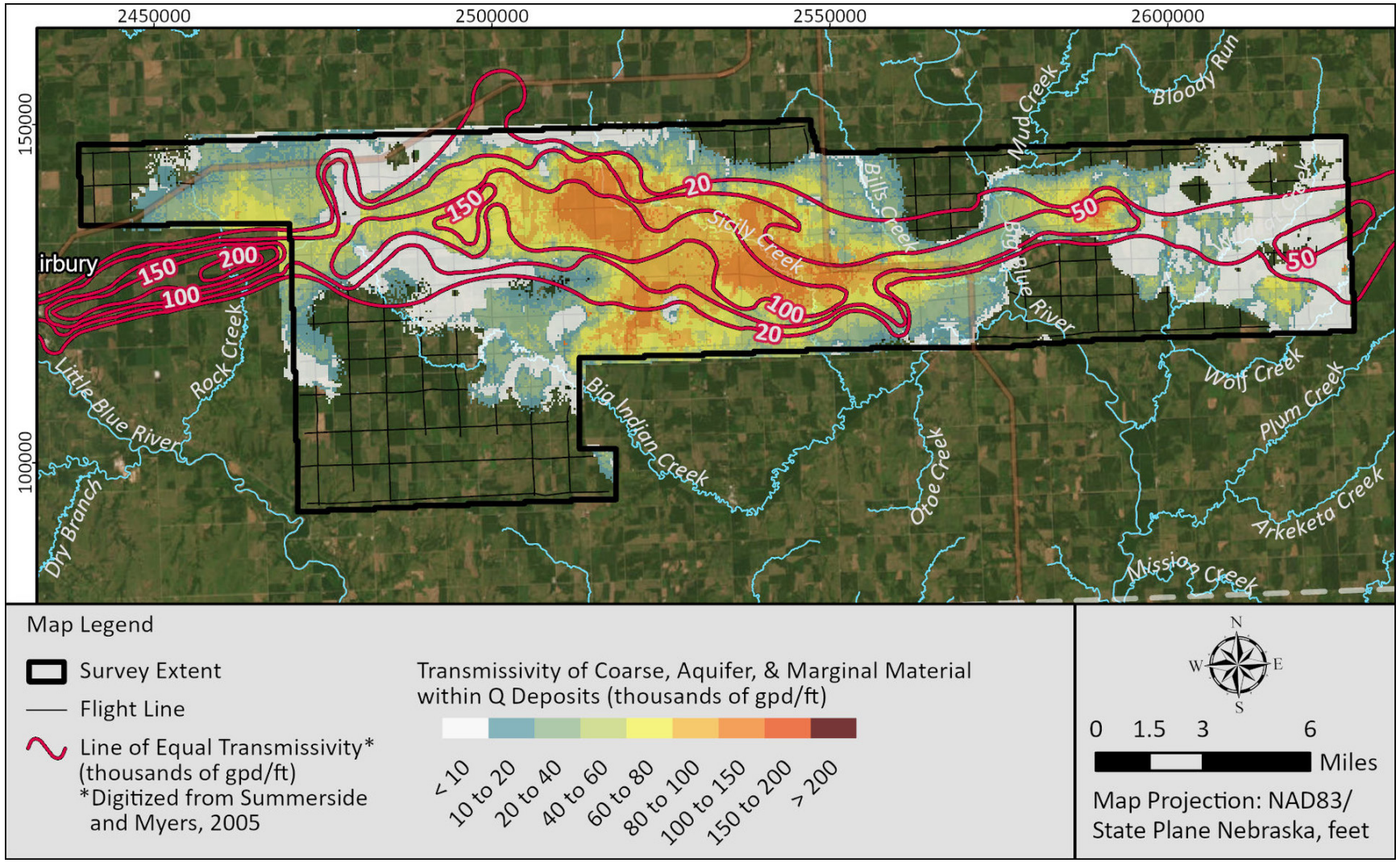


Figure 5-47. Map of the estimated transmissivity (gpf/feet) of the Quaternary (*Q*) marginal aquifer materials, aquifer materials, and coarse aquifer material transmissivity within the LBBNRD 2023 AEM survey area. Overlain with the transmissivity contours from Summerside and Myers (2005).

5.3.2 Hydrogeology of the Cretaceous Dakota Group

The ***Kd*** is in the western part of the survey area and is directly deposited on the undifferentiated Permian (***P***) units. The ***Kd*** was eroded from the eastern two thirds of the survey area before and during the glacial period. The ***Kd*** is composed of consolidated and semi consolidated clay, silt, sand, sandstone, siltstone, and shale. The deposits are in fluvial deposits associated with the delta front that existed and underwent multiple regressive and transgressive sequences in the Cretaceous (Witzke et al., 1983).

These materials overlie the Permian Chase ***Pc*** in the western section of the survey area and serve as the regional aquicludes. A map of the elevation of the top of the undifferentiated Permian (***P***) bedrock, which can be considered the base of ***Kd***, is presented in Figure 5-48. The top of the ***P*** influenced the depositional environment of the ***Kd*** due to the control the surface had on the stream gradient at the time of deposition where sediments were deposited. A majority of the ***Kd*** is saturated throughout the survey area.

Figure 5-49 is a 3D voxel model looking north showing the distribution of ***Kd*** cemented sand and sand dominant materials along with the sand/silt dominant materials. This represents resistivities > 18 ohm-m. Similarly, Figure 5-50 presents a 3D voxel model, looking north, showing the distribution of ***Kd*** materials with resistivities over 25 ohm-m. This threshold illuminates several channel structures within the ***Kd***.

Figure 5-51 presents the profile of north-south Line L400801 on the western edge of the survey area. The lithologies of the wells on the southern end of the line indicated sandstone within the ***Kd***. Several wells are completed within the ***Kd*** and show specific capacities from 5 to 10 gpm/ft. Well *138505* looks to be completed in both the ***Kd*** and the ***Q*** and has a specific capacity (SC) of > 20 gpm/ft.

The ***Kd*** varies in thickness from 0 ft in the east to approximately 220 Feet thick in the west (Figure 5-52). The saturated thickness is similar to the total thickness as the majority of the ***Kd*** is saturated (Figure 5-53).

As discussed above, the aquifer materials within the ***Kd*** indicated fluvial and deltaic sediment paleochannel systems and can be seen in Figure 5-54 which shows the saturated sandstone and sand dominant materials > 25 ohm-m. When present, they are from <25 feet to >150 feet thick. The well completions in the area indicated that these sandstone and sand dominant materials have had significant well development.

Figure 5-55 is a map of the saturated thickness of the sandstone and sand dominant materials > 25 ohm-m and the SC of the wells which are completed in the ***Kd***. There is a strong correlation of the > 25 ohm-m materials to the location of the best wells in the area and the higher SC values.

Using a similar approach as was used to calculate transmissivity maps (Section 5.1.7) for the ***Q***, an attempt was made to estimate the transmissivity of the ***Kd*** aquifer. In review of the literature in the area of eastern Nebraska, two references were found on the transmissivity within the ***Kd***. One is O'Connor (1987) with a value of 5.56×10^{-4} feet/sec. This value is from northeastern Nebraska, north of the Platte

River. The second value, from southwestern Iowa from Gannon and Vogelgesang (2015), is 6.48×10^{-4} feet/sec. We elected to use the average of the two values of 6.02×10^{-4} feet/sec. The saturated thickness of the ***Kd***, using the > 18 ohm-m threshold, was used, composed of cemented sand and sand dominant material along with the sand/silt dominant materials.

Unlike the ***Q*** we have no map for the ***Kd*** to compare with as in Summerside and Myers (2005) that can be used to adjust our values as pumping tests are almost nonexistent within the ***Kd***. This is one of the first estimations of the ***Kd*** transmissivity in Nebraska and needs to be used carefully and as a guide and not as a firm value.

When the SC values from the NE-DNR registered wells are placed on the ***Kd*** AEM estimated transmissivity map (Figure 5-56), a good general agreement is observed, and more details revealed by the AEM due to the high density of observations.

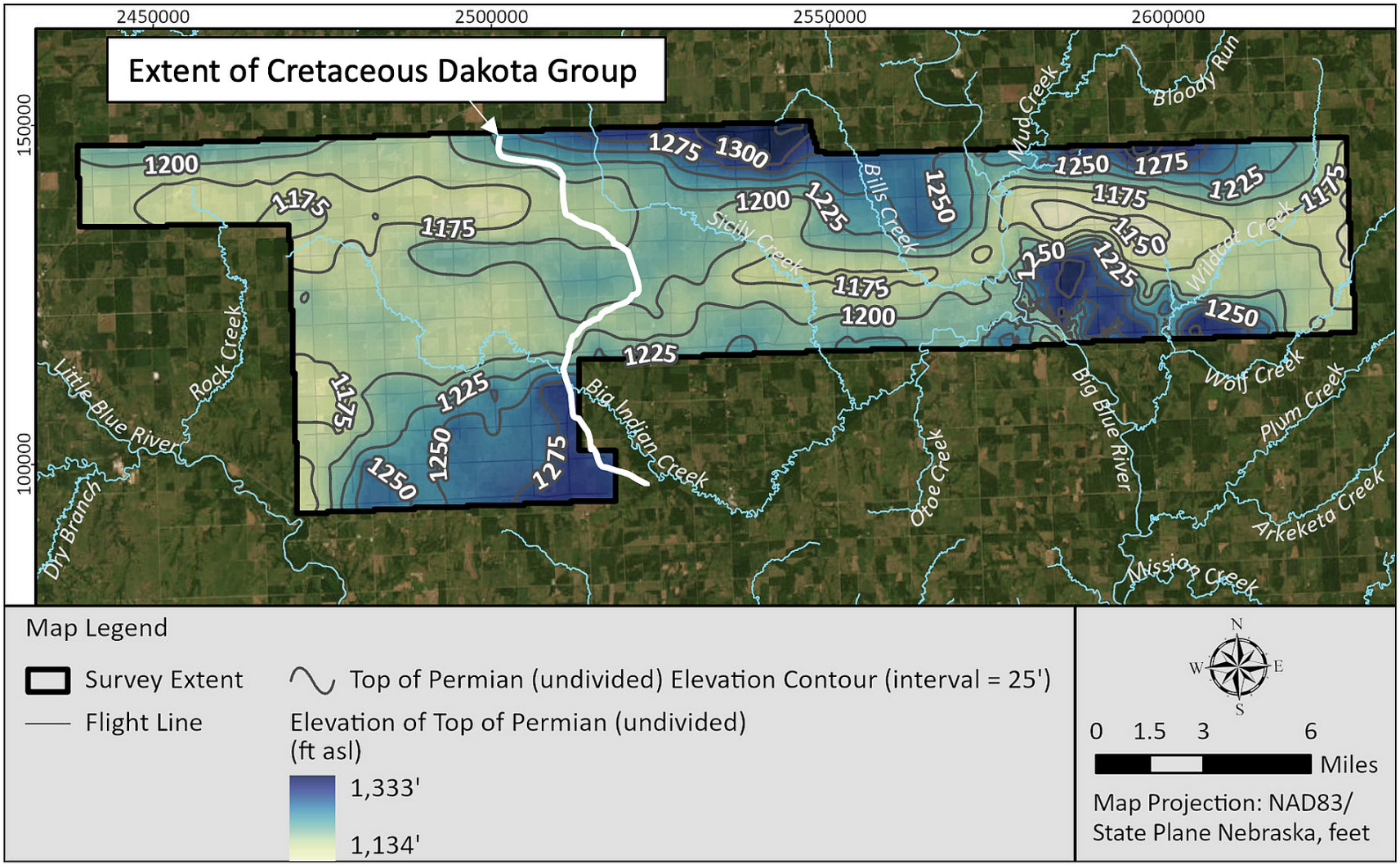


Figure 5-48. Map of the undifferentiated Permian (*P*) bedrock surface elevation. The extent of the Cretaceous Dakota Group (*Kd*) is indicated by the white line.

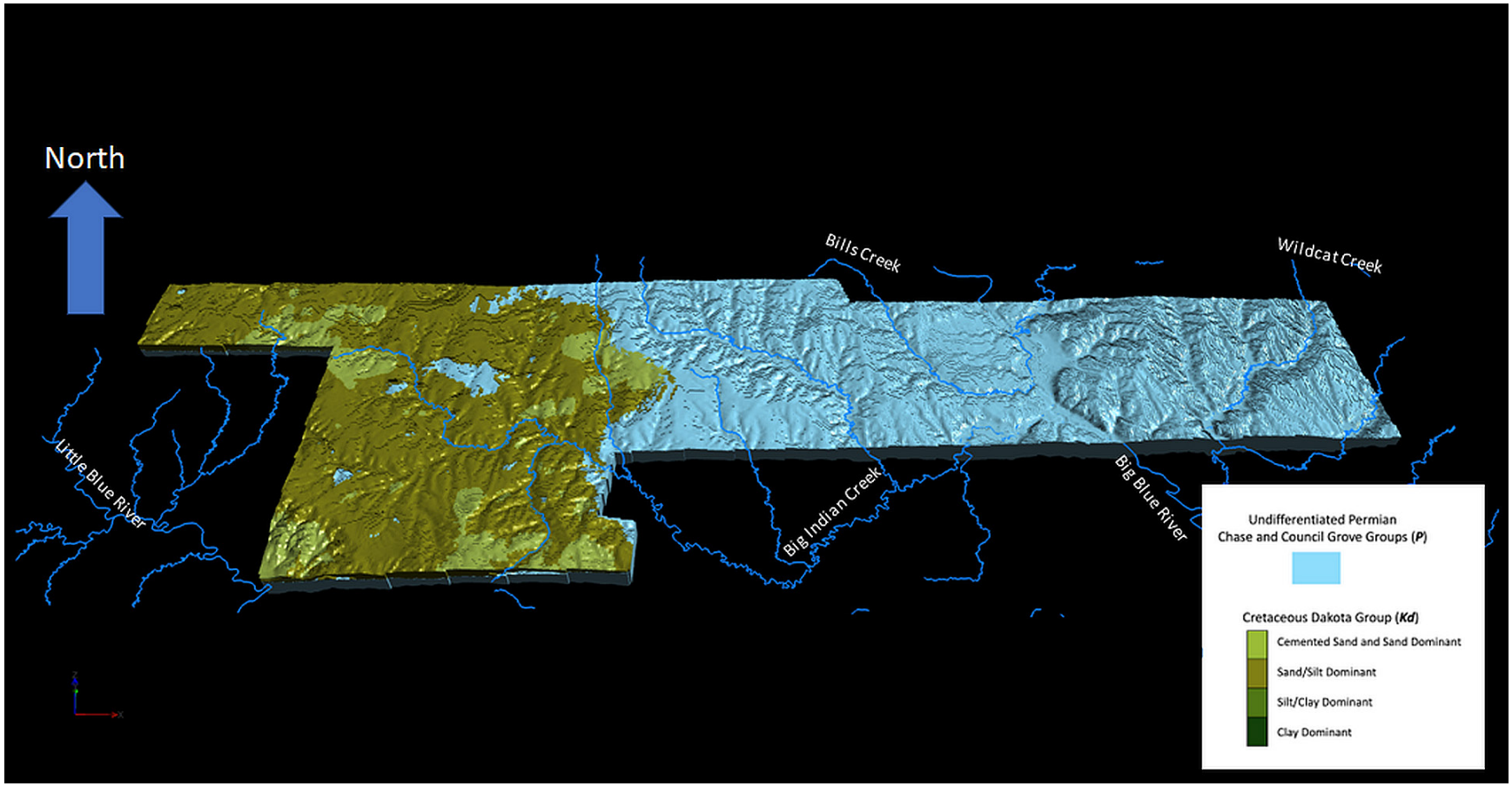


Figure 5-49. 3D Voxel diagram looking to the north of the interpreted Cretaceous Dakota Group (*Kd*) distributions of cemented sand and sand dominant as well as sand and silt dominant material > 18 ohm-m within the LBBNRD 2023 AEM survey area. V.E.=20x.

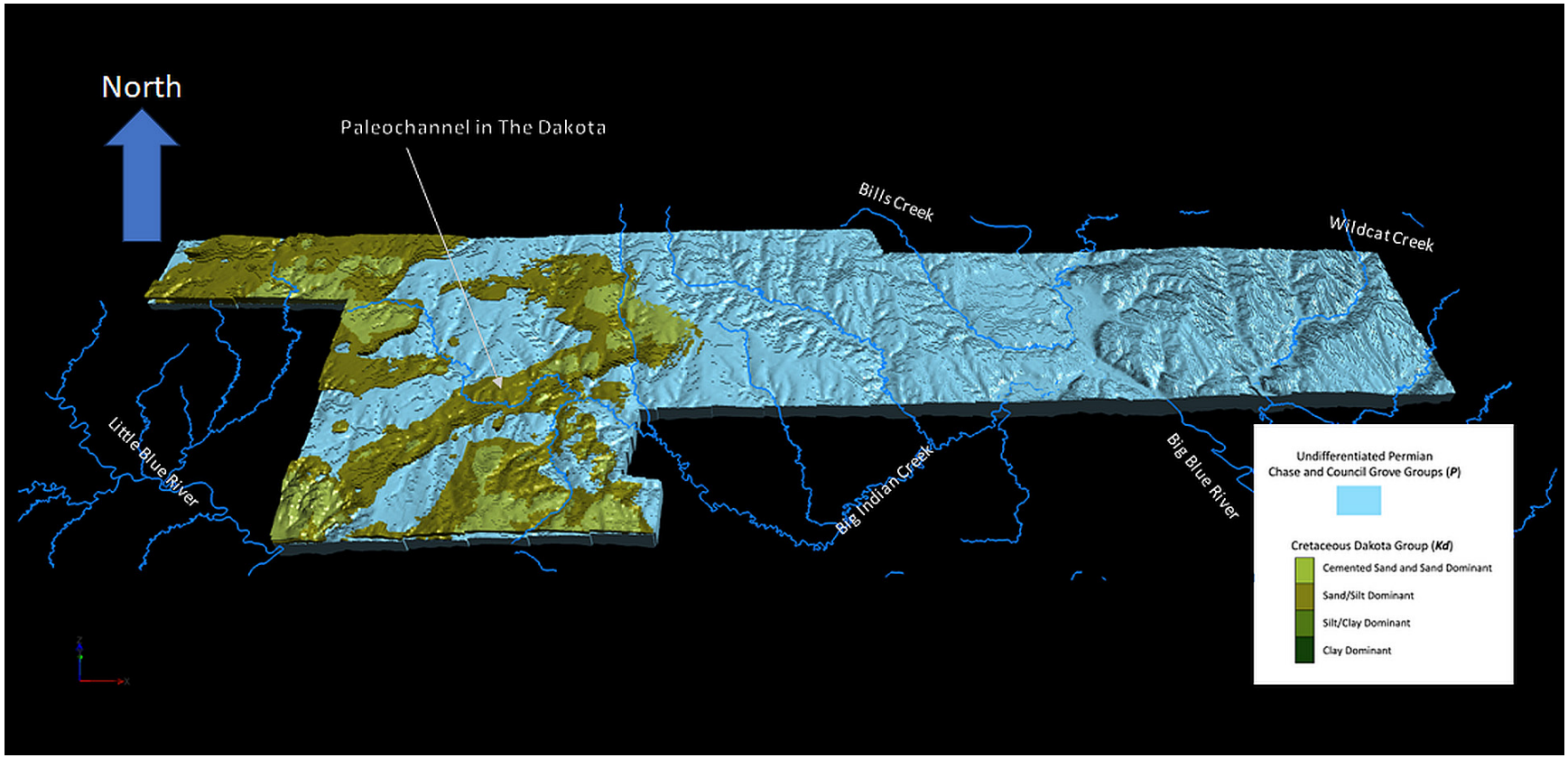


Figure 5-50. 3D Voxel diagram looking to the north of the interpreted Cretaceous Dakota Group (*Kd*) distributions of cemented sand and sand dominant material > 25 ohm-m within the LBBNRD 2023 AEM survey area. V.E.=20x.

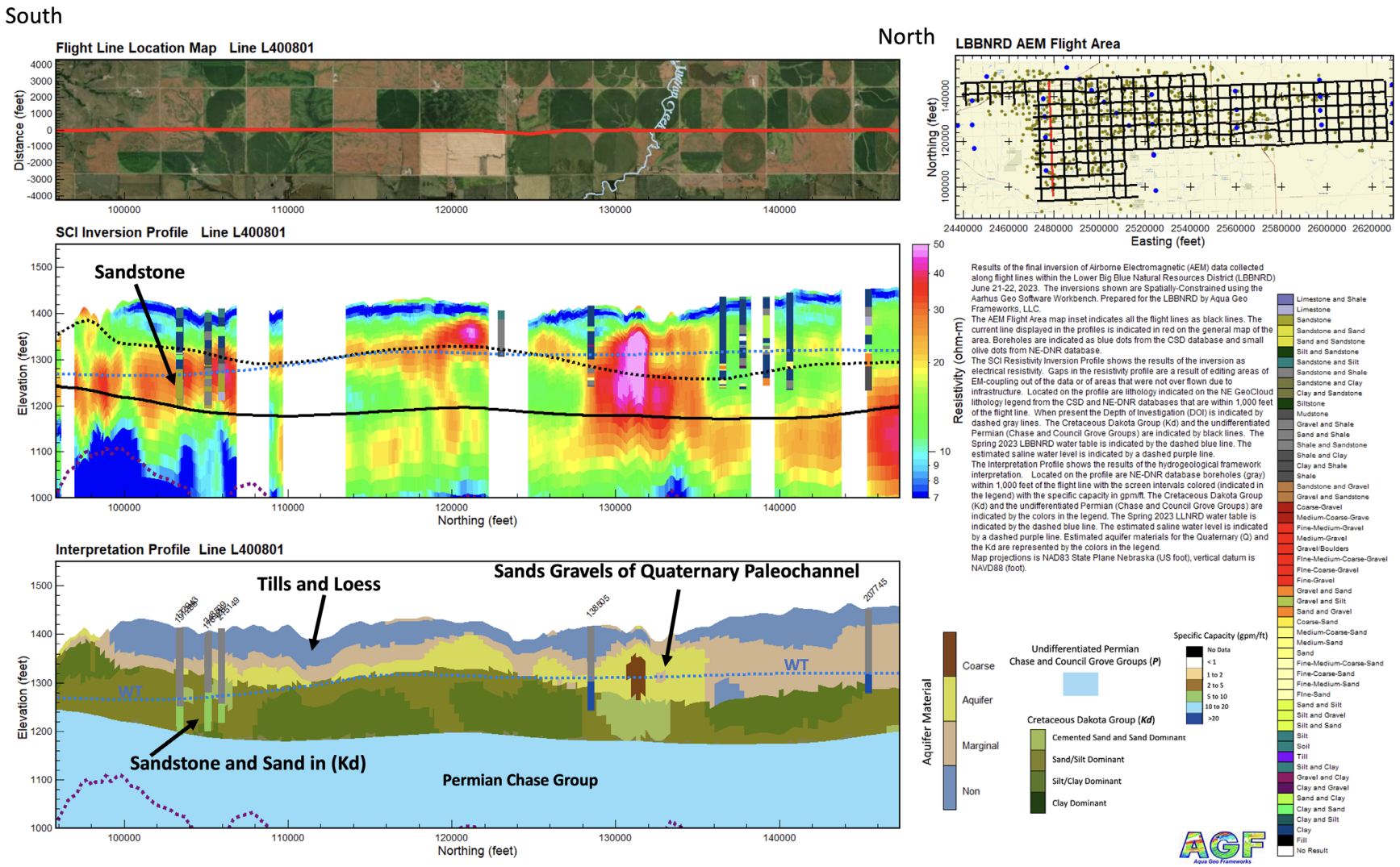


Figure 5-51. North-south AEM flight line L400801. A location map is on the upper right. On the left the top profile shows the air photo along the flight line. The middle profile is the SCI resistivity inversion result showing borehole lithologies and the bottom profile is an interpretative section showing the undifferentiated Permian (*P*) underlying Quaternary (*Q*) subdivide into interpreted aquifer materials. Boreholes in the bottom section indicate measured Specific Capacity.

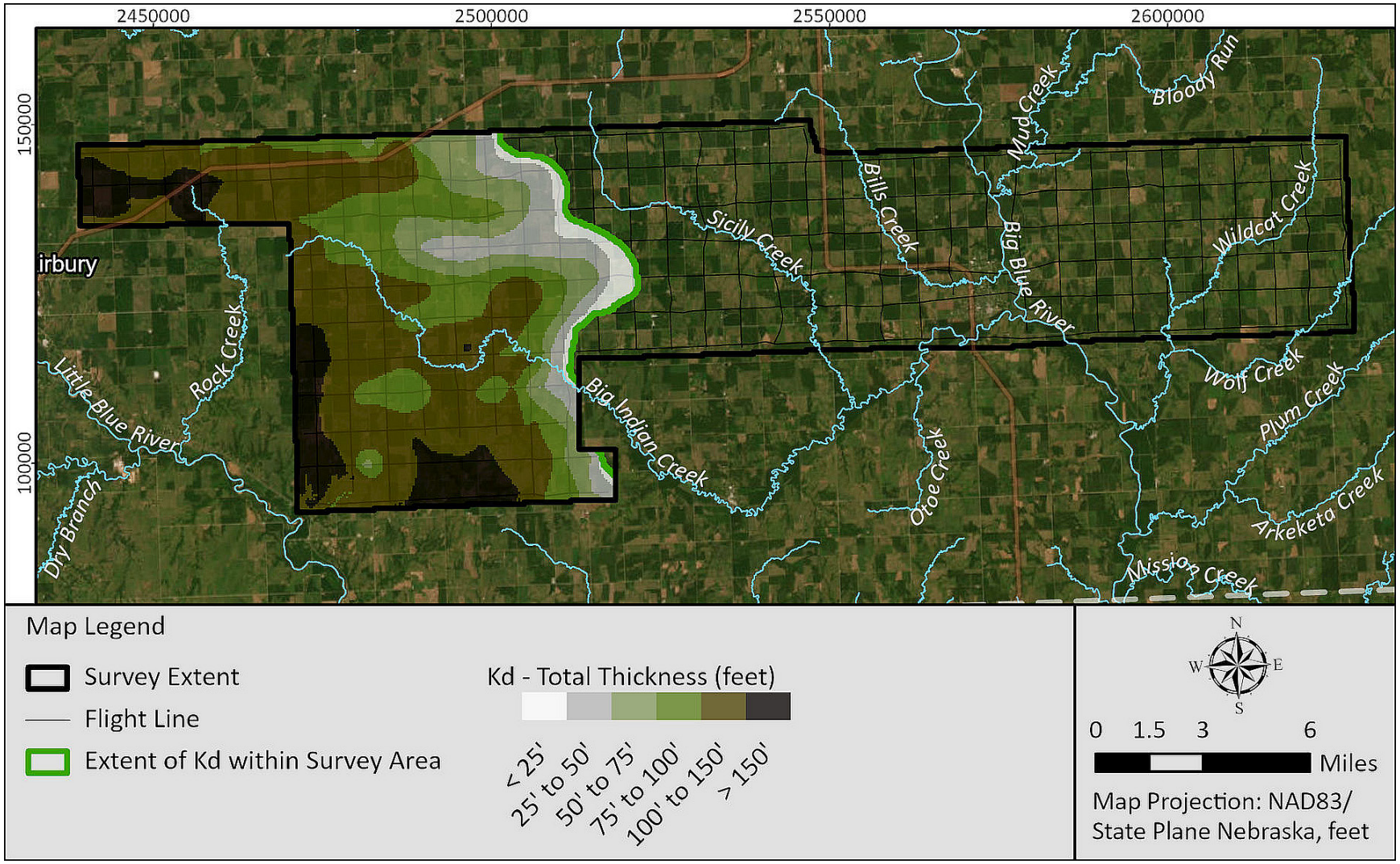


Figure 5-52. Map of the total Cretaceous Dakota Group (*Kd*) total thickness within the LBBNRD 2023 AEM survey area.

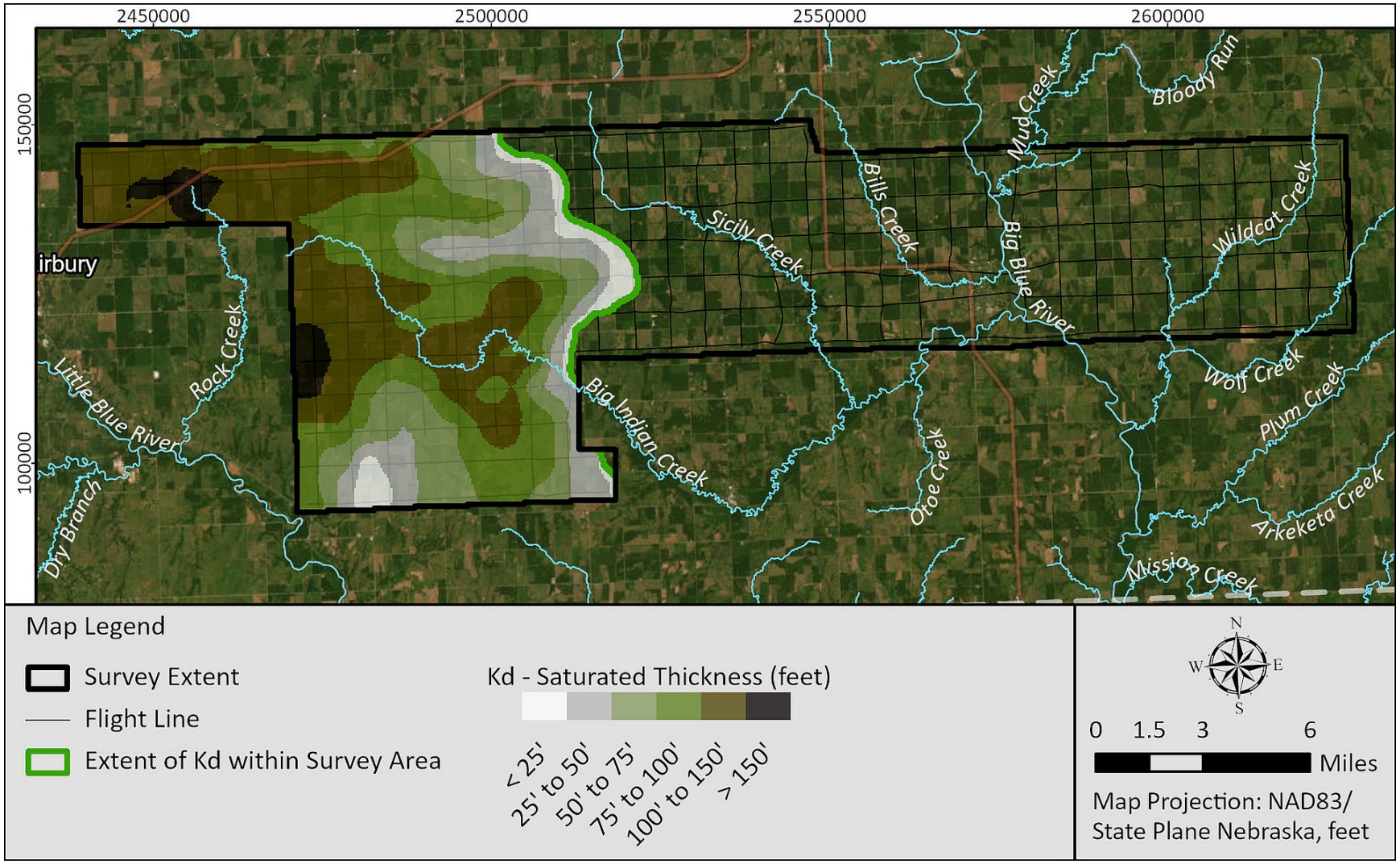


Figure 5-53. Map of the Cretaceous Dakota Group (*Kd*) total saturated thickness within the LBBNRD 2023 AEM survey area.

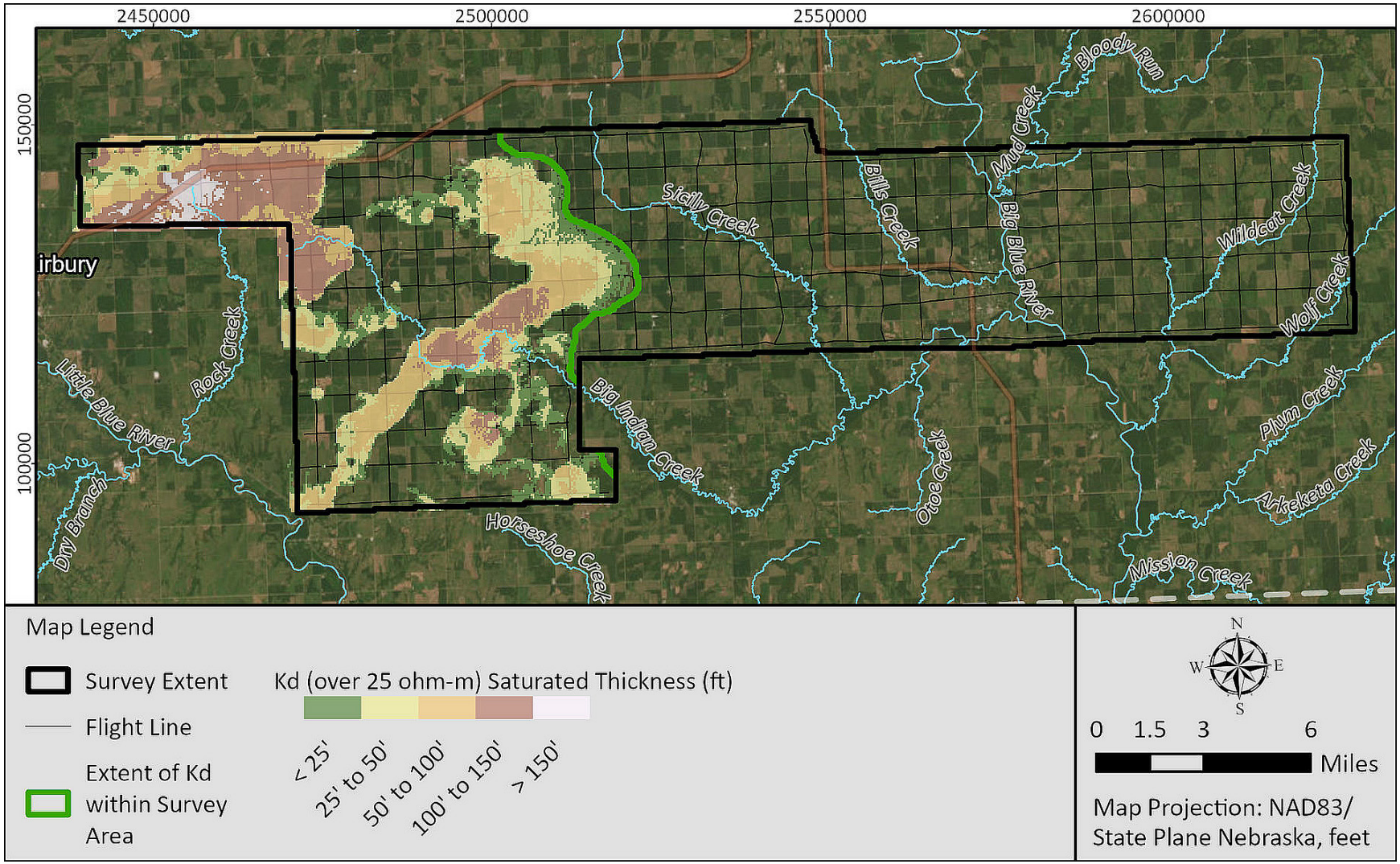


Figure 5-54. Map of the Cretaceous Dakota Group (*Kd*) total saturated thickness of the sandstone and sand-dominant materials within the LBBNRD 2023 AEM survey area with resistivities >25 ohm-m.

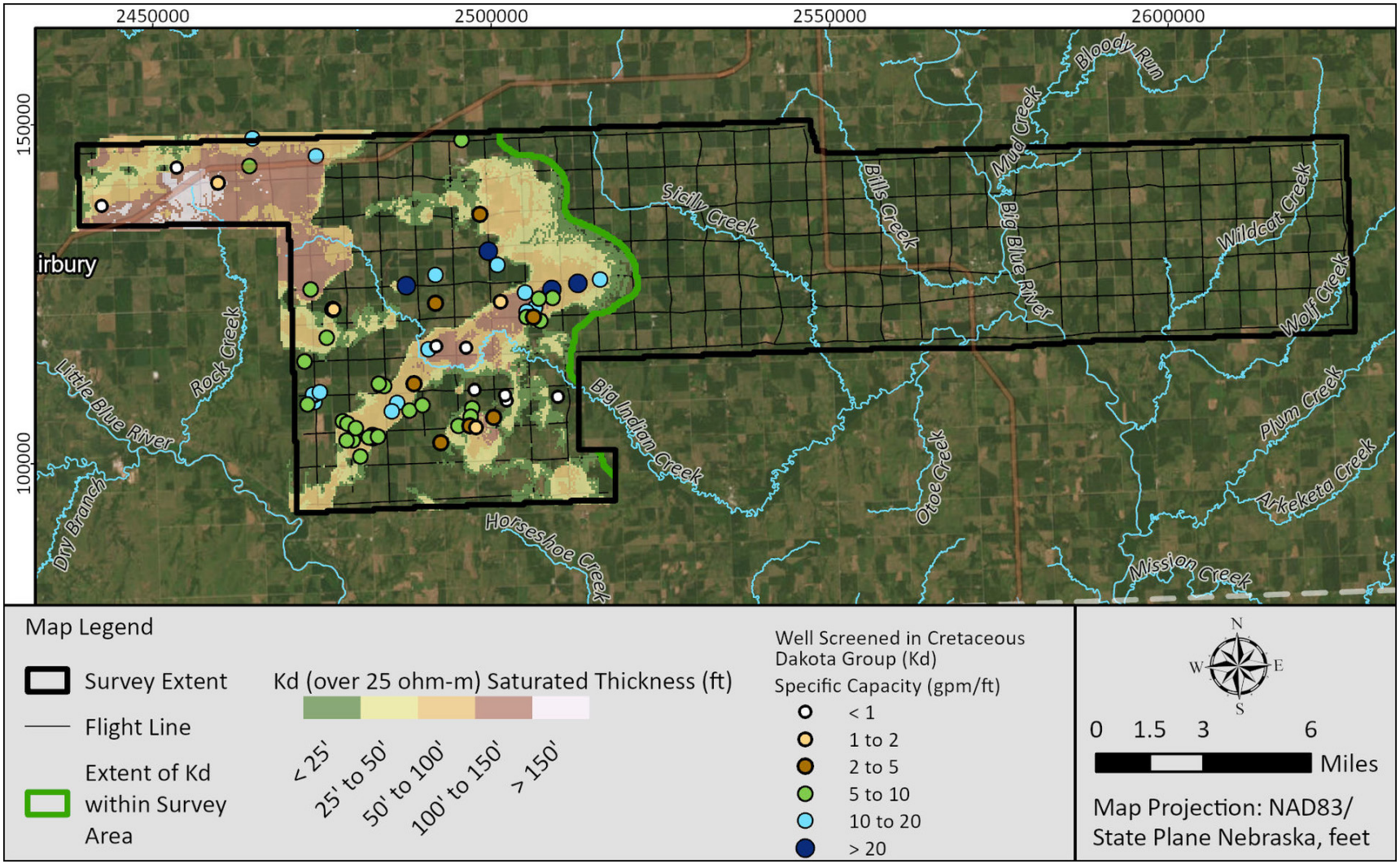


Figure 5-55. Map of the estimated transmissivity (gpf/feet) of the Cretaceous Dakota Group (*Kd*) saturated thickness of the sandstone and sand dominant materials with resistivities > 25 ohm-m within the LBBNRD 2023 AEM survey area. Specific capacity values from the NE-DNR registered well database for wells screen in the *Kd* are shown as indicated by the legend.

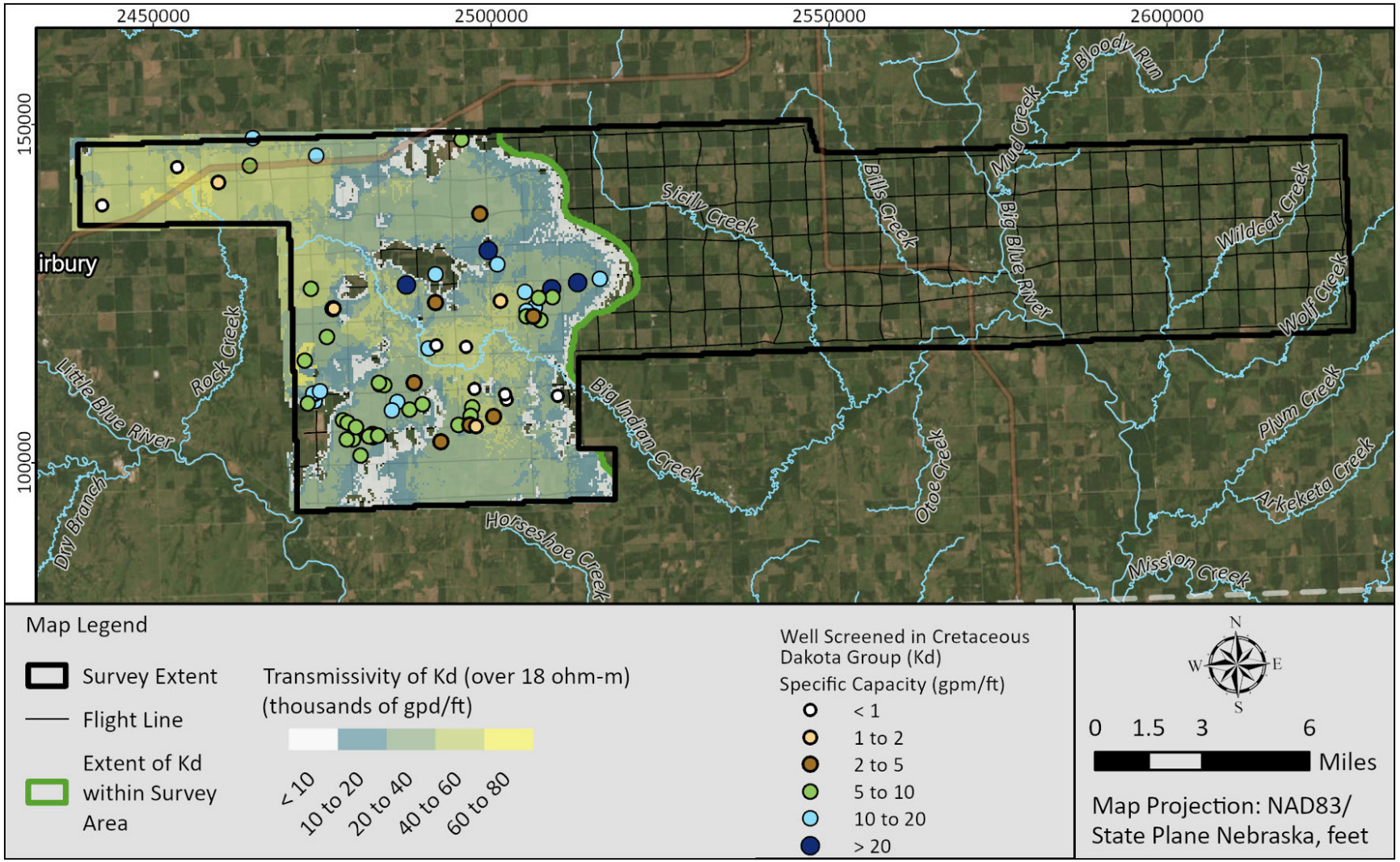


Figure 5-56. Map of the estimated transmissivity (gpf/feet) of the Cretaceous Dakota Group (*Kd*) saturated thickness of the sandstone and sand dominant as well as the sand/silt dominant materials > 18 ohm-m within the LBBNRD 2023 AEM survey area. Specific capacity values from the NE-DNR registered well database for wells screen in the *Kd* are shown as indicated by the legend.

5.3.3 The Permian Bedrock Hydrology

The Permian bedrock is made up of the Permian Chase Group (***Pc***) and Permian Council Grove Group (***Pcg***) which underlies the ***Kd*** (when present) and the ***Q.*** These units are considered aquicludes in this area. There is some use of the fractured limestone within the southern area of Nebraska as an aquifer, but that is not common, and the fractures need to be in hydrogeological connection to a water source, typically a stream or a good aquifer in the ***Q***.

Within the ***P*** unit of the LBBNRD 2023 AEM survey area a low resistivity layer of < 7 ohm-m is interpreted as a regional saline water interface. The interface is shallower in the easter portion of the survey area with a minimum of 70 feet and is deepest in the western portion of the survey area at > 700 feet (Figure 5-57) depth.

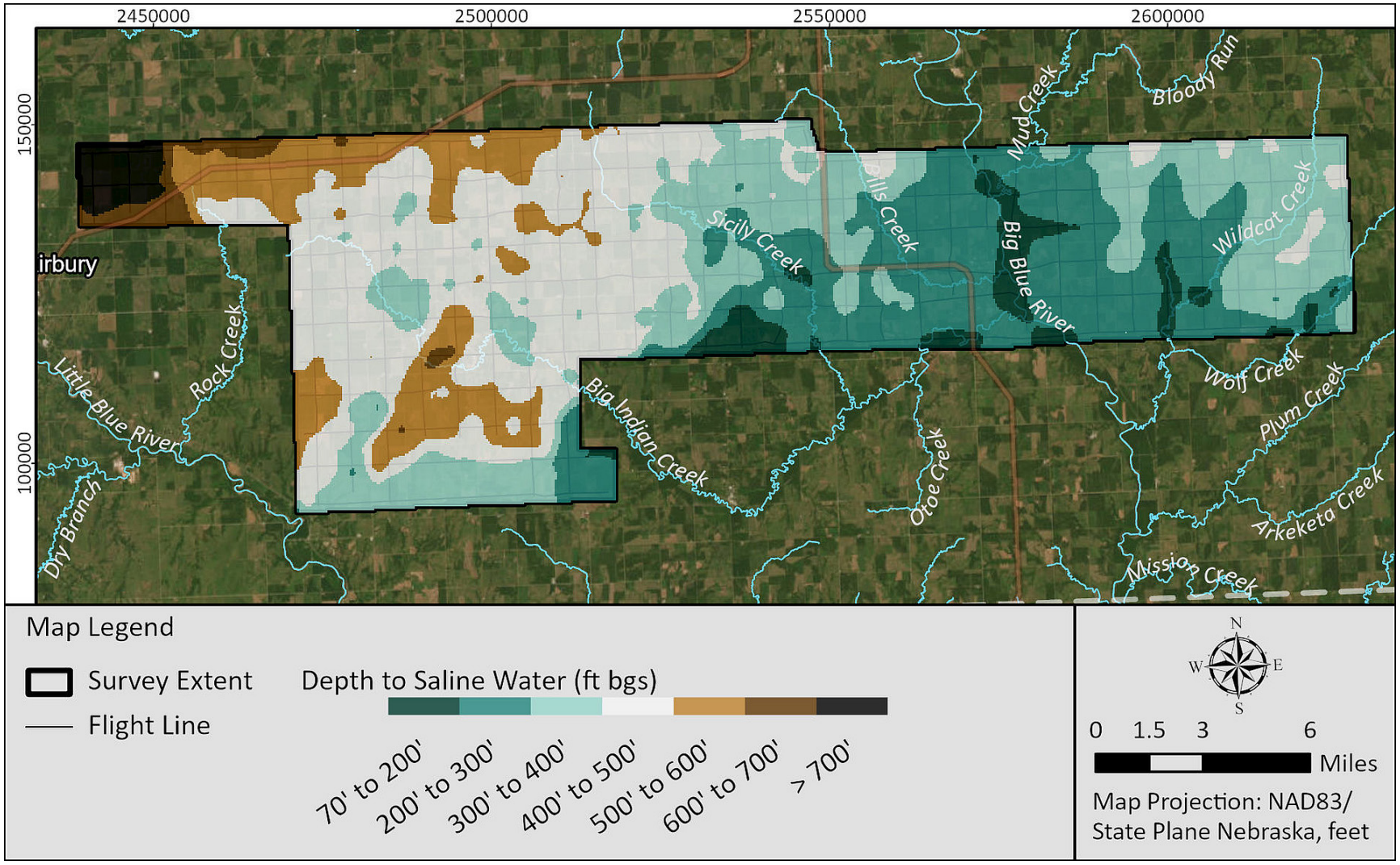


Figure 5-57. Map of the depth to the interpreted saline water surface within the undifferentiated Permian (P) units over the LBBNRD 2023 AEM survey area.

5.3.4 Groundwater in LBBNRD 2023 AEM Survey Area

As discussed above, the groundwater within LBBNRD 2023 AEM survey area is within the limited alluvial sediments of the present streams, glacial sediments, and the paleovalley sediments of the Quaternary (***Q***). There is also groundwater in the fluvial and deltaic sediments of the Cretaceous Dakota Group (***Kd***). The groundwater availability is governed by both the ***Q*** and ***Kd.*** In the western third of the survey area, the ***Q*** overlies the ***Kd*** and is in hydrogeological connection with the ***Kd***. In general, the ***Q*** groundwater is within paleovalley sediments, and the ***Kd*** groundwater is in the sandstone and sand deposits of the fluvial deposits. Some wells show completions in both units the ***Q*** and the ***Kd***.

Figure 5-58 shows the NE-DNR specific capacities (SC) of the wells competed within the ***Q*** on the estimated transmissivity of the ***Q*** aquifers. Most of the SC values that we have calculated from the NE-DNR database are within the higher estimated transmissivity (**T**) values of the paleovalley. A clear decrease in T is observed on the eastern side of the survey area where the paleovalley sediments area reduced to the thick glacial till deposits. Some isolated deposits of outwash gravel exist within the upper portions of the till and may be related to glacial-tectonic features associated with thrust sheets of outwash as was observed in other areas of central Nebraska by Korus et al. (2021). Many of these sand and gravel deposits are unsaturated or partially saturated. Locally they can provide domestic water sources but are seldom large enough for sustainable large production wells.

Figure 5-59 shows the NE-DNR SC of the wells competed within the ***Kd*** on the estimated T of the ***Kd*** aquifers with resistivities >18 ohm-m representing the cemented sands and sand dominant as well as the sand/silt dominant materials. As discussed above in Section 5.3.2, there have been many assumptions made in the estimates of the T map, but it does provide a useful way of examining the T of the ***Kd***. Many of the higher ***Kd*** SC are along a trend that is associated with a high electrical resistivity fluvial channel deposits within the ***Kd***.

As was discussed in Section 5.2.2, the calculation of the T is governed by the selection of hydraulic conductivity and the saturated thickness of the unit. When looking at the interaction of the groundwater within both units, a composite image of both the ***Q*** coarse, aquifer, and marginal and the ***Kd*** > 25 ohm-m sand dominant section is useful (Figure 5-60). This image shows the SC values for the wells completed in both the ***Q*** and the ***Kd***, and indicates areas that have aquifer materials in both units. This is not an improbable outcome in many areas as the top of the ***Kd*** is difficult to differentiate from the bottom of the ***Q*** in many cases as there is unconsolidated sands in both units. Mud rotary drilling also makes this subtill contact difficult to detect.

Inspecting 3D voxel images of the area can provide more clarification on the location of the wells and the SC in relation to the aquifer materials. Figure 5-61 is a view from the south looking to the northeast of the aquifer and coarse aquifer material of the ***Q*** and the > 25 ohm-m sand dominant ***Kd*** with the specific capacity SC (gpd/ft) displayed as sized and colored disks. This figure shows the higher specific capacity wells along the paleovalley aquifer and the paleochannel within the ***Kd***. Note the area displaying no aquifer material (transparent zones), are mostly marginal and non-aquifer material of the ***Q*** as well as the silt and clay dominant materials of the ***Kd***.

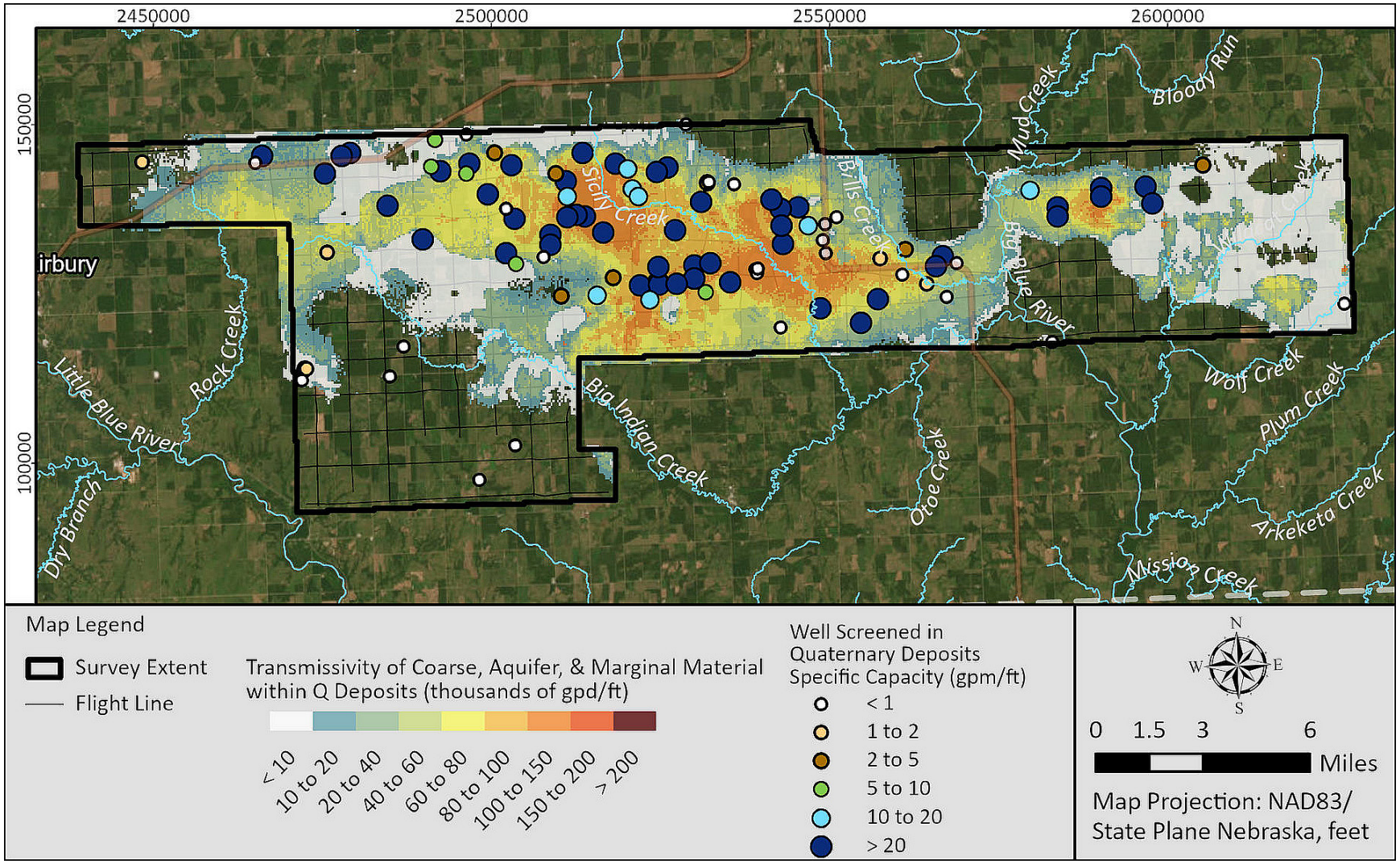


Figure 5-58. Map of the estimated Transmissivity (T) (gpd/ft) of the Quaternary (*Q*) coarse, aquifer, and marginal aquifer materials with the Specific Capacity (SC) of the NE-DNR registered wells completed within the *Q*.

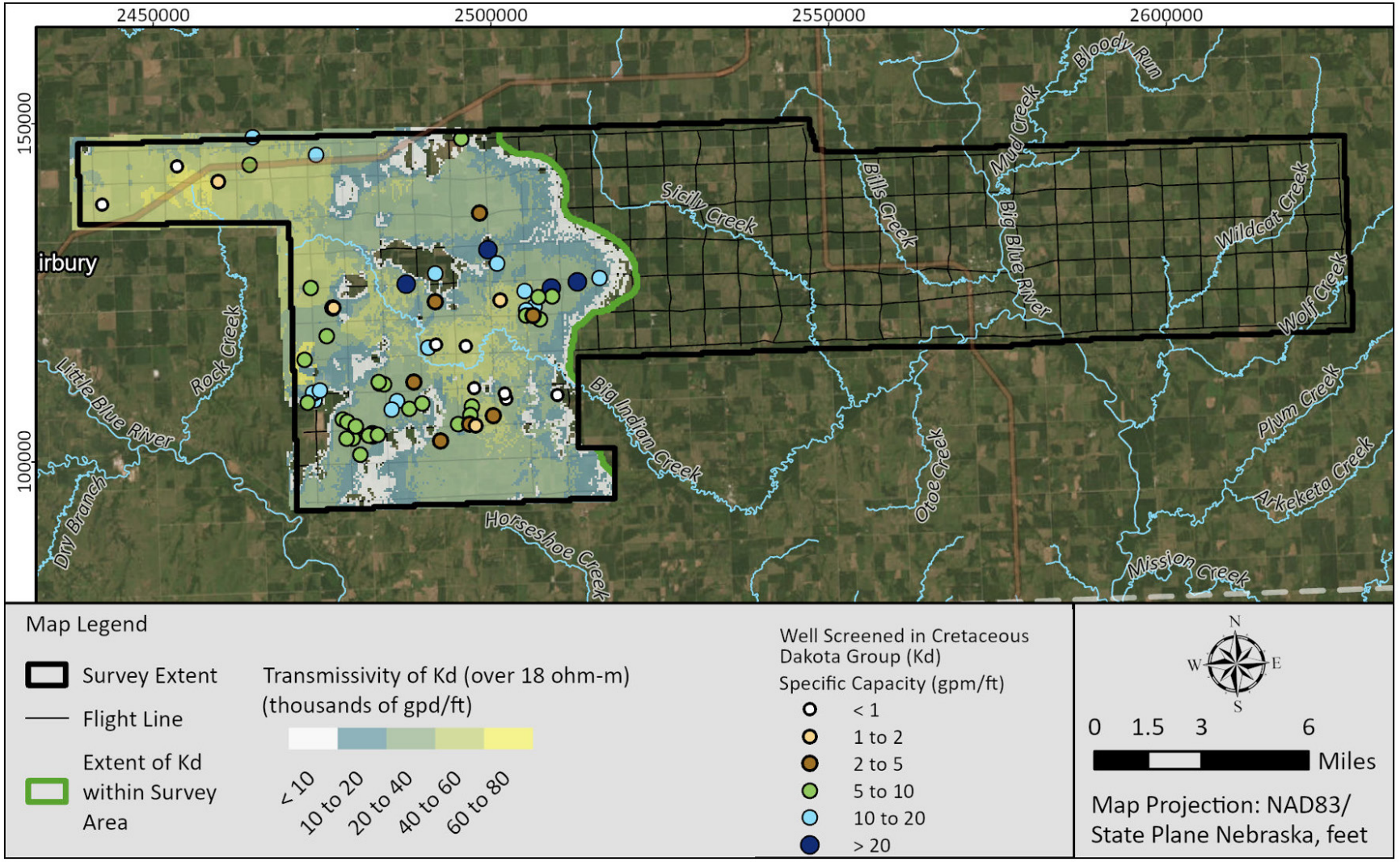


Figure 5-59. Map of the estimated Transmissivity (T) (gpd/ft) of the Cretaceous Dakota Group (*Kd*) with resistivities > 18 ohm-m cemented sand and sand dominant as well as the sand/silt dominant aquifer materials with the Specific Capacity (SC) of the NE-DNR registered wells completed within the *Kd*.

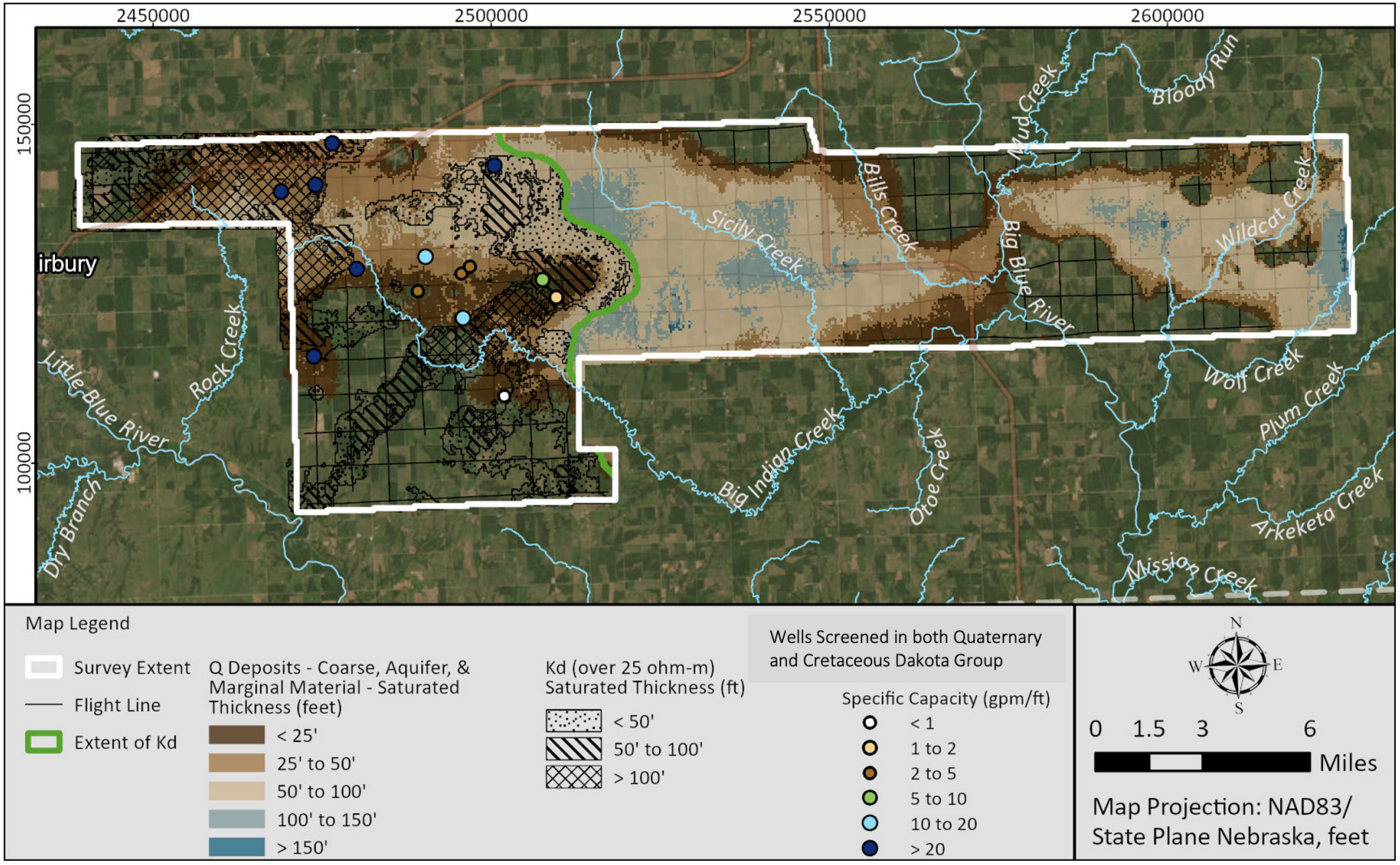


Figure 5-60. Map of the saturated Quaternary (*Q*) coarse, aquifer, and marginal aquifer materials plus the saturated Cretaceous Dakota Group (*Kd*) with resistivities >25 ohm-m cemented sand and sand dominant with the Specific Capacity (SC) of the NE-DNR registered wells completed within the *Q* and *Kd*.

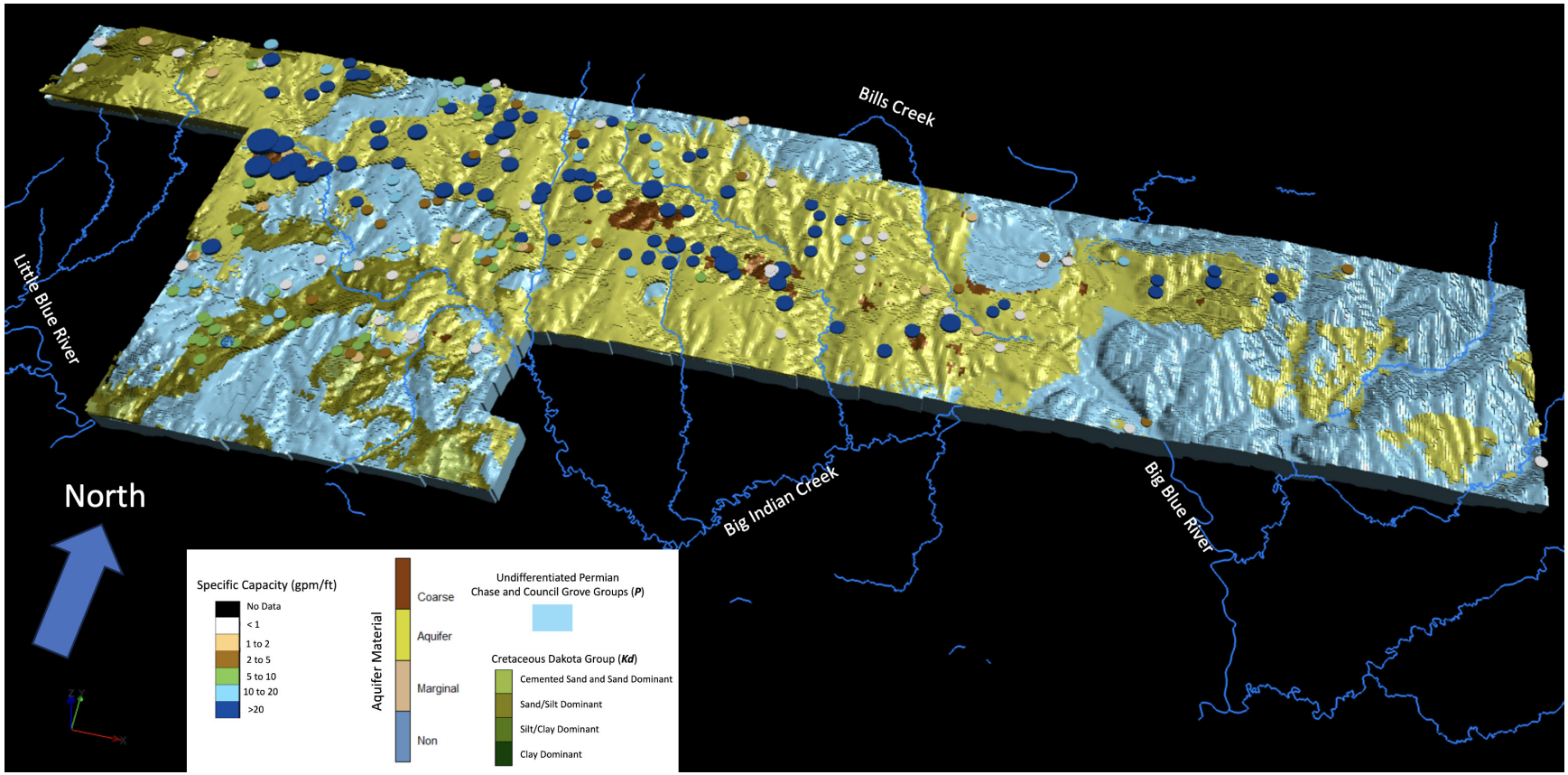


Figure 5-61. 3D voxel model of the saturated Quaternary (*Q*) coarse and aquifer materials plus the saturated Cretaceous Dakota Group (*Kd*) with resistivities > 25 ohm-m cemented sand and sand dominant material with the Specific Capacity (SC) of the all NE-DNR registered wells completed within the area.

5.3.5 Estimation of Aquifer Volume/Water Storage for the 2023 LBBNRD AEM Survey Area

Three-dimensional digital representation of the subsurface resulting from the AEM method provides users the ability to estimate total unsaturated and saturated aquifer volume and the amount of extractable water more accurately. An area of approximately 234 square miles (approximately 149,632 acres) of AEM data were collected in the LBBNRD 2023 AEM survey as shown by the map of 'as flown' flight lines in Figure 5-1.

The criteria for determining the basis for the range of resistivity values used in calculating the volumes of interpreted aquifer material for both ***Q*** and ***Kd*** are provided in Section 5.2. The resistivity ranges for ***Q*** interpreted non-aquifer, marginal aquifer, aquifer, and coarse aquifer materials are also found in Section 5.2.1. The resistivity ranges for the ***Kd*** includes clay dominant, silt/clay dominant, sand/silt dominant, and cemented sand and sand dominant materials are also found in Section 5.2.2. The mapped deposits of the ***Q*** and ***Kd*** provide information from which the volumes of selected aquifer materials combined with estimated average values for porosity and specific yield are the best estimates for calculation of aquifer volume in acre/ft, groundwater in storage in acre-ft, and extractable water in acre-ft. The area beneath the survey area included in these calculations and represented in Figure 5-1 were created in Datamine Discover PA, version 2023, Release Build 18.0.133 (Datamine Discover, 2024).

All aquifer materials including non-aquifer material, marginal aquifer material, aquifer material, and coarse aquifer material are used for calculating the groundwater in storage volume and the extractable water volumes for the survey area. Reported values of the average porosity for aquifer materials present are based on values from Freeze and Cherry (1979). Clay porosity ranges from 40%-70%, silt ranges from 35%-50%, sand ranges from 25%-50%, and gravel is from 25%-40%. Conservative estimates for the porosity values used in these calculations within the survey area are 40% for non-aquifer material, 35% for marginal aquifer material, 22% for the aquifer material, and 25% for the coarse aquifer material.

Specific yield values for all ***Q*** aquifer materials were selected by estimating values from Heath (1983). Specific yield for non-aquifer materials was chosen at 0.02 (Heath, 1983) and for marginal aquifer materials a value of 0.05 was selected (Heath, 1983). The specific yield value for aquifer material is 0.20 (Heath, 1983). While coarse aquifer materials exist as localized deposits in the survey area, estimates of specific yield for the coarse aquifer material is 0.19 (Heath, 1983). The aquifer and marginal aquifer materials represent the dominant material types by total volume for groundwater storage in the survey area. For specific yield, maps of the area would be improved if new maps were produced using this new AEM survey information plus the addition of aquifer tests or other methods of gaining new data including Nuclear Magnetic Resonance (NMR) surveys to capture aquifer characteristics including: mobile water, total porosity, and hydraulic conductivity.

All ***Kd*** aquifer materials including clay dominant, silt/clay dominant, sand/silt dominant, and cemented sand and sand dominant materials were used for calculating the groundwater in storage volume and the extractable water volumes for the survey area. Values for the ***Kd*** are problematic at best due to the limited reported values. Thus, information from Freeze and Cherry (1979), O'Conner (1987), Dominico

and Schwartz (1998), Fetter (1988), Gannon and Vogelgesang (2015), and Divine and Sibray (2017) was used to estimate volumes. These publications indicate that clay dominant porosity ranges from 35%-60%, clay/silt dominant material ranges from 35%-60%, sand/silt dominant material ranges from 25%-50%, and cemented sand and sand dominant material is from 5%-40%. The conservative estimates for the ***Kd*** porosity values used in these calculations within the survey area are 40% for Clay dominant material, 40% for clay/silt dominant material, 30% for the sand/silt material, and 35% for the cemented sand and sand dominant material.

Specific yield values for all ***Kd*** aquifer materials were selected by estimating values. Specific yield for clay dominant materials was chosen at 0.01 (Heath, 1983) and for clay/silt materials a value of 0.05 was selected (Heath, 1983). The specific yield for the sand/silt dominant is 0.08 (Heath, 1983). The specific yield for the cemented sand and sand dominant material is 0.10 (Heath, 1983). The aquifer and marginal aquifer materials represent the dominant material types by total volume for groundwater storage in the 2023 LBBNRD AEM survey area. For specific yield, maps of the area would be improved if new maps were produced using this new AEM survey information plus the addition of aquifer tests or other methods of gaining new data including Nuclear Magnetic Resonance (NMR) surveys to capture aquifer characteristics including: mobile water, total porosity, and hydraulic conductivity.

Table 5-5 shows the results of calculations of the amount of groundwater in storage calculated by volume of the saturated ***Q*** materials multiplied by the estimated porosity and estimated specific yield. 33% of the ***Q*** materials are saturated.

The values in the Table 5-5 are for the saturated (based on the LBBNRD Spring 2023 water table) ***Q*** materials, and have a total volume of **5,757,715** acre-ft. The estimated volume of groundwater in storage for ***Q*** aquifer material is **1,559,226** acre-ft. The estimated extractable volume of groundwater in ***Q*** aquifer materials is **826,072** acre-ft.

There is only a small portion of the ***Kd*** that is unsaturated based on the LBBNRD 2023 Spring water table. The values in the Table 5-6 are for the saturated ***Kd*** materials and have a total volume of **6,010,404** acre-ft which is 84% of the total ***Kd***. The estimated volume of groundwater in storage for ***Kd*** is **1,988,522** acre-ft. The estimated extractable volume of groundwater in ***Kd*** aquifer materials is **457,577** acre-ft.

A useful calculation would be combining the saturated ***Q*** and ***Kd*** of all materials. Again, this is using the LBBNRD Spring 2023 water table and the assumed values for the porosity and specific yield as discussed above for Table 5-5 and Table 5-6. The total estimated volume of the saturated ***Q*** and ***Kd*** aquifer materials is **11,768,119** acre-ft, which is 48 % of the total combined ***Q*** and ***Kd*** aquifer materials. The total groundwater in storage is **3,547,747** acre-ft. The total extractable water is **1,283,649** acre-ft.

As stated above, these estimates are based on the water table map as calculated from the LBBNRD Spring 2023 water levels (Section 5.1.6). Also, these volumetric estimates consider only the volume of water assumed in the pore spaces of the aquifer material defined by the resistivity threshold levels and do not account for the possible “confined or semi-confined” water under pressure (head above the aquifer). Note that additional analysis of data for the confined, or semi-confined, areas of the AEM

survey area would need to be completed before any designation of these areas can be made. Aquifer testing may be the only way to confidently ascertain the confining condition of the overlying loess.

An estimate of the area that may be confined can be provided by looking at the unsaturated ***Q*** non-aquifer material and marginal aquifer material thicknesses (Figure 5-62). This volume of water would add to the values reported in Table 5-5 and Table 5-6. However, too much uncertainty exists in developing an average level of head above the top of the aquifer across the entire project area, as well as defining a representative storativity term for the confined or semi-confined aquifers. Thus, the volumes listed in Table 5-5 and Table 5-6 are conservative estimates and the amount released from the decline in pressure is not considered.

Table 5-5. Volumes for Saturated Quaternary (*Q*) aquifer materials underlying the LBBNRD 2023 AEM survey area.

Q Aquifer Material	Aquifer Volume (ft3)	Aquifer Volume (Acre-Ft)	Average Porosity	Groundwater Potential in Storage Volume (Acre-Ft)	Average Specific Yield	Extractable Potential Water Volume (Acre-Ft)
Coarse > 50 ohm-m	8,572,074,022	196,788	0.25	49197	0.19	37390
Aquifer 20-50 ohm-m	151,521,594,386	3,478,457	0.22	765261	0.2	695691
Marginal 12-20 ohm-m	76,857,249,363	1,764,400	0.35	617540	0.05	88220
Non 0-12 ohm-m	13,855,165,184	318,071	0.4	127228	0.02	4771
Totals		5,757,715		1,559,226		826,072

Table 5-6. Volumes for Saturated Cretaceous Dakota Group (*Kd*) aquifer materials underlying the LBBNRD 2023 AEM survey area.

Kd Aquifer Material	Aquifer Volume (ft3)	Aquifer Volume (Acre-Ft)	Average Porosity	Groundwater Potential in Storage Volume (Acre-Ft)	Average Specific Yield	Extractable Potential Water Volume (Acre-Ft)
Cemented Sand and Sand Dominant >35 ohm-m	40,280,672,232	924,717	0.35	323651	0.1	92472
Sand/Silt Dominant 35-18 ohm-m	160,912,427,147	3,694,041	0.3	1108212	0.08	295523
Silt/Clay Dominant 18-3 ohm-m	60,619,303,760	1,391,628	0.4	556651	0.05	69581
Clay Dominant < 3 ohm-m	783,257	18	0.4	7	0.01	0
Totals		6,010,404		1,988,522		457,577

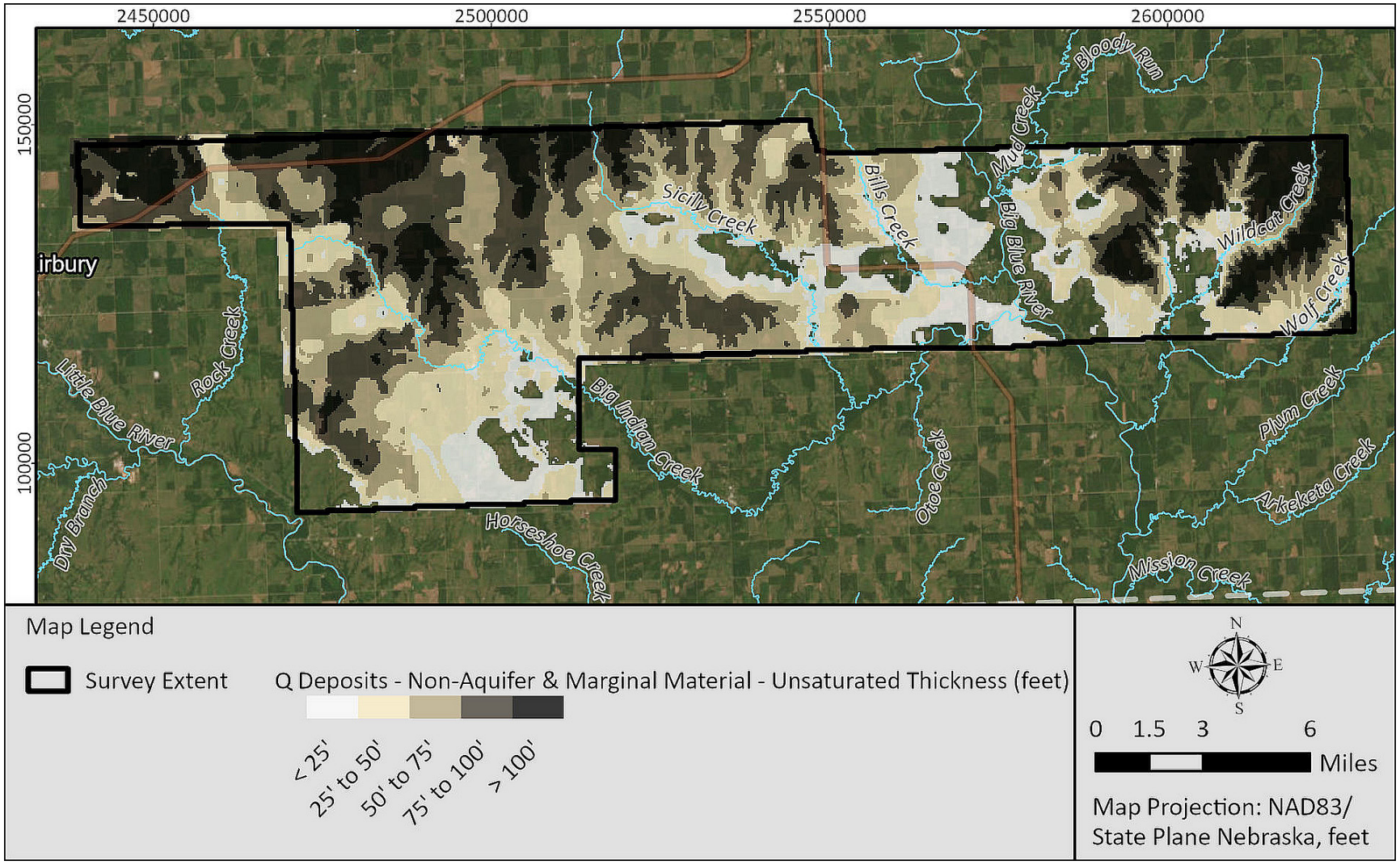


Figure 5-62. Map of the Non- and Marginal Aquifer material within the unsaturated portion of the Quaternary (*Q*) potentially creating a confined aquifer beneath.

5.3.6 Groundwater Quality in the LBBNRD 2023 AEM Survey Area

The primary contaminants of concern throughout the Lower Big Blue NRD are nitrates. As such, the LBBNRD annually samples dedicated monitoring wells and registered irrigation wells for nitrate analysis. In 2021, sample results in the project area indicated one monitoring well (MW9 south of Ellis) and 20 registered irrigation wells with nitrate concentration levels at or above the Environmental Protection Agency's (EPA's) maximum contaminant level (MCL) of 10 parts per million (ppm), with the bulk of these wells located in an approximate township-sized area. There are also 21 registered irrigation wells, located in the northwest portion of the project area, with nitrate concentrations at or above 6.0 ppm, which, if sustained, would qualify for NRD Phase II delineation for groundwater quality (60% of MCL).

The AEM provided information on the near surface materials in the LBBNRD AEM survey area. Near surface occurrences of sandy soils and sand deposits (aquifer materials) provide conduits for contaminants to migrate into the groundwater.

Using the 3D interpretation of the AEM, a near surface occurrence of the aquifer materials map can be generated. Using the water quality data collected by the LBBNRD (Personal Communication, Tyler Weishahn, January 2024), the data was overlain on the aquifer material map of the unsaturated coarse and aquifer material. Illustrated in Figure 5-63 is the correlation of nitrate samples and the areas of the aquifer materials along the trend of the paleovalley aquifer.

Additionally, when the thickness of the unsaturated marginal and non-aquifer materials are plotted with the nitrate values, a weak to no correlation to the areas without non-aquifer and marginal materials or thin non-aquifer and marginal materials can be seen (Figure 5-64). There is a slight pattern around Sicily Creek, but again it is weak.

There are some areas of higher nitrates in areas of the northwestern area of the survey. These are not related to the surface materials and may be related to deeper elevated nitrates in the sandy portions of the ***Q*** paleovalley aquifers in that area. With the thick non- and marginal aquifer material in the area, it is unlikely that the nitrates are migrating through the clay-rich thicker till and loess deposits.

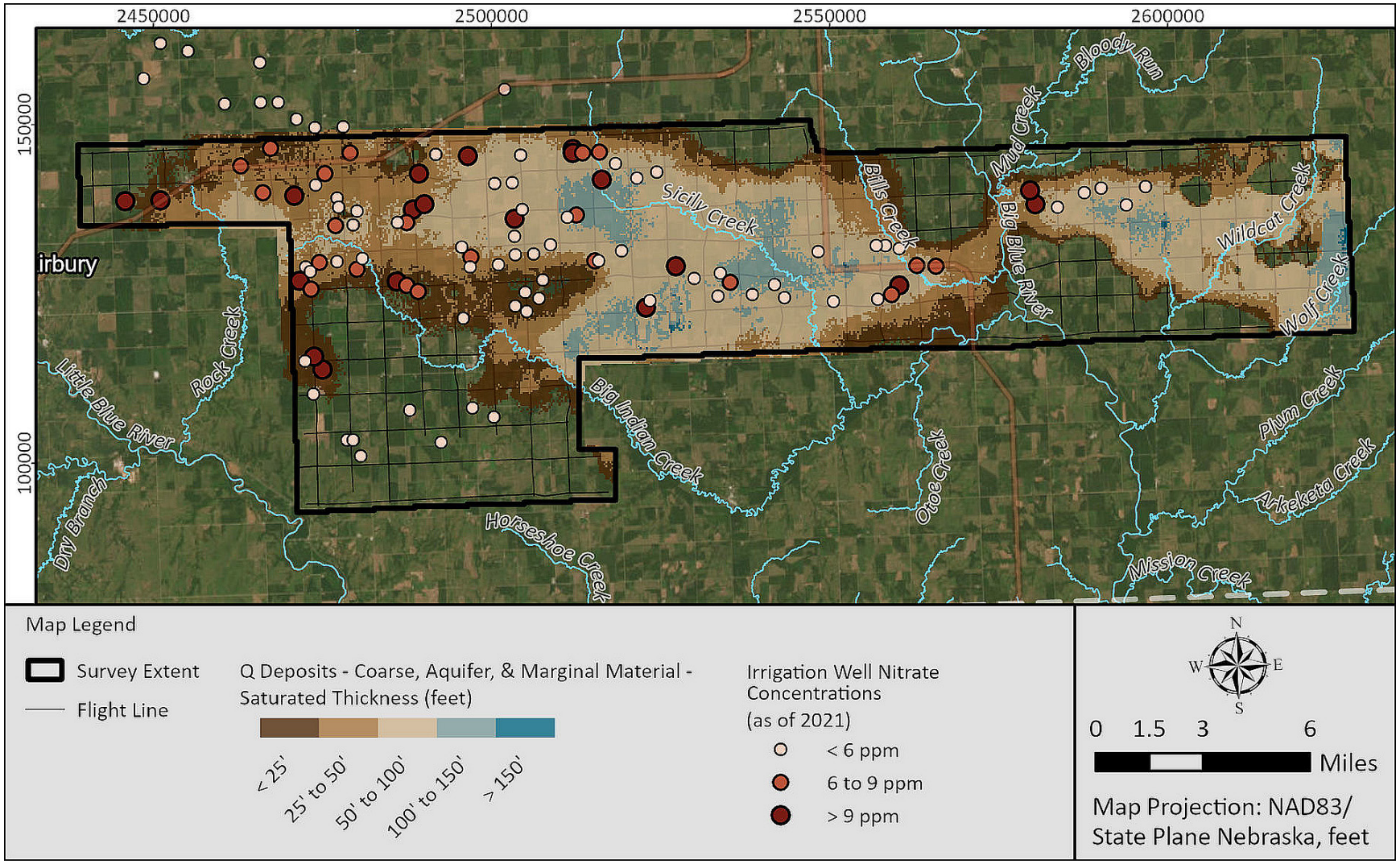


Figure 5-63. Map of the thickness of the unsaturated coarse and aquifer material and the LBBNRD nitrate samples.

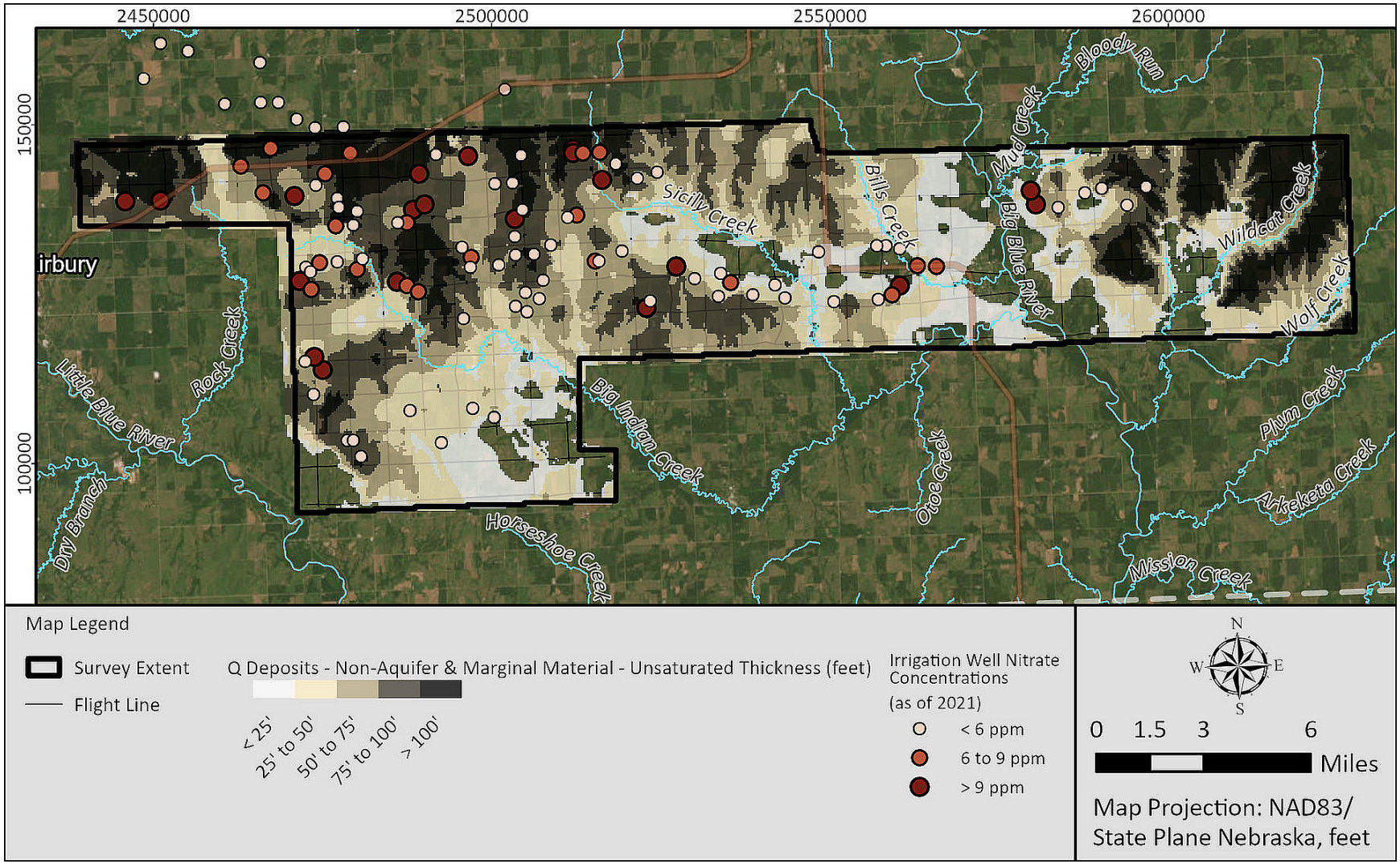


Figure 5-64. Map of the thickness of the unsaturated non- and marginal aquifer material and the LBBNRD nitrate samples.

5.3.7 Recharge in ***the LBBNRD 2023 AEM Survey Area***

An important question that is required to be assessed in any groundwater availability study is the location of recharge sites. The AEM has the unique ability to map the near-surface aquifer materials as indicated above to help determine potential areas of recharge.

Using a similar approach to what was utilized in the water quality section (Section 5.3.6), near surface ***Q*** materials composed of coarse and aquifer material were mapped using the following criteria: 1) Greater than 6 feet thickness of coarse and aquifer material; 2) The top of the coarse and aquifer material is less than or equal to 3 feet below the ground surface; and 3) There is greater than 10 feet of depth between the top of the coarse and aquifer material and the top of the bedrock. These criteria are based on the idea that a recharge area within the survey area would require relatively thick coarse and aquifer material close to ground surface, with bedrock deep enough to allow for water to recharge to depth.

Figure 5-65 is the map of the thickness of the coarse and aquifer material that meet those criteria. Many of these areas are along the stream where the till and loess have been eroded away exposing the deeper coarse and aquifer material. These are windows into the lower aquifer materials. On the eastern side of the survey area many of these deposits are the outwash in the upper section and may not have potential beneficial impacts as they may be not connected to the deeper aquifer materials. The area along Sicily Creek is a great area to look at as it is underlain by the main paleovalley aquifer.

The areas in the southwest are areas that are underlain by **Kd** and may not have a large recharge benefit. Examining the profiles can help to understand the 3D connections of the near-surface materials to the deeper aquifer. Figure 5-66 is the east-west profile of line L500500. The areas along Sicily Creek and Bills Creek show the aquifer materials going from the surface down to the saturated materials. Figure 5-67 is the east-west profile of line L500401 (one line to the north of Figure 5-66). The areas along Sicily Creek show the aquifer materials going from the surface down to the saturated materials. Figure 5-68 is a north-south profile of line L401901 that is along Sicily Creek also displaying the aquifer materials going from the surface down to the saturated materials.

A recharge area target map has been developed to help identify areas that could be investigated in the future for recharge locations (Figure5-69). The areas within the ***Kd*** and the eastern areas have been removed and only the best targets have been indicated. A Google Earth KMZ, *LBBNRD2023_Potential Areas of Recharge.kmz* (included in *Appendix 3-Deliverables/KMZ*), has also been created that shows the locations of the best estimated recharge areas within the 2023 LBBNRD AEM survey area.

Utilizing the above maps to target recharge areas can be done. However, it is imperative that accurate test holes are used to assess the geological materials which may include sonic cores. Any possible thin clay layers that were not detected with the AEM or may have been missed in the test hole drilling may be detected by calibrated borehole geophysical induction logs. Infiltration tests also need to be conducted to fully evaluate recharge rates.

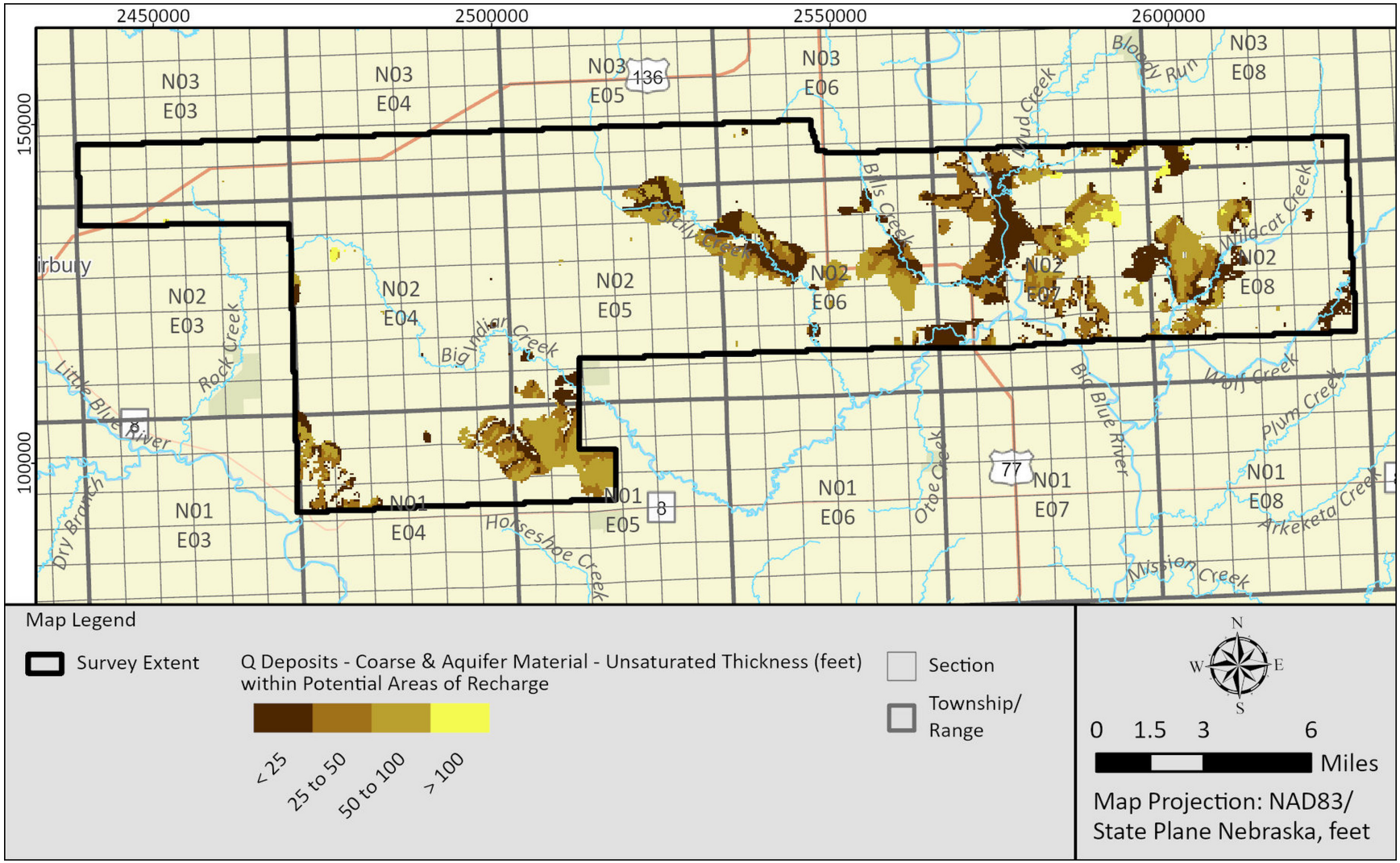


Figure 5-65. Map of the thickness of the unsaturated coarse and aquifer material that is in the near surface that may provide recharge pathway to lower aquifers.

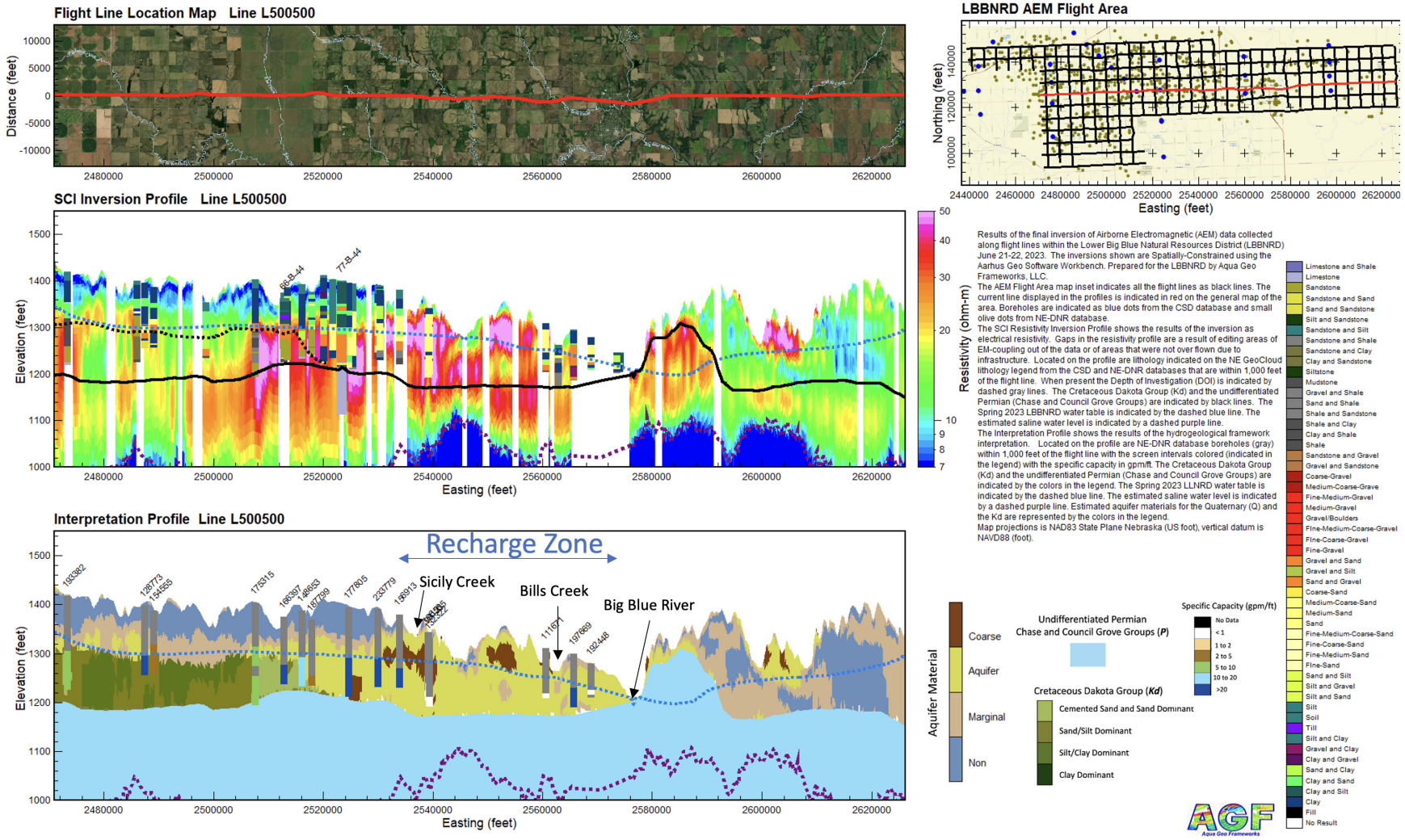


Figure 5-66. East-west AEM flight line L500500. A location map is on the upper right. On the left the top profile shows the air photo along the flight line. The middle profile is the SCI resistivity inversion result showing borehole lithologies and the bottom profile is an interpretative section showing the undifferentiated Permian (*P*) underlying Quaternary (*Q*) subdivided into interpreted aquifer materials. Boreholes in the bottom section indicate measured Specific Capacity.

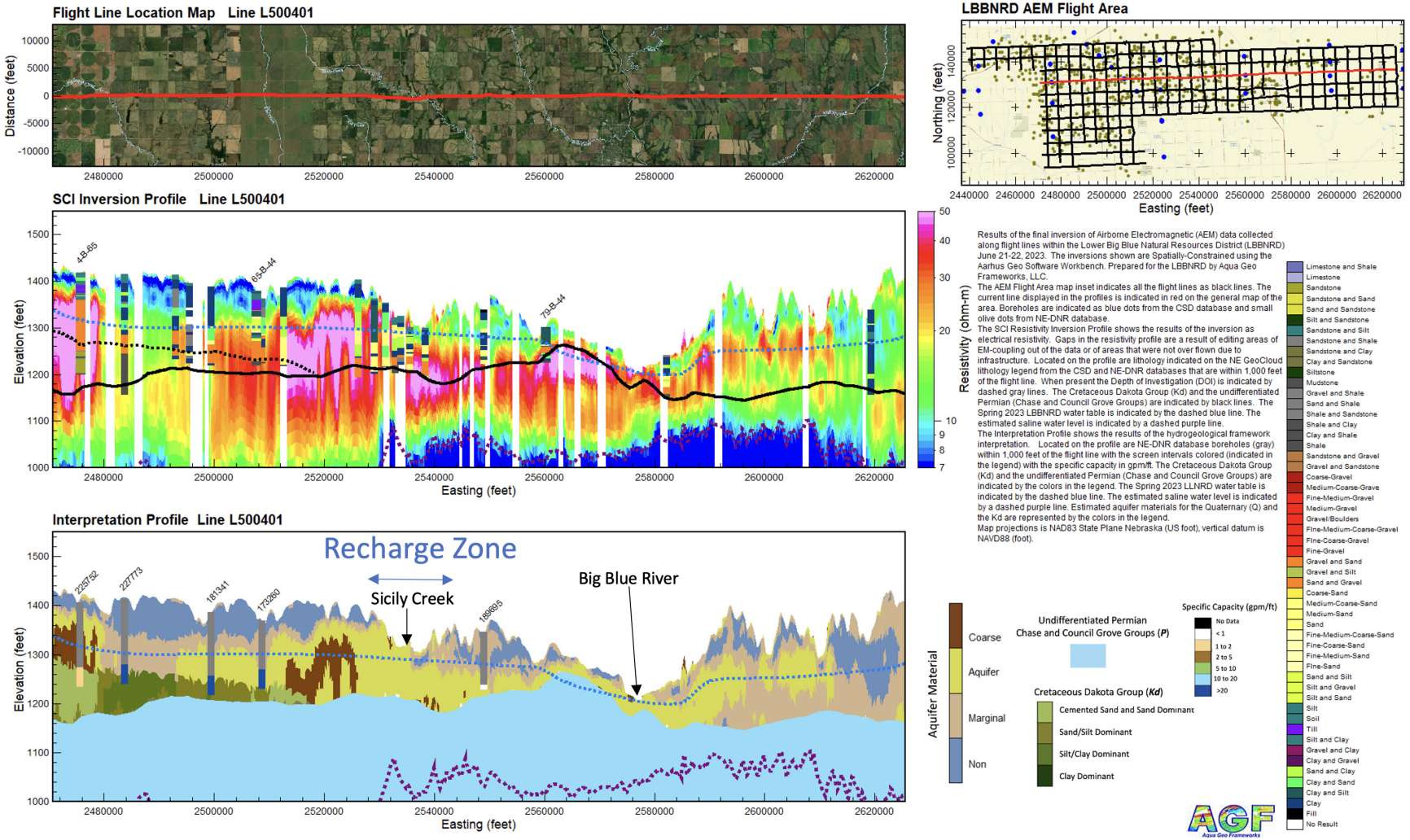


Figure 5-67. East-west AEM flight line L500401. A location map is on the upper right. On the left the top profile shows the air photo along the flight line. The middle profile is the SCI resistivity inversion result showing borehole lithologies and the bottom profile is an interpretative section showing the undifferentiated Permian (*P*) underlying Quaternary (*Q*) subdivide into interpreted aquifer materials. Boreholes in the bottom section indicate measured Specific Capacity.

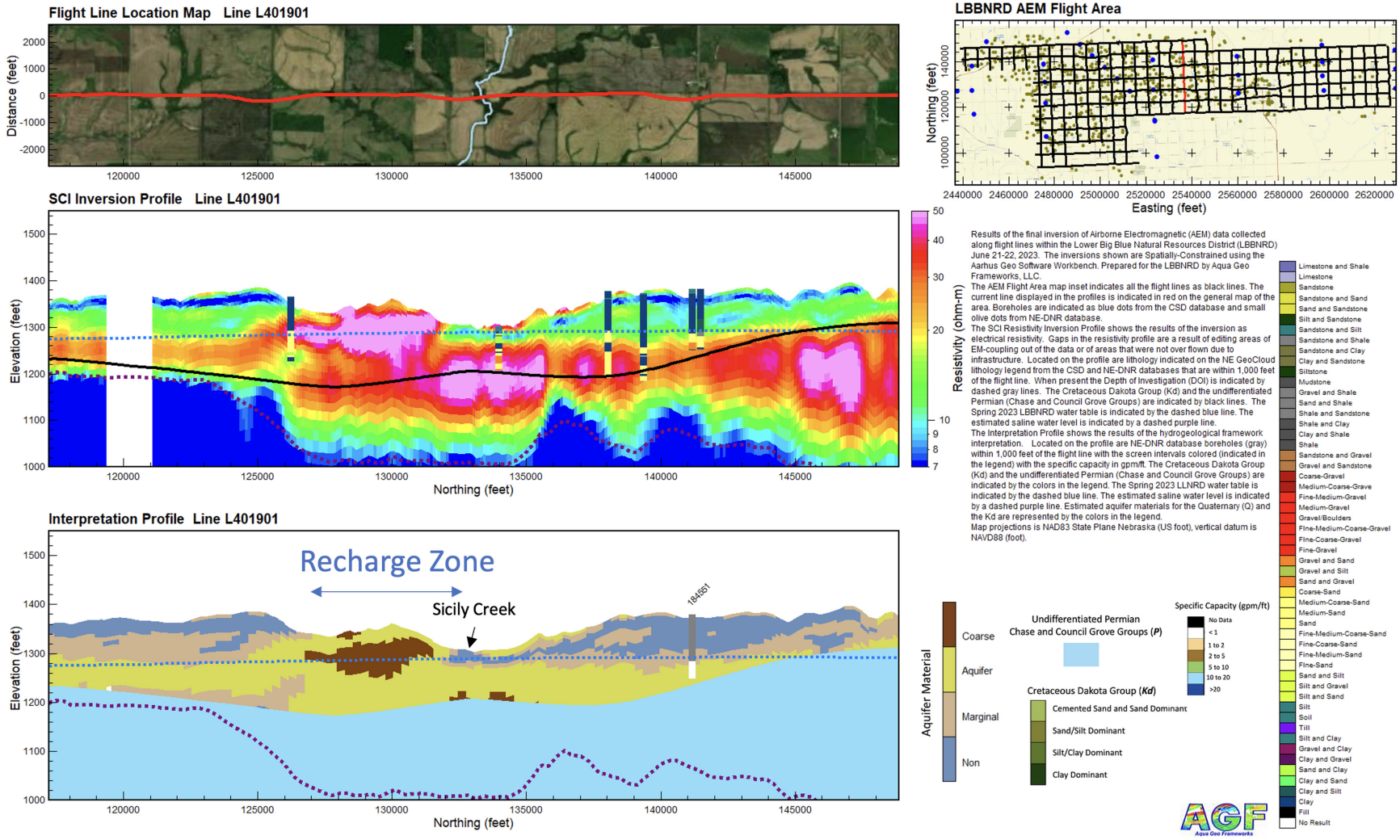


Figure 5-68. North-south AEM flight line L401901. A location map is on the upper right. On the left the top profile shows the air photo along the flight line. The middle profile is the SCI resistivity inversion result showing borehole lithologies and the bottom profile is an interpretative section showing the undifferentiated Permian (*P*) underlying Quaternary (*Q*) subdivide into interpreted aquifer materials. Boreholes in the bottom section indicate measured Specific Capacity.

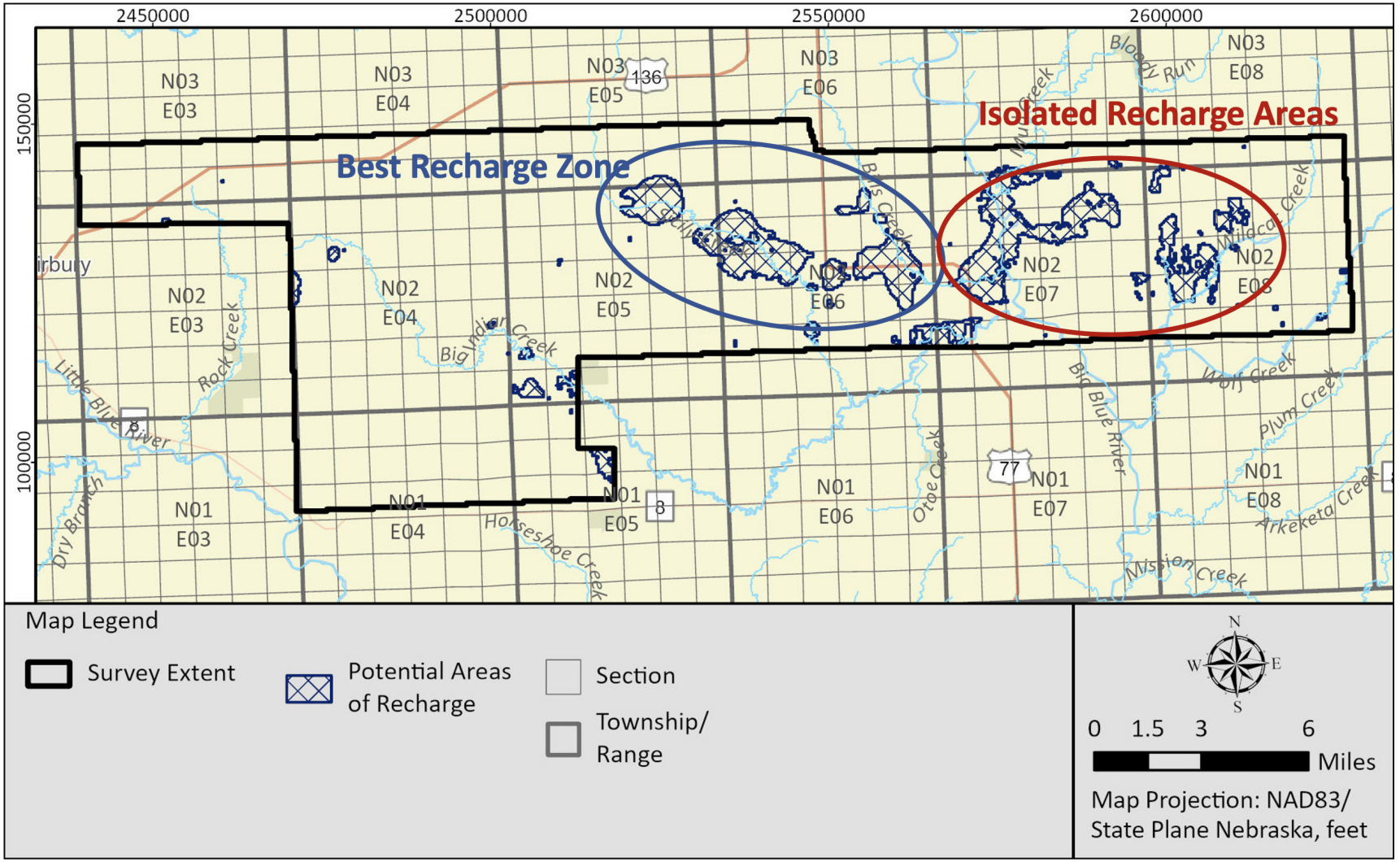


Figure 5-69. Map of the potential recharge locations based on the presence of coarse and aquifer materials in the near surface with connections to the deeper aquifers.

5.4 New Understanding of AEM Framework Applied to Water Management Efforts in in the LBBNRD 2023 AEM Survey Area

All management plans can be improved as new information is gathered and considered for modifying the management practices. Much of this study was focused on the determination of the groundwater availability within the LBBNRD AEM survey area. Previous mapping was based on surficial mapping and limited test hole drilling coupled with monitoring well networks. While this provided some understanding of the hydrogeology it raised more questions.

The AEM provides a much higher resolution of the aquifer configuration. The important findings that can have an impact on the management of the area are related to the estimated shape and configuration of the aquifers. Examples are estimates of both the ***Q*** and the ***Kd*** aquifers transmissivities as was determined in this study. The ***Q*** transmissivity map is also in general agreement with the map produced by Summerside and Myers (2005). The AEM provides a much higher resolution view of the area as compared with the previous mapping, but that is expected and the goal of this study.

Additionally estimates of the transmissivity of the ***Kd*** aquifer were produced. The uncertainties in the hydrogeological parameters used in the ***Kd*** transmissivity estimates need to be acknowledged, but the maps can serve as a starting point to the understanding of the area.

Determining the areas that are impacted by nitrates due to the configuration of the near-surface materials is critical. These same areas can also be targets for recharge. The maps produced in this study can guide both management of nitrate control areas as well as allow implementation of recharge projects.

5.5 Key AEM Findings

5.5.1 Boreholes

Information from boreholes was used to analyze the AEM inversion results. These included CSD information on 27 test holes containing lithology and stratigraphic information, and four (4) test holes containing geophysical information. NE-DNR wells totaled 715 registered well records containing usable lithology information. These boreholes were essential in the interpretation of the AEM.

5.5.2 Digitizing Interpreted Geological Contacts

Characterization and interpretation of the subsurface was performed in cross-section and in derived surface grid formats. Contacts between the geologic units were digitized in 2D including: Quaternary (***Q***), Cretaceous Dakota Group (***Kd***), and the undifferentiated Permian (***P***) composed of the Permian Chase (***Pc***) and Council Grove Groups (***Pcg***). The interpretive process benefited from the use of CSD and NE-DNR borehole logs. Geological outcrop maps previously published were also used and critical in developing the geological contacts. Surface grids of the interpreted geologic formations were then produced. Each flight line profile with interpretation including the Quaternary/Cretaceous Dakota Group aquifer material mapping is included in the appendices as well as interpretative surface grids.

5.5.3 Resistivity/Lithology Relationship

Assessment of the sediment character in both the Quaternary (***Q***) and Cretaceous Dakota Group (***Kd***) aquifer system and the undifferentiated Permian bedrock was conducted to determine the overall composition of the major categories used to define the aquifer and aquitards in the survey area. A numerical assessment of the resistivity thresholds within the ***Q*** was used to characterize non-aquifer (<12 ohm-m), marginal (12-25 ohm-m), and aquifer (25-50 ohm-m), including coarse sand-rich intervals (>50 ohm-m), material.

The ***Kd*** within the LBBNRD AEM survey area was split into four parts based on empirical comparisons to lithology logs. The four parts were classified as follows: 1) 0-3 ohm-m as Shale/Clay Dominant materials; 2) 3-18 ohm-m as Siltstone/Silt Dominant materials; 3) 18-35 ohm-m as Sand/Silt Dominant; and 4) 35 ohm-m and greater as Sandstone/Sand Dominant materials. This is a modification of the splits that were used in the P-MRNRD reports from AGF (2021). Additional unpublished work in the Nebraska ***Kd*** using AEM data has led to a better understanding of the resistivity versus lithology within the ***Kd***.

The undifferentiated Permian bedrock varied greatly but generally had moderate resistivities in the range of 15-30 ohm-m with the exception of the areas that contain saline waters; these areas had resistivities <7 ohm-m.

5.5.4 Hydrogeological Framework of the LBBNRD 2023 AEM Survey Area

The AEM reveals considerable variability in the Quaternary (***Q***) and Cretaceous Dakota Group (***Kd***) deposits across the AEM survey area. The groundwater within the LBBNRD 2023 AEM survey area is within the limited alluvial sediments of the present streams, glacial sediments, and the paleovalley sediments of the ***Q***. There is also groundwater in the fluvial and deltaic sediments of the ***Kd***. The actual groundwater availability is dependent upon the material type of both the ***Q*** and ***Kd***. In the western third of the survey area, the ***Q*** overlies the ***Kd*** and is in hydrogeological connection with the ***Kd***. In general, the ***Q*** groundwater is available within paleovalley sediments, and the ***Kd*** groundwater is available in the sandstone and sand deposits of the fluvial deposits. Some NE-DNR wells are completed in both the ***Q*** and the ***Kd***.

An estimated Transmissivity (**T**) map was developed for the ***Q*** aquifers. This is related to the thickness of the saturated aquifer material and the estimated hydraulic conductivities. Most of the higher Specific Capacity (**SC**) values calculated from the NE-DNR well database are within the higher estimated **T** values of the paleovalley. A clear decrease in **T** is observed on the eastern side of the survey area where the paleovalley sediments thickness is reduced and the geology is dominated by thick glacial till deposits. Some isolated deposits of outwash gravel exist within the upper portions of the till and may be related to glacial-tectonic features associated with thrust sheets of outwash as was observed in areas of central Nebraska by Korus et al. (2021). Many of these sand and gravel deposits are unsaturated or partially saturated. Locally they can provide domestic water sources but are seldom large enough for sustainable large production wells.

The AEM successfully mapped the sand rich deposits of the ***Kd***. Many of the ***Kd*** completed wells are in this sand dominant region that has electrical resistivity > 25 ohm-m; these would be the sand dominant materials of the fluvial deposits of a paleochannel. The paleochannel deposits mapped by the AEM have many wells completed within it with SC on the order of 2 to 10 gallons per minute per foot (gpm/ft). While most of the ***Kd*** is saturated, the low yielding shales, siltstone, silts, and clays reduce the actual Specific Yield.

An estimated **T** map was developed for the ***Kd*** in the 2023 LBBNRD AEM survey area using the thickness of the sand dominant materials and hydraulic conductivities from published references (e.g., O'Connor (1987) and Gannon and Vogelgesang (2015)) in the area of eastern Nebraska and western Iowa. This map can be helpful, but needs to be used with caution due to the lack of local hydrogeological information on the ***Kd***.

5.5.5 Estimation of Aquifer Volume and Water in Storage in the LBBNRD AEM Survey Area

The values for the saturated Quaternary (***Q***) aquifer (based on the LBBNRD spring 2023 water table) and Cretaceous Dakota Group (***Kd***) aquifer volumes were calculated. Three-dimensional digital representation (3-D Voxel model) of the subsurface resulting from the AEM interpretation allowed the total saturated aquifer volume and the amount of extractable water to be estimated more accurately. An area of approximately 234 square miles (approximately 149,632 acres) of AEM data were collected in the LBBNRD 2023 AEM survey, and using estimates of porosity and specific yield from the published literature as well as the 3-D Voxel models, the total volume of groundwater in storage and the total volume of extractable groundwater within the saturated ***Q***, ***Kd***, and ***Q*** and ***Kd*** combined were calculated and are as follows:

- ***Q***
    - Total volume of saturated ***Q*** materials: **5,757,715** acre-ft (or approximately 33% of total ***Q*** material volume)
    - Estimated groundwater in storage: **1,559,226** acre-ft
    - Estimated extractable volume of groundwater: **826,072** acre-ft
- ***Kd***
    - Total volume of saturated ***Kd***: **6,010,404** acre-ft (or approximately 84% of total ***Kd*** volume)
    - Estimated groundwater in storage: **1,988,522** acre-ft
    - Estimated extractable volume of groundwater: **457,577** acre-ft
- ***Q*** and ***Kd*** combined
    - Total volume of saturated ***Q*** and ***Kd*** combined: **11,768,119** acre-ft (or approximately 48% of total ***Q*** and ***Kd*** combined volume)
    - Estimated groundwater in storage: **3,547,747** acre-ft
    - Estimated extractable volume of groundwater: **1,283,649** acre-ft

5.5.6 Groundwater Quality in the LBBNRD 2023 AEM Survey Area

The AEM provided information on the near-surface (unsaturated) materials in the 2023 LBBNRD AEM survey area. Near-surface occurrences of sandy soils and sand deposits (aquifer materials) may provide conduits for contaminants to migrate into the groundwater. Using the 3D interpretation of the AEM, a near-surface occurrence of the aquifer materials 2D grid was generated. A map depicting water quality (nitrate) data collected by the LBBNRD (*Personal Communication, Tyler Weishahn, January 2024*) overlying the near-surface occurrence of aquifer materials grid was made to visually determine if there is a correlation between the near-surface material type and water quality. While there is a very weak visual correlation of the nitrate concentrations within an area of near-surface sandy aquifer material along a portion of Sicily Creek, no other strong pattern exists. With the thick non- and marginal aquifer material in the survey area, it is unlikely that the nitrates are migrating through the clay-rich thicker till and loess deposits.

There is, however, a visual correlation of relatively high nitrate concentrations and the areas of the aquifer materials along the trend of the paleovalley aquifer (west-east).

5.5.7 Potential Recharge Zones within the LBBNRD 2023 AEM Survey Area

Using the AEM near-surface (unsaturated) 2D grid of the coarse and aquifer materials, a map was developed to assist in identifying and investigating areas where these materials could be used for recharge. Many of these areas are along the streams where the till and loess have been eroded away exposing the deeper coarse aquifer and aquifer material and may be considered windows into these deeper aquifer materials. On the eastern side of the survey area, many of the areas of coarse and aquifer materials that are depicted on the map are the isolated deposits of outwash in the upper portions of the till and may not have potential beneficial recharge impacts as they may not be connected to the deeper aquifer materials. The area along Sicily Creek is a good area to consider for recharge as it is underlain by the main paleovalley aquifer.

Utilizing the recharge target map to locate recharge areas can be done. However, it is imperative that accurate test holes, which may include sonic cores, are used to assess the geological materials. Any possible thin clay layers that were not detected with the AEM or may have been missed in the test hole drilling may be detected by calibrated borehole geophysical induction logs and natural gamma. Infiltration tests also need to be conducted to fully evaluate recharge rates. Additionally, determining the areas that are impacted by nitrates due to the configuration of the near-surface materials is critical because these same areas can also be targets for recharge due to the nature of the material type. The maps produced in this study can guide both management of nitrate control areas as well as allow implementation of recharge projects.

5.5.8 Using AEM Results to Implement Groundwater Management

All management plans can be improved as new information is gathered and considered for modifying the management practices. Much of this study was focused on the determination of the groundwater availability within the LBBNRD AEM survey area. Previous mapping was based on surficial exposures and limited test hole drilling coupled with monitoring well networks. While this provided some understanding of the hydrogeology, the AEM provides a much higher resolution of the aquifer configuration. The important findings that can have an impact on the management of the area are related to the estimated shape and configuration of the aquifers. Examples of these estimates are the transmissivity (**T**) maps that were made of both the ***Q*** and the ***Kd*** aquifers as part of this study. The hydraulic conductivity values used to estimate the ***Q*** transmissivity were based on the known material type (established with interpretation of the AEM) present within the survey area. The estimated transmissivity produced a **T** map that is in general agreement with the map produced by Summerside and Myers (2005). The AEM-produced **T** map provides a much higher resolution view of the area as compared with the previous mapping, but that is expected and is the goal of this study. The hydraulic conductivity value used to estimate the transmissivity of the ***Kd*** aquifer was based on an average of two published values. The uncertainties in the hydrogeological parameters used in the ***Kd*** transmissivity

estimates need to be acknowledged, but the map can serve as a starting point to the understanding of the area.

5.6 Recommendations

Recommendations provided to the LBBNRD in this section are based on the interpretation and understanding gained from the addition of the AEM data to existing information and from discussions with the LBBNRD about their management challenges.

5.6.1 Additional AEM Mapping

The aquifer maps provided in this report represent the detailed hydrogeologic framework developed for the LBBNRD 2023 AEM survey area. The AEM interpretations used to create the aquifer maps match well with the CSD and NE-DNR borehole lithologic, stratigraphic, and/or geophysical logs. It is recommended that additional areas be flown in the LBBNRD so that these aquifer maps may be broadened to cover a larger geographic extent. Additional survey flight lines can be of a reconnaissance nature to begin with but, later, closely spaced lines or “block flights” should be collected over project areas such as well fields, well head protection areas, and/or areas of detailed recharge projects to develop more detailed frameworks. The line spacing for the block flights should be on the order of 0.25 mile (1,320 ft). It is important to note that AEM data is not meant to replace existing data, such as borehole lithology or aquifer tests, but to provide a framework in which to place the existing hydrogeological data. Therefore, AEM mapping can assist with targeting areas where more expensive technologies including borehole drilling can be implemented, especially when a block flight is flown over an area.

Future AEM mapping projects could potentially be done in cooperation with the neighboring NRDs to get details on the continuous aquifer system that is shared in the area. The Little Blue NRD is a great example of an NRD the LBBNRD can partner with to share an AEM mapping project. A benefit for partnering with other NRDs is to have a combined comprehension of the estimates of groundwater storage capacity, which may be calculated by understanding the aquifer characteristics through AEM interpretation.

5.6.2 Siting new test holes and production wells

The AEM framework maps and profiles provided in this report give insight into the 3D relationship between current test holes and production groundwater wells and the material in which they are drilled into. At the time of this report, the current available lithology data for the LBBNRD area was used to help build the framework maps and profiles. It is recommended that the results from this report be used to site new test holes, monitoring wells, and/or water supply wells. Based on more data, the AEM framework maps and profiles provide detail in areas where the previously existing data may have been more regional in nature; this enables better decision-making when siting new wells.

The location of any future water supply wells can also use the results in this report to guide development of new water supply wells. Planners should locate wells in areas of greatest saturated thickness with the least potential for non-point source pollution.

5.6.3 Aquifer testing and borehole logging

Aquifer tests are recommended to improve estimates of aquifer characteristics. A robust aquifer characterization program is highly recommended at the state, regional (NRD's), and smaller municipal levels. Aquifer tests can be designed based on the results of AEM surveys and existing production wells.

Additional test holes with detailed, functional, and well calibrated geophysical logging for aquifer characteristics is highly recommended. The few test holes with calibrated geophysical logs in the LBBNRD survey area were inadequate. The borehole geophysical logs provided for this investigation demonstrate that additional calibrated and verified geophysical logs are required in the LBBNRD.

Examples of additional logging would be borehole flow meter logs and geophysical logs including gamma, neutron, electrical, and induction logs. Detailed aquifer characteristics can be accomplished with nuclear magnetic resonance logging (NMR). This is a quick and effective way to characterize porosity and water content, estimates of permeability, mobile/bound water fraction, and pore-size distributions with depth. This is very cost effective when compared to traditional aquifer tests.

5.6.4 Groundwater Management: Control Areas, Recharge areas

The hydrogeologic framework in this report provides the location and extent of high transmissive and saturated aquifers. Conversely, it also shows areas where high-capacity wells may be limited due to the aquifer characteristics. It is recommended that these areas be used to define the control areas based on empirical data of the AEM coupled with water quality and groundwater levels. The geospatial data products delivered with this report can be directly opened in ESRI's ArcGIS Pro and can be used to provide guidance in the establishment on control areas. These data can also be invaluable to the producers/developers within the area in replacing wells and drilling new wells. These data can be used by the LBBNRD in assessing the well permits of the area and assisting the interested parties to drill successful wells.

This study mapped areas that are windows to the deeper paleovalley aquifer. These areas may be considered for special recharge projects. These areas also may require additional protections to be added to avoid groundwater quality issues due to the direct conduit of the surface to the deeper aquifer systems. Any management decisions that would propose recharge would need to be weighed against current land use and recharge water availability.

6 Description of Data Delivered

6.1 Tables Describing Included Data Files

Table 6-1 describes the raw data files included in Appendix 3_Deliverables \Raw_Data. As discussed above, six (6) flights were required to acquire the 2023 LBBNRD AEM data (Figure 4-5). Grouped by flight date, there are four (4) data files included in Appendix 3\Raw_Data for each flight. These files have extensions of "*.sps" and "*.skb". The "*.sps" files include navigation and DGPS location data and the "*.skb" files include the raw AEM data that have been PFC-corrections (discussed in Section 4.4.1). Two additional files are used for all the flights. These are the system description and specifications file (with the extension "*.gex") in the GEO subdirectory and the 'mask' file (with the extension "*.lin"), in the MASK subdirectory, which correlates the flight dates, flight numbers, and assigned line numbers.

Table 6-2 describes the data columns in the ASCII *.xyz file *LBBNRD2023_EM_MAG_AUX.xyz*. This file contains the electromagnetic data, plus the magnetic and navigational data, as supplied directly from SkyTEM.

The result of the SCI is included in *LBBNRD2023_AEM_SCI02_INV_v1.xyz* and the data columns of these databases are described in Table 6-3.

The interpretation results are included in the data file *LBBNRD2023_InterpSurfaces.xyz* in ASCII format. Table 6-4 describes the data columns of those files.

ESRI ArcGIS raster grids of the surfaces (*.tif and *.flt formats) that were used in the interpretation (DEM, water table) and derived from the interpretation (top of geological units) of the AEM and borehole are listed in Table 6-5 and stored in Appendix 3 - Deliverables\ESRI. Included shapefiles are listed in Table 6-6.

In addition, a data file, *LBBNRD2023_SCI02_InvResults_GeoCloud_v1.xyz*, with the Nebraska Geocloud format is included in Appendix 3_Deliverables\GeoCloud. The format is listed in Table 6-7.

Finally, Table 6-8 describes the columns in the LBBNRD 2023 AEM 3D voxel files included in this data delivery.

In summary, the following are included as deliverables:

- Raw Data Files - SkyTEM files *.gex, *skb, *.lin (Table 6-1)
- Raw EM Mag data as ASCII *.xyz (Table 6-2)
- SCI inversion as ASCII *.xyz in array column format (Table 6-3)
- Interpretations as ASCII *.xyz (Table 6-4)
- ESRI GIS files – raster grids (*.flt) and ESRI ArcGIS Pro map package (.mpkx) (Table 6-5)
- 2D profiles, Surfaces, and 3D fence diagrams of the AEM survey inversion results
- Files compatible with GeoScene 3D and the Nebraska GeoCloud (Table 6-7)
- LBBNRD 2023 AEM 3D voxel files (Table 6-8)
- KMZs for LBBNRD AEM flight lines (Discussed in Section 6.2).

Table 6-1. Raw SkyTEM data files

Folder	File Name	Description
Data	..NavSys.sps, ...PaPc.sps, ...RawData_PFC.skb, ...PPP.sps	Raw data files included for each flight used in importing to Aarhus Workbench
Geo	20230615_20065_USA_AGF_NE_304M_SKB.gex	304HM System Description
	20065_USA_AGF_CO_304M_SR2.gex	
	20065_USA_AGF_CO_304M_SR2.sr2	
Mask	20065_USA_AGF_Colorado_304M_Prod.lin	Production file listing dates, flights, and assigned line numbers

Table 6-2: Channel name, description, and units for LBBNRD2023_EM_MAG_AUX.xyz with DEM, magnetic, DGPS, Inclinometer, altitude, and associated data.

Parameter	Description	Unit
Line	Line Number	
E_UTM14Nm	Easting, NAD83 UTM Zone 14N	Meters [m]
N_UTM14Nm	Northing, NAD83 UTM Zone 14N	Meters [m]
DEM_m	Digital Elevation	Meters [m]
E_NESPCS83ft	Easting, NAD83 Nebraska State Plane	Feet [ft]
N_NESPCS83ft	Northing, NAD83 Nebraska State Plane	Feet [ft]
DEM_ft	Digital Elevation	Feet [ft]
Fid	Unique Fiducial Number	
Flight	Name of Flight	yyyymmdd.ff
DateTime	DateTime Format	Decimal days
Date	DateTime Format	yyyymmdd
Time	Time UTC	hhmmss.sss
AngleX	Angle (in flight direction)	Degrees
AngleY	Angle (perpendicular to flight direction)	Degrees
Height_m	System Height Measurement Above Ground	Meters [m]
Height_ft	System Height Measurement Above Ground	Feet [ft]
Lon	Longitude, WGS84	Decimal Degrees
Lat	Latitude, WGS84	Decimal Degrees
Alt	DGPS Altitude above sea level (elevation)	Meters [m]
GDSpeedL	Ground Speed	Kilometers/hour [km/h]
LMcurrent	Current, Low Moment	Amps [A]
HMcurrent	Current, High Moment	Amps [A]
LM_Z_dBdt_G01	Normalized (PFC-Corrected) Low Moment Z-RxCoil values array	$pV/(m^4*A)$

LM_X_dBdt_G01	**Normalized (PFC-Corrected) Low Moment X-RxCoil values array**	**pV/(m^4*A)**
HM_Z_dBdt_G01	**Normalized (PFC-Corrected) High Moment Z-RxCoil values array**	**pV/(m^4*A)**
HM_X_dBdt_G01	**Normalized (PFC-Corrected) High Moment X-RxCoil values array**	**pV/(m^4*A)**
PLNI	**Power Line Noise Intensity monitor**	**V/m^2**
Bmag_Raw	**Raw Base Station Mag Data filtered**	**nanoTesla [nT]**
Diurnal	**Diurnal Mag Data**	**nanoTesla [nT]**
MAG_Raw	**Raw Mag Data**	**nanoTesla [nT]**
MAG_COR	**Corrected Magnetic Data**	**nanoTesla [nT]**
RMF	**Residual Magnetic Field**	**nanoTesla [nT]**
TMI	**Total Magnetic Intensity**	**nanoTesla [nT]**

Table 6-3. Channel name, description, and units for LBBNRD2023_AEM_SCI02_INV_v1.xyz with EM inversion results.

/Parameter	Description	Unit
LINE	**Line Number**	
E_NESPCS83ft	**Easting NAD83, Nebraska State Plane**	**Feet (ft)**
N_NESPCS83ft	**Northing NAD83, Nebraska State Plane**	**Feet [ft]**
DEM_ft	**DEM from 100 ft grid NED NAVD88**	**Feet [ft]**
E_UTM14N_m	**Easting NAD83, UTM Zone 14**	**Meters [m]**
N_UTM14N_m	**Northing NAD83, UTM Zone 14**	**Meters [m]**
DEM_m	**DEM from survey**	**Meters [m]**
Alt_m	**Measured altitude of system above ground**	**Meters [m]**
Invalt_M	**Inverted Altitude of system above ground**	**Meters [m]**
Resdata	**Residual of individual sounding**	
ResTotal	**Total residual for inverted section**	
RHO_I_0 through RHO_I_38	**Inverted resistivity of each layer**	**Ohm-m**
RHO_I_STD_0 through RHO_I_STD_38	**Inverted resistivity error per layer**	
SIGMA_I_0 through SIGMA_I_38	**Conductivity**	**S/m**
DEP_TOP_0_ft through DEP_TOP_38_ft	**Depth to the top of individual layers**	**Feet [ft]**
DEP_BOT_0_ft through DEP_BOT_38_ft	**Depth to the bottom of individual layers**	**Feet [ft]**
THK_0_FT through THK_38_FT	**Thickness of individual layers**	**Feet [ft]**
DEP_TOP_0_m through DEP_TOP_38_M	**Depth to the top of individual layers**	**Meters [m]**

DEP_BOT_0_M through DEP_BOT_38_m	**Depth to the bottom of individual layers**	**Meters [m]**
THK_0_m through THK_38_m	**Thickness of individual layers**	**Meters [m]**
DOI_UPPER_FT	**More conservative estimate of DOI**	**Feet [ft]**
DOI_LOWER_ft	**Less conservative estimate of DOI**	**Feet [ft]**
DOI_UPPER_M	**More conservative estimate of DOI**	**Meters [m]**
DOI_LOWER_M	**Less conservative estimate of DOI**	**Meters [m]**

Table 6-4. Channel name description and units for the interpretation results file LBBNRD2023_InterpSurfaces.xyz.

Parameter	Description	Unit
LINE	**Line Number**	
E_NESP83ft	**Easting NAD83, Nebraska State Plane**	**Feet [ft]**
N_NESP83ft	**Northing NAD83, Nebraska State Plane**	**Feet [ft]**
DEM_ft	**Topography at 100ft sampling (NAVD 1988)**	**Feet [ft]**
E_UTM14Nm	**Easting UTM Zone 14**	**Meters (m)**
N_UTM14Nm	**Northing UTM Zone 14**	**Meters (m)**
DEM_m	**Topography at 100ft sampling (NAVD 1988)**	**Meters (m)**
RESDATA	**Inversion model residuals of each individual sounding**	
RESTOTAL	**Inversion model average of all residuals**	
RHO [0] through RHO [38]	**Array of Inverted model resistivities of each layer**	**Ohm-m**
RHO_STD[0] through RHO_STD[38]	**Array of Standard Deviations of Inverted model resistivities for each layer**	**Ohm-m**
DEP_TOP_FT [0] through DEP_TOP_FT [38]	**Depth to the top of 39 individual layers**	**Feet [ft]**
DEP_BOT_FT [0] through DEP_BOT_FT [38]	**Depth to the bottom of 39 individual layers**	**Feet [ft]**
DOI_UPPER_FT	**More conservative estimate of DOI from Workbench**	**Feet [ft]**
DOI_LOWER_FT	**Less conservative estimate of DOI from Workbench**	**Feet [ft]**
WT_1995	**Elevation of the top of the water table from the Nebraska School of Natural Resources Configuration Report, 1995**	**Feet [ft]**
WT_2023	**Elevation of the top of the water table as measured in 2023**	**Feet [ft]**
Kd	**Elevation of the top of the Cretaceous Dakota Group surface**	**Feet [ft]**
Permian	**Elevation of the top of the Undifferentiated Permian**	**Feet [ft]**
SalineWater	**Elevation of the top of the Saline Water at depth**	**Feet [ft]**

Table 6-5. Files containing LBBNRD 2023 raster datasets (.flt format). All datasets projected to NAD83/State Plane Nebraska, feet and extend throughout the entire LBBNRD AEM Survey Area, unless otherwise stated. Resolution of all grids is 300 ft.

Grid File Name	Description
LBBNRD_bedrock_depthto	Depth to the top of bedrock (ft bgs).
LBBNRD_bedrock_topelevation	Elevation of the top of bedrock (ft asl).
LBBNRD_groundsurface_dem	Ground surface elevation (ft asl).
LBBNRD_Kd_depthto	Depth to the top of the Cretaceous Dakota (*Kd*) (ft bgs).
LBBNRD_Kd_thickness_saturated	Saturated thickness of the *Kd* (ft).
LBBNRD_Kd_thickness_total	Total Thickness of the *Kd* (ft).
LBBNRD_Kd_topelevation	Elevation of the top of *Kd* (ft asl).
LBBNRD_Permian_depthto	Depth to the Undivided Permian (Permian) (ft bgs).
LBBNRD_Permian_topelevation	Elevation of the top of Permian (ft asl).
LBBNRD_Q_thickness_saturated	Saturated thickness of the *Q* deposits (ft).
LBBNRD_Q_thickness_total	Total thickness of *Q* (ft).
LBBNRD_watertable_depthto	Depth to the top of the water table (ft bgs).
LBBNRD_watertable_topelevation	Elevation of the top of the water table (ft asl).
LBBNRD_Kd_thickness_over18ohm_saturated	Saturated thickness of the *Kd* (over 18 ohm) (ft).
LBBNRD_Kd_thickness_over18ohm_total	Total thickness of the *Kd* (over 18 ohm) (ft).
LBBNRD_Kd_thickness_over18ohm_transmissivity	Transmissivity of Kd (over 18ohm-m) (gpd/ft)
LBBNRD_Kd_thickness_over18ohm_unsaturated	Unsaturated thickness of the *Kd* (over 18 ohm) (ft).
LBBNRD_Kd_thickness_over25ohm_saturated	Saturated thickness of the *Kd* (over 25 ohm) (ft).
LBBNRD_Kd_thickness_over25ohm_total	Total thickness of the *Kd* (over 25 ohm) (ft).
LBBNRD_Kd_thickness_over25ohm_unsaturated	Unsaturated thickness of the *Kd* (over 25 ohm) (ft).
LBBNRD_Q_coarse_aquifer_thickness_saturated	Saturated thickness of coarse and aquifer material within the *Q* (ft).
LBBNRD_Q_coarse_aquifer_thickness_total	Total thickness of coarse and aquifer material within the *Q* (ft).
LBBNRD_Q_coarse_aquifer_thickness_unsaturated	Unsaturated thickness of coarse and aquifer material within the *Q* (ft).
LBBNRD_Q_coarse_thickness_total	Total thickness of coarse material within the *Q* (ft).

LBBNRD_Q_coarse_aquifer_marginal_thickness_saturated	**Saturated thickness of coarse, aquifer, and marginal material within the *Q* (ft).**
LBBNRD_Q_coarse_aquifer_marginal_transmissivity	**Transmissivity of the coarse, aquifer, and marginal material within the *Q* (gpd/ft).**
LBBNRD_Q_marginal_thickness_saturated	**Saturated thickness of marginal material within the *Q* (ft).**
LBBNRD_Q_non_marginal_thickness_unsaturated	**Unsaturated thickness of non-aquifer and marginal materials within the *Q* (ft).**
LBBNRD_Q_nonaquifer_thickness_saturated	**Saturated thickness of nonaquifer material within the *Q* (ft).**
LBBNRD_salinewater_depthto	**Depth to the saline water surface (ft bgs).**
LBBNRD_salinewater_elevation	**Elevation of the saline water surface (ft asl).**
LBBNRD_potentialrechargeareas_coarseaquiferq_thickness_unsaturated	**Unsaturated thickness of coarse and aquifer material within the *Q* (ft) within the potential recharge areas extent only**

Table 6-6. Relevant features and extents as LBBNRD 2023 ESRI Shapefiles. NAD83/State Plane Nebraska, feet.

LBBNRD_DNRWells_SpecificCapacity	**Nebraska DNR wells that had all elements to calculate specific capacity and assign the wells to either *Q* deposits or bedrock, including: screen interval, static water level, pumping water level, and well yield.**
LBBNRD_Kd_Extent	**Extent of the Cretaceous Dakota (*Kd*); revised from Burchett (1986) based on AEM data.**
LBBNRD_WaterTable_ControlPoints	**Data points used to create the water table surface including monitoring wells, DNR wells, and river control points.**
LBBNRD_Project_Extent	**Extent of the AEM survey area and interpolation area for the 2023 LBBNRD AEM survey.**
LBBNRD_Outcrops.shp	**Bedrock outcrops digitized from Burchett et al., 1972. Used for reference only.**
LBBNRD_Wells_UsedForInterp	**CSD and NE-DNR wells/boreholes used to help guide the AEM interpretation.**
LBBNRD_WellsWithGeophysicalLogs	**CSD boreholes with geophysical logs within the survey area.**
LBBNRD_FlightLines_AsFlown	**AEM survey flight lines as flown in the field.**
LBBNRD_FlightLines_AsFlown_Merged	**AEM survey flight lines merged for this report.**
LBBNRD_PotentialAreasOfRecharge	**Potential areas of recharge**

TransmissivityContours_Digitized_SummersideMyer	**Digitized lines of equal transmissivity from published data used for comparison (Summerside and Myers, 2005)**

Table 6-7. Nebraska Geocloud-import file: LBBNRD2023_SCI02_InvResults_GeoCloud_v1.xyz. (*_geocloud.xyz)

LINE	**Original Line Number**
X_SP_FT	**Easting Nebraska State Plane (feet) NAD83**
Y_SP_FT	**Northing Nebraska State Plane (feet) NAD83**
ELEV_FT	**Elevation above sea level (feet) from USGS Data Elevation Model**
X_SP_M	**Easting Nebraska State Plane (meters) NAD83**
Y_SP_M	**Northing Nebraska State Plane (meters) NAD83**
ELEV_M	**Elevation above sea level (meters) from USGS Data Elevation Model**
INV_ALT_FT	**Inverted altitude of AEM system (feet)**
RESDATA	**Data residual of sounding**
RESTOTAL	**Total data residual of inversion**
RHO_0 to 38	**Resistivity of layers 1 to 39 (Ohm-m)**
RHO_STD_0 to 38	**Standard deviation of resistivity of layers 1 to 39**
DEP_TOP_FT_0 to 38	**Depth to top of layer 1 to 39 (positive feet for GeoCloud)**
DEP_BOT_FT_0 to 38	**Depth to bottom of layer 1 to 39 (positive feet for GeoCloud)**
DEP_TOP_M_0 to 38	**Depth to top of layer 1 to 39 (negative meters)**
DEP_BOT_M_0 to 38	**Depth to bottom of layer 1 to 39 (negative meters)**
DOI_UPPER_FT	**Upper Depth of Investigation calculation (negative feet)**
DOI_LOWER_FT	**Lower Depth of Investigation calculation (negative feet)**
DOI_UPPER_M	**Upper Depth of Investigation calculation (negative meter)**
DEP_LOWER_M	**Lower Depth of Investigation calculation (negative meter)**

Table 6-8. Columns in LBBNRD 2023 AEM 3D Voxel files LBBNR23_Rho_Voxel_ALL, _Kd, _Q.

E_NESPCS83ft	**Easting, NAD83 Nebraska State Plane, in feet**
N_NESPCS83ft	**Northing, NAD83 Nebraska State Plane, in feet**
Depth_ft	**Northing Nebraska State Plane (feet) NAD83**
LBBNRD_Rho_Voxel_XX	**Interpolated LBBNRD 2023 3D voxel model resistivity**

6.2 Description of Included Google Earth KMZ Data and Profiles

In addition to the data delivered in XYZ format, Google Earth .KMZ files were generated to view the geophysical AEM flight line locations and interpreted geologic data. KMZ files for all "*As-Flown*" flight lines and data "*Retained*" for inversion after editing are included in the folder "*Appendix_3_Deliverables\KMZ\Flight Lines*".

Unique KMZ files were created for each individual flight line in approximately 10-12-mile segments or shorter. Within these specialized KMZ files, the AEM flight line is shown as well as place marks at each location where there are interpreted geologic results. The attribute data for each unique place mark contains location information as well as bedrock and the water table. These KMZ files are located within the "*Appendix_3_Deliverables\KMZ\LBBNRD23_Profiles*" folder. In this folder is a "*GoogleE_Readme.pdf*" file that provides instructions regarding the "*Settings*" changes that need to be made in Google Earth, and how to use the KMZ files in Google Earth including a legend of what attributes are displayed when an AEM sounding location is clicked. This LBBNRD 2023 GoogleE_Readme.pdf file is repeated below as a convenience. An image of the LBBNRD 2023 KMZ layout is presented in Figure 6-1 and an example of clicking on points is presented in Figure 6-2. A 2D profile of line L401401 is presented in Figure 6-3.

6.2.1 Included README for the LBBNRD 2023 Interpretation KMZ

README for: **LBBNRD23_SCI02_Interp_KMZ.kmz**

Data Files - Please copy the folder *LBBNRD23_Profiles* to your C:\ drive. Do not rename any of the images within the folder.

Google Earth Instructions:

STEP 1: In Google Earth, click "*Tools*", then "*Options*".

STEP 2: In the Google Earth Options box, click the "*General*" tab.

STEP 3: Under "*KML Content Security*", make sure the box is checked to allow access to local files (the profiles).

STEP 4: Under "*Display*", make sure the box is checked to show web results in external browser.

STEP 5: The LBBNRD23_SCI02_Interp_KMZ interpretation file within the folder named *LBBNRD23_Profiles* can now be opened and viewed in Google Earth.

Data:

East (m) – Easting coordinate in NAD83, UTM 14N, in meters.

North (m) – Northing coordinate in NAD83, UTM 14N, in meters.

East (ft) – Easting coordinate in NAD83, Nebraska State Plane, in feet.

North (ft) – Northing coordinate in NAD83, Nebraska State Plane, in feet.

Elevation (ft) – Digital Elevation Model (DEM) ground surface elevation in feet.

Elevation WaterTable1995 (ft) – Elevation of the 1995 water table, in feet.

Elevation WaterTable2023 (ft) – Elevation of the 2023 water table, in feet.

Elevation Cretaceous Dakota Gp (ft) – Estimated elevation of Cretaceous Dakota Group Fm., ***Kd***, in feet.

Elevation Permian Units (ft) – Estimated elevation of the Permian Chase (***Pc***) and Council Grove (***Pcg***) geological formations, in feet.

Elevation Saline Water (ft) – Estimated elevation of the saline water, where present, in feet.

Profile – Link to Interpreted AEM profile images.

Legend – Link to this write-up describing data channels listed here.

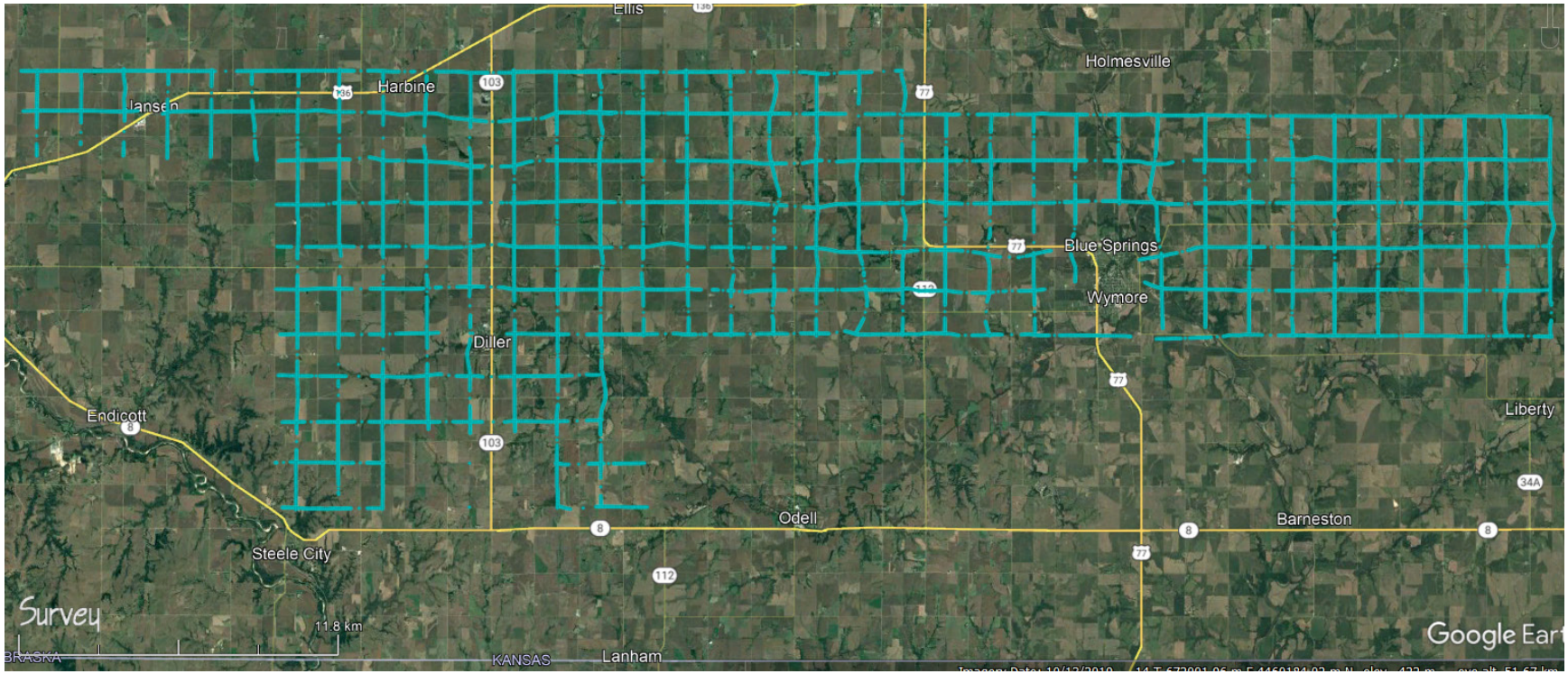


Figure 6-1. Google Earth KMZ of the LBBNRD 2023 AEM survey area showing the AEM Interpretation locations.

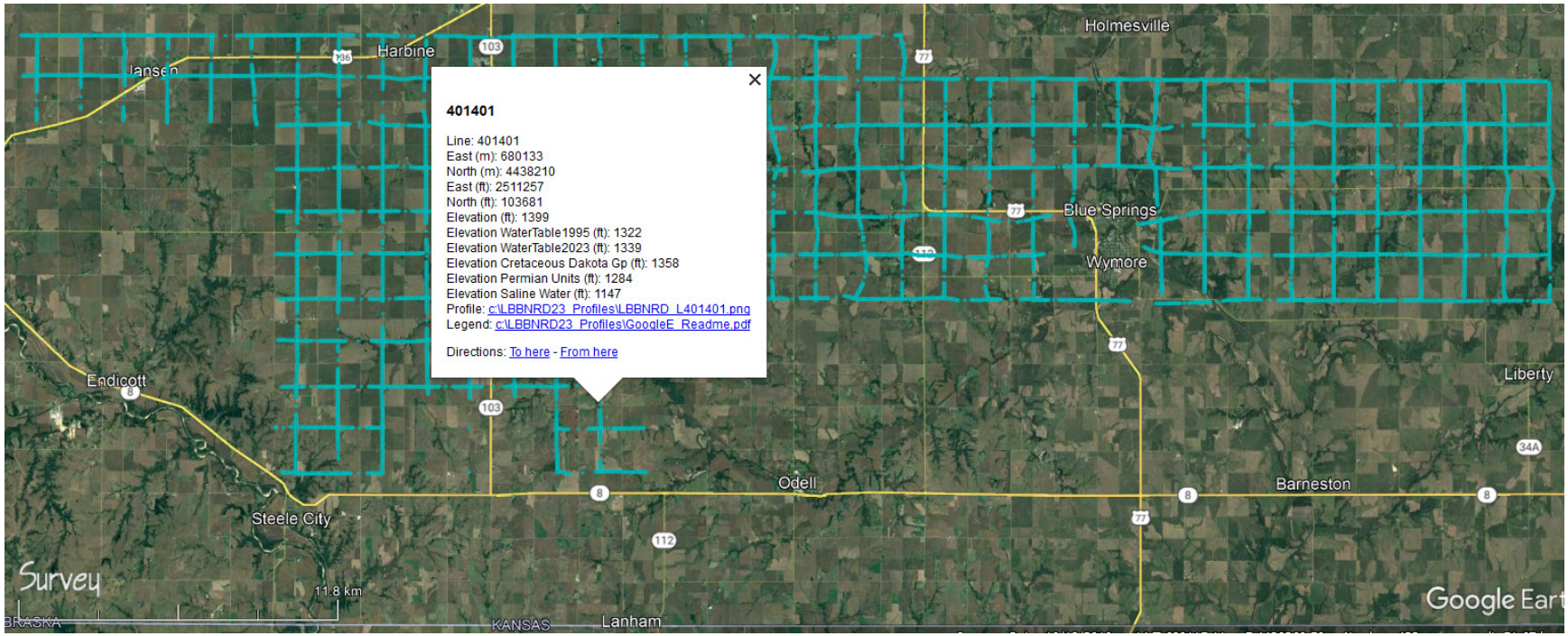


Figure 6-2. Example of clicking on a location in the LBBNRD 2023 AEM survey area. Profile L401401 is presented in Figure 6-3 below.

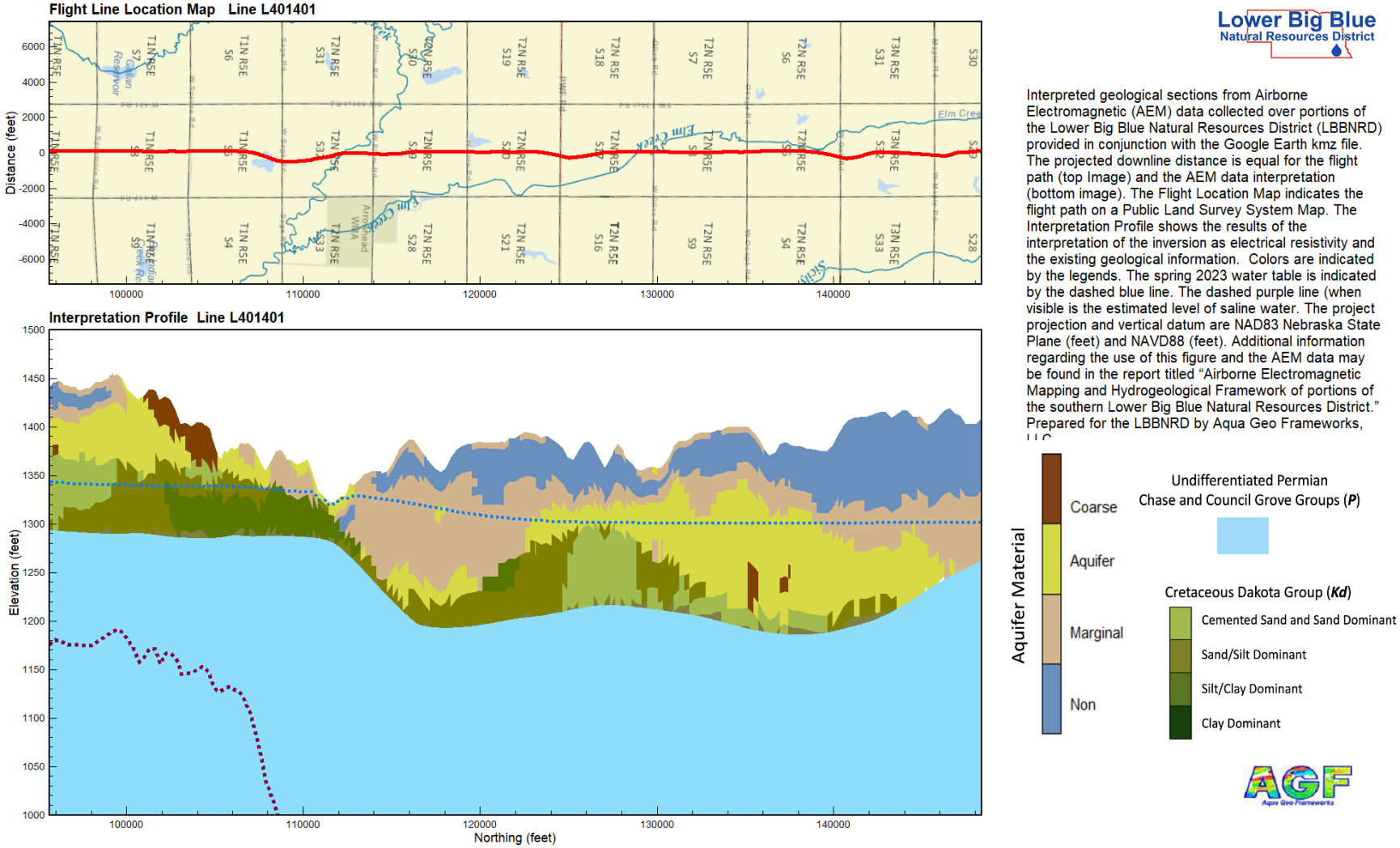


Figure 6-3. Example of clicking on link to Profile image for line L401401 in the LBBNRD 2023 interpretation KMZ.

7 References

AGF, 2019, Summary Report on "Airborne Electromagnetic Mapping and Hydrogeologic Framework of Selected Regions of the Eastern Nebraska Water Resources Assessment Area" Chapters Completed for Lewis and Clark, Lower Elkhorn, Lower Platte North, Lower Platte South, Nemaha, and Papio-Missouri River Natural Resources Districts: Prepared for Eastern Nebraska Water Resources Assessment by Aqua Geo Frameworks, LLC, Mitchell, NE, 13 December 2019, 22p., (accessed on February 24, 2023) http://www.enwra.org/aem2018.html

AGF, 2021, Airborne Electromagnetic Mapping and Hydrogeologic Framework of Selected Regions of the Papio-Missouri River Natural Resources District: Prepared for the Papio-Missouri River Natural Resources District by Aqua Geo Frameworks, LLC, Laramie, WY, 22 February 2021, 232pp., http://www.enwra.org/aem2020.html

Asch, T.H., Abraham, J.D., and Irons, T., 2015, "A discussion on depth of investigation in geophysics and AEM inversion results", Presented at the Society of Exploration Geophysicists Annual Meeting, New Orleans. (accessed on February 24, 2023). https://library.seg.org/doi/reader/10.1190/segam2015-5915199.1

Burchett, R. R. and Reed, E. C., 1967, Centennial guidebook to the geology of southeastern Nebraska: Conservation and Survey Division, 621, https://digitalcommons.unl.edu/conservationsurvey/621

Burchett, R.R., Dreeszen, V.H., Reed, E.C., and Prichard, G.E., 1972, Bedrock geologic map showing thickness of overlying Quaternary deposits, Lincoln Quadrangle and part of Nebraska City Quadrangle, Nebraska and Kansas: U.S. Geological Survey, Report IMAP-729, https://doi.org/10.3133/i729

Burchett, R.R., 1986, Geologic bedrock map of Nebraska: Nebraska Geological Survey. Scale 1:1,000,000, Geologic Maps and Charts (GMS)-1, https://ngmdb.usgs.gov/Prodesc/proddesc_39227.htm

Burchett, R.R. and Pabian, R.K., 1992, Geologic bedrock map of Nebraska: Nebraska Geological Survey, Nebraska Geonotes, Conservation and Survey Division, No. 763, University of Nebraska GIM-48, 4pp., https://digitalcommons.unl.edu/conservationsurvey/763

Cannia, J.C., Woodward, D.W., and Cast, L.D., 2006, Cooperative Hydrology Study hydrostratigraphic units and aquifer characterization report: Cooperative Hydrology Study, 91 p., accessed February 18, 2023, at http://cohyst.dnr.ne.gov/document/dc012hydro_aquifer_022406.pdf

Carney, C.P., Abraham, J.D., Cannia, J.C., and Steele, G.V., 2015, Final Report on Airborne Electromagnetic Geophysical Surveys and Hydrogeologic Framework Development for the Eastern Nebraska Water Resources Assessment – Volume II, including the Lower Platte North, Lower Platte South, and Nemaha Natural Resources Districts: Prepared for the Eastern Nebraska Water Resources Assessment (ENWRA) by Exploration Resources International Geophysics LLC, Vicksburg, MS. http://www.enwra.org/aem%20data%20download.html (accessed on February 20, 2023

Christensen, N. B., Reid, J. E., and Halkjaer, M., 2009, "Fast, laterally smooth inversion of airborne time-domain elecromagnetic data." *Near Surface Geophysics* 599-612. https://doi.org/10.3997/1873-0604.2009047

Christiansen, A. V., and Auken, E., 2012, "A global measure for depth of investigation." *Geophysics,Vol. 77, No. 4* WB171-177. (accessed on February 24, 2023). https://library.seg.org/doi/abs/10.1190/geo2011-0393.1

Datamine Discover, 2024, Datamine Discover Profile Analyst, (accessed on December 22, 2023). https://www.dataminesoftware.com/solutions/discover-exploration-gis/.

Divine, D., Joeckel, R.M., Korus, J.T., Hanson, P.R., and Lackey, S.O., 2009, Eastern Nebraska Water Resources Assessment (ENWRA): Introduction to a Hydrogeological Study: Nebraska Conservation and Survey Division, School of Natural Resources, University of Nebraska- Lincoln, No41, (accessed on December 22, 2023), http://digitalcommons.unl.edu/conservationsurvey/41

Divine, D.P. and Sibray, S.S., 2017, An Overview of Secondary Aquifers in Nebraska: Lincoln, NE, Nebraska Conservation and Survey Division, Educational Circular No. 26, pp 44, (accessed on December 22, 2023), https://digitalcommons.unl.edu/conservationsurvey/138/.

Domenico, P.A. and Schwartz, F.W., 1998, Physical and Chemical Hydrogeology (2nd edition): John Wiley and Sons, Inc., New York, 506pp, (accessed December 22, 2023), https://www.wiley.com/en-us/Physical+and+Chemical+Hydrogeology,+2nd+Edition-p-9780471597629

Fetter, C., 1988, Applied Hydrogeology. Merrill Publishing, Columbus, 592pp., https://www.amazon.com/Applied-hydrogeology-C-W-Fetter/dp/0675208874

Foged, N., Auken, E., Christiansen, A.V., and Sorensen, K.I., 2013, "Test-site calibration and validation of airborne and ground based TEM systems.": Geophysics, v.78, No.2: E95-E106. (accessed on https://doi.org/10.1190/GEO2012-0244.1). https://doi.org/10.1190/GEO2012-0244.1

Freeze, R.A. and Cherry, J.A., 1979, “Groundwater”: Published by Prentice Hall, New Jersey, ISBN 0-13-365312-9.

Gannon, J.M., and Vogelgesang, J.A., 2015, Groundwater resources evaluation of the lower Dakota Aquifer in north-central and southwestern Iowa, Water Resources Investigation Report 12, Iowa Geological Survey The University of Iowa01/2015 DOI: 10.17077/rep.006473, https://iro.uiowa.edu/esploro/outputs/report/Groundwater-Resource-Evaluation-of-the-Lower/9984109991002771?institution=01IOWA_INST#file-0

Geosoft, 2023, Oasis montaj, (accessed on December 22, 2023). https://www.seequent.com/products-solutions/geosoft-oasis-montaj/

Heath, R.C., 1983, Basic ground-water hydrology, U.S. Geological Survey Water-Supply Paper 2220, 86p., http://pubs.er.usgs.gov/publication/wsp2220 (accessed February 23, 2023)

HGG, 2023, AarhusInv64 – 1D Electromagnetic inversion algorithm; Developed by HydroGeophysics Group at Aarhus University, Aarhus, Denmark, (accessed on January 10, 2024). https://hgg.au.dk/software/aarhusinv/

HydroGeophysics Group, Aarhus University, 2010, "Validation of the SkyTEM system at the extended TEM test site." Aarhus, Denmark.

HydroGeophysics Group, Aarhus University, 2011, "Guide for processing and inversion of SkyTEM data in Aarhus Workbench, Version 2.0."

Joeckel, R. M., Diffendal, R.F., Hanson, P R., and Korus, J.T., 2018, Geologic mapping of Nebraska: Old rocks, new maps, fresh insights: Robert F. Diffendal, Jr., Publications, no 73, (accessed December 22, 2023), http://digitalcommons.unl.edu/diffendal/73

Joeckel, R.M., Divine, D., Howard, L.M., Cameron, K., and Waszgis, M.M., 2019, Geology of southeastern Nebraska: Nebraska Conservation and Survey Division, No. 671, (accessed December 22, 2023), https://digitalcommons.unl.edu/conservationsurvey/671

Korus, J.T., Howard, L.M., Young, A.R., Divine, D.P., Burbach, M.E., and Hallum, D.R., 2013, The Groundwater Atlas of Nebraska, Third Edition: Conservation and Survey Division, School of Natural Resources, Institute of Agriculture and Natural Resources, University of Nebraska–Lincoln, Resource Atlas No. 4b/2013, 76pp., (accessed December 22, 2023), https://newsroom.unl.edu/announce/snr/2922/16031

Korus, J.T., Joeckel, R.M., Abraham, J.D., Høyer, A.S., Jørgensen. F., 2021, Reconstruction of pre-Illinoian ice margins and glaciotectonic structures from airborne electromagnetic (AEM) surveys at the western limit of Laurentide glaciation, Midcontinent U.S.A.: Elsevier Quaternary Science Advances, Issue 100026, v. 4, October 2021, https://doi.org/10.1016/j.qsa.2021.100026

Ley-Cooper, Y. and Davis, A., 2010. Can a borehole conductivity log discredit a whole AEM survey? : in Extended abstracts of the Australian Society of Exploration Geophysicists Annual meeting Aug 20-24, Sydney, Australia

Nebraska Department of Natural Resources, 2023, Registered Groundwater Wells Data Retrieval, (accessed December 22,2023). https://dnr.nebraska.gov/data/groundwater-data .

Nebraska GeoCloud, 2023, (https://snr.unl.edu/csd/geology/nebraskageocloud.aspx

O'Connor, T.M., 1987, A Preliminary Study of the Hydrogeology of the Dakota Formation in Douglas, Sarpy and Washington Counties, Eastern Nebraska: M.S. Thesis, Department of Geology, University of Nebraska.

Reed, E. C., 1959, The geological section of Nebraska: Conservation and Survey Division, No. 670, Revisions to Condra, G.E. and Reed, E.C., The geological section of Nebraska, Geological Survey Bulletin, No. 14A, 1959, 82pp., (accessed December 22,2023), https://digitalcommons.unl.edu/conservationsurvey/670

Schamper, C., Auken, E., and Sorensen, K., 2014, Coil response inversion for very early time modelling of helicopter-borne time-domain electromagnetic data and mapping of near-surface Geologic Layers. European Association of Geoscientistis & Engineers, Geophysical Prospecting, v. 62, Issue 3, p. 658–674, https://doi.org/10.1111/1365-2478.12104.

SkyTem Airborne Surveys Worldwide, 2023, SkyTEM304M, (accessed on December 22, 2023). https://skytem.com/transient-electromagnetic-tem-systems/.

Souders, V.L., 2000, Geologic Map and Cross Sections Showing Configurations of Bedrock Surfaces, Broken Bow 1° x 2° Quadrangle, East-Central Nebraska: U.S. Geological Survey Geologic Investigations Series I-2725, V.1, https://pubs.usgs.gov/imap/i-2725/ .

Stoeser, D.B., Green, G.N., Morath, L.C., Heran, W.D., Wilson, A.B., Moore, D.W., and Van Gosen, B.S., 2005, Preliminary integrated geologic map databases for the United States: Central States: Montana, Wyoming, Colorado, New Mexico, North Dakota, South Dakota, Nebraska, Kansas, Oklahoma, Texas, Iowa, Missouri, Arkansas, and Louisiana: U.S.G.S. Open File Report 2005-1351, https://pubs.usgs.gov/of/2005/1351/

Summerside, S. A., Olafsen-Lackey, S., Goeke, J., and Myers, W., 2005, Mapping of Aquifer Properties - Transmissivity and Specific Yield - for Selected River Basins in Central and Eastern Nebraska: Conservation and Survey Division Open-File Report 71, 37 pp, https://marketplace.unl.edu/nemaps/mapping-of-aquifer-properties-transmissivity-and-specific-yield-for-selected-river-basins-in-central-and-eastern-nebraska-ofr-71.html .

Summerside, S. and Myers, W., 2005, Transmissivity of the principal aquifer, Lincoln and Nebraska City Quadrangles, Nebraska. Conservation and Survey Division, School of Natural Resources, University of Nebraska–Lincoln GM-65, scale 1:250:000

Szilagyi, J. and Jozsa, J., 2012, MODIS-aided statewide net groundwater-recharge estimation in Nebraska: Ground Water 50, 1–10, (accessed December 22, 2023), https://www.google.com/url?sa=t&rct=j&q=&esrc=s&source=web&cd=&cad=rja&uact=8&ved=2ahUKEwj7rdGuoaSDAxWNkyYFHX25Aj4QFnoECBQQAQ&url=https%3A%2F%2Fsnr.unl.edu%2Fszilagyi%2FGWPublishedpaper.pdf&usg=AOvVaw1p-xIfF46YK6fvXTUDwgBK&opi=89978449

University of Nebraska-Lincoln (UNL) School of Natural Resources, 2023, Nebraska statewide test-hole database. (accessed December 9, 2023), http://snr.unl.edu/csd/geology/testholes.aspx.

U.S. Geological Survey (USGS), 2023, The National Map, 2023, 3DEP products and services: The National Map, 3D Elevation Program Web page, (accessed December 22, 2023). https://www.usgs.gov/the-national-map-data-delivery

USGS-MrData, 2023, “MrData” website on geologic units, by state and county, across the United States, (accessed December 22, 2023). https://mrdata.usgs.gov/geology/state/geog-units.html

Viezzoli, A., Christiansen, A. V., Auken, E., and Sorensen, K., 2008, "Quasi-3D modeling of airborne TEM data by spatially constrainted inversion." *Geophysics Vol. 73 No. 3* F105-F11. (accessed February 24, 2023). http://www.aarhusgeo.com/images/pdf/viezzoli2008.pdf

Witzke, B.J., Ludvigson, G.A., Poppe, J.R., and Ravn, R.L., 1983, Cretaceous Paleogeography along the Eastern Margin of the Western Interior Seaway, Iowa Southern Minnesota, and Eastern Nebraska and South Dakota: Mesozoic Paleogeography of the West-Central United States: Rocky Mountain Symposium 2, p. 225-252, https://archives.datapages.com/data/rocky_sepm/data/011/011001/225_rocky_mount110225.htm

Witzke, B.J. and Ludvigson, G.A., 1994, The Dakota Formation in Iowa and the type area: Book Chapter in Geological Society of America Special Paper 287, Perspectives on the Eastern Margin of the Cretaceous Western Interior Basin, Shurr, G.W., Ludvigson, G.A., and Hammond, R.H., https://doi.org/10.1130/SPE287-p43